

For Reference

NOT TO BE TAKEN FROM THIS ROOM

For Reference

NOT TO BE TAKEN FROM THIS ROOM

Ex LIBRIS
UNIVERSITATIS
ALBERTAENSIS





Digitized by the Internet Archive
in 2019 with funding from
University of Alberta Libraries

<https://archive.org/details/DuPlessis1965>

THE UNIVERSITY OF CHICAGO

THE UNIVERSITY OF CHICAGO
CHICAGO, ILLINOIS 60637

1

THE UNIVERSITY OF CHICAGO

2

THE UNIVERSITY OF CHICAGO
CHICAGO, ILLINOIS 60637

THE UNIVERSITY OF CHICAGO

THE UNIVERSITY OF CHICAGO

THE UNIVERSITY OF CHICAGO

CHICAGO, ILLINOIS 60637

Thesis
1968
61

THE UNIVERSITY OF ALBERTA

i

INVESTIGATION OF CONCENTRATION GRADIENT
OF FLUIDIZED SOLIDS IN PIPELINE TRANSPORT

by

MORNÉ PIER DUPLESSIS, B.Sc., M.Sc.

A THESIS

SUBMITTED TO THE FACULTY OF GRADUATE STUDIES
IN PARTIAL FULFILMENT OF THE REQUIREMENTS
FOR THE DEGREE OF

DOCTOR OF PHILOSOPHY

DEPARTMENT OF CIVIL ENGINEERING

EDMONTON, ALBERTA

April, 1965

UNIVERSITY OF ALBERTA

FACULTY OF GRADUATE STUDIES

The undersigned certify that they have read, and recommend to the Faculty of Graduate Studies for acceptance, a thesis entitled

"INVESTIGATION OF CONCENTRATION GRADIENT
OF FLUIDIZED SOLIDS IN PIPELINE TRANSPORT"

submitted by

Morné Pier duPlessis

in partial fulfilment of the requirements for the degree of
Doctor of Philosophy

ABSTRACT

A Gamma-ray scanning instrument was developed to investigate the concentration gradient of fluidized solids transport in a 4" horizontal pipeline.

A simplified model of the flow mechanism is formulated and confirmed experimentally for sand-water mixtures. The model equates the measured pressure gradient acting over the entire pipe flow section to the sum of the wall shear stresses, acting respectively in the top low solids concentration region and in the bottom high concentration region. The pipe wall shear stress in the bottom region was estimated from the Bagnold "Dispersive Stress" Concept which relates the shear stress to the submerged weight of the solids and a "dynamic" coefficient of friction, $\tan \phi$. The values of $\tan \phi$ were found to fall close to the predicted values and were reasonably constant (0.20 to 0.27) for conditions where the high concentration zone exceeded depths of approximately 1.5".

An empirical equation for the concentration gradient in the dense solids transport region which shows a fairly constant solids distribution is developed and although subject to further experimental verification, gives practical significance to the investigation at this stage.

ACKNOWLEDGMENTS

A major equipment grant from the National Research Council of Canada made this research work possible. Much of the ancillary equipment was loaned to the author by Syncrude of Canada Limited. To a large extent this study is a continuation of work initiated by Dr. R. W. Ansley.

Mr. G. Shook was of invaluable assistance in development and installation of the instruments. Prof. A. W. Peterson and the Hydraulics laboratory staff were active in numerous phases of the work.

Dr. T. Blench provided helpful advice throughout the entire program.

TABLE OF CONTENTS

	<u>PAGE</u>
Title Page	i
Approval Sheet	ii
Abstract	iii
Acknowledgments	iv
Table of Contents	v

PART A - Investigation of Critical Deposit Condition in 4 Inch Pipeline

List of Tables	vii
List of Figures	ix
List of Plates	xi
List of Nomenclature	xii

CHAPTER

I	INTRODUCTION	1
II	EXPERIMENTAL PROGRAM	15
III	EXPERIMENTAL RESULTS	60
IV	INTERPRETATION OF EXPERIMENTAL RESULTS .	81
V	DISCUSSION OF RESULTS	97
VI	CONCLUSIONS AND RECOMMENDATIONS	99

TABLE OF CONTENTS - continued

	<u>PAGE</u>
 <u>PART B - Settling Behaviour of Silica Particles in Non-Newtonian Clay Slurry</u>	
List of Figures and Plates	104
 <u>CHAPTER</u>	
I INTRODUCTION	105
II EXPERIMENTAL PROGRAM	106
III EXPERIMENTAL RESULTS	112
List of References	101
 <u>APPENDIX</u>	
A Data Processing	A 1
B Calibration Data	B 1
C Experimental Data and Accuracy of Results and Concentration Profiles - Original Curves	C 1
D Settling Test Data	D 1

LIST OF TABLES

<u>TABLE</u>		<u>PAGE</u>
II - 1	Average Values of Absorption Coefficient k_w from Pipe Scanning Tests	51a
III - 7	Accuracy of Point Concentrations	78
IV - 1	Calculated Values of G^2 and $\tan \alpha$	90
B - 1	Magnetic Flow Meter Calibration with Water ..	B1
B - 2	Magnetic Flow Meter Calibration with Sand-Water Mixtures	B2
B - 3.1	Gamma Attenuation in Water	B4
B - 3.2	Gamma Attenuation in Sand	B5
B - 3.3	Standard Absorption Curves of Pipe with Water - Top Horizontal	B6
B - 3.4	Standard Absorption Curves of Pipe with Water - Bottom Horizontal	B7
B - 3.5	Standard Absorption Curves of Pipe with Water - Vertical Beam	B8
B - 3.6	Standard Pipe Wall Absorption Curves and Calculated Values of k_w - Top Horizontal.	B9
B - 3.7	Standard Pipe Wall Absorption Curves and Calculated Values of k_w - Bottom Horizontal .	B10
B - 3.8	Standard Pipe Wall Absorption Curves and Calculated Values of k_w - North Vertical	B11
B - 3.9	Standard Pipe Wall Absorption Curves and Calculated Values of k_w - South Vertical	B12
B - 4	Random Variation of Gamma-Ray Output Signal .	B13
B - 5	Pipe Inside Diameter and Pipe Wall Measurements	B14
B - 6	Scanner and Chart Displacement Measurements .	B15
B - 7	Comparison of Pipe Center Located by Chart Measurement and Physical Measurement	B16

LIST OF TABLES - continued

<u>TABLE</u>		<u>PAGE</u>
B - 8.1	Sampling Accuracy	B17
B - 8.2	Sampling Accuracy	B18
B - 9	Typical Sand Sieve Analysis	B19
C - 1	Clear Water Runs in 4" Line	C1
C - 2	Sand Water Runs	C3
C - 3	Gamma-Ray Point Concentrations, C_s	C9
C - 4	Flow Accuracy	C13
C - 5	Accuracy of Transport Concentration During Test Runs	C15
C - 5.2	Accuracy of k_w	C16
C - 5.4	Standard Deviations of $\ln(E_p)$ from Horizontal Beam Scanning Tests	C17
C - 5.5	Accuracy of $\ln e$	C18
C - 5.6	Sample Calculation for Accuracy of Concentration by Gamma-Ray Instrument	C20
C - 6	Comparison of Sand Concentration from Integrated Gamma-Ray Concentration Profiles \bar{C}_s with Transport Concentration C_t Obtained by Sampling at Pipe Discharge	C21
D - 1	Settling Test Results	D1
D - 2	Settling Test Data	D4

LIST OF FIGURES

<u>FIGURE</u>		<u>PAGE</u>
I - 2	Fundamental Head Loss Curve	7
II - 1	Flow Diagram of Experimental Equipment	16
II - 2	Air-Lift Pump	22
II - 3	Detail of Pressure Tap	25
II - 4	Simplified Circuit of Magnetic Flow Meter ...	27
II - 5	Magnetic Flow Recorder Chart	27
II - 6	Water Calibration Chart of Flow Meter	28
II - 7	Sand-Water Mixture Flow Meter Calibration Chart	29
II - 8	Differential Pressure Recorder Chart	31
II - 9	Gamma-Ray Scanner - Mechanical Details	38
II - 10	Scanner Circuit	39
II - 11	Simplified Gamma-Ray Instrument (Qualicon) Circuit	42
II - 12	Gamma Attenuation in Water	47
II - 13	Gamma Attenuation in Sand	48
II - 14	Typical X-Y Recorder Chart	49
II - 15	Sampling Device	55
II - 16	Typical Grain-Size Curve	57
II - 17	Nondimensional Grain-Size Plot	58
III - 1	Clear-Water Friction Factor - Reynolds Number Plot	62
III - 2	Concentration Profiles Test Series 122300 ...	66
III - 3.1	Concentration Profiles Test Series 122400 ...	67
III - 3.2	Concentration Profiles Test Series 122400 ...	68

LIST OF FIGURES - continued

<u>FIGURE</u>		<u>PAGE</u>
III - 4.1	Concentration Profiles Test Series 123000 ...	69
III - 4.2	Concentration Profiles Test Series 123000 ...	70
III - 4.3	Concentration Profiles Test Series 123000 ...	71
III - 5.1	Concentration Profiles Test Series 123100 ...	72
III - 5.2	Concentration Profiles Test Series 123100 ...	73
III - 6	Summary of Concentration Profiles	74
IV - 1	Simplified Sketch for Force Balance	84
IV - 2	Plot of $\tan \alpha$ vs G_w^2	90a
IV - 3	Plot of RE/FN^2 vs ϕ	94
IV - 4	Semi-Log Plot of $C_s/C_s(w)$ vs y'/y'_B For Zone with C_s Greater Than 10%	96
B - 4	Random Variation of Gamma Output Signal	B13b
C	Standard Pipe Wall Absorption Curves	Tests # 122001 to 122003
C	Standard Absorption Curves of Pipe with Water	Tests # 1221S1 to 1223S3
C	Test Run Absorption Curves	Tests # 122303 to 123106

LIST OF PLATES

<u>PLATE</u>		<u>PAGE</u>
II - 1	View from Operating Platform	18
II - 2	Instrument Panel	19
II - 3	View of 4" Test Pipe	19
II - 4	3" Magnetic Flow Tube	20
II - 5	Gamma-Ray Scanner	20
II - 6	Glass Inspection Section	20
II - 7	Gamma-Ray Scanner - Horizontal Beam	36
II - 8	Gamma-Ray Scanner - Vertical Beam	37
II - 9	Photo-micrographs of Test Sand	59

LIST OF NOMENCLATURE

A	= Total internal pipe area = 0.8374 sq. ft.
A _w	= Top clear-water flow area, sq. ft.
A _B	= Bottom sand flow area, sq. ft., $C_s > 10\%$.
A _C	= Center flow area, sq. ft., $C_s < 10\%$.
C _s	= Sand concentration by volume.
C _s (w)	= Sand concentration at pipe floor.
\bar{C}_s	= Average sand concentration by volume in area A _B .
C _t	= Sand discharge concentration by volume.
C _D	= Drag coefficient.
D	= Internal pipe diameter = 3.916 inches = 0.3263 ft.
d	= Mean particle diameter.
E	= Recorded point voltage for calculation of C _s .
E _o	= Voltage for gamma beam in air.
E _{op}	= Voltage for gamma beam in air during calibration tests with water in pipe.
E _p	= Voltage during calibration tests with water in pipe.
e	= E_p/E
F	= Factor converting horizontal chart distances to true displacements of gamma scanner carriage = 1.008
f	= Friction factor defined by Darcy-Weisbach Equation = $2i_w g D / V_m^2$.
FN	= Froude Number = V_m / \sqrt{gD}
g	= Acceleration due to gravity = 32.2 ft/sec ² .
He	= Hedstrom Number = $\frac{\tau_y d^2 \rho_f}{\eta^2}$

NOMENCLATURE - continued

i	= Hydraulic gradient of mixture measured in ft. of water per ft. of pipe.
i_w	= Hydraulic gradient of water.
k	= Linear absorption coefficient for gamma rays, inch^{-1} .
k_w	= Linear absorption coefficient for gamma rays in water, inch^{-1} .
k_s	= Linear absorption coefficient for gamma rays in sand, inch^{-1} .
L_T	= Inside pipe perimeter for flow area $A_w + A_C$.
L_B	= Inside pipe perimeter for flow area A_B .
L_C	= Inside pipe perimeter for flow area A_C .
P	= "Bagnold" dispersive stress, lb/ft^2 .
Q	= Discharge in ft^3/sec .
R	= Pipe inside radius = 1.958 inches = 0.1632 ft.
Re	= Reynolds Number.
S_s	= Specific gravity of sand = 2.64.
S	= Specific gravity of sand divided by specific gravity of water.
s	= Standard deviation.
V_m	= Mean velocity ft/sec .
V^*	= Friction velocity, $\text{ft/sec} = \sqrt{f/8} \cdot V_m$
W	= Terminal settling velocity, ft/sec .
x	= Gamma path length, inches.
y	= Distance from pipe center, inches.
y'	= Distance from interface, inches.
y'_B	= Height of zone where $C_s > 10\%$.

NOMENCLATURE - continued

Y_C	= Chart distance from pipe center, inches.
γ_W	= Specific weight of water, lb/ft ³ .
γ_S	= Specific weight of sand = 164.82 lb/ft ³ .
γ_m	= Specific weight of sand-water mixture.
ρ_S	= Mass density of sand = 5.12 slugs/ft ³ .
ρ_W	= Mass density of water = 1.94 slugs/ft ³ .
ν	= Kinematic viscosity, ft ² /sec.
μ	= Absolute viscosity of water lb. sec/ft ² .
τ_T	= Average pipe wall stress in area, A_T , lb/ft ² .
τ_B	= Average pipe wall stress in area, A_B , lb/ft ² .
τ	= Shear stress, lb/ft ² .
τ_y	= Yield stress in Bingham model, lb/ft ² .
η	= Coefficient of rigidity in Bingham model, lb. sec/ft ² .

CHAPTER I

INTRODUCTION

1.1 HYDRAULIC TRANSPORT OF FLUIDIZED SOLIDS IN PIPELINES

Hydraulic transport is used extensively in road and dam construction, land and harbor reclamation and in process effluent streams in the mining and chemical industries, where large tonnages of bulk material are involved. Non-Newtonian carrying fluids such as clay suspensions are frequently encountered in the latter industries.

A very broad classification of transport regimes is: (1) A fully suspended regime; solids do not appear as a separate phase in the lower pipe section. (2) A fully developed bed regime; the bulk of the solids appear as a separate phase in the lower pipe section. (3) A transition regime or critical deposit regime where part of the solids appear as a separate phase moving along the pipe floor. Many classifications based on particle size, terminal settling velocity and average flow velocity (Govier and Charles, 1961; Newitt et al, 1955; Durand, 1952) have been proposed, none of which accounts for the actual differences in vertical concentration gradients between the flow regimes.

A hydraulic transport task force at the 1960 ASCE Hydraulics Division Conference stated that "It is unfortunate,

considering the many applications of fluid transport of sediment in pipes, that no unified theory has been developed to form a solid foundation for experimental and design work". The trend has been to vastly overdesign commercial installations. This approach is acceptable in applications where equipment is used for a multitude of services. In most other applications handling abrasive solids, closer design tolerances are required since maintenance costs due to pipe wear far exceed operating costs. A rule of thumb is that the pipe wear rate is proportional to the third power of the average flow velocity. The critical deposit regime, although associated with higher pressure gradients, is therefore the most economical operating region.

1.2 WORK TO DATE

Several excellent, up-to-date, historical reviews of published literature (Chamberlain et al, 1960; Babcock, 1962; Thomas, 1962; Condolios and Chapus, 1963; Ansley, 1963) are available and it would be redundant to repeat these in detail. However, for the sake of completeness a brief summary of the more prominent design formulae is given in SECTION 1.3.

Research on this topic is currently in progress. The most active centers have been at Grenoble (France), University of London (England) and the University of Colorado (U.S.A.). Recent impetus was given by a task force appointed by the American Steel Institute (1963). Since the turn

of the century the critical deposit regime has been recognized as the most economical operating condition (Blatch, 1906).

Experimental work to date has been confined for the most part to measuring pressure gradients of various solid-fluid mixtures. This is due to two reasons. Firstly, this has been the conventional approach in developing friction factors for water flow. Secondly, it was the only experimental technique available. This has resulted in empirical and semi-theoretical techniques of predicting pressure drop.

The critical deposit condition was first postulated from the characteristic plot of pressure drop versus mean velocity (FIGURE I-1). It was postulated (Blatch, 1906) that the increased gradient at low velocities resulted from partial restriction of the flow area and increased friction drag of the settled sand. At present there is still not agreement as to whether the characteristic curves converge or diverge from the clear water line. Observation of the different bed conditions is not as simple as it may seem. Only recently has there been disagreement with the generally accepted concept of a bed with flat surface. It was demonstrated that bed movement by dune formation exists as a stable transport mechanism in the critical region (Ansley, 1963). This corresponds to similar phenomena observed for bed load transport (Blench, 1957) in rivers and sand dune movement by wind (Bagnold, 1956).

Historically the most successful approach has been a theoretical dimensional argument based on simplified models. This approach was used independently by several workers and has been compared with experimental results from both large and small scale testing units (Newitt, 1955; Ansley, 1963). The variables used were pressure gradient, density of solids, shape of solids, size of solids, density and viscosity of fluid, mean flow velocity, volume concentration of solids, roughness height of conduit wall, and hydraulic radius of conduit. Although it was recognized that concentration gradient should enter as a variable, the absence of a reliable method of measurement precluded its use. In developing the equations the trend has been to lump the five variables - solid density, shape, size, fluid density and viscosity into one parameter of either terminal settling velocity W or drag coefficient C_D . In fact these actually became the measured variable. In view of this it is hardly surprising that even the more prominent published correlations are not in agreement. This lack of agreement is particularly noted in the critical flow regime. This is obviously true for more than one reason. By far the bulk of the data has been taken for fully suspended clean bed conditions, but, more important, the measured variable W or C_D has very little if any physical meaning, particularly in the critical deposit flow condition. The drag coefficient measured from settling tests in clear water (or more often taken from published tables) is not a very meaningful parameter when applied to

hindered settling in turbulent flow of material with a concentration gradient. In addition it is difficult to determine a characteristic length and a shape factor for mixed solid sizes. Values of W based on a median particle diameter and a weighted average value of C_D have been used. It has only recently been recognized that appreciable quantities of fine solids can alter the rheological properties of the carrying fluid. However, the formulae summarized in SECTION 1.3 are still being used extensively for commercial design in the absence of anything better and despite a growing awareness of their limitations. In many instances a design is preceded by pilot testing on a large scale which at times approaches 100% of full size.

Another approach to the problem has been an investigation directed towards isolating the dynamics of solid-fluid interaction (Banister, 1959; Hinze, 1961; Worster, 1952; Hunt, 1954; Friedlander, 1957). Unfortunately the results have been in terms of variables which cannot be measured or related to the external parameters such as hydraulic gradient, mean velocity and solids concentration. In this respect these attempts are still considered to be inconclusive by their authors. However, they have aided in recognizing pertinent parameters.

1.3 SUMMARY OF DESIGN FORMULAE FOR PIPELINE TRANSPORTATION OF SOLIDS

Only the more important experimental work and resulting design formulae will be reviewed. A general discussion

of these approaches is given in the preceeding section.

1.3.1 HAZEN AND HARDY (1906), BLATCH (1906)

The work by Hazen and Hardy formulated the first investigation into hydraulic transport of fluidized solids in pipelines. Discussion of their results and an independent investigation by Blatch with 60 - 100 mesh sand in a 1" pipe resulted in the fundamental plot (FIGURE I-1) of mean velocity, V_m versus hydraulic gradient, i (ft of water per ft of pipe) and the following observations;

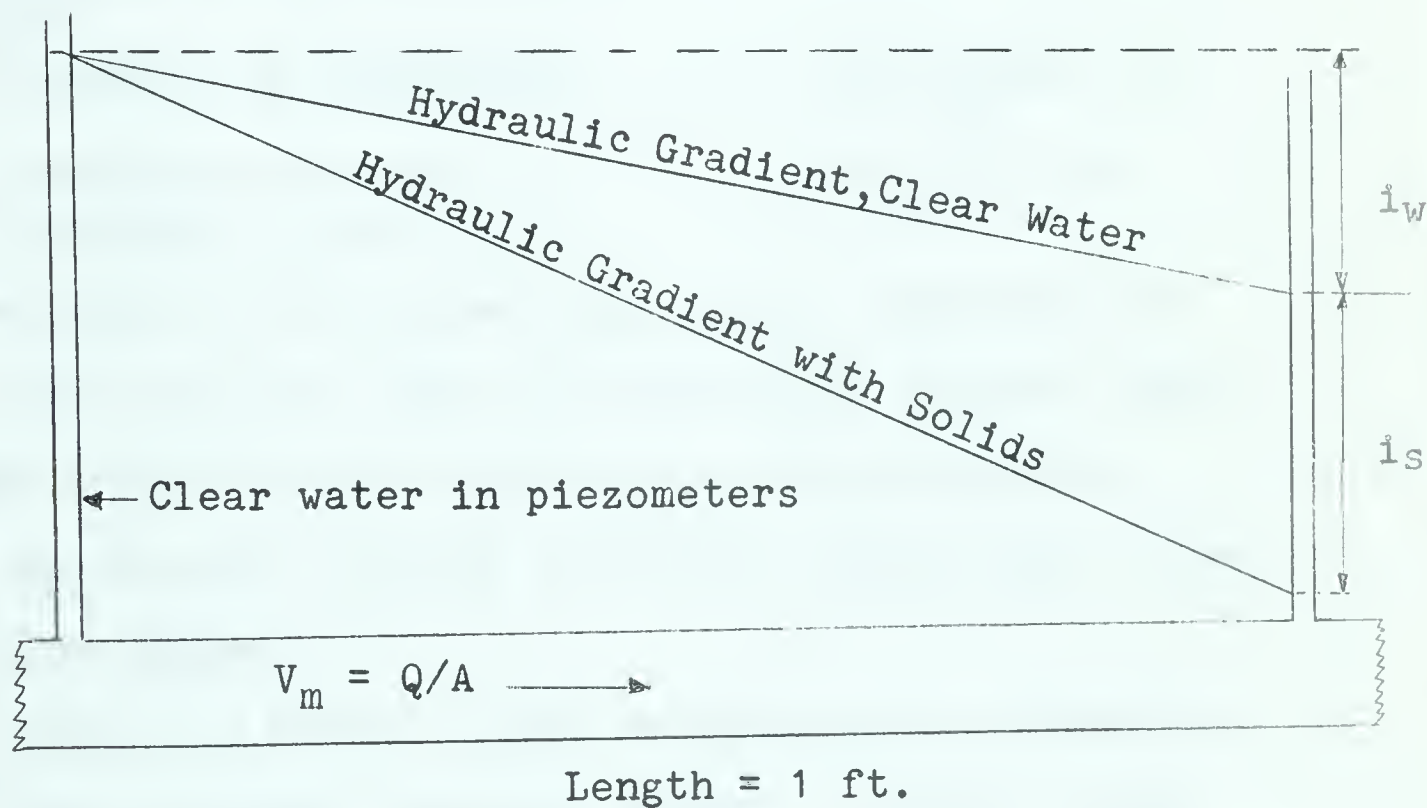
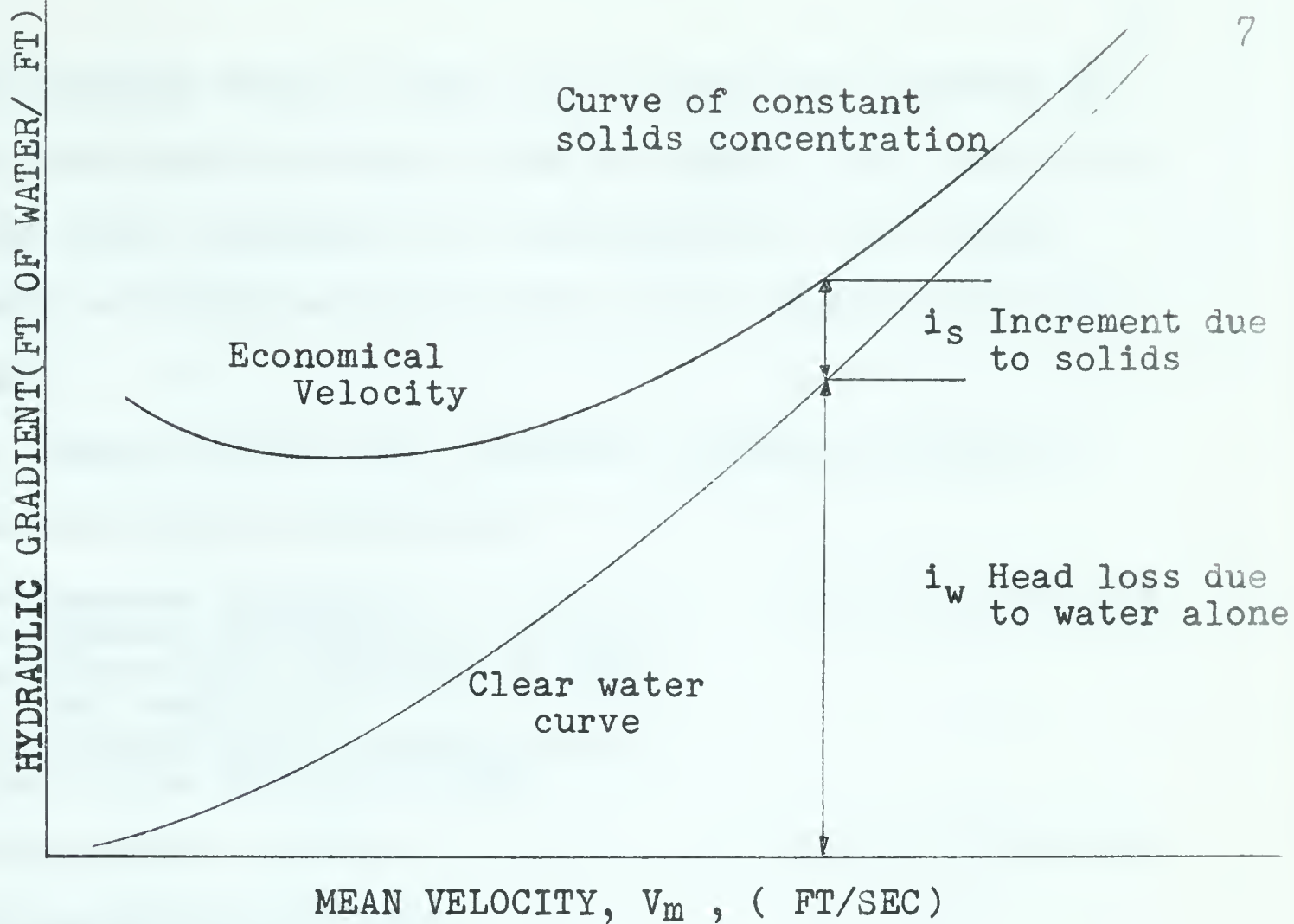
- (i) At low velocities, $i = \text{fn}(C_s)$.
- (ii) At high velocities, $i = \text{fn}(V_m, C_s)$. Experimental data indicated $i \propto V_m^n$ where $n = 1.75$ to 1.86 .
- (iii) A "critical deposit velocity" exists below which a bed forms in the pipe. Blatch found it to be 3.5 ft/sec.
- (iv) The increased value of i at low velocities results from partial restriction of the flow channel and increased friction drag of a dense sand layer on the pipe floor.

These workers concluded that the hydraulic gradient of a slurry could be expressed as the hydraulic gradient due to water alone (i_w) at the given slurry velocity plus an incremental value (i_s) which is a function of the sand concentration.

$$\text{i.e. } i = i_w + f(C_s)$$

1.3.2 DURAND AND CONDOLIOS (1952)

The work carried out at the Neypric Hydraulic Transport Laboratory in France by Durand et al represents the most exhaustive study in this field. Test conditions covered pipe diameters from 1" to 28", solids with specific



FUNDAMENTAL HEAD LOSS CURVE

FIGURE I-1

gravities ranging from 1.5 for coal to 3.95 for corundum and transport concentrations up to 60% by weight. All tests were run in the fully suspended or "heterogeneous" flow regime with graded material having particle sizes ranging from 0.02 to 100 mm.

Durand defined the transport regimes according to solid particle sizes as follows;

1. Homogeneous mixtures. $d < 25$ to 30 microns.
Considered equivalent to a fluid and classified according to rheological behaviour.
No concentration gradient exists from top to bottom of pipe.
2. Intermediate mixtures. $d = 25$ to 50 microns.
3. Heterogeneous mixtures.
A concentration gradient exists from the top to the bottom of the pipe.
 - (a) transport by suspension. . . $d = 50$ microns to 0.2 mm.
 - (b) transition category. $d = 0.2$ to 2 mm.
 - (c) transport by saltation. . . . $d > 2$ mm.

Saltation referred to the arched flow path of particles being lifted from the floor only to be deposited further along.

The objective was to develop a non-dimensional correlation which could be used to predict mixture head losses in all the flow regimes.

O'Brien and Folsom (1939) recognized the potential of grouping the variables, specific weight of solids, shape and size of solids particles and specific weight and viscosity of the homogeneous fluid phase into the one parameter of settling velocity of the solids particles. Durand instead

used the drag coefficient, C_D , as a measure of these five variables after the hydraulic gradient was found to be independent of the particle size for particles larger than 2 mm. He explained this phenomenon by the fact that the drag coefficient for spherical particles became independent of the Reynolds number in the range 1000 to 200,000. His results were best fitted by the equation:

$$\Phi = \frac{i-i_w}{C_s i_w} = 81 \left[\frac{gD(S-1)}{V_m^2} \cdot \frac{1}{\sqrt{C_D}} \right]^{1.5} \dots \dots \dots (1.3.1)$$

The critical deposit velocity was found to be:

$$V_C = F_L [2gD(S-1)]^{1/2} \text{ ft/sec} \dots \dots \dots (1.3.2)$$

where F_L is a function of particle diameter and solids concentration.

The Durand - Condolios equation relates i to V_m^{-3} which is contrary to the findings of Blatch.

1.3.3 CONDOLIOS AND CHAPUS (1963)

Condolios and Chapus conducted some tests with ungraded solids as an extension of their earlier work with graded solids. They came to the conclusion that the critical deposit velocity could still be predicted from EQUATION 1.3.2 but an apparent drag coefficient was introduced to accommodate the irregularity of particle shape. They also used a weighted drag coefficient to account for the different particle sizes. It was further claimed that the equation could be used for the case where a bed exists in the pipe. In this case the diameter was replaced by the hydraulic radius of the flow area

above the pipe.

The final equation for this condition is:

$$\Phi = \frac{i - i_w}{C_s i_w} = 180 \left[\frac{4gR_h}{V_e} \cdot \frac{1}{\sqrt{C_{x'}}} \right]^{3/2} \dots \dots \dots (1.3.3)$$

where V_e = true velocity above the fixed bed.

R_h = hydraulic radius of flow area above the bed.

$$\sqrt{C_{x'}} = P_1 \sqrt{\frac{C_{D1}}{\psi}} + P_2 \sqrt{\frac{C_{D2}}{\psi}} + \dots \dots \dots$$

C_{D1}, C_{D2} = true drag coefficient of solid sizes d_1, d_2 .

ψ = sphericity of solid particles.

$$= \frac{\text{cross-section of sphere of diameter } d}{\text{maximum cross-section of particle of diameter } d}$$

P_1, P_2 = weight percentages of fractions with diameters d_1, d_2 .

1.3.4 NEWITT ET AL (1955)

Newitt et al derived equations for homogeneous flow, heterogeneous flow and for flow with a sliding bed. Their use of the term $(i - i_w)$ at the same mean velocity as a measure of the energy required for conveying the solids is not justified since the presence of solids will almost certainly modify the flow pattern. As a first approximation the hydraulic gradient due to fluid alone (i_w) and the increase due to the solids (i_s) were assumed to be additive.

$$\text{i.e. } i = i_w + i_s \dots \dots \dots (1.3.4)$$

By using i_s as a measure of the work done by the fluid on the particle and the terminal settling velocity W and apparent weight of solids as measures of the work done by the particle

on the fluid and equating these, they derived the following expression for heterogeneous mixtures without a bed condition.

$$\Phi = \frac{i-i_w}{C_s i_w} = 1100(S-1) \frac{g^{DW}}{V_m^3} \dots \dots \dots (1.3.5)$$

For flow with a moving bed, i_s was related to the work done in pushing particles over the floor. In the simplified model this friction force was taken as proportional to a coefficient of friction and the apparent weight of the solids in water.

This expression is given as:

$$\Phi = 66(S-1) \frac{g^D}{V_m^2} \dots \dots \dots (1.3.6)$$

The constants in the above equations were obtained by experiments in 1" brass pipes using narrow particle size fractions. The effect of mixtures of two sizes was also studied. The critical deposit velocity equation of Durand (EQUATION 1.3.2) was shown to hold fairly well for their data.

1.4 WORK TO BE DONE

The less rigorous theoretical approach based on simplified models of the flow mechanism appears to be the most promising in developing more reliable design equations. The main deterrent is still the lack of reliable experimental instruments for measuring the conditions from point to point in the flow section. Velocity and concentration variations undoubtedly are the most important of these variables and an accurate measurement of the difference or "slip" velocity between fluid and solids would constitute a major break-through

in this field. More general use of radiation techniques in recent years has led to development of instruments capable of measuring densities in a flow section without disturbing the flow pattern. Measurement of velocity variations in a slurry is a much more formidable problem. Shook and Daniel (1964) are currently using the gamma-ray technique for measuring concentration gradients in a 1" x 4" closed rectangular channel. They also developed a technique for measuring the variation of mixture velocity over the flow section.

To the best of the author's knowledge, no reliable investigation of the concentration gradient in horizontal pipelines has yet been carried out. Undoubtedly such an investigation will lead to a better understanding of the transport mechanism than has hitherto been possible.

1.5 SCOPE OF INVESTIGATIONS

PART A

It appeared desirable to study the concentration gradient and its associated bed condition close to the critical deposit region as a first step in a research program in which development of the gamma-ray instrument would take up a major portion of the time. A thin-walled 4" test pipe was chosen as the smallest size which would have a sufficiently long path length close to the wall to give meaningful readings in this area. The solid type was limited to an easily obtainable silica sand of consistent size distribution in the range 30 to

100 mesh (median diameter 0.355 mm). The basic objectives were to attempt to;

- (i) classify the flow regimes by their concentration gradients.
- (ii) formulate simplified models of the flow mechanism based on the information gained.
- (iii) test the validity of these models with the test data.

Delays in delivery of the gamma-ray instrument and in obtaining a licence from the Federal Health authorities for the use of a radio-active source in the Hydraulics Laboratory curtailed the scope of the concentration gradient investigation.

Calibration of the instrument was carried out in November 1964 and the test runs were made during December 1964.

PART B

PART B is not directly related to PART A and is a separate investigation of an observation by Ansley (1963) that there is a so-called boosting effect in transport capacity when a clay suspension up to a certain clay concentration is used as the carrying fluid. The present investigation used the Rheological data obtained by Ansley in an attempt to explain this boosting effect and optimum clay concentration.

It was decided to investigate the phenomenon in as simple a system as possible, i.e. a study of the settling

behaviour of single particles in a stationary clay suspension. The high turbidity of the clay suspension necessitated development of an electrical technique to replace visual observation of settling particles. This experimental work was carried out during the summer of 1964 concurrently with development work on the gamma-ray instrument and preparation of the 4" pipeline system.

CHAPTER II

EXPERIMENTAL PROGRAM

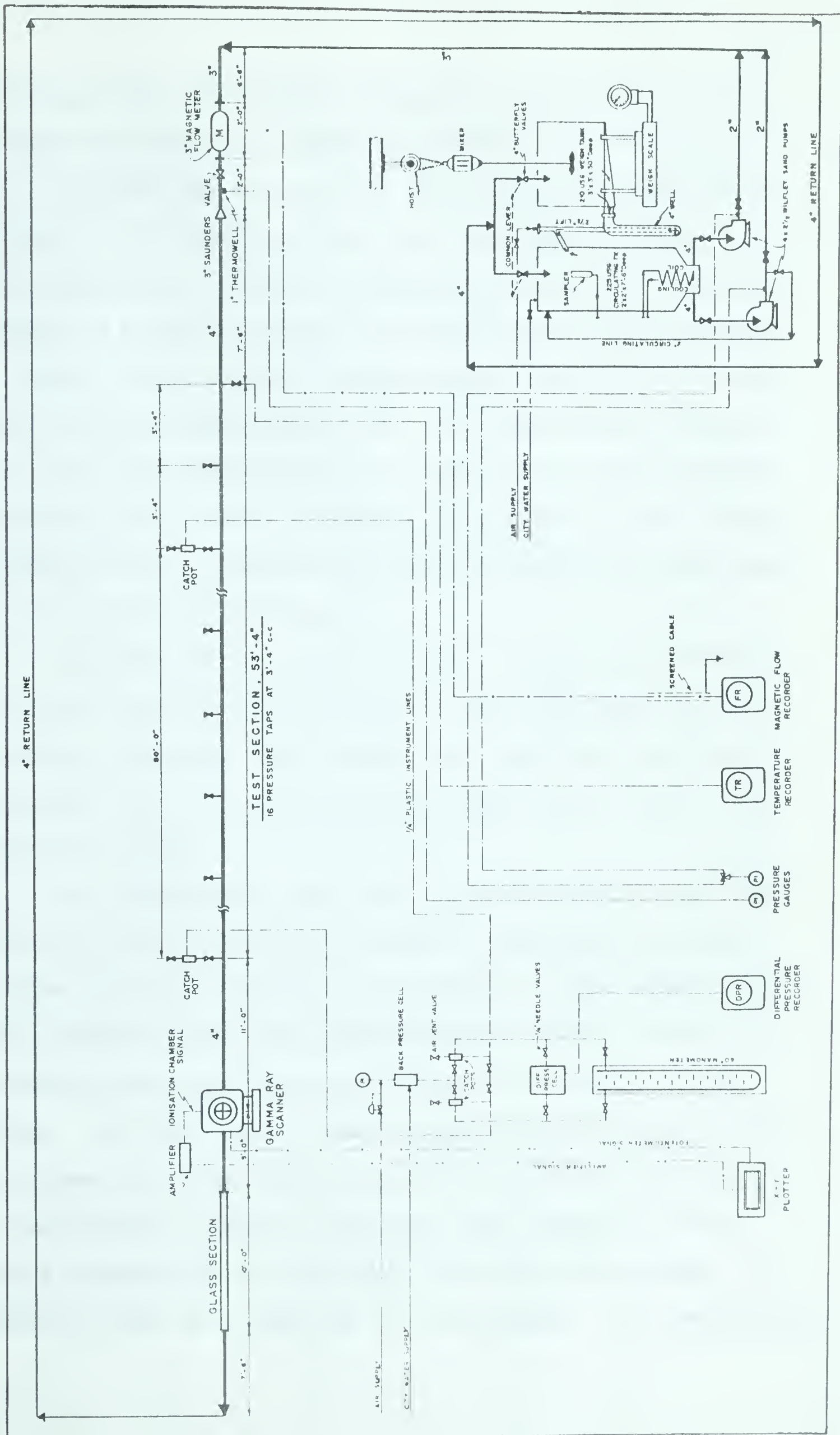
This chapter describes the experimental equipment and discusses calibration of the instruments.

2.1 GENERAL DESCRIPTION OF FOUR INCH TEST PIPE INSTALLATION

A sketch of the experimental apparatus can be seen in FIGURE II-1 entitled "Flow Diagram".

The basic concept of this equipment is to provide a circulating system capable of handling dense slurries of solids in water. The capacity of the existing test unit in the hydraulics laboratory was increased to accommodate a 100 feet long, 4" diameter horizontal test pipe in which the density gradients were measured. A 4" diameter thin walled aluminum test pipe was selected as the smallest size to provide a gamma ray absorption path of sufficient length to give the desired accuracy in the region immediately above the pipe floor.

This unit has a circulating capacity of approximately 450 USGPM and is considered to be a large test unit. Considerable effort has been made to ensure operating stability and adequate control of operating variables as well as minimizing the problems involved in starting the unit up and shutting it down. The magnitude of operating problems are best understood when it is borne in mind that the sand holdup in



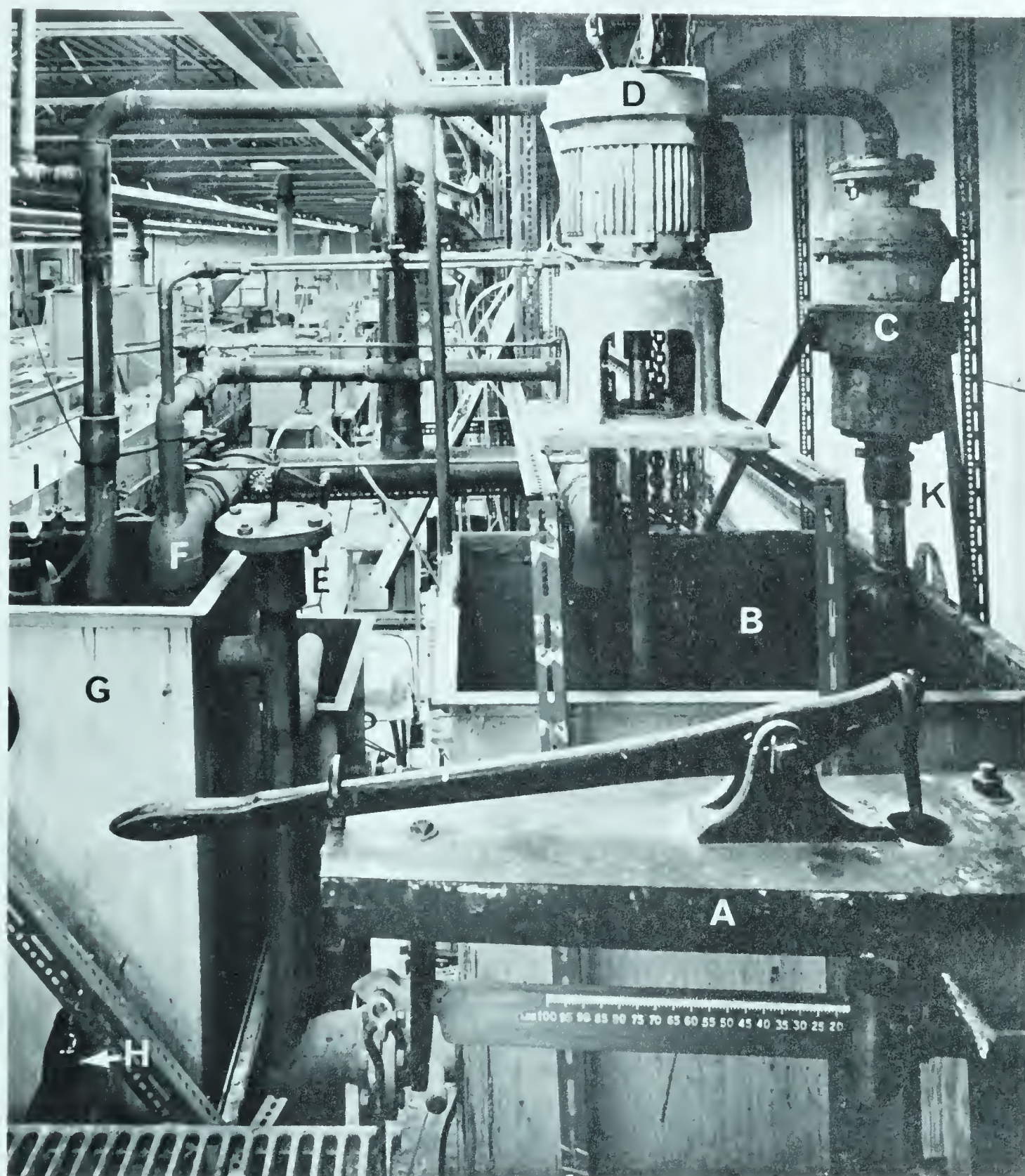
FLOW DIAGRAM
FIGURE IH

circulating tanks and complete plugging of lines at low flow rates must be continually guarded against.

Operability of the unit was greatly improved by installation of a 6" cyclone above the weigh tank. Solids could be separated from the circulating system in a short time and stored as a dense mixture (75 weight % sand) in the weigh tank. These solids could be reintroduced simply by diverting part of the circulating stream into the weigh tank, turning on the mixer and transferring the suspension to the circulating tank via the air lift. The air lift proved to be a simple and reliable way of transferring dense slurries from the weigh tank to the circulating tank.

Another useful feature of this design is that the test line can fairly well be cleared after shut-down by back pressuring it with air thus blowing the fluid back into the circulating tank. All these features enabled the unit to be operated by one man.

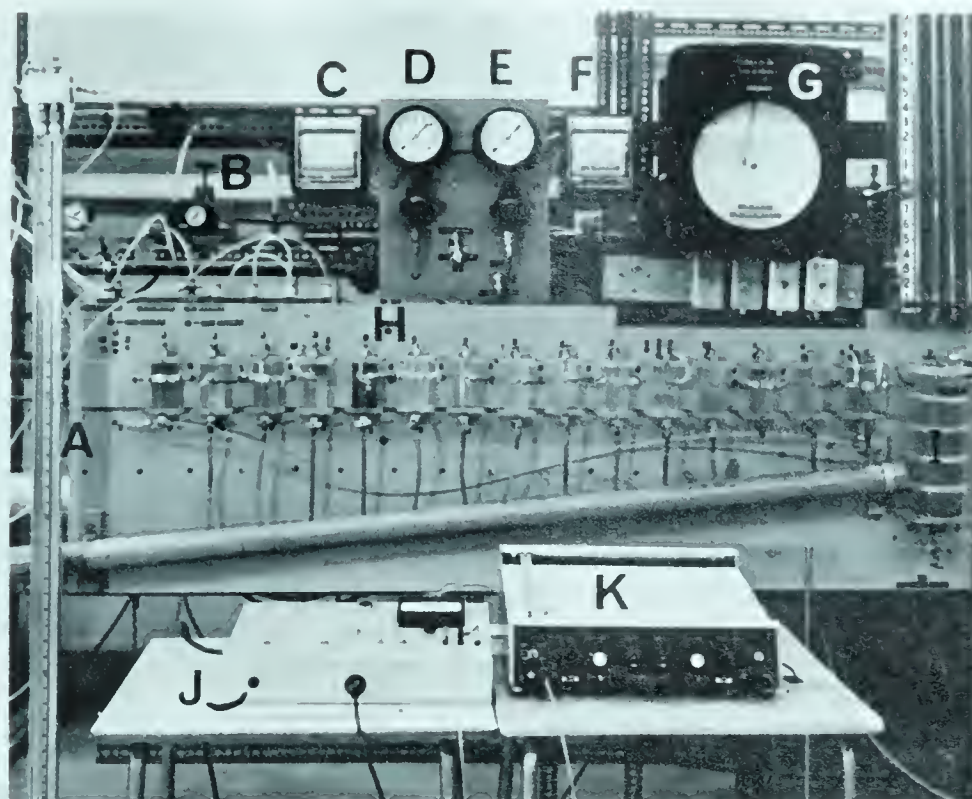
The circulating flow rate is controlled by setting the valve in the circulating line and is measured by a magnetic flow meter and continuously recorded. This unit is not used for absolute flow rate determination but only as an instantaneous and continuous approximate flow guide during operation. The flow rate is determined by deflecting the discharge stream into the weigh tank over a measured time interval. The pressure gradient along the test section is continuously recorded by a differential pressure instrument. A manometer is used as a check on the instrument. The temperature



- | | | | |
|-----|------------------|-----|-------------------|
| [A] | WEIGH BEAM | [G] | CIRCULATING TANK |
| [B] | WEIGH TANK | [H] | SAMPLE BOTTLE |
| [C] | 6 INCH CYCLONE | [I] | SAMPLER HANDLE |
| [D] | MIXER | [K] | CYCLONE UNDERFLOW |
| [E] | AIR LIFT | | |
| [F] | 4 INCH DISCHARGE | | |

VIEW FROM OPERATING PLATFORM

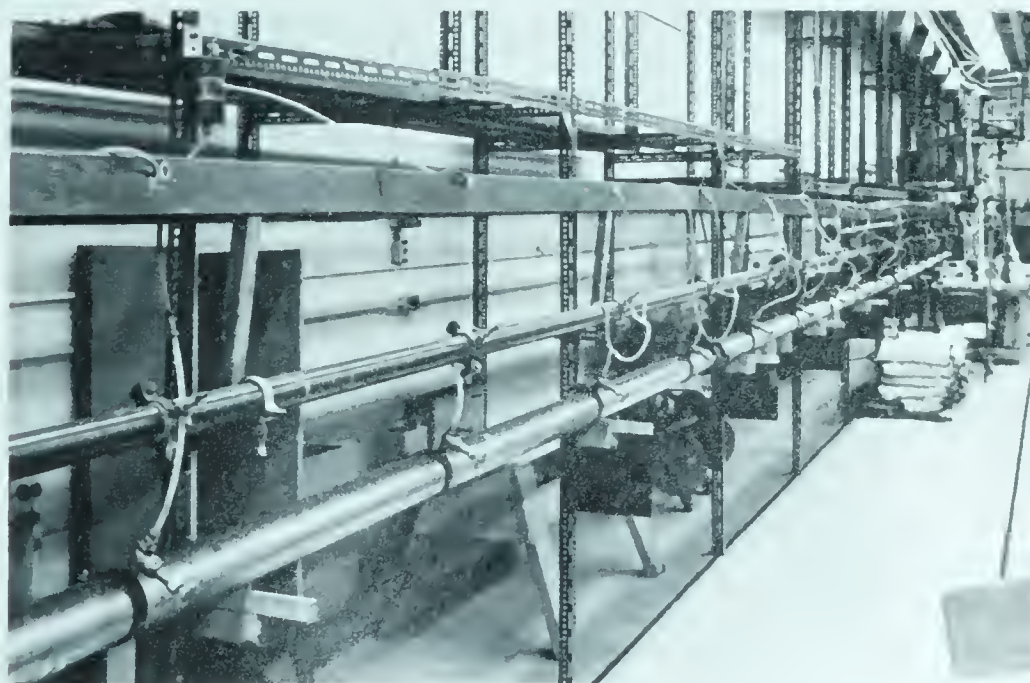
PLATE II-I



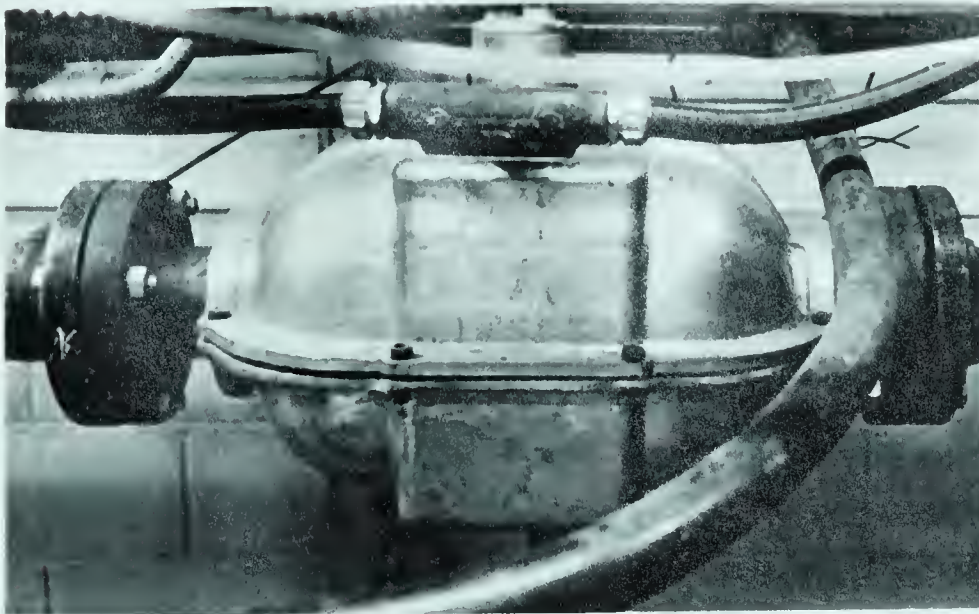
- | | |
|------------------------------------|-------------------------|
| [A] 60 INCH MANOMETER | [G] FLOW RECORDER |
| [B] AIR PRESSURE REGULATOR | [H] BOARD CATCH POTS |
| [C] DIFFERENTIAL PRESSURE RECORDER | [I] RESERVOIR CELL |
| [D] PIPE PRESSURE GAUGE | [J] SCANNER CONTROL BOX |
| [E] PUMP PRESSURE GAUGE | [K] X-Y PLOTTER |
| [F] TEMPERATURE RECORDER | |

INSTRUMENT PANEL

PLATE II - 2

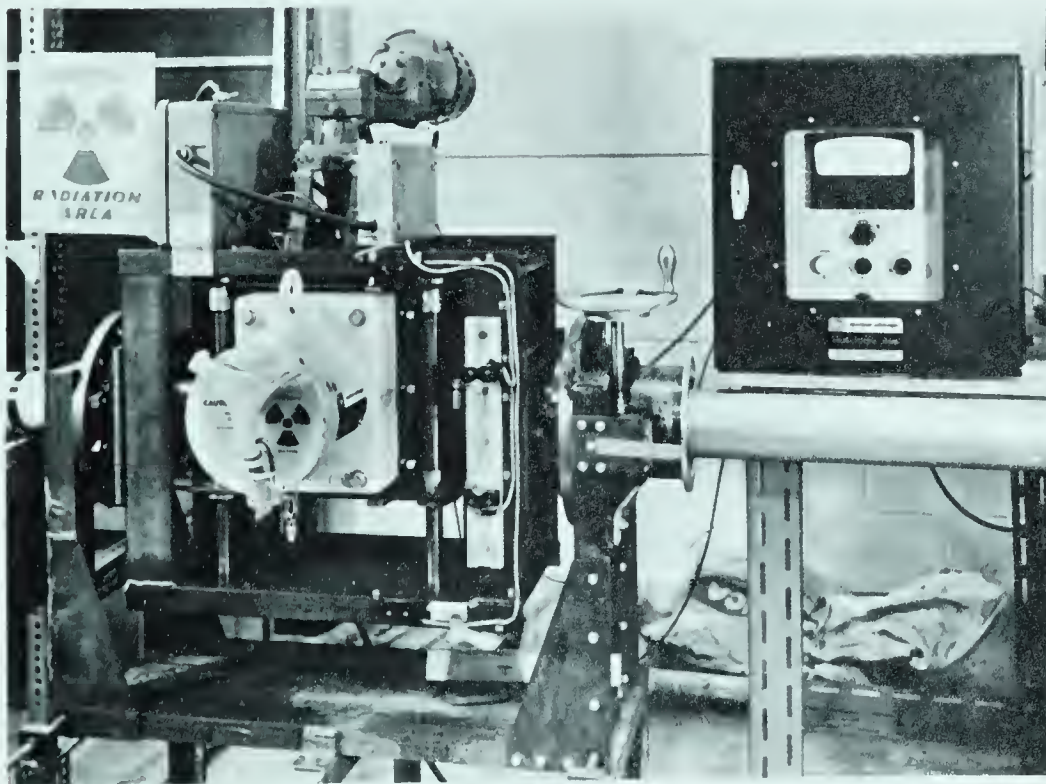


VIEW OF 4 INCH TEST PIPE SHOWING PRESSURE TAPS
AND CATCH POT
PLATE II-3



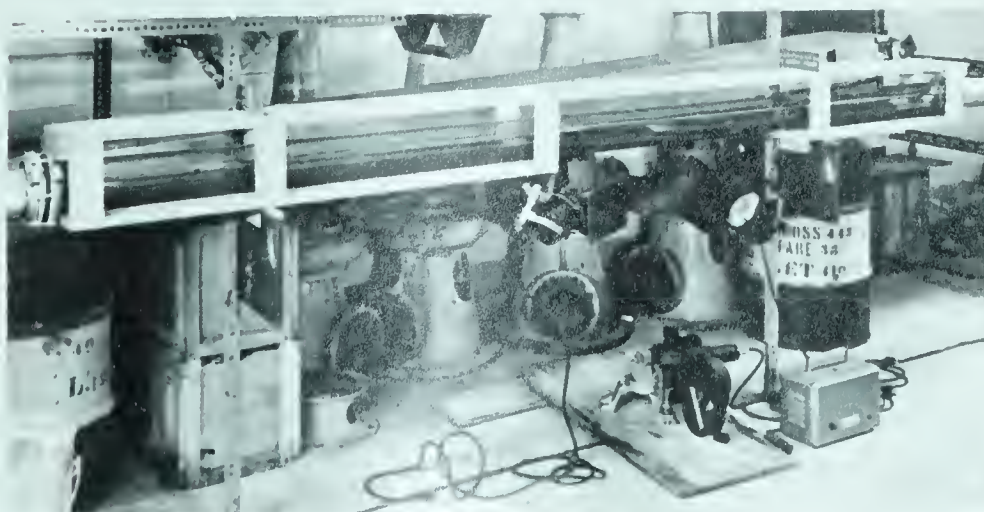
3 INCH MAGNETIC
FLOW TUBE

PLATE II-4



GAMMA RAY
SCANNER

PLATE II-5



GLASS INSPECTION
SECTION

PLATE II-6

at the entrance to the test section is continuously recorded and a cooling coil in the circulating tank maintains the system close to room temperature. An additional dial thermometer indicates the temperature in the circulating tank. The gamma ray instrument scans the vertical and horizontal flow sections and the amplifier signal is recorded on an X-Y plotter together with the signal indicating the scanner position. General details of the installation are shown in PLATES II-1 to 6.

2.2 PUMPS

The two 4" x 2½" Wilfley centrifugal sand pumps are equipped with mechanical seals and driven at 1760 RPM by 15 HP motors. Initially considerable trouble was experienced with air entrainment through these seals but it was found that this problem was associated with worn seal rings. The pumps have a maximum water capacity of 225 USGPM each at a discharge pressure of 40 psi and suction head of 3 to 6 feet. FIGURE II-2 shows details of the air lift pump.

2.3 GENERAL TANKS, PIPING AND VALVES

Dimensions of the weigh tank and circulating tank are given in FIGURE II-1. PLATE II-1 shows the top view of these together with the cyclone, mixer, weigh beam, air lift and discharge piping. The tanks are of rectangular steel construction and are described by Ansley (1963) and Howard (1962). The height of the circulating tank was increased when it was found that free fall of the discharge stream

contributed to air entrainment. In the final layout the circulating tank was operated at a level of 5 feet from the bottom with only the 2 feet of free fall required for the sampling device. The circulating tank also contains a 1" copper cooling coil 12" in diameter and containing 8 turns. The city water supply entering this coil at 50 to 60° F removed sufficient heat to maintain the fluid temperature within 5° F during a test run. Without this cooling the fluid temperature would rise to 100° F within a one to two hour period. All the pump suction and discharge piping including the flow meter pipe is schedule 40 steel pipe with flanged and welded fittings. The cyclone mounted on the weigh tank is connected with a removable 2" neoprene hose so as not to interfere with weighing accuracy.

The weigh tank is mounted on a 5000 lb Fairbanks - Morse scale measuring to one half pound increments. The scale and weights were checked and calibrated by the manufacturer at frequent intervals during the testing period.

A 3/4 HP, 440 RPM Lightning Mixer with one 6" diameter propeller was suspended from a hoist above the weigh tank and could be lowered onto a supporting framework after each weighing.

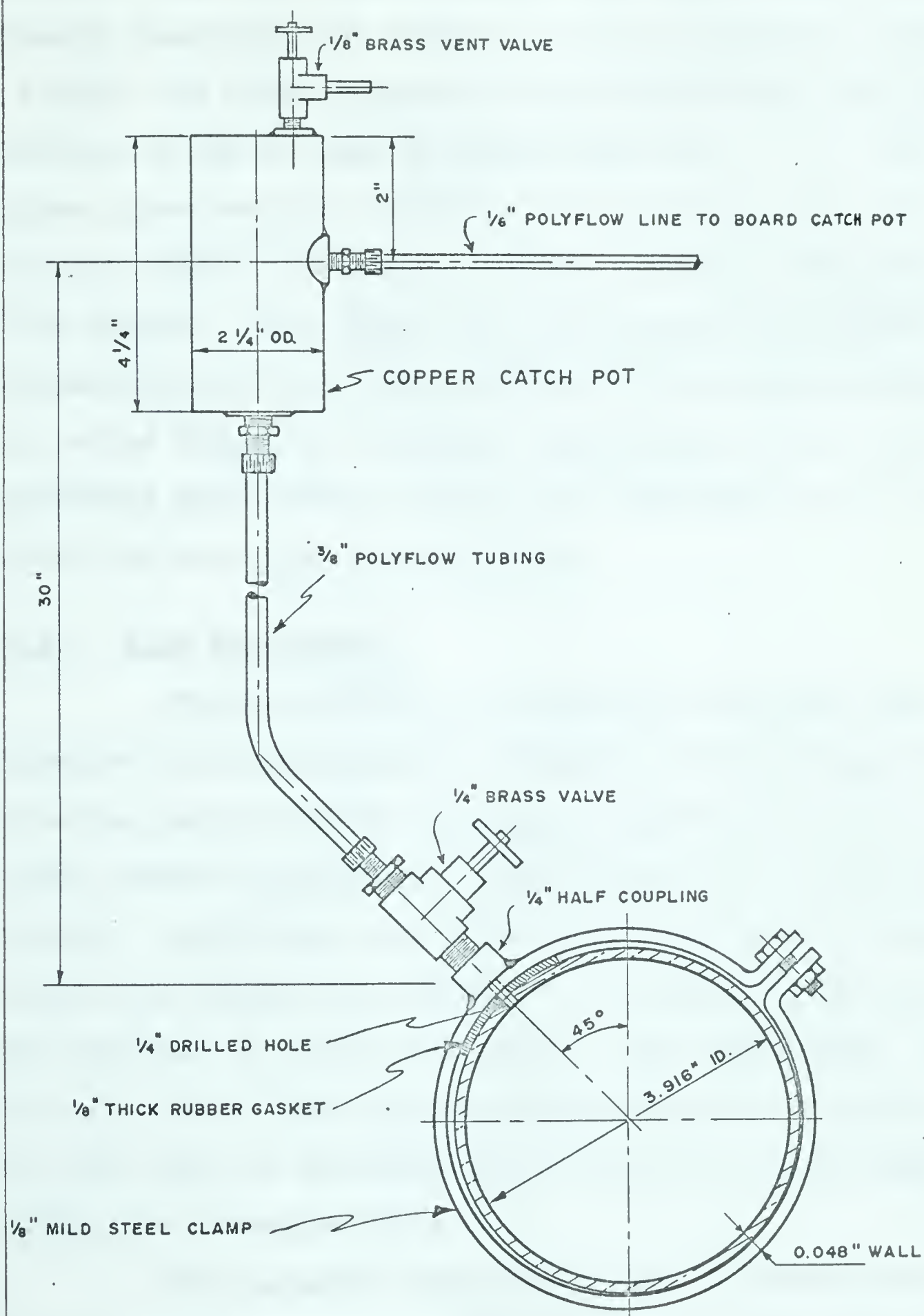
Four types of valves were used. Pump suction and discharge were steel plug valves with grease ports in the plug. The circulating line contained a neoprene rubber pinch valve. A 3" "Saunders" neoprene diaphragm is located at the entrance to the test section. At low flow rates this valve was used

to throttle the flow. Two 4" butterfly valves with neoprene O-rings and actuated by a common lever arm enabled instantaneous deflection of the discharge stream into either the weigh tank or circulating tank.

2.2.4 FOUR INCH TEST PIPE

The 100 feet of aluminum test pipe has an average internal diameter of 3.916", a wall thickness of 0.048" and is mounted on wooden brackets supported from the dexion frame work. (See PLATE II-3). There was some concern that these brackets were not rigid enough but frequent checks with a precision level showed no sagging at all. The return line consists of a 4" plastic pipe. The pipe internal diameter was checked at several locations after about 40 hours of operation. Although pipe wear was apparent from discoloration of the fluid after several hours of operation no change in average pipe diameter could be detected. Fresh water was used each day to prevent accumulation of erosion products in the system. The magnetic flow tube is located in a section of steel pipe 2 feet upstream of the 4" test pipe. (See PLATE II-4).

The test section is comprised of three test sections joined with "dresser" couplings. Care was taken to accurately match the joining ends so as to give a smooth transition. Sixteen piezometer orifices equally spaced at 40" intervals are located 6 feet downstream of the 3" throttle valve. It was originally intended to measure the pressure gradient over



DETAIL OF PRESSURE TAP

FIGURE II-3

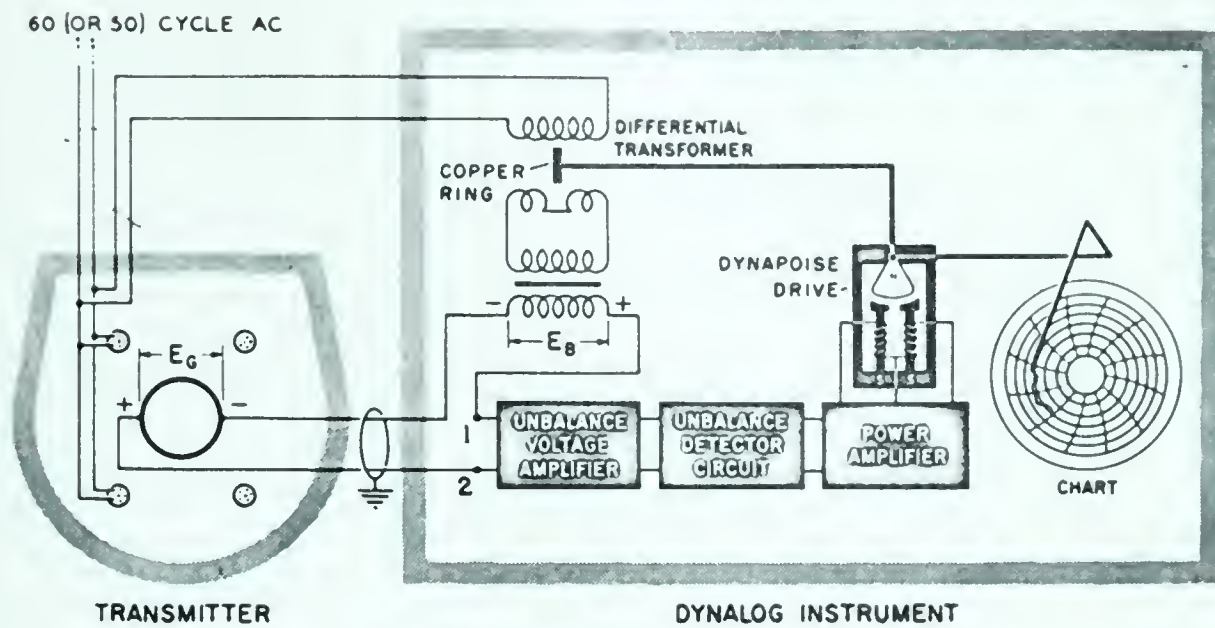
all or several of these locations. This was done during the initial tests but later readings were taken only over a 600" length comprising the second and last piezometer orifices.

FIGURE II-3 shows details of the pressure taps and tubing leading to the air and sediment catch pots. A 10 feet long pyrex glass section located at the far end of the test line enabled visual observation and photography of the different flow phases. (See PLATE II-6). The gamma ray scanning instrument is located 5 feet upstream of the glass section and is bolted firmly to the floor. (See PLATE II-5). A 15 feet removable pipe section enabled the instrument to be located after the test pipe was installed.

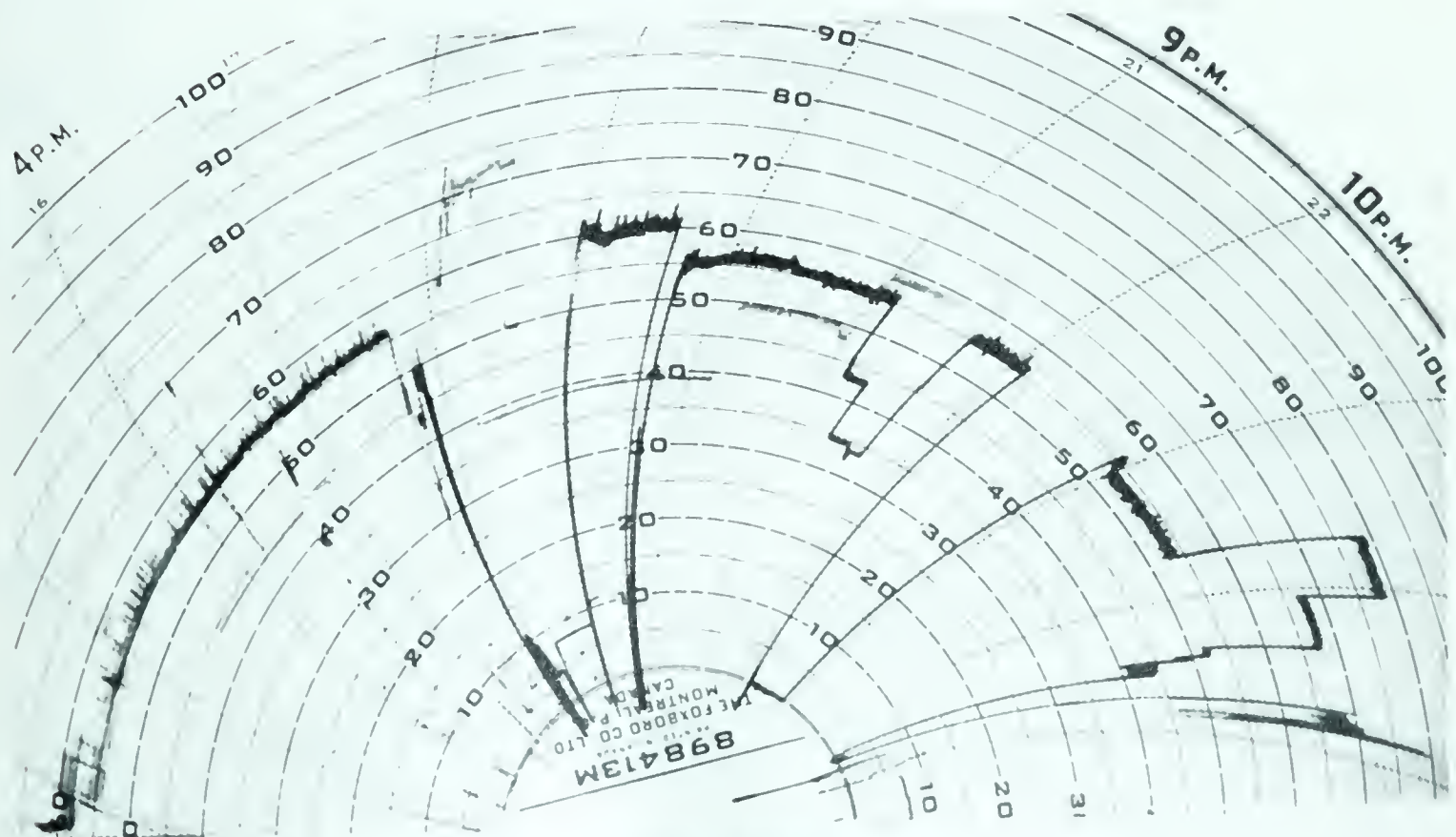
2.2.5 FLOW MEASUREMENT

The flow rates for water-solid mixtures were determined by instantaneously diverting the discharge stream into the weigh tank for usually a minimum period of 10 seconds, thereby accumulating approximately 100 to 600 lbs of slurry. An electric stop watch measuring to the nearest tenth of a second and mounted at the common valve arm enabled the operator to obtain an accurate time measurement. The 2 to 3 ft drop of level in the circulating tank did not affect the flow rate as indicated by a steady flow meter reading during the diversion time.

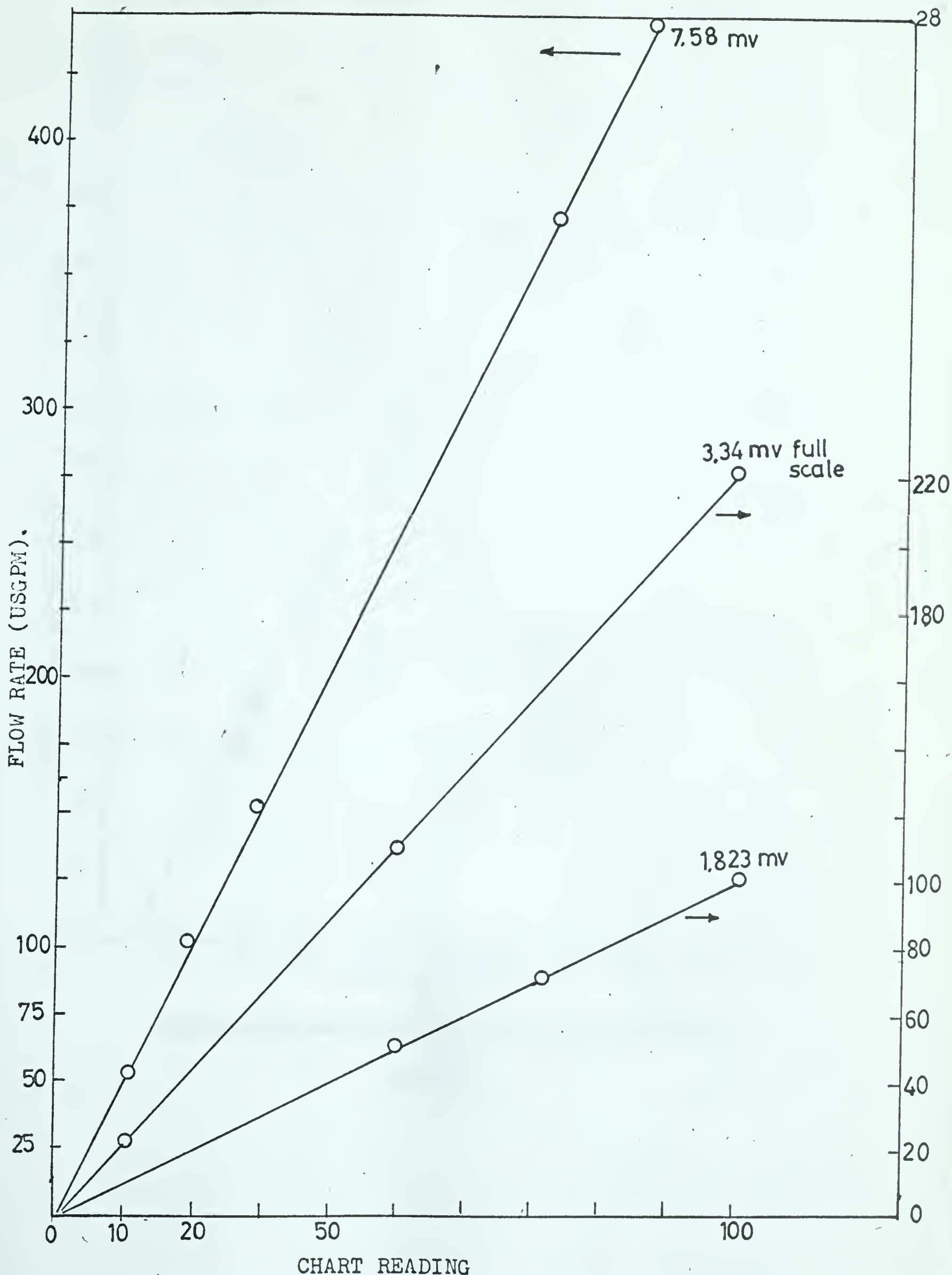
The magnetic flow meters were calibrated and found to be reliable with clear water but calibration with different water-solid concentrations indicated that they would not be



SIMPLIFIED CIRCUIT OF MAGNETIC FLOW METER
FIGURE II-4

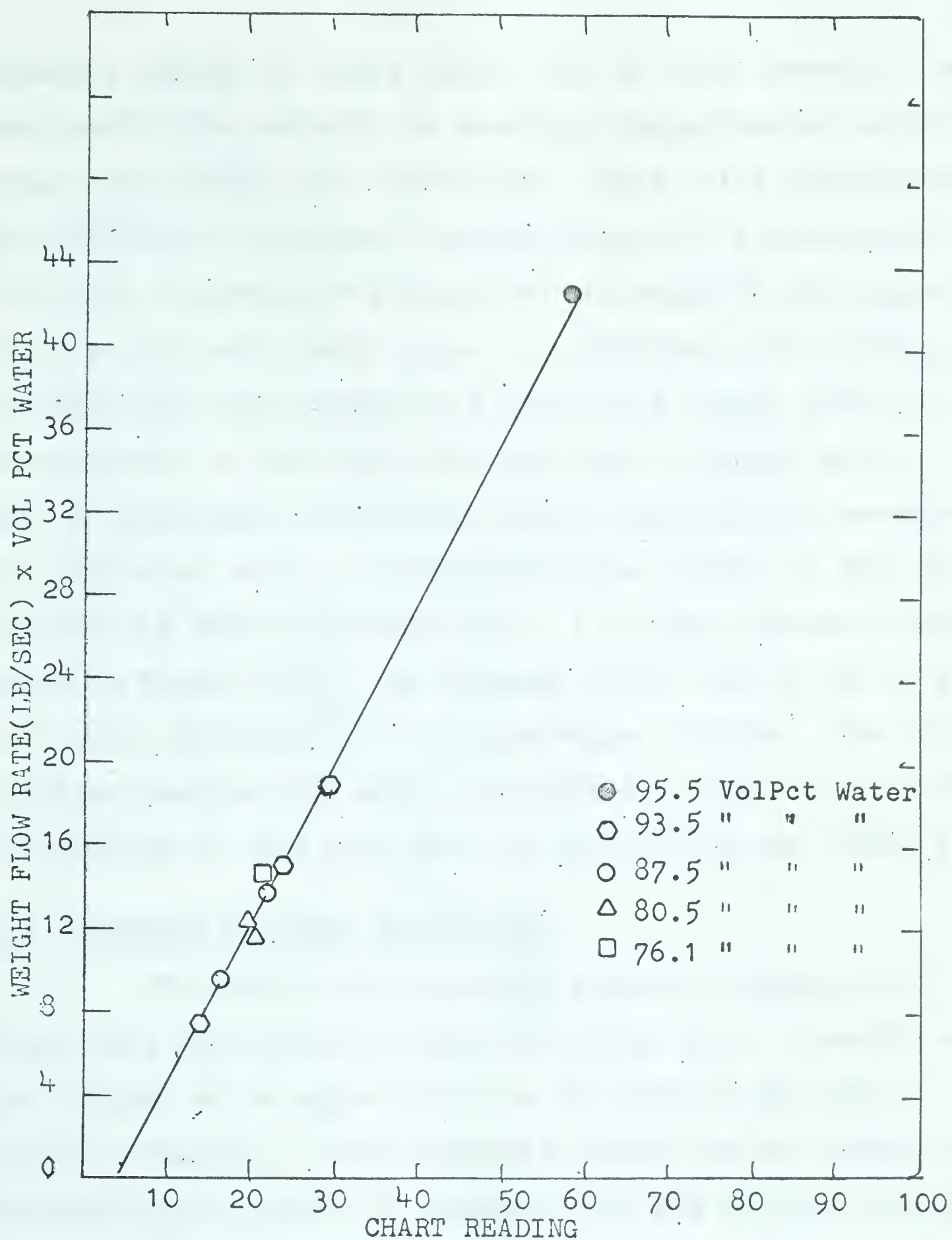


MAGNETIC FLOW RECORDER CHART
FIGURE II-5



WATER CALIBRATION CHART OF FLOW METER

FIGURE II-6



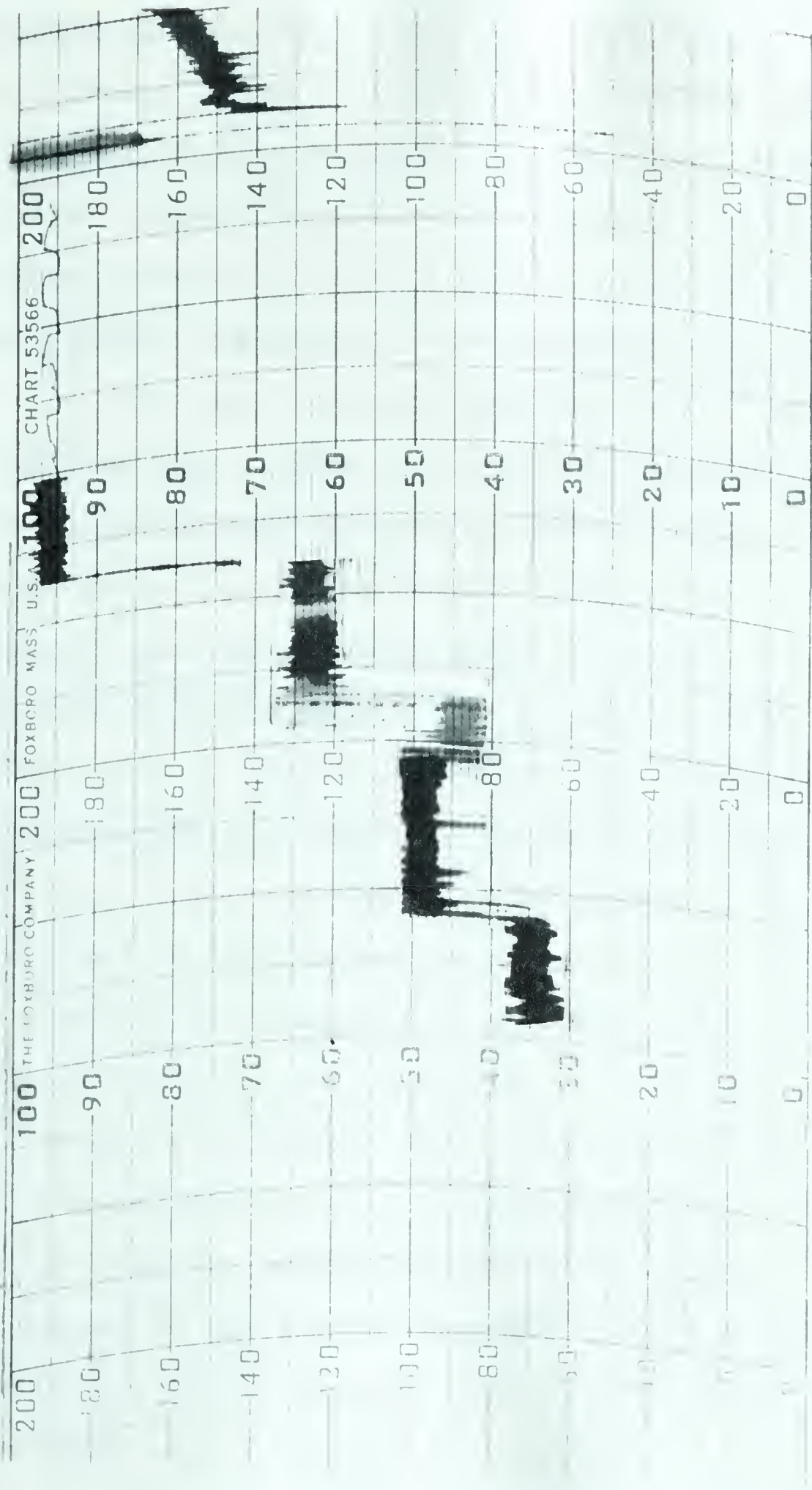
SAND-WATER MIXTURE FLOW METER CALIBRATION.
CHART

FIGURE II-7

accurate enough for these tests. The 3" meter proved to be most useful and reliable in providing instantaneous relative flow rates during test conditions. These units manufactured by the Foxboro Instrument Company consist of a non-magnetic flow tube (neoprene or fiberglass) subjected to the magnetic field of 110 volt field coils. A conducting fluid passing through this field generates a milli-volt signal which is proportional to the fluid flow rate and is picked up by a pair of electrodes in the pipe wall, amplified and recorded in a "Dynalog" unit. A simplified flow circuit of this instrument is shown in FIGURE II-4. A typical recorder chart is shown in FIGURE II-5. The Dynalog circuit can be set to give full scale deflection over a wide range of flows. The calibration results with water and water-sand mixtures are given in APPENDIX B-1 and also shown in FIGURE II-6 and FIGURE II-7.

2.6 PRESSURE GRADIENT MEASUREMENT

The bulk of the pressure gradient readings were taken with the system as shown in FIGURE II-1. Pressure taps are mounted at an angle of 45° to the side of the pipe to minimize plugging. Each clamp was secured on the outside of the pipe after which a $\frac{1}{4}$ " diameter hole was drilled through the packing and pipe wall, taking care not to leave burrs on the inner wall. A sediment and air catch pot is mounted above each pressure tap with the interconnecting $\frac{3}{8}$ " plastic tubing as straight as possible between the two locations. All catch pots were levelled with a precision level. The pressure tubes



DIFFERENTIAL PRESSURE RECORDER CHART

FIGURE II-8

from the two pots are connected to similar pots on the instrument board. These pots are independently connected to a 0-200" water Honeywell differential pressure cell (DP - Cell), a 60" glass U-tube manometer and to a back pressure cell which provides fluorescien-dyed water to the pressure taps. A line between the two catch pots permits the pressures to be equalized and the instrument to be checked at zero differential.

The DP - cell is supplied with 15 psi instrument air and can be set to give a 3 to 15 psi output signal for differential pressures from 20" to 200" of water. This output signal is recorded on a 4" wide strip chart. A typical undampened recorder chart is shown in FIGURE II-8. This instrument gave reliable results in the high pressure drop ranges (50" to 100" of water) but proved to be unreliable for the low differential pressures frequently encountered over the 600" test section at the low flow rates. Although the unit is claimed to be accurate in the 0" to 20" water range it was not specifically designed to operate in this range and frequent calibrations were required. It is also quite possible that better performance would have resulted if the unit had been relocated half way between the pressure taps with high and low pressure connections of equal length. More reliance was placed in the simpler manometer which was used with water over Carbon Tetrachloride ($SG = 1.595$) in the low ranges and with water over Bromoform ($SG = 2.872$).

Instantaneous differential pressure readings in fluidized solids flow are subject to fluctuations especially

in the high solids concentration region. Very little has been said about this in literature and it is generally accepted that an average-steady state condition prevails. This approach appears reasonable when it is considered that any one condition can be maintained for long periods at a time and this condition can also constantly be reproduced. Good average differential pressure readings were obtained by closing down on the needle valves on the manometer tubes. Each set of readings was preceded by back-flushing the pressure taps and testing the air bleed valves on the catch pots to remove any accumulated air.

2.7 TEMPERATURE MEASUREMENT

A 1" thermometer well located immediately downstream of the magnetic flow meter and protruding into the pipe contains a gas-filled bulb which is the sensing element of a "Foxboro" Temperature Transmitter. This unit transmits a 3 to 15 psi signal to a recording instrument with a 4" chart reading from 0 to 250° F. This provided a continuous temperature record during the test runs. Another gas-filled bulb dial thermometer is located in the circulating tank and was used as a check on the recorded temperature. No discrepancy was ever observed between the two instruments. The cooling coil heat exchange capacity was somewhat marginal and a rise of approximately 5° F occurred during test runs. This was not considered too serious since the fluid properties were taken at the actual test temperature.

2.8 CONCENTRATION GRADIENT MEASUREMENT

Daniel (1963) discusses the various techniques for concentration gradient measurement. These are briefly summarized below.

Danel (1939), Howard (1939), Vanoni (1946), Ismail (1952) and others have made concentration gradient measurement by withdrawing samples from the flow sections. This method has the serious drawback of disturbing the flow pattern by insertion of a sampling probe and results of such studies will therefore always be suspect. Durand (1951) and Halbronne (1951) measured concentration gradients by an electrical conductivity technique. Calibration difficulties appeared to have been formidable, probably because of the sensitivity of the reading to changes of the electrode surfaces. Shook (1960) used a flow splitting device at the discharge end of a channel but found it to have rather poor accuracy. Daniel and Shook (1963) have been using a narrowly collimated beam of gamma rays to determine the vertical concentration gradient in a horizontal rectangular flow section.

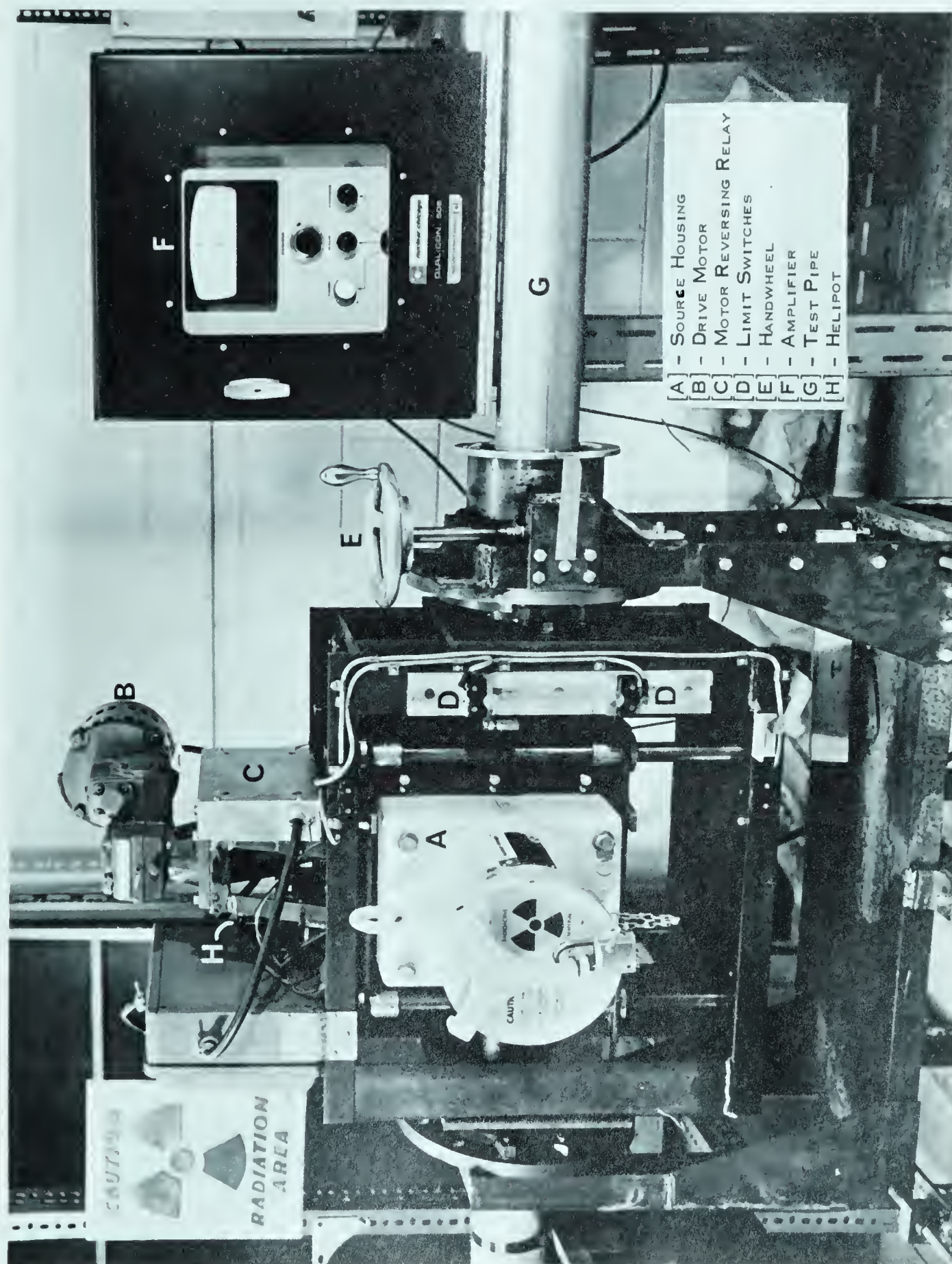
This method has the advantage of not causing any flow disturbance but also the disadvantage of giving an average value of energy attenuation along its path. Irregular concentration profiles can therefore not be detected in any one scanning direction, and relating the degree of attenuation to a concentration also requires an accurate knowledge of the path length. These factors become more complicated when dealing with a circular flow section and it was realized that

some accuracy would have to be sacrificed. It still appeared to be the most promising approach since reliable measurement of the average concentration gradient in a vertical plane would constitute a substantial contribution to the present state of knowledge.

2.9 GAMMA-RAY SCANNER: GENERAL DESCRIPTION

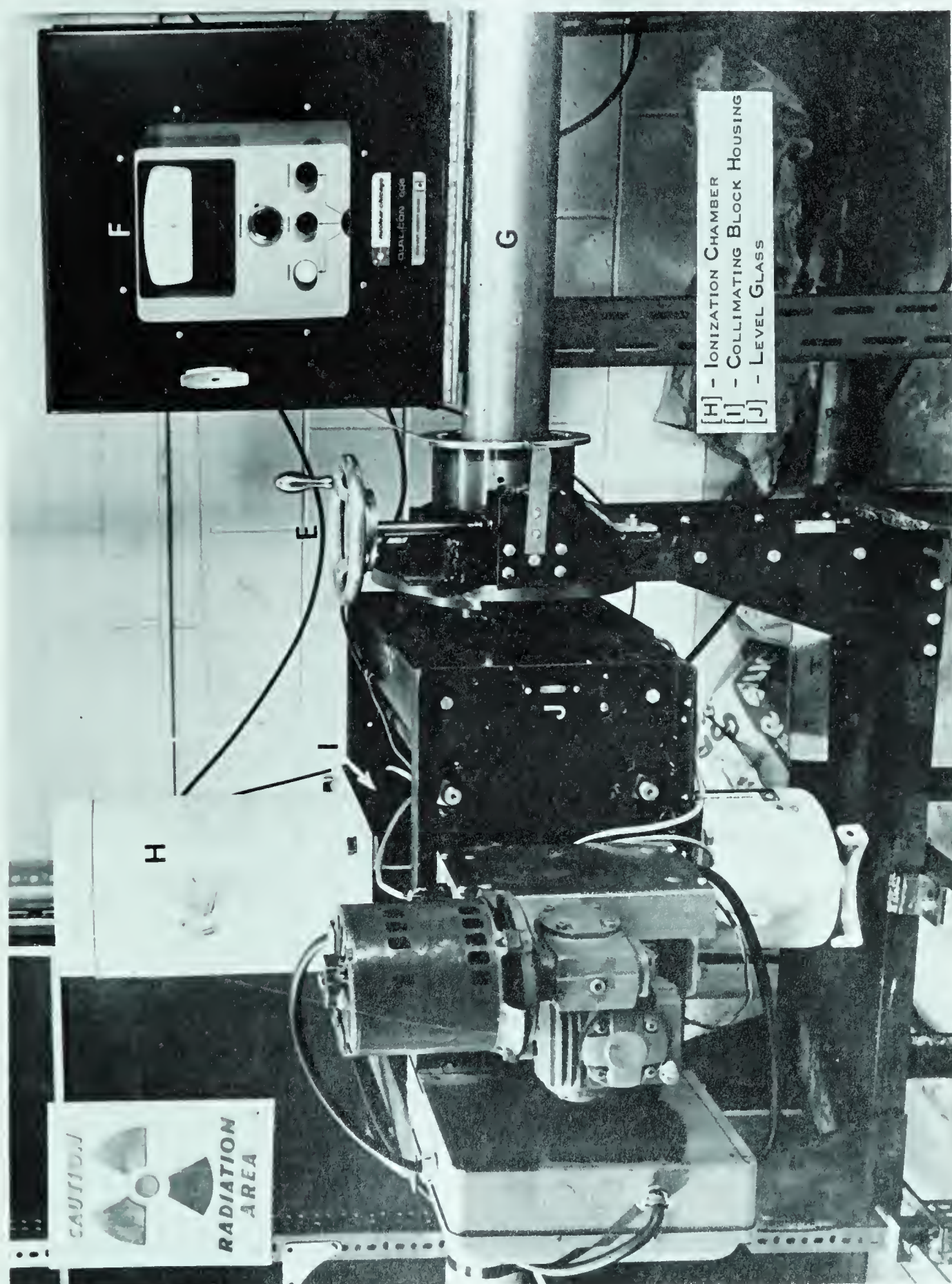
Gamma-ray instruments are used extensively in industry as density gauges and level indicators at fixed locations. The radioactive source is usually Cesium - 137. Gamma-ray intensity is measured either by a scintillation-counter system or by an ionization chamber, both of which emit electrical pulses proportional to the intensity of the incident radiation.

It was originally intended to develop an instrument capable of measuring specific gravities in the range 1.000 to 2.000 ± 0.005 in a minimum path length of 2" and having an overall response time of 1 second, since it was hoped that bed movement rates could be detected and measured by such an instrument. The specifications necessitated using a high intensity Cesium source and involved counting rates exceeding the maximum limit of conventional scintillation-counter systems. The ionization chamber seemed to be a more flexible system and was claimed by the manufacturer to be capable of response times of 1 second if used in combination with a 2 Curie Cesium - 137 source and a modified low-capacitance amplification circuit. It also has the advantage of producing



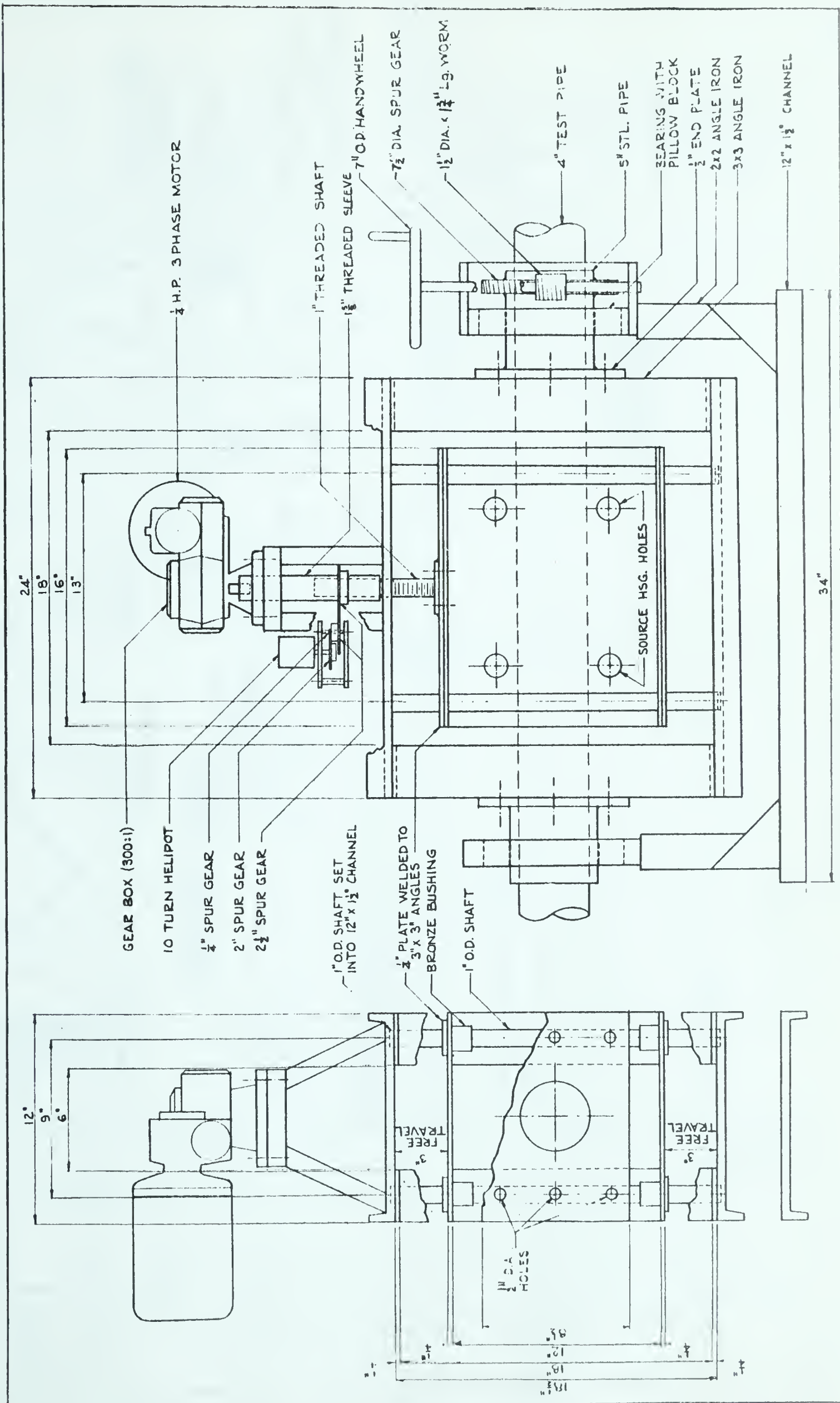
GAMMA-RAY SCANNER - HORIZONTAL BEAM

PLATE II-7

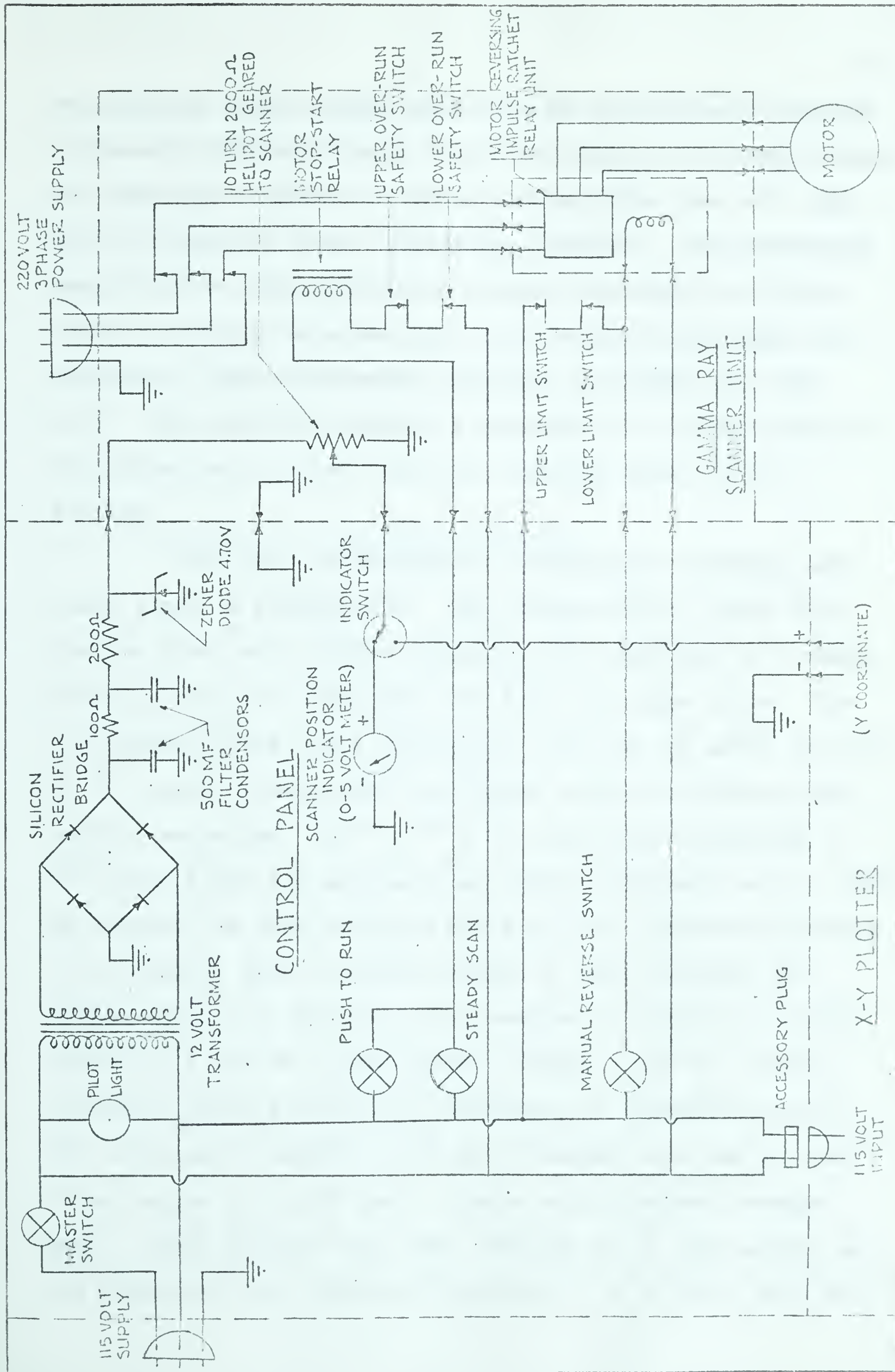


GAMMA-RAY SCANNER - VERTICAL BEAM

PLATE II-8



GAMMA-RAY SCANNER
FIGURE II-9



SCANNER CIRCUIT

FIGURE II-10

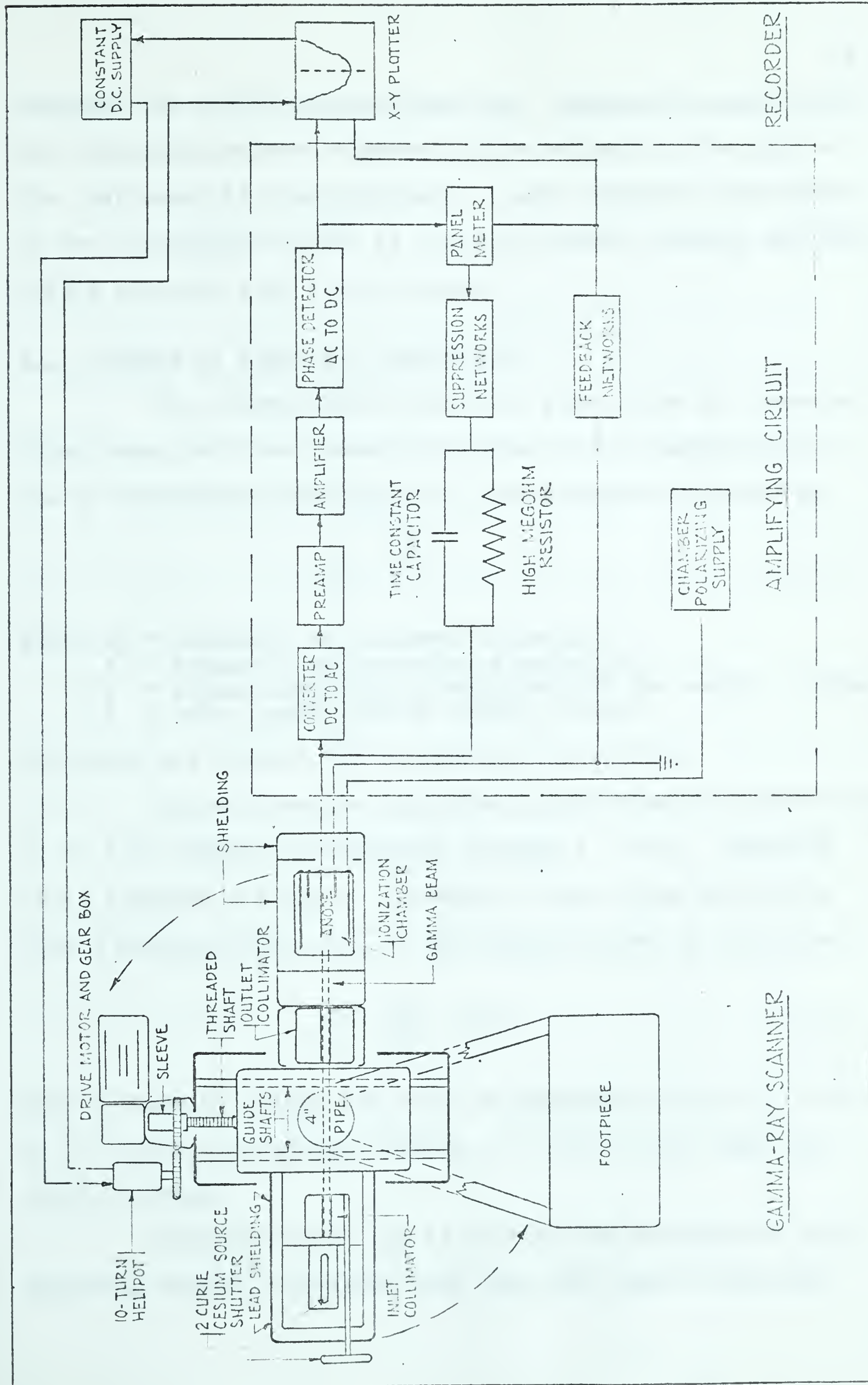
an analogue output signal which can be continuously recorded. A standard Nuclear-Chicago "Qualicon" Model 5060 Density Gauge was modified to house a 2 Curie Cesium Source and a 4" long by 1/4" diameter inlet collimating aperture. This measuring head together with ionization chamber and amplifier (Model 5302) was bought as a package from the Nuclear-Chicago Corporation. These components are shown in PLATES II-7 and II-8. The amplifier signal is recorded at 0.2 Volts/inch or 0.5 Volts/inch on the X-axis of a Moseley Model 2D X-Y Plotter.

The unit is mounted on a mechanical scanning mechanism shown in FIGURE II-9. The Cesium-source, inlet collimating block and shutter mechanism are contained in a single housing which is bolted onto the front carriage plate. The collimating block and a "shut-off" block can be moved in front of the capsule containing the Cesium source by rotating the shutter mechanism. A 4" x 4" x 4" lead block containing a 1/4" hole along its axis acts as outlet collimator and is bolted between the back carriage plate and the ionization chamber. It is rigidly held in place between 4" wide channels by a sulphur-fire clay mixture. The scanner is driven at 0.415"/minute by a 1/4 HP 3 phase motor through a 300 to 1 double reduction gearbox and shaft containing 14 threads per inch. The carriage is mounted on 5" ball bearings and can be set at any angle by a spur gear, pinion and handwheel arrangement. Level glasses allow the carriage to be set exactly in the horizontal and vertical directions. A 10 turn, 2000 ohm

"helipot" driven from the carriage shaft and connected to a constant 4 Volt DC Circuit gives a signal varying linearly with the carriage position and is recorded on the Y-axis of the Moseley X-Y Plotter. Micro-switches set on the supporting structure and connected to a ratchet relay circuit instantly reverses the motor direction when they are tripped at the end of each scan. These circuits are shown in FIGURE II-10. This unit was designed and built in the Hydraulics workshop.

2.10 PRINCIPLE OF INSTRUMENT OPERATION

A simplified block diagram (FIGURE II-11) demonstrates the principle of operation. The ionization current developed in the high pressure ionization chamber is directly proportional to the incident radiation. This current develops a DC voltage across a high meg ohm resistor. (10^9 to 10^{11} ohm). The Qualicon instrument is essentially an extremely high impedance vibrating reed electrometer capable of measuring voltages developed across this high meg ohm resistor. The converter unit produces a sinusoidal voltage from the impressed DC voltage. This AC voltage is amplified and then compared in a phase sensitive detector to a reference voltage. This results in a maximum DC signal of approximately ± 1 volt which is directly proportional to the original voltage developed across the high meg ohm resistor and has sufficient power to drive the panel meter and associated recorder. Inverse DC feedback is applied across the ionization chamber and high meg



QUALICON CIRCUIT

FIGURE II-II

resistor for stability and linearity. Adjustable sensitivity and ionization current suppression for adjusting the span of the instrument is also provided. A more detailed description of the electronic circuit is given in Nuclear Chicago Bulletin 712370 provided with the instrument.

2.11 THEORY OF GAMMA RAY ABSORPTION

The attenuation of parallel gamma-rays in a beam of fixed cross sectional area is governed by the Lambert-Beer's Law of exponential absorption of electromagnetic radiation:

$$\frac{I_0}{I} = e^{kx} \quad (2.1)$$

where I_0 = intensity of incident radiation.

I = intensity of transmitted radiation.

k = linear absorption coefficient of the medium, inches⁻¹.

x = path length through medium, inches.

This does not account for attenuation by scatter.

In our case the radiation intensities are proportional to a DC voltage, fluctuating through ± 1 volt. EQUATION (2.1) requires a range of voltages of equal sign decreasing from a maximum value, E_0 , to the minimum value, E , such that:

$$\frac{I_0}{I} = \frac{E_0}{E} = e^{kx} \quad (2.2)$$

Such a range of values was found by experiment to be 1.7 volts to 3.7 volts and involved adding 2.5 volts to the amplifier output voltage.

EQUATION (2.2) can be written for attenuation in an absorbing medium containing more than one type of material.

Attenuation of a beam passing through a pipe filled with water will be given by:

$$\frac{E_{op}}{E_p} = e^{k_m x_m + k_w x} \quad (2.3)$$

where k_m , k_w = linear absorption coefficients of the metal wall and the water respectively.

and x_m , x = path lengths of beam through the metal and water respectively.

Taking the natural logarithm on both sides results in:

$$\ln\left(\frac{E_{op}}{E_p}\right) = k_m x_m + k_w x \quad (2.4)$$

The preceeding assumes that absorber position has no effect on attenuation. A similar relation can be written for a 2 component sand-water mixture in a pipeline.

$$\ln\left(\frac{E_o}{E}\right) = k_m x_m + k_w x_w + k_s x_s \quad (2.5)$$

where k_s = linear absorption coefficient of sand.

x_s = path length occupied by sand.

x_w = path length occupied by water.

If EQUATIONS (2.4) and (2.5) refer to the same location of the beam, the overall path length between the metal walls will be the same. i.e.

$$x = x_w + x_s \quad (2.6)$$

Also for a narrow beam of fixed cross-sectional area the volume concentration, C_s , of solids in the path of the beam is given by:

$$C_s = \left(\frac{x_s}{x}\right)(100) = \frac{x_s}{x_s + x_w} (100) \quad (2.7)$$

The term $x_m k_m$ can be eliminated from EQUATIONS (2.4) and (2.5) by subtraction. i.e.

$$\begin{aligned} \ln\left(\frac{E_o}{E}\right) - \ln\left(\frac{E_{op}}{E_p}\right) &= k_w x_w + k_s x_s - k_w x \\ &= k_s x_s - k_w (x - x_w) \\ &= k_s x_s - k_w x_s \\ &= x_s (k_s - k_w) \text{ from EQUATION (2.6)} \\ &= x C_s (k_s - k_w) / 100 \text{ from EQUATION (2.7)} \end{aligned}$$

or
$$C_s = 100 \ln\left(\frac{E_o}{E_{op}} \cdot \frac{E_p}{E}\right) / x(k_s - k_w) \quad (2.8)$$

If the signals E_o and E_{op} proportional to the intensity of incident radiation are constant, the equation becomes:

$$C_s = 100 \ln\left(\frac{E_p}{E}\right) / x(k_s - k_w) \quad (2.9)$$

E_o , E_{op} , E_p , and E are quantities measured by the gamma-ray instrument. x can be calculated from the average pipe radius, R , and the distance from the pipe center, y :

$$x = 2(R^2 - y^2)^{0.5} \quad (2.10)$$

When y is measured as a chart distance a correction factor, F , has to be applied to convert it to a true carriage displacement. i.e.

$$x = 2(R^2 - F^2 \cdot y^2)^{0.5} \quad (2.10.1)$$

k_s and k_w are determined by calibration and by application of EQUATION (2.2). EQUATION (2.9) can therefore be solved for C_s as the unknown.

2.2.12 CALIBRATION OF GAMMA-RAY INSTRUMENT

EQUATION (2.2) was verified experimentally using

first water and then sand as the absorption material. The values of the linear absorption coefficients k_w and k_s for sand and water were obtained from these experiments. The value of k_w was then checked independently by scanning first the empty pipe to obtain values of $x_m k_m$ from the equation;

$$\ln\left(\frac{E_{om}}{E_m}\right) = x_m k_m \quad (2.2.1)$$

and then the pipe filled with water.

EQUATION (2.4) - (2.2.1) solved for k_w results in:

$$k_w = \ln\left(\frac{E_{op}}{E_p} \cdot \frac{E_m}{E_{om}}\right) / x \quad (2.11)$$

Calculation of x from EQUATION (2.10) at different displacements from the pipe centerline permits calculation of k_w at the corresponding points.

Values of k_w were calculated at 23 points in the horizontal scan direction and at 23 points in the vertical scan direction. APPENDIX B-3 describes the calibration procedure and lists the attenuation values in sand and water. FIGURES II-12 and II-13 show these results plotted as $\ln \frac{E_o}{E}$ vs. x_w and x_s with average values of $x_w = 0.166/\text{inch}$ and $x_s = 0.433/\text{inch}$. The maximum deviation from the average line in FIGURE II-12 occurs at the high and low x -values indicating deviation from EQUATION (2.2) outside this range. FIGURE II-13 does not show this trend but has more scatter probably due to uneven compacting and levelling of the dry sand in the test cylinder.

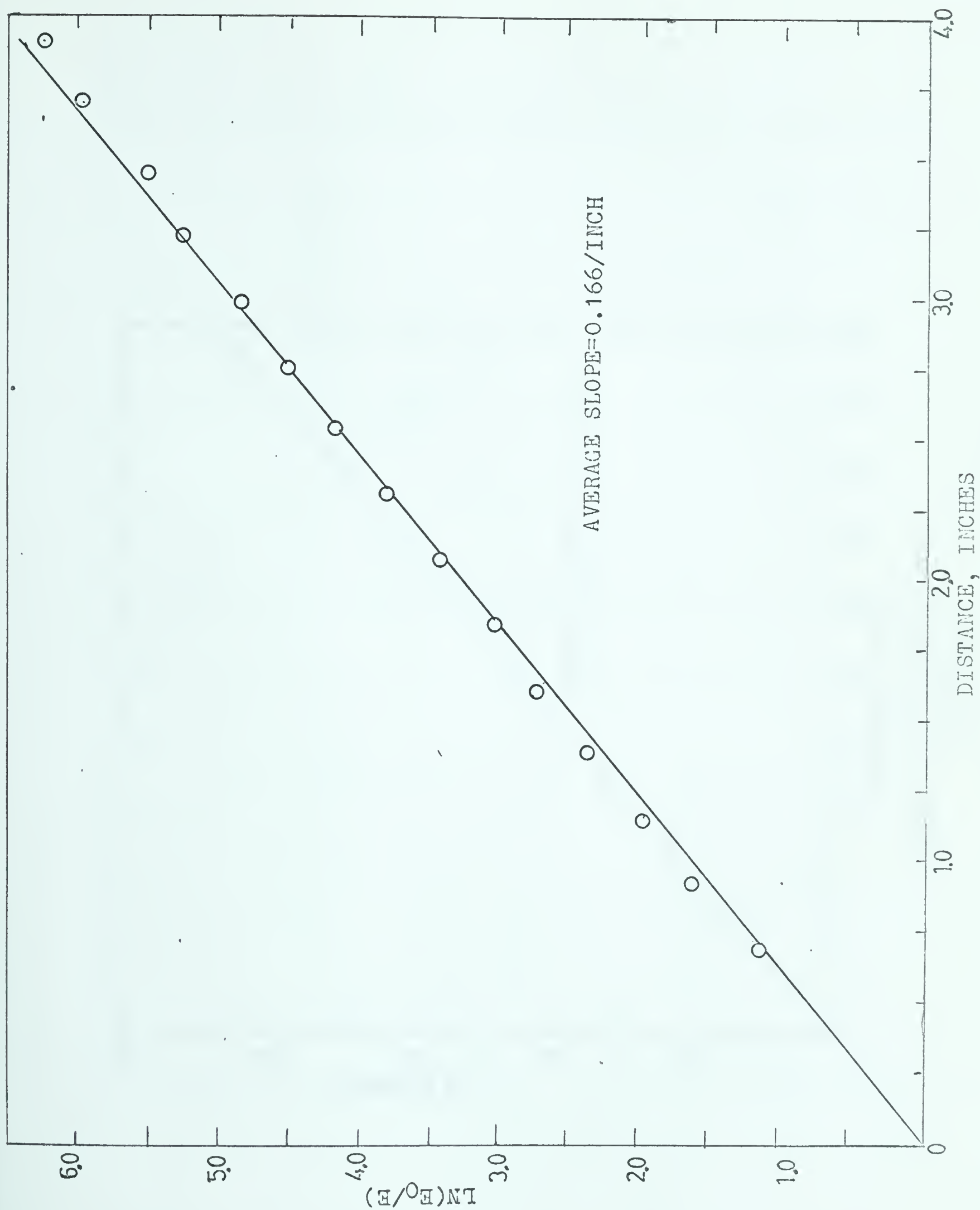
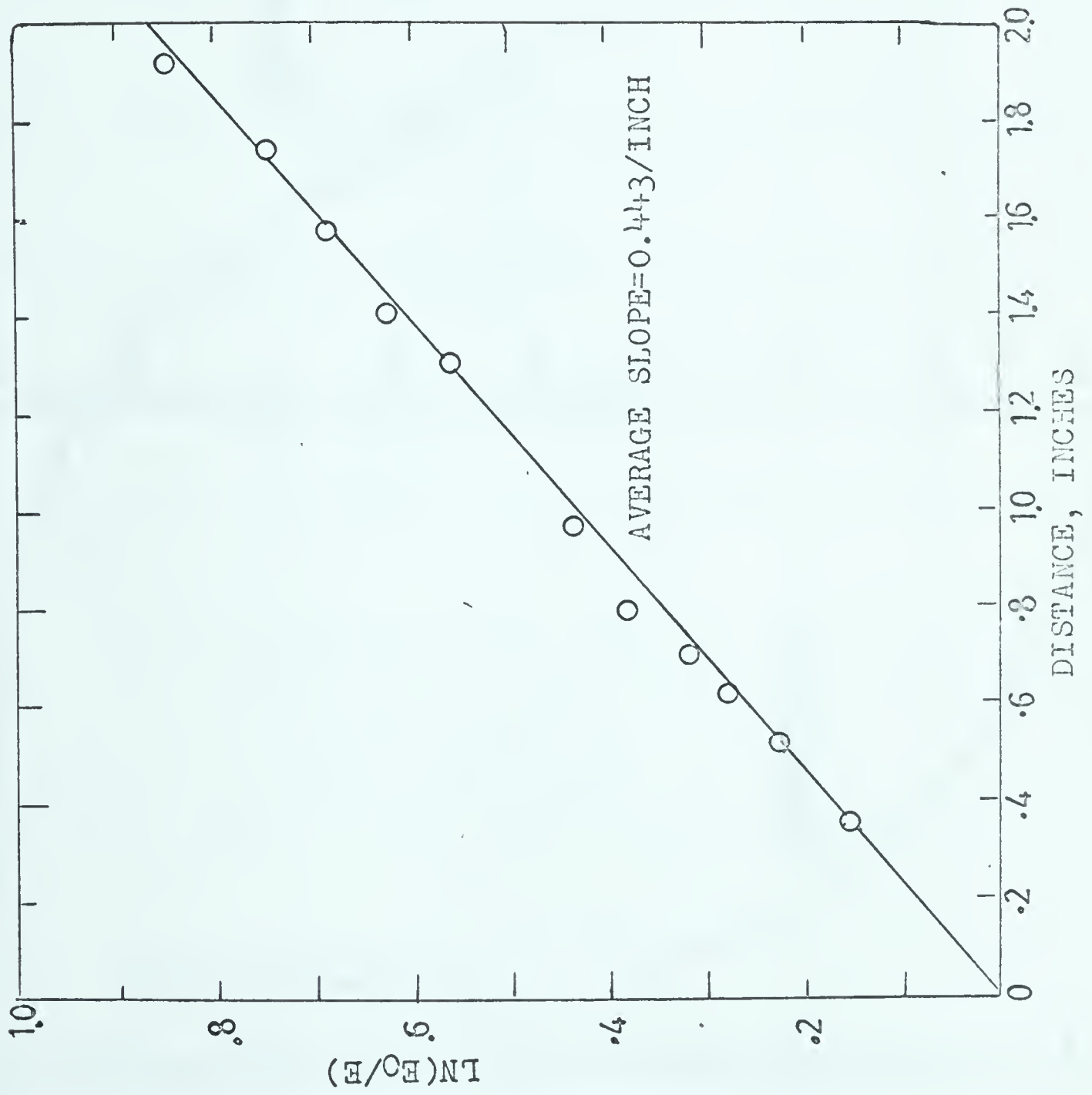


FIGURE 11-12



GAMMA ATTENUATION IN SAND

FIGURE II-13

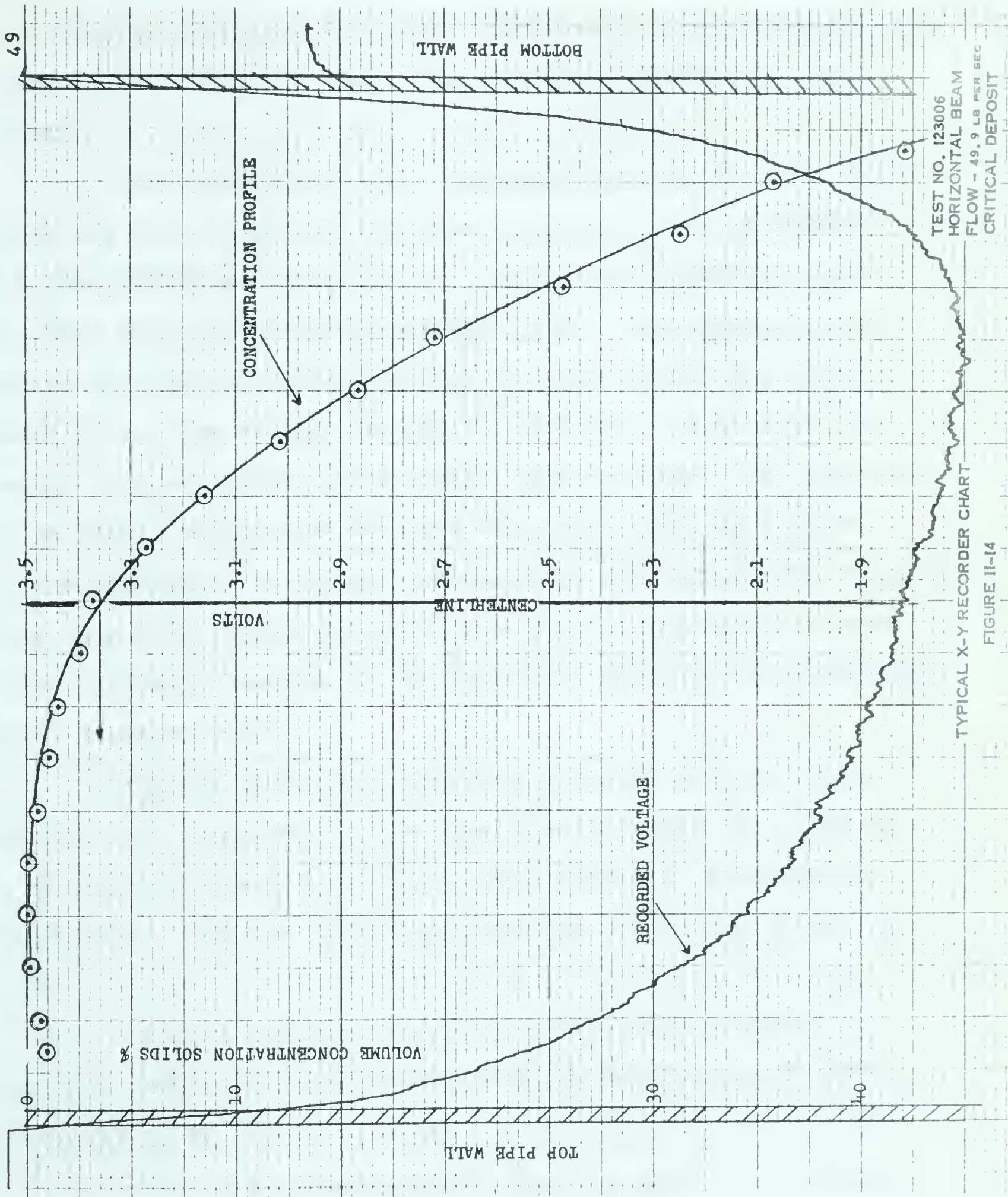


FIGURE II-14

Effects of particle size and location in the beam have been investigated by Daniel (1963) and it was shown to have a negligible effect on the values of linear absorption coefficient.

The results of the 7 scanning tests of the pipe with water and the 5 tests of the pipe wall are listed in APPENDIX B-3, and TABLES B-3.3 to B-3.9. Typical X-Y recorder charts of these tests are shown in FIGURE II-14. The average k_w values at the various distances from the pipe center are given in TABLE II-1. The values for the 17 locations $\pm 1.6"$ from the center line and having path lengths greater than 2.20" appeared to be fairly consistent and were averaged, yielding a value $k_w = 0.165/\text{inch}$. k_w values for the 8 points having path lengths less than 2.22 inches differed considerably from this average value, probably because of the increased angle of the pipe wall with the gamma-beam.

The k_w value of 0.166/inch obtained by direct calibration was considered to be more accurate than the value of 0.165 which was derived from a larger number of experimental quantities. The two values nevertheless still only differ by 0.7%.

Solids concentrations at the 17 points closest to the pipe center were calculated from the EQUATION (2.8) after substitution of the value of $k_s - k_w = 0.433 - 0.166 = 0.267$.

$$\text{i.e. } C_s = 100 \ln\left(\frac{E_o}{E_{op}} \cdot \frac{E_p}{E}\right) / 0.267x \quad \dots (2.12)$$

Linear absorption coefficients for sand and water are

approximately related by:

$$\frac{k_S}{k_W} \approx \frac{\rho_S}{\rho_W} = \frac{2.64}{1.0} \dots \dots \dots (2.13)$$

The actual experimental ratio was:

$$\frac{k_S}{k_W} = \frac{0.433}{0.166} = 2.61 \dots \dots \dots (2.14)$$

In the absence of a reliable technique of determining the value of k_S in this section of the pipe, the equation;

$$k_S - k_W = 2.61 k_W - k_W = 1.61 k_W \dots (2.15)$$

was used.

The solids concentration could then be calculated from EQUATION (2.8) with the appropriate value of k_W taken from TABLE II-1. i.e.

$$C_S = 100 \ln\left(\frac{E_o}{E_{op}} \cdot \frac{E_p}{E}\right) / 1.61 k_W x \dots (2.16)$$

2.13 RANDOM VARIATION OF GAMMA-RAY OUTPUT SIGNAL; RESPONSE TIME AND SCANNING SPEED

The random emission rate of the radio-active source necessitates that the average value of the recorded signal be taken over a certain time period. A time recording of the signal was made at 1.5 inches/minute at an increased recorder sensitivity (50 mv/inch). Point values were taken from this graph and the standard deviation calculated for consecutive 20 second intervals for a total elapsed time of 2 minutes. None of the averages differed from the 2 minute average by more than 0.33%. The maximum standard deviation in any one 20 second interval was 0.31%. The scanning speed had to take

TABLE II-1AVERAGE VALUES OF ABSORPTION COEFFICIENT k_w FROM PIPE SCANNING TESTS

Location Inches from Chart Center Line	Path Length Inches x_w	<u>Horizontal Scans</u>		<u>Vertical Scans</u>		Aver- ages	Overall Average	Std Dev
		Top Half	Bottom Half	North Half	South Half			
0	3.916	.1637		.1629		.1633		
0.5	3.893	.1665	.1631	.1646	.1646	.1647		
1.0	3.832	.1639	.1636	.1646	.1626	.1637		
1.5	3.724	.1644	.1643	.1645	.1653	.1646		
2.0	3.568	.1639	.1636	.1664	.1657	.1649		
2.5	3.367	.1651	.1638	.1659	.1650	.1649		
3.0	3.038	.1670	.1666	.1686	.1682	.1676		
3.5	2.714	.1645	.1652	.1676	.1635	.1656		
4.0	2.220	.1649	.1645	.1683	.1618	.1649	.1649	
4.3	1.820	.1613	.1619	.1619	.1561	.1603	.1605*	.0044
4.5	1.472	.1521	.1521	.1480	.1372	.1473	.1495*	.0070
4.7	0.985	.1237	.1127	.1408	.1275	.1261	.1242*	.0159

* Overall average of individual tests.

into account both the length of time required to give a good statistical average at one position and the response time of the instrument. The latter was found by observation to be 5 to 10 seconds. A total time of 30 seconds would therefore be required to obtain the average value at an instantaneous change of density. A first approximation of the scanning speed was a full beam diameter ($1/4"$) displacement in approximately 30 seconds. i.e. $0.5"/\text{minute}$. A slightly slower speed of $0.415"/\text{minute}$ resulted from practical considerations and was found to give good reproducible curves. APPENDIX FIGURE B-4 shows the time recording of the output signal at 50 mv/inch and 0.2 volt/inch. TABLE B-4 lists the values and standard deviations of this signal.

2.14 PIPE DIAMETER, CARRIAGE DISPLACEMENT, CHART DISTANCES

The path length, x , is calculated from the mean pipe diameter and distance from the pipe centerline (y) according to EQUATION (2.10.1). This involves locating the pipe centerline on the chart and relating distances from the centerline to true displacements of the beam. The pipe inside diameter was taken at 36 points at the gamma-test section with a feeler-gauge and was shown to be slightly oval in cross-section but not sufficiently so to prevent using an average diameter. TABLE B-5 lists the readings averaging $3.916" \pm 0.015"$.

The total carriage displacement between the limit switches was measured by micrometer during several test runs and compared with the corresponding chart distances between

the reversal points which constitute the extremities of the recorded line on the x-axis. Prior to this the helipot in the constant DC voltage supply circuit was set to approximately give a chart displacement 2.5 times that of the true carriage displacement. The chart distances could therefore be measured directly to the nearest .005 inch on a precision scale. APPENDIX TABLE B-6 lists these measurements together with the measurements from the chart centerline to the reversal points. The factor, F , converting chart distances was found to have an average value of 1.008.

The center of the chart in each case was located by bisecting the x-distance of the recorded curve at several locations and drawing a vertical line through these points. This procedure gave remarkably consistent results as evidenced by the close agreement of the readings obtained in TABLES B-3.4 to 3.9.

A further check by physical measurement confirmed the reliability of this procedure. The scanner carriage was stopped at the top reversal point and a precision 1/4" diameter steel shaft was inserted in the back collimating hole so that it extended over the top of the pipe. The distance between the shaft and top of the pipe was measured with a feeler-gauge. The pipe centerline location obtained by adding the pipe wall thickness and radii of the shaft and pipe compared well with the chart measurements of the same distance. These readings are given in APPENDIX TABLE B-7.

2.15 SAMPLING OF SOLIDS IN CIRCULATING STREAM

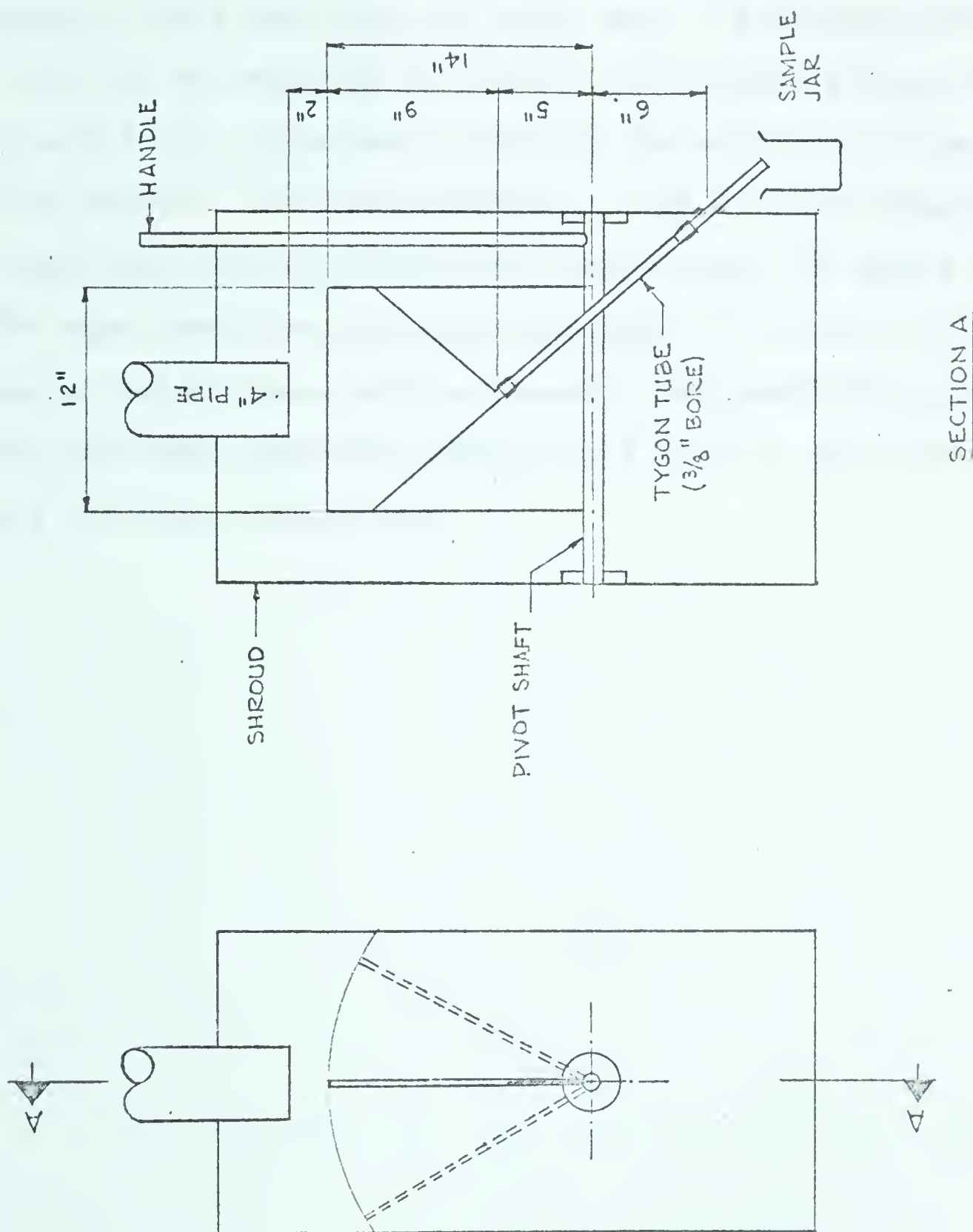
The average concentration of solids being transported was determined by taking samples from the stream entering the circulating tank. A sampling device was devised by which relatively small representative samples could be taken. FIGURE II-15 is a sketch of this sampler. It consists of an approximately 1/4" wide x 12" long slot formed between two parallel thin-walled sheet metal plates. The inside narrow wall slopes at 60° towards a 1/2" inside diameter pipe which is connected to a similar pipe in the tank wall by a "tygon" tube. All the sides and tubing have a minimum slope of 60° to the horizontal so as to minimize solids hold up. The sampler collects a 20 to 30 oz sample when moved through the fluid stream twice. A large number of tests were made at two solid concentrations to determine the reliability of the sampler. The results, given in APPENDIX B-8 show low standard deviations under the conditions tested. i.e. 84.9 ± 1.9 weight % water and 61.4 ± 1.2 weight % water at a flow rate of 20 lb/second. At high flow rates care had to be taken to move the sampler through the stream at such a rate that no fluid spilt over the edges.

2.16 SAND USED IN TESTS

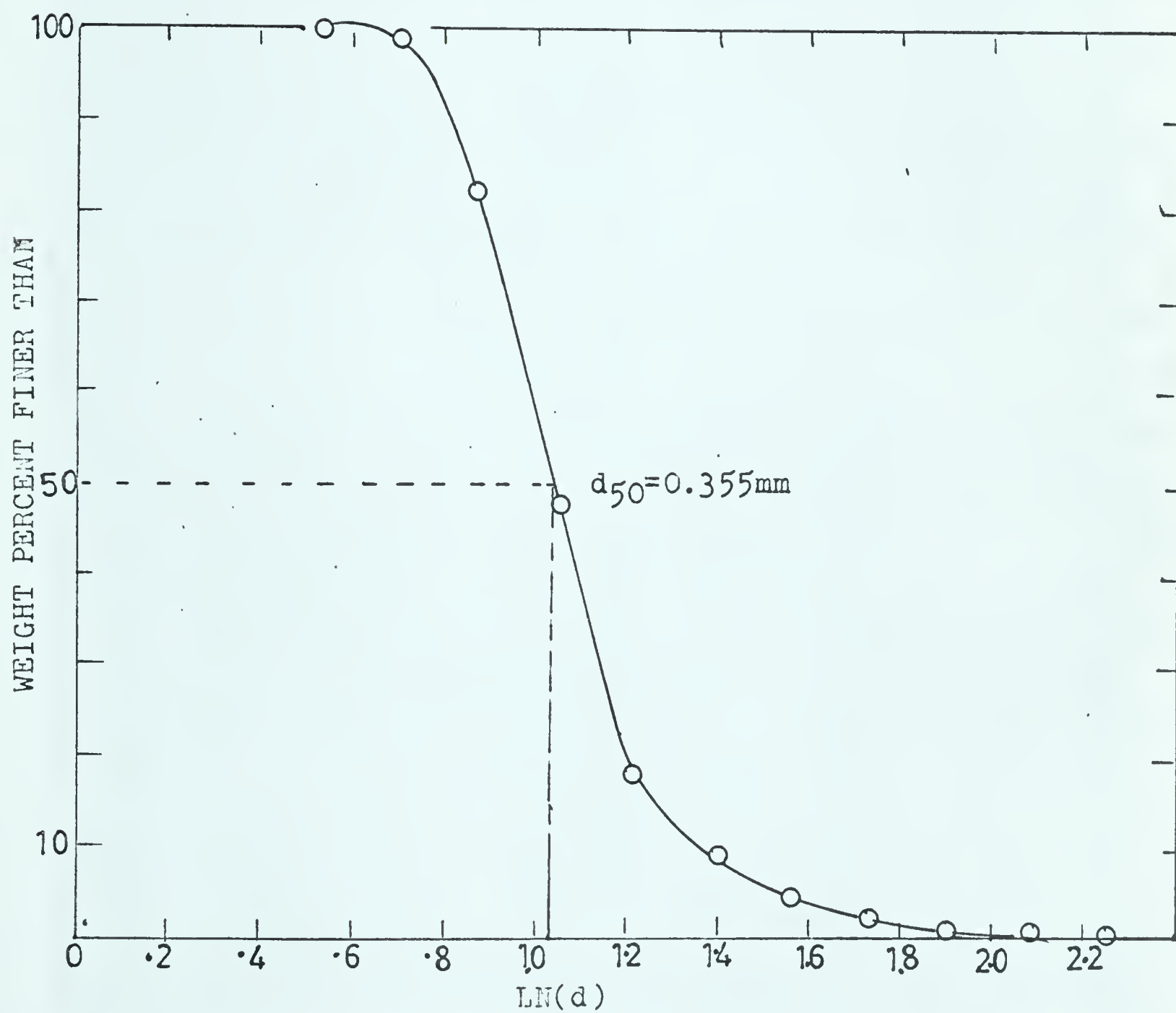
Ottawa sand conforming to ASTM C-109 specifications was the only type of solids used in these tests. The specified sieve analysis of this sand is given below:

+100 Mesh	98	$\pm 2\%$
+ 50 Mesh	72	$\pm 5\%$
+ 30 Mesh	2	$\pm 1\%$

SAMPLING DEVICE
FIGURE II-15

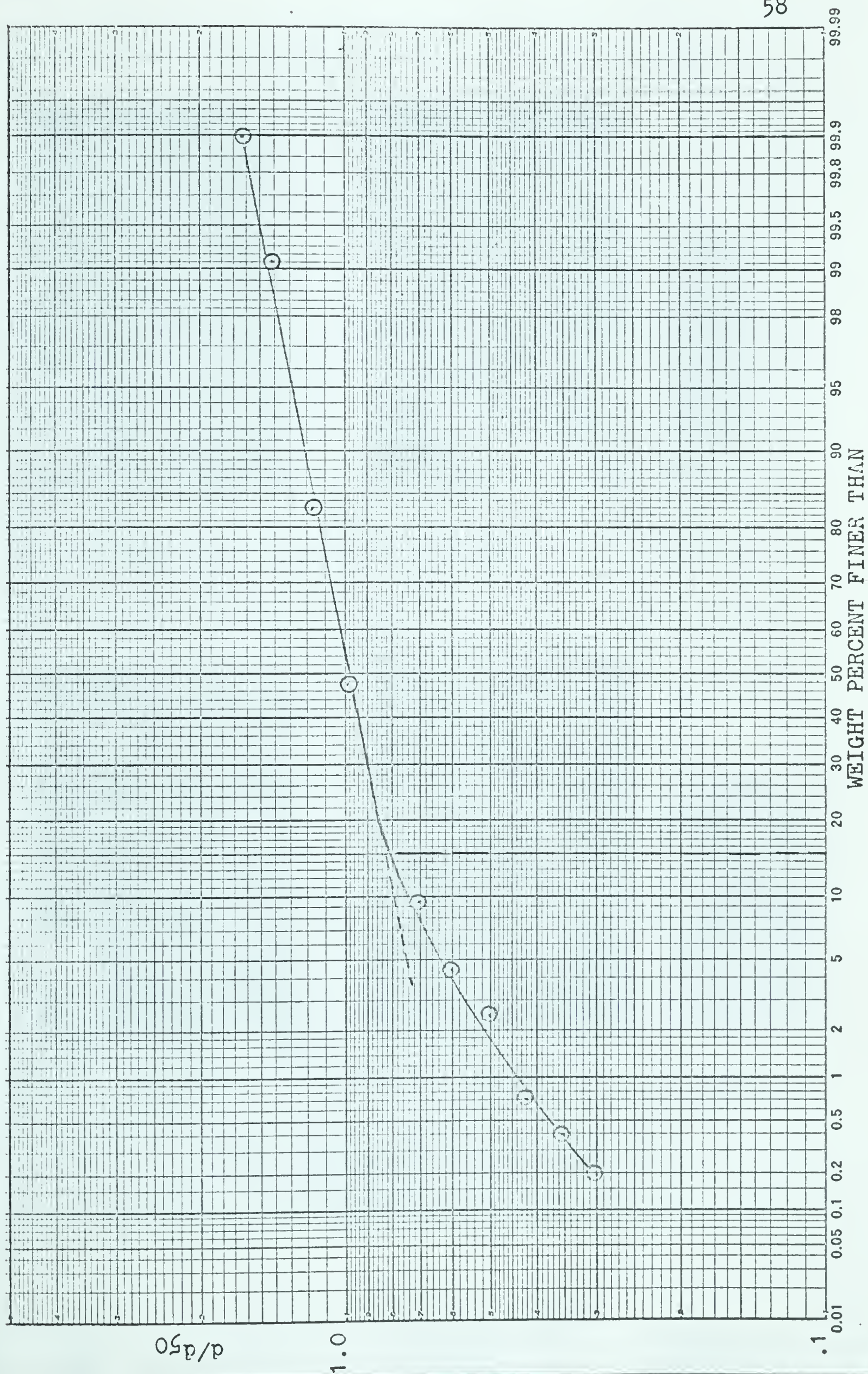


Several sieve analyses were carried out on the material as received which confirmed this broad classification. A typical analysis over narrower size fractions is given in TABLE B-9 and the results as plotted in FIGURE II-16 show a median diameter (50% finer than) of 0.355 mm. A frequency plot (FIGURE II-17) as recommended by Blench (1952) shows a fair straight-line fit for approximately 85% of the material in the larger size ranges. By this criterion the sand can be regarded as simulating naturally-deposited sands found in canals and rivers. The sand particles as shown in PLATE II-9 appear well rounded and no attempt was made to measure the geometric properties. The published specific gravity of 2.64 is a well accepted figure for this silica sand.

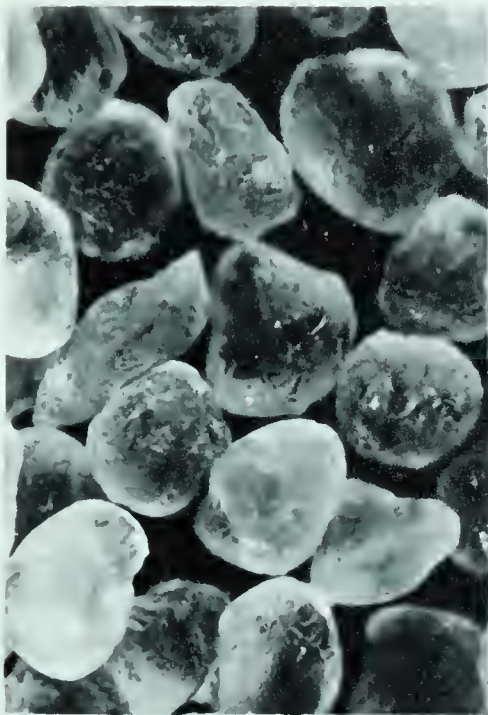


TYPICAL GRAIN-SIZE CURVE

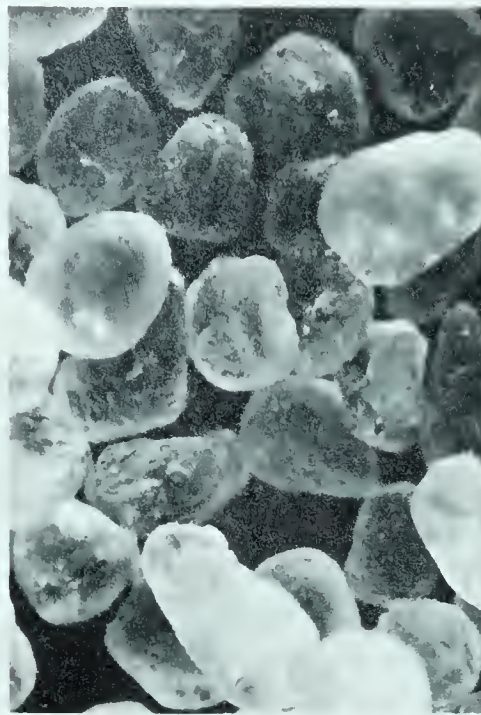
FIGURE II-16



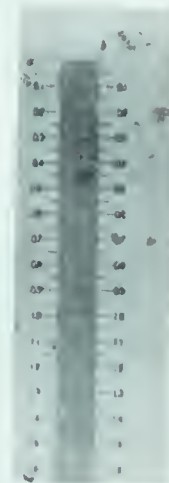
NONDIMENSIONAL GRAIN-SIZE PLOT
FIGURE II-17



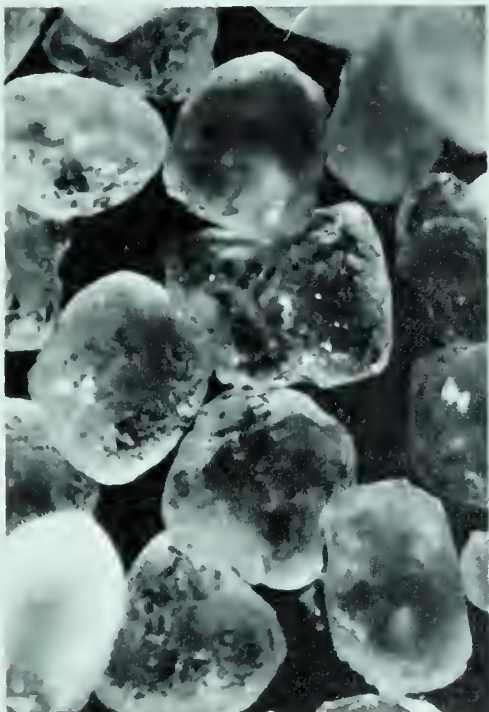
30 TO 35
MESH



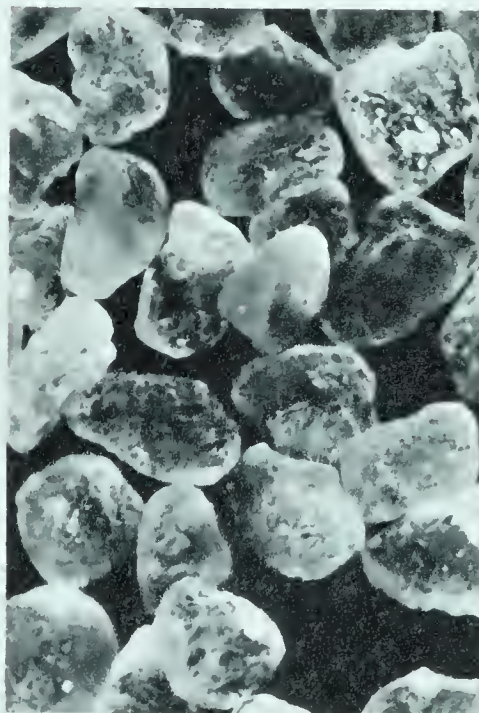
40 TO 45
MESH



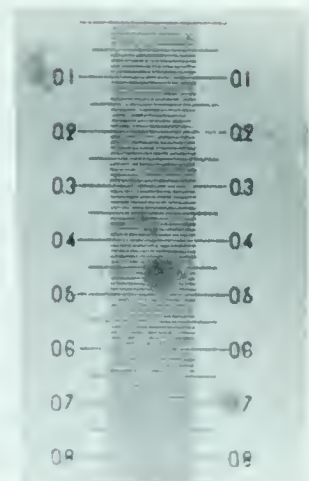
SCALE
MM



50 TO 60
MESH



70 TO 80
MESH



SCALE
MM

PHOTO - MICROGRAPHS OF TEST SAND

PLATE II - 9

CHAPTER III

EXPERIMENTAL RESULTS

3.1 GENERAL

The initial phase of the work consisted of designing an operable experimental unit and in selecting, purchasing, installing and calibrating the necessary instrumentation. The final test unit and associated equipment have been described in the preceeding chapter. Instrument calibration has also been briefly dealt with in CHAPTER II.

This chapter outlines the data collected from the experimental equipment and the accuracy of the data. All terms are defined and listed in APPENDIX A. Original test data and calculated quantities are tabulated in APPENDIX C.

3.2 CHRONOLOGY

The experimental equipment exclusive of the gamma-ray scanner was completed during the summer of 1964. Preliminary testing of the unit commenced in June, 1963 but delays in delivery of the gamma-ray instrument and in obtaining a licence from the Federal Health Authorities for operating this instrument postponed final installation until September 1964. Further delays were caused by a faulty pre-amplifier section of the "Qualicon" system. Final calibration was carried out during November 1964 and final test runs were made during December 1964.

3.3 CLEAR WATER RUNS

These tests were carried out as a check on the differential pressure instruments and also to test the general operability of the unit. The results have been plotted in FIGURE III-1 and tabulated in APPENDIX C-1 as friction factor vs. the Reynolds number on log-log coordinates which is a convenient and conventional way of comparing the results with those of other workers. The straight line shown is a plot of the Blasius formula $f = \frac{0.316}{Re^{\frac{1}{4}}}$ over the range of Reynolds numbers 10^3 to 10^6 . As can be seen the data follow the Blasius line quite well. Increased scatter in the lower Reynolds numbers is due to the increased error in reading the small differential pressures from the manometer or chart.

3.4 SAND-WATER RUNS

3.4.1 OPERATING PROCEDURE

The operating procedure consisted of circulating water through the unit at a high rate and then adding the sand contained in individual 50 lb bags to the circulating tank until the desired concentration was reached. This was most conveniently achieved by setting the gamma-ray scanner in the vertical position over the pipe centerline and calculating the reading required for a desired concentration. A reasonably close check could usually be obtained between this reading and the transport concentration by the sampling and drying procedure providing fully suspended flow conditions prevailed.

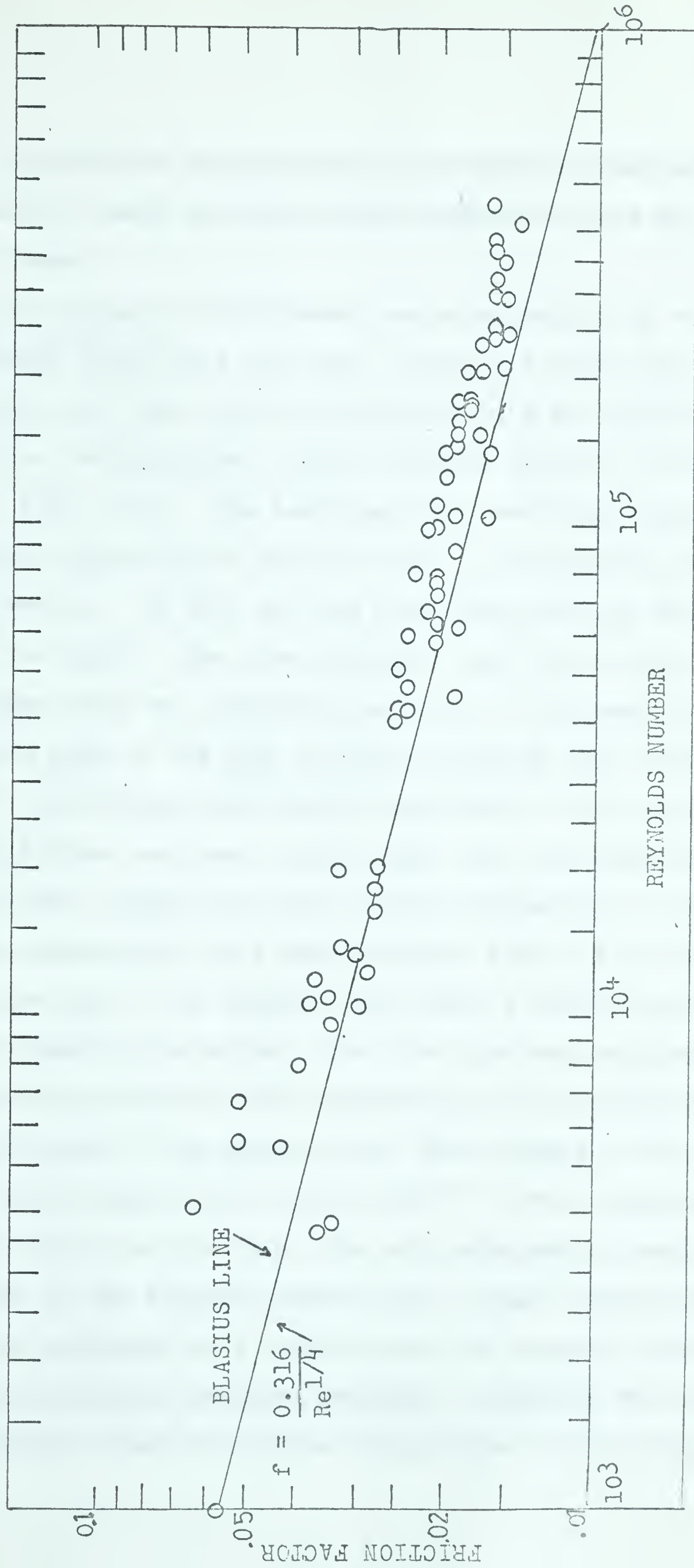


FIGURE III-1

A period of approximately 15 minutes was allowed for the unit to reach an equilibrium condition before any readings were taken.

The gamma-ray instrument was standardized by running the horizontal beam above the pipe, clamping a $3/8$ " thick reference plate over the outlet collimating hole and adjusting the amplifier "standardize" 10-turn helipot to give a recorder reading of 2.59 volts. The scanning motor was then started in the ascending direction so that it would be reversed by the top limit switch. In this way the reversing position would be marked on the chart. The same procedure was followed for the vertical beam which was standardized with the reference plate on the north side of the pipe and then scanning from north to south. The horizontal scan always commenced at the top of the pipe because there was some concern that the instrument would not respond fast enough from the minimum attenuation in air to the maximum attenuation in a dense settled sand bed at the bottom of the pipe. Two samples were taken 5 minutes apart during the scanning operation. The flow rate was measured by the weigh tank procedure after completion of the horizontal and vertical scans. The samples were then weighed to the nearest 0.05 gm and dried in an oven at 250° F. After completion of one flow condition the flow rate was decreased by opening up the valve in the by-pass line to give a small reduction in flow rate as evidenced by a drop in both the magnetic flow meter and differential pressure readings. Readings were taken at progressively lower flow rates through the critical deposit

regime. Several tests established that any one condition could be reproduced by simply adjusting the flow rate to duplicate the flow meter reading and differential pressure.

3.4.2 TEST CONDITIONS

Test conditions were confined to sand transport concentrations ranging from approximately 2 to 20 volume % and to transport rates immediately above or below the critical deposit condition. It was not the intention to collect pressure gradient data over a wide range of flow rates since this has been adequately covered in experimental work to date.

The different tests are most conveniently classified by the maximum sand transport concentration as follows:

<u>TEST SERIES</u>	<u>VOLUME CONCENTRATION OF SAND</u>
122300	1-3
122400	3-8
123000	8-12
123100	12-18

These test numbers were used to identify the gamma-ray recorder charts which are reproduced in APPENDIX C. 23 point values were taken from each chart and punched on IBM cards from which a computer programme of EQUATIONS 2.10.1, 2.12 and 2.16 calculated the sand concentration.

All other readings such as flow rate weighings and time, differential pressure readings and conversion factor, temperature, sample weighings before and after drying, were also punched on IBM cards from which a computer programme calculated the weight flow rate, pressure gradient, volumetric flow rate, mean velocity, sand transport concentration and

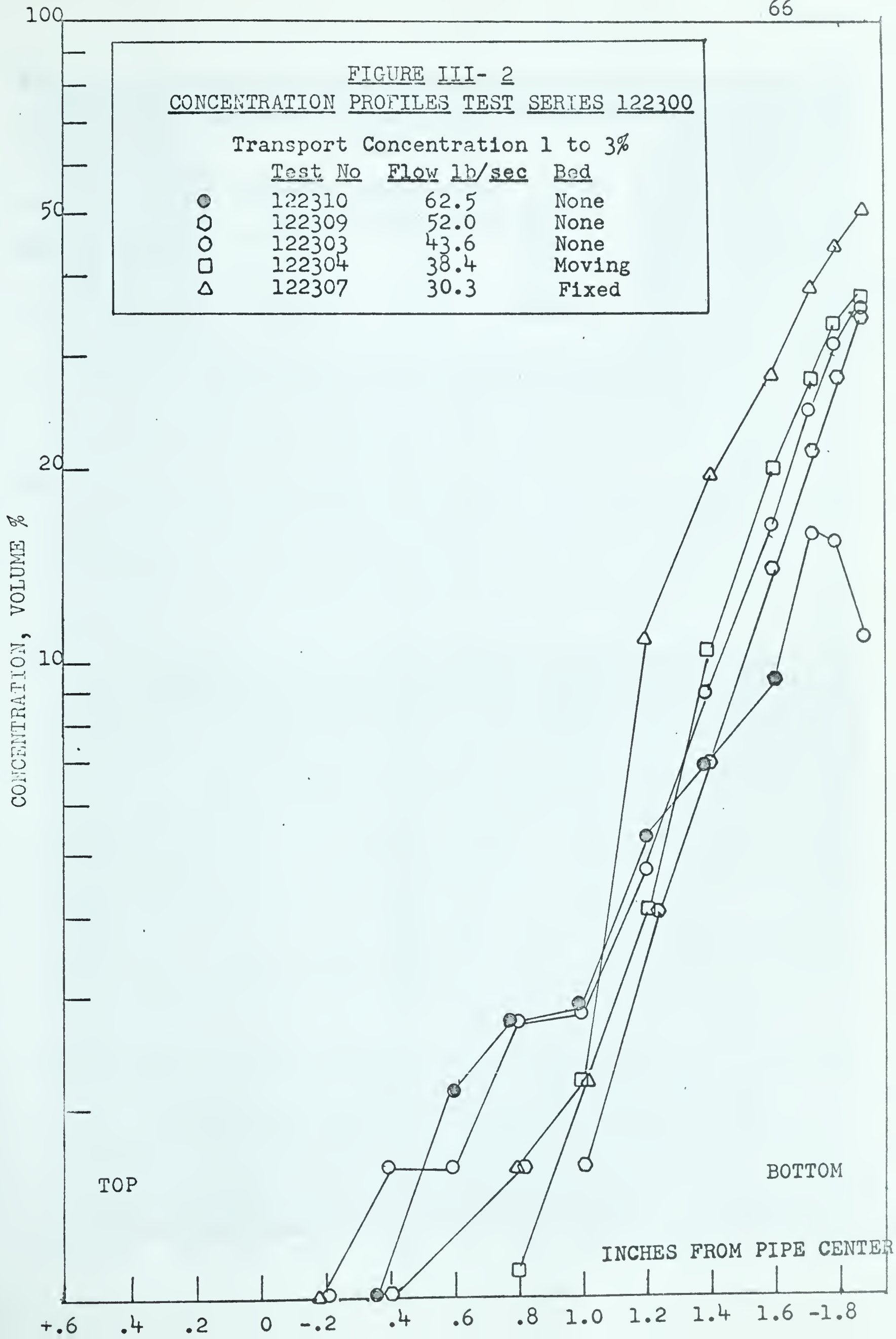
relevant non-dimensional numbers.

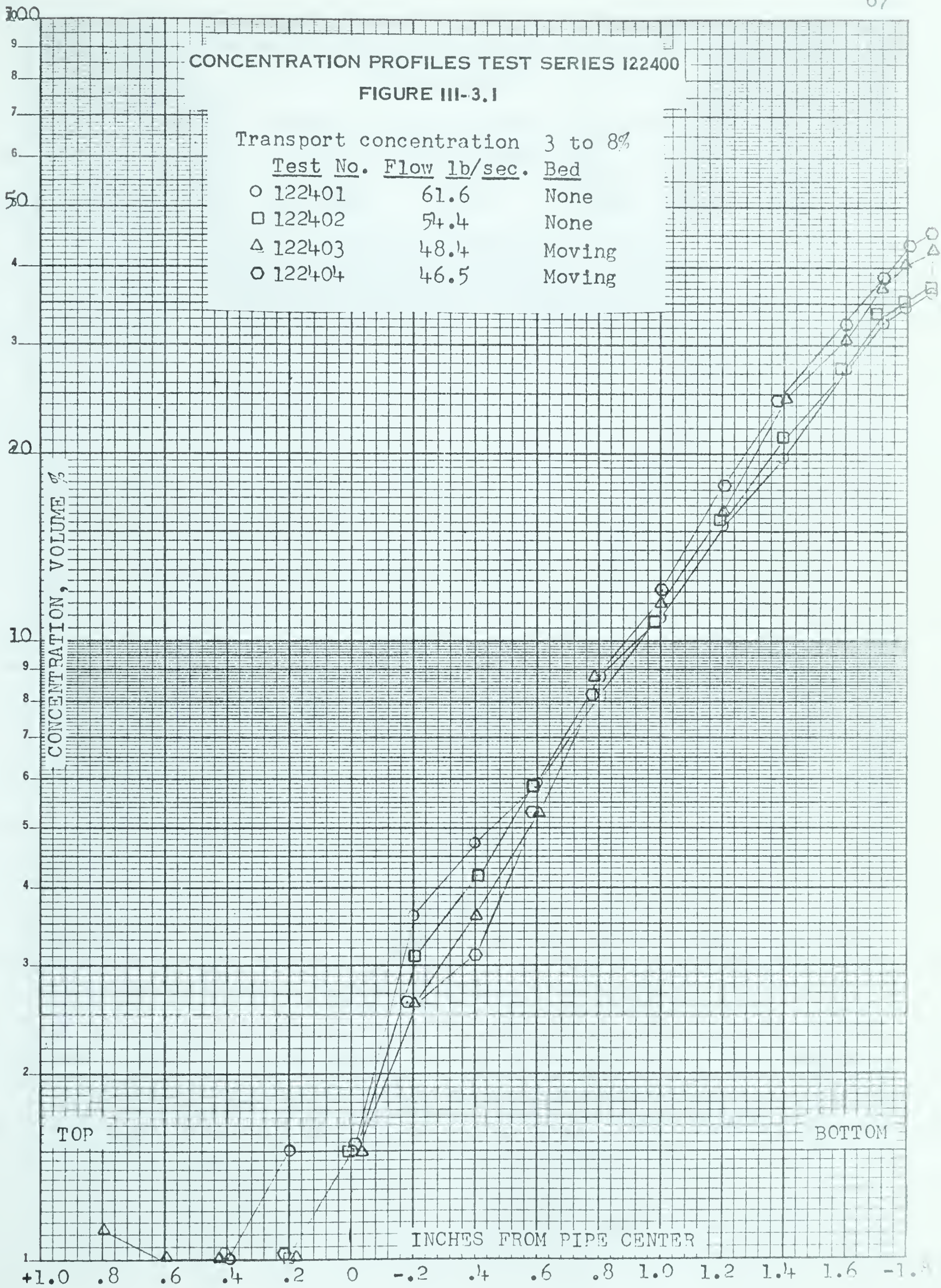
APPENDIX TABLE C-2 lists the test conditions with the values of the above variables and TABLE C-3 lists the point concentrations for each run. The concentration profiles are also plotted on each recorder chart, and all the profiles of each series are shown in FIGURES III-2 to 5. They are further summarized in one plot in FIGURE III-6 to facilitate comparison of the different test conditions. The bed condition for each test is summarized under the categories "no bed", "moving bed", and "fixed bed". An attempt was made to further classify the moving bed according to the type of bed surface and "dune" formation but this was abandoned when it became apparent that no significant change in type of bed movement occurred over the range of test conditions in the critical deposit region. The critical deposit condition was defined as that condition between fully-suspended flow and a moving bed where slugs of dense sand would first form on the pipe floor and then be dissipated after travelling a short distance. This condition could be classified as a type of "slug" flow in the bottom of the pipe. The moving bed was identified by a small continuous ribbon of settled sand having a "peristaltic" movement along the lowest pipe sector. The fixed bed was stationary at the pipe wall but had a moving dune-like interface with the suspended phase. These "dunes" never exceeded $\frac{1}{4}$ " to $\frac{1}{2}$ " in height and did not seem to move in a well defined pattern thereby precluding any quantitative evaluation of their behaviour. It was initially hoped that the gamma-ray instrument could be

FIGURE III- 2
CONCENTRATION PROFILES TEST SERIES 122300

Transport Concentration 1 to 3%

	<u>Test No</u>	<u>Flow lb/sec</u>	<u>Bed</u>
●	122310	62.5	None
◊	122309	52.0	None
○	122303	43.6	None
□	122304	38.4	Moving
△	122307	30.3	Fixed





100

CONCENTRATION PROFILES TEST SERIES 122400

FIGURE III-3.2

Transport concentration 3 to 8%

Test No.	Flow lb/sec.	Bed
○ 122405	41.2	Moving
□ 122406	35.0	Fixed

CONCENTRATION, VOLUME %

TOP

BOTTOM

INCHES FROM PIPE CENTER

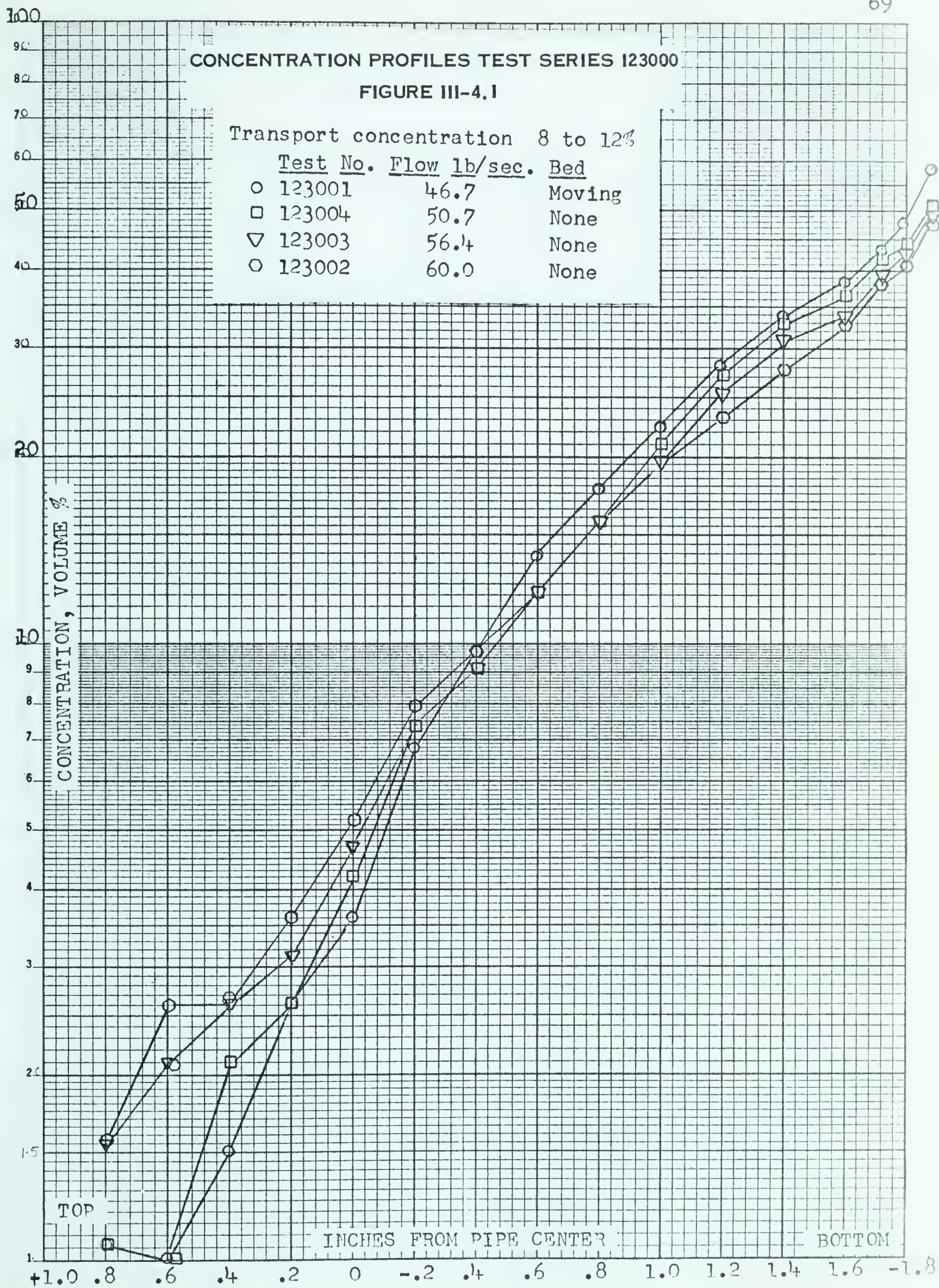
+1.0 .8 .6 .4 .2 0 -.2 .4 .6 .8 1.0 1.2 1.4 1.6 -1.8

10

2

1

9
8
7
6
5
4
3
2
1
9
8
7
6
5
4
3
2
1



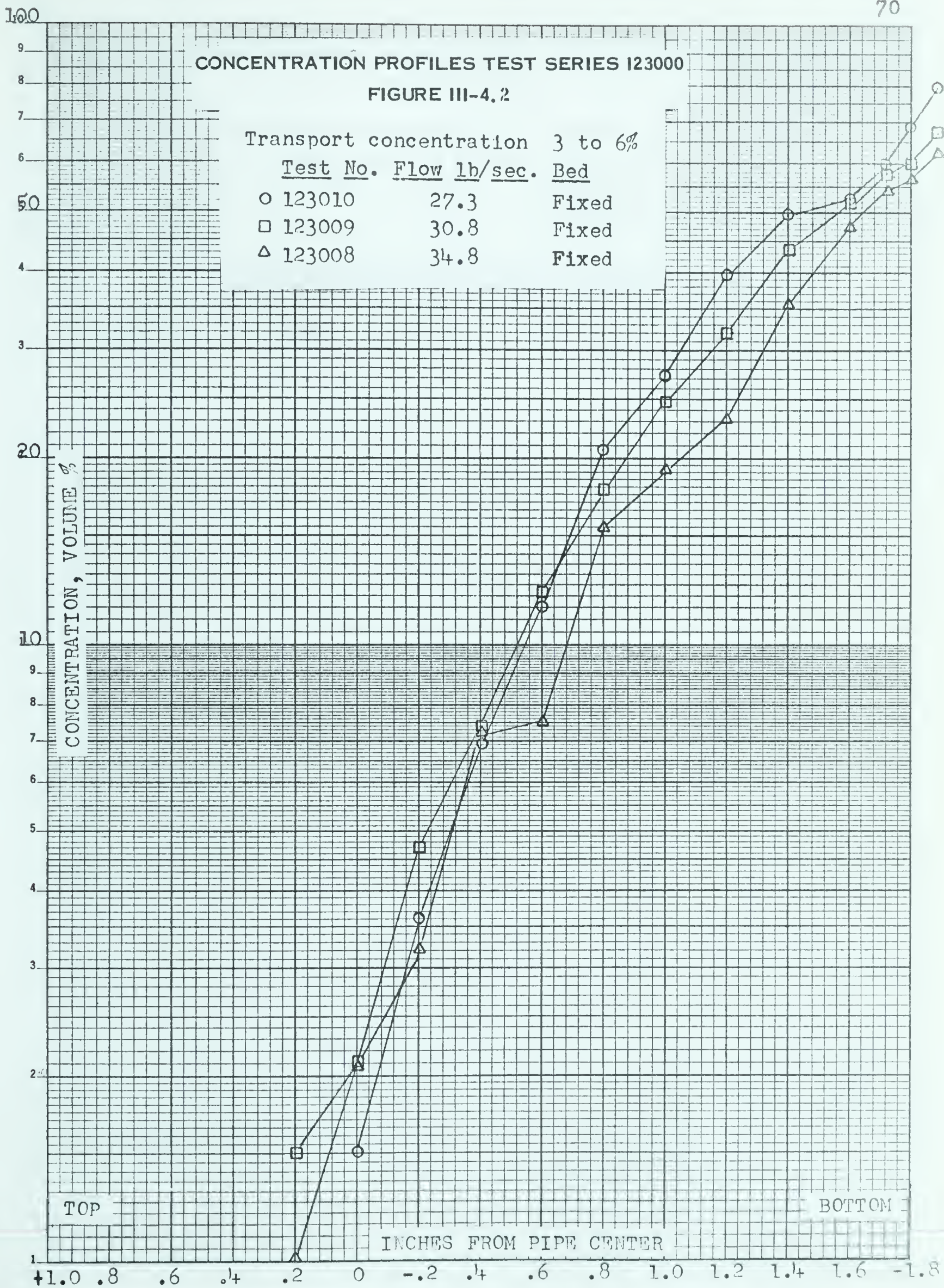
CONCENTRATION PROFILES TEST SERIES 123000

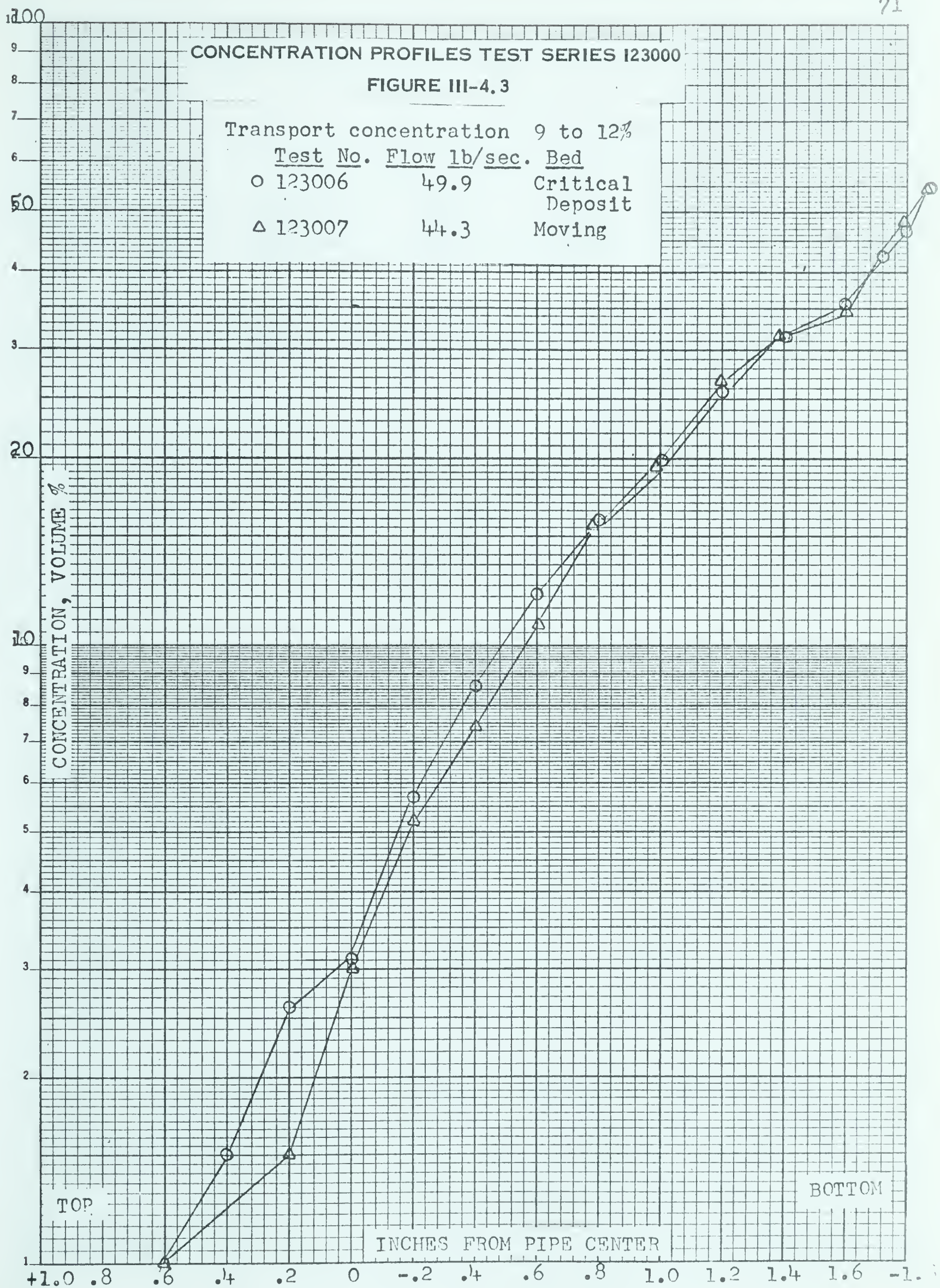
FIGURE III-4.2

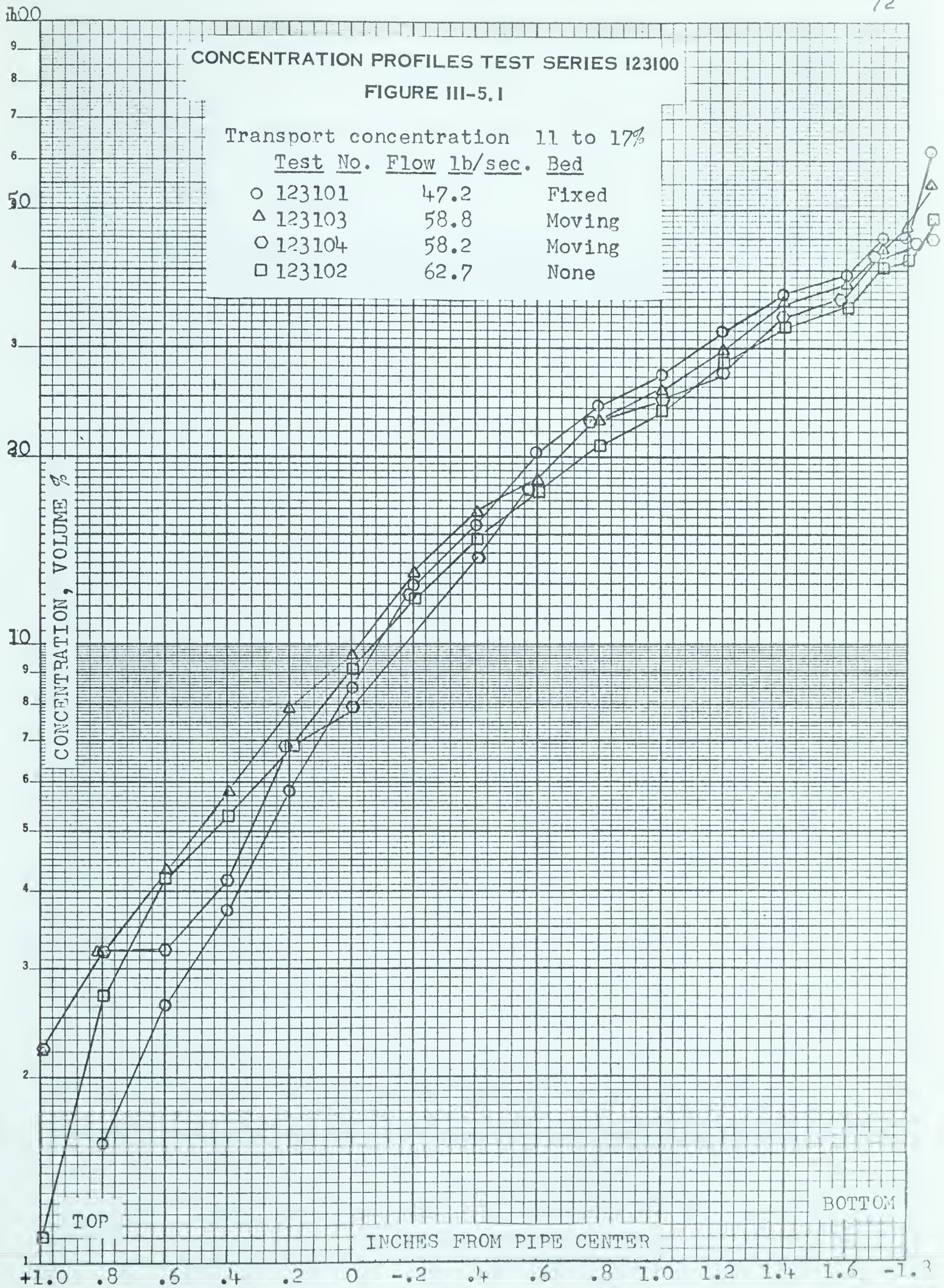
Transport concentration 3 to 6%

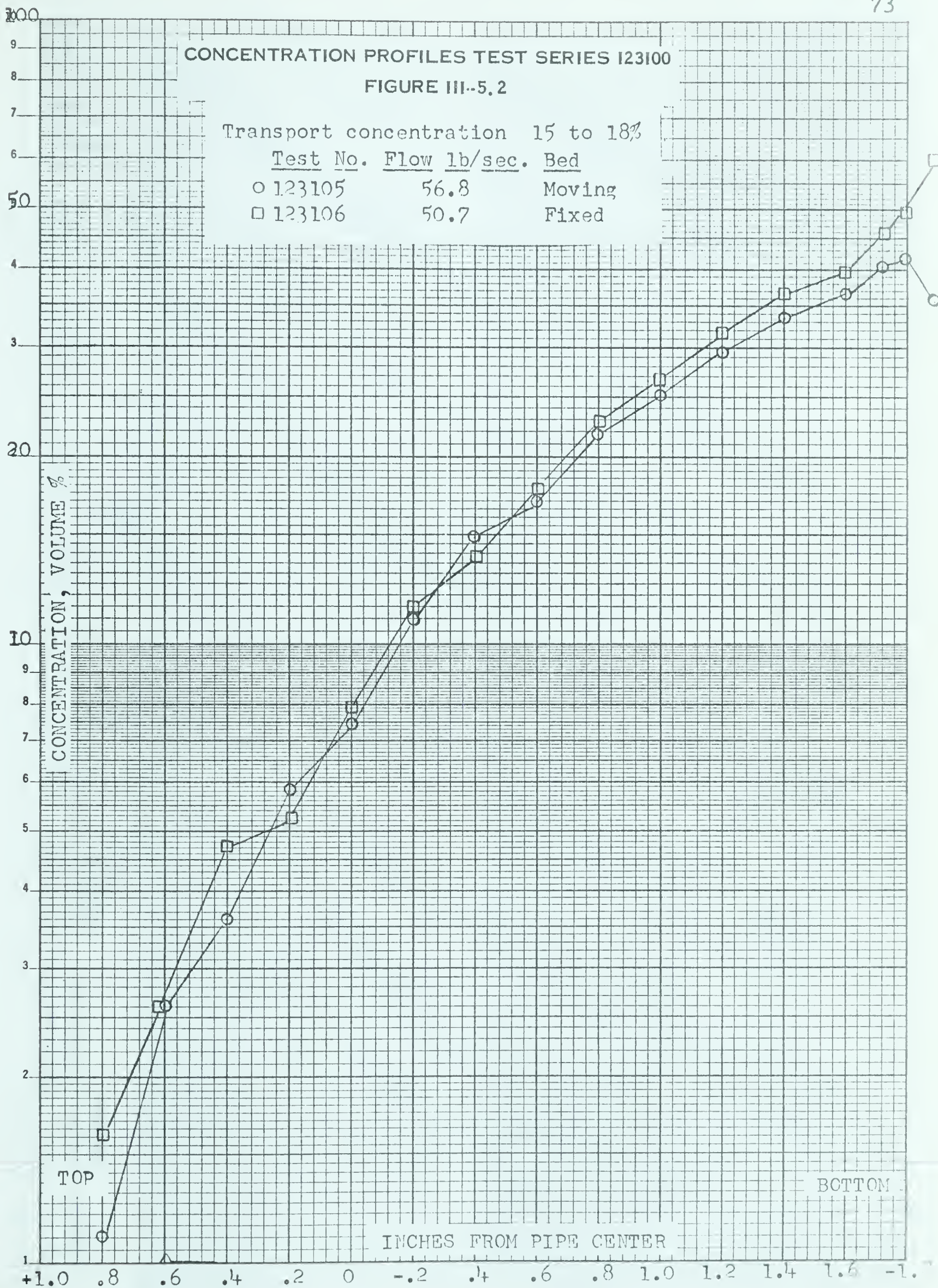
Test No. Flow lb/sec. Bed

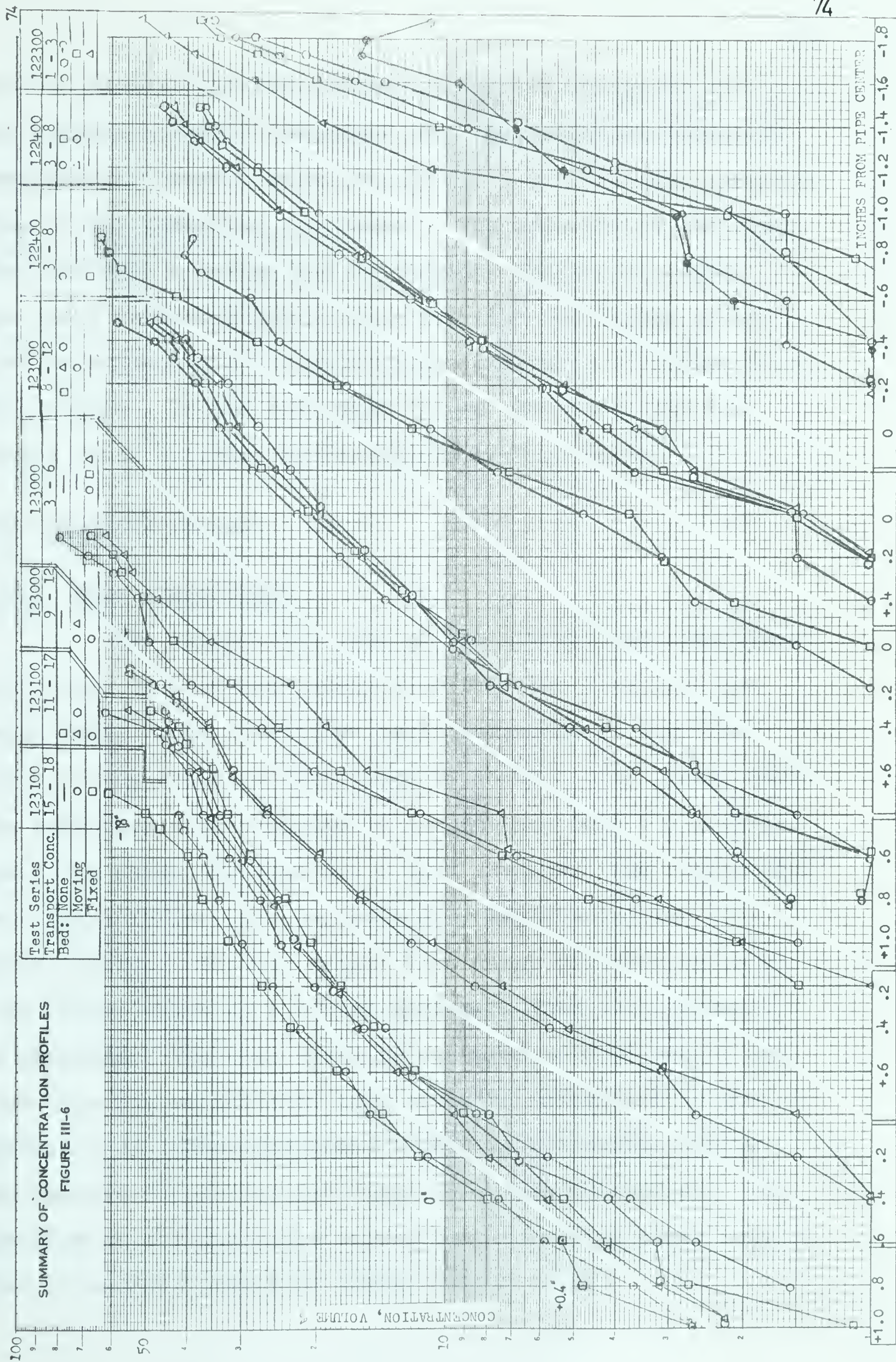
○ 123010	27.3	Fixed
□ 123009	30.8	Fixed
△ 123008	34.8	Fixed











used to identify different dune geometries and velocities, but several attempts indicated that concentration fluxes by dune movement were blanked out by the 5 to 10 second response time of the gamma-ray instrument. The majority of the tests were run with a moving bed or complete absence of a bed. A few tests (FIGURE III-4.2) were run with bed depths up to $3/4$ " as evidenced by concentrations exceeding 45 Volume % in this region. In the remaining "fixed bed" tests the bed height never exceeded approximately $1/4$ " in depth.

3.5 ACCURACY OF DATA

3.5.1 FLOW MEASUREMENT

The weight flow rate of the mixture was determined accurately by instantaneously diverting the flow into the weigh tank. Some repetitive tests were done at low flow rates giving standard deviations of 14.80 ± 0.13 lb/sec where the measuring time exceeded 10 seconds and 20.5 ± 0.2 lb/sec where the measuring time was 6 to 7 seconds. One higher flow rate (43.6 lb/sec) was reproduced by duplicating the flow meter reading. The two weight flow rates differed by only 0.04 lb/sec which is a closer agreement than would normally be expected. The time could be measured to 0.05 second and from this the weight flow rate could be determined to the nearest 0.05 lb/sec for times exceeding 10 seconds and to the nearest 0.5 lb/sec for times less than 10 seconds. Inspection of all the tests showed that measuring times less than 10 seconds prevailed during only 2 tests.

Standard deviations of $\pm 1\%$ and $\pm 2.5\%$ corresponding to measuring times greater and less than 10 seconds were assigned to the flow rate measurements.

3.5.2 PRESSURE GRADIENT

The large number of clear water tests yielding reproducible results was regarded as sufficient evidence that the instrumentation was reliable and accurate to $\pm 0.1''$ of water. The manometer could be read to $0.05''$ corresponding to a differential pressure of $0.094''$ with the water over bromoform system. Differential pressure fluctuations with sand-water mixtures reduced the accuracy to $\pm 0.2''$ of water. Total differential pressures during the test runs varied from approximately 18 to $60''$ of water giving errors ranging from $\pm 1\%$ to 0.3% . Room temperatures varied from 72°F to 77°F and it was not considered necessary to make a temperature correction for density changes of the manometer fluids. The "reagent grade" bromoform reacted slowly with the water at the manometer interfaces and was replaced whenever a permanent discoloration developed. The bromoform was entirely contained in the glass U-tube of the manometer.

3.5.2 TEMPERATURE

Temperatures could be read to 0.5°F on the strip chart or dial thermometer. Specific weights and kinematic viscosities of the water at the operating temperature were used in all computations.

3.5.3 SAND TRANSPORT CONCENTRATION

SECTION 2.2.15 dealt with the sampling procedure and accuracy of sampling at relatively low flow rates. A good measure of the sampling accuracy during the test runs is given by the root mean square of the deviations from the average for each pair of samples. These values are given in APPENDIX TABLE C-5 and are summarized below.

$$C_t \pm 0.44 \text{ Volume } \% \text{ for } C_s < 10\%$$

$$C_t \pm 0.80 \text{ Volume } \% \text{ for } C_s > 10\%$$

$$C_t \pm 0.61 \text{ Volume } \% \text{ for all tests}$$

3.5.4 CONCENTRATION GRADIENT

The accuracy of the point values of sand concentration, C_s , obtained from the gamma-ray instrument depends on the accuracy of the measured quantities in EQUATIONS 2.12 and 2.16.

$$C_s = 100 \ln\left(\frac{E_o}{E_{op}} \cdot \frac{E_p}{E}\right) / 0.267x \text{ for } y \leq \pm 1.6''$$

$$C_s = 100 \ln\left(\frac{E_o}{E_{op}} \cdot \frac{E_p}{E}\right) / 1.61 k_w x \text{ for } y > \pm 1.6''$$

These can be combined in the form,

$$C_s = 100 \ln e / kx \quad (3.5.4)$$

for the actual test conditions where E_o equalled E_{op} and

$$\ln e = \ln\left(\frac{E_p}{E}\right)$$

$$k = 0.267 \text{ for } y \leq \pm 1.6''$$

$$k = 1.61 \cdot k_w \text{ for } y > \pm 1.6''$$

The standard deviations of the preceeding three groups were obtained from the approximate general statistical relationship:

$$s_Y \simeq \left[\left(\frac{\partial F}{\partial z} \cdot s_{z_1} \right)^2 + \left(\frac{\partial F}{\partial z_2} \cdot s_{z_2} \right)^2 + \dots \right]^{\frac{1}{2}} \dots (3.5.5)$$

where $y = F(z_1, z_2, \dots)$, and it is assumed that the changes in values of z are independent of one another. Application of EQUATION 3.5.5 to 3.5.4 enabled calculation of an approximate value of the standard deviation of C_s at 4 locations in the pipe and at concentrations close to the test conditions.

Summaries of the calculation procedures are given in APPENDIX C-5. The standard deviations of $\ln e$, k , x and C_s at these 4 points are listed below.

TABLE III-2

Location Inches Below Pipe Center	0	0.6	1.2	1.8
$C_s, \%$	5.00 \pm .61	10.0 \pm 1.0	30.0 \pm 3.0	50.0 \pm 11.0
$\ln e$.0523 \pm .0045	.0994 \pm .0045	.2466 \pm .0048	.1772 \pm .0085
$x, "$	3.916 \pm .015	3.724 \pm .016	3.079 \pm .020	1.472 \pm .048
k/inch	.267 \pm .019	.267 \pm .019	.267 \pm .019	.241 \pm .020

It should be noted that these calculated standard deviations assume that the readings with sand-water mixtures could be obtained with the same accuracy as the readings with water only. They therefore do not necessarily reflect actual

fluctuations in pipeline concentration. In addition it may not reflect the increased error in obtaining the 3 point readings on the curve having a greater slope in the bottom pipe region. Insufficient runs at set conditions were made to obtain standard deviations at different points and with different solids concentrations. Fluctuations in solids concentration with frequencies less than approximately 10 seconds would be "averaged-out" by the combined effect of the slow scanning speed and instrument time constant. Fluctuations of lower frequency could be expected to show up in the recorded signal, but their effect could be minimized by taking the smoothed curve value at each point. Sufficient readings at the 3 points greater than 1.6" from the centerline were made to convince the author that they could be obtained with the same degree of accuracy as corresponding points on the water calibration curve. The standard deviations of C_s of TABLE III-7 can be expected to give a good indication of the variation of the concentration measurements during the test runs.

A further indication of the relative accuracy of \bar{C}_s can be obtained by comparing the average concentration obtained by integrating the horizontal and vertical concentration profiles with the sampled transport concentration C_t . These values are summarized in TABLE C-6 and show a root mean square discrepancy of ± 1.09 volume % sand for $C_s < 10\%$ and ± 1.95 volume % for $C_s > 10\%$ for the runs without a fixed bed. The difference in these two concentrations is in part due to the hold-up of solids in the pipe. The integrated values show

a reasonably random distribution of values higher and lower than the transport concentration indicating that the hold-up ratio could not be determined within these limits of accuracy.

CHAPTER IV

INTERPRETATION OF EXPERIMENTAL RESULTS

4.1 GENERAL

Virtually all the data and theory of pipeline transport of fluidized solids published to date have been confined to the fully suspended flow regime far above the critical deposit region. This study was confined to the critical deposit region and hardly any data are therefore available with which to compare these test results.

This chapter outlines the approach taken in an attempt to quantitatively describe the critical deposit regime.

4.2 SIMPLIFIED THEORETICAL ARGUMENT FOR SUSPENDED FLOW IN PIPELINES USING THE BAGNOLD (1956) DISPERSIVE STRESS CONCEPT

SUMMARY:

Bagnold introduced a novel concept in the flow of fluid-solid suspensions. He was able to measure both the shear stress (τ) and the normal or "dispersive" stress component (P) of non-settling suspensions in a concentric cylinder viscometer and showed that these could be related by;

$$\frac{\tau}{P} = \tan \phi \dots \dots \dots (4.2.1)$$

where $\tan \phi$ can be regarded as the dynamic analogue of the static coefficient of friction and has a value ranging from 0.75 to 0.32 for suspension concentrations larger than 10%.

$\tan \phi$ in turn was found to be a function of the particle and fluid properties. These properties were expressed in the form of a non-dimensional "dispersion" number, G .

$$\tan \phi = \text{Fn} \left[\frac{\rho_s d^2 p}{\mu_f^2 \lambda} \right] = \text{Fn}(G^2) \quad (4.2.2)$$

where $\lambda = \frac{d}{a}$ and a = average distance between particle surfaces. This parameter was used to broadly classify high shearing rates as "Inertial" and low shearing rates as "Viscous". In these regions constant values could be assigned to $\tan \phi$. This classification with the numerical values of $\tan \phi$ and G^2 are listed below.

<u>REGIME</u>	<u>TAN ϕ</u>	<u>G^2</u>	<u>C_s</u>
Viscous	0.75	< 28	> 10%
Inertial	0.32	> 3700	

In studying sand transport by saltation as found in wind-driven sand and bed-load transport in streams and canals, Bagnold suggested that the transition from a moving to a fixed bed corresponded to a transition from Inertial to Viscous shearing.

A brief review of Bagnold's work and its limitations is given in SECTION 4.4.

4.3 APPLICATION TO SIMPLIFIED MODEL OF PIPELINE FLOW

Inspection of the concentration gradients shows that the vertical flow section consists of a clear water section occupying as much as half of the top flow section and a

fluidized solids section with a concentration gradient increasing from zero % solids at the interface to 40 to 60% solids at the pipe floor. The latter section can further be subdivided into a top region with $C_s < 10\%$ and a bottom region with $C_s > 10\%$. The Bagnold dispersive stress concept and classification of SECTION 4.2 would then apply to this bottom region.

Values of the average pipe wall shear stresses in these regions can be approximately calculated from the procedure outlined below. Refer to FIGURE IV-1.

A force balance over the length of pipe dL yields;

$$|dP| A = (\tau_w L_w + \tau_c L_c + \tau_b L_b) dL$$

$$\left| \frac{dP}{dL} \right| = i \gamma_w = \tau_w \left(\frac{L_w}{A} \right) + \tau_c \left(\frac{L_c}{A} \right) + \tau_b \left(\frac{L_b}{A} \right) \dots (4.3.1)$$

where τ_w, τ_c, τ_b = average wall shear stresses in the water, center, and bottom regions respectively in lb/ft^2 ; and where L_w, L_c, L_b = wall perimeters in the 3 regions, in ft.

The approximate values of τ_w and τ_c can be calculated from the mean flow velocity V_m and a friction factor. Extensive experimentation has verified that in highly turbulent flow (Reynolds numbers greater than approximately 150,000) the friction factors for low concentration sand-water mixtures differ only slightly from the clear water friction factor at the same mean velocity (Condolios and Chapus, 1963; Ansley, 1963). In this region the friction factor is also a very weak function of the velocity if changes in velocity distribution

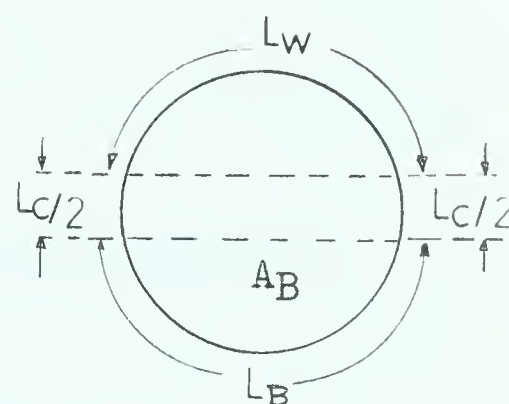
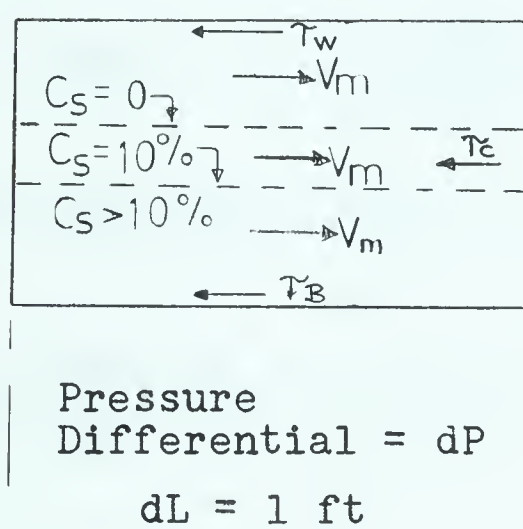
The first of these is the fact that the
government has been unable to
obtain the necessary funds to
carry out its policy. This is due
to the fact that the government
has been unable to raise the
necessary funds to carry out its
policy. This is due to the fact
that the government has been
unable to raise the necessary funds
to carry out its policy.

The second of these is the fact that
the government has been unable to
obtain the necessary funds to
carry out its policy. This is due
to the fact that the government
has been unable to raise the
necessary funds to carry out its
policy. This is due to the fact
that the government has been
unable to raise the necessary funds
to carry out its policy.

The third of these is the fact that
the government has been unable to
obtain the necessary funds to
carry out its policy. This is due
to the fact that the government
has been unable to raise the
necessary funds to carry out its
policy. This is due to the fact
that the government has been
unable to raise the necessary funds
to carry out its policy.

The fourth of these is the fact that
the government has been unable to
obtain the necessary funds to
carry out its policy. This is due
to the fact that the government
has been unable to raise the
necessary funds to carry out its
policy. This is due to the fact
that the government has been
unable to raise the necessary funds
to carry out its policy.

The fifth of these is the fact that
the government has been unable to
obtain the necessary funds to
carry out its policy. This is due
to the fact that the government
has been unable to raise the
necessary funds to carry out its
policy. This is due to the fact
that the government has been
unable to raise the necessary funds
to carry out its policy.



$\tau_{w,C,B}$ are average wall shear stresses in water, center and bottom regions respectively.

SIMPLIFIED SKETCH FOR FORCE BALANCE

FIGURE IV-1

due to presence of the dense bottom layer are neglected. The approximate value of the wall shear stress in the two top regions can be obtained from;

$$\tau_T = \tau_W \triangleq \tau_C = \frac{\gamma_w f V_m^2}{8g} \quad (4.3.2)$$

also
$$L_T = L_W + L_C \quad (4.3.3)$$

As a first approximation τ_B can be obtained from the Bagnold dispersive stress concept, EQUATION 4.2.1 where P can be regarded as the submerged weight of sand per unit projected area of pipe floor.

i.e.
$$\tau_B = P \tan \alpha = (\gamma_s - \gamma_w) \left(\frac{\bar{C}_s A_B}{x_B} \right) \tan \alpha \quad (4.3.4)$$

Substitution of EQUATIONS 4.3.2; 4.3.3 and 4.3.4 in 4.3.1 gives:

$$i \gamma_w = \gamma_w \left(\frac{f V_m^2}{8g} \right) \left(\frac{L_T}{A} \right) + (\gamma_s - \gamma_w) \left(\frac{A_B L_B}{A x_B} \right) \bar{C}_s \tan \alpha$$

or
$$i = \left(\frac{f V_m^2}{8g} \right) \left(\frac{L_T}{A} \right) + (S-1) \left(\frac{A_B L_B}{A x_B} \right) \bar{C}_s \tan \alpha \quad (4.3.5)$$

All terms except $\tan \alpha$ in this equation are measured variables. The values of $\tan \alpha$ (from EQUATION 4.3.5) and G^2 (from EQUATION 4.2.2) could therefore be calculated for all test conditions and compared with the values obtained by Bagnold.

4.4 REVIEW OF WORK BY BAGNOLD (1954, 1956)

Bagnold argued that a static mass of solids cannot

be sheared without some degree of dilation or dispersion. For fluid-solids flow systems he postulated a dispersive pressure resulting from momentum transfer between successive layers of the mixture of fluid and solids. This pressure acts normal to the plane of shearing and in horizontal flow acts against the force of gravity. In this way Bagnold was able to explain how solids could remain suspended under conditions where lifting action by fluid turbulence was insufficient.

A simplified model of particle interaction was used to relate the dispersive pressure, P , with the fluid and solids properties as outlined below.

A mass of rigid elastic spheres with uniform diameter, d , arranged in a tetrahedral-rectangular pattern which gives a minimum static void space (corresponding to C_0 volume % solids) is uniformly dispersed so that the distance, d , between centres is increased to bd . If the resulting free distance is a , we have:

$$b = \frac{a}{d} + 1 = \frac{1}{\lambda} + 1, \quad \text{and}$$

$$\lambda = d/a \quad (4.4.1)$$

which represents the "linear concentration" and is related to the volume concentration by;

$$\lambda = \frac{1}{(C_0/C)^{.333} - 1} \quad (4.4.2)$$

The following simplifying assumptions were made regarding the

solids and fluid motion.

- (i) Zero "slip" velocity between fluid and solids.
- (ii) A steady uniform velocity gradient $\frac{dV}{dy}$ prevails throughout the mixture.
- (iii) The kinetic energy per unit volume is maintained constant by frictional losses.
- (iv) In addition to the average velocity V , the motion of each sphere consists of three dimensional oscillations caused by a succession of collisions between spheres in faster and slower moving layers.

Adjacent layers have mean relative velocities $\delta V = kbd \frac{dV}{dy}$
 $\dots\dots\dots(4.4.3)$

where k is a constant. In $\frac{a}{\delta V}$ seconds the number of collisions

is a function of λ , i.e. $F_n(\lambda) \delta V/a$ collisions occur in unit time. The number of grains per unit area in each layer is $\frac{1}{(bd)^2}$. Each grain collides at some unknown angle \angle with

the slower moving spheres in the adjacent layer thereby experiencing a total momentum change $2m\delta V \cos \angle$ in the y direction and $2m\delta V \sin \angle$ in the V direction. (m = mass of sphere).

A repulsive pressure $P = \frac{1}{b^2 d^2} \cdot \frac{F_n(\lambda) \delta V}{a} 2m \delta V \cos \angle$ and

shear stress $\tau = P \tan \angle \dots\dots\dots(4.4.4)$

therefore exist between adjacent layers. The expression for P can also be written;

$$P = k \rho_s \lambda F_n(\lambda) d^2 (dV/dy)^2 \cos \angle \dots\dots\dots(4.4.5)$$

by substituting $m = \frac{\pi d^3}{6} \rho_s$ and the values of a and δV from EQUATIONS (4.4.1) and (4.4.3). k is a constant.

Any momentum transfer due to fluid turbulence will be in addition to τ . There will also be dispersive pressure components of unknown magnitude in other directions.

The theory as outlined above is obviously weak because it neglects fluid-particle interaction. Bagnolds main contribution lies in experimental justification of EQUATION 4.2.1 for two limiting conditions of shear rate and within a range of concentrations of approximately 10 to 60%. The experimental work was confined to spheres of uniform diameter and of the same density as the fluid. The shear stress necessary to prevent movement of the inner cylinder of a coaxial viscometer was measured together with the dispersive pressure on the inner wall. The fluid viscosity was treated as a separate variable and was varied by a factor of 7 during tests.

At high shear rates (inertial region) $\tan \alpha$ seemed to approach a constant average value of 0.32 and the constant of EQUATION (4.2.12) could be calculated giving an empirical expression for P.

$$P = 0.042 (\lambda d)^2 (dV/dy)^2 \cos \alpha \dots \dots \dots (4.2.13)$$

The pressure P persisted even in the low shear rate (Viscous) region where the fluid viscosity becomes important and $\tan \alpha$ approached a constant average value of 0.75 giving an empirical expression;

$$\tau = 1.3P = 2.25 \lambda^{3/2} \mu_f dV/dy \dots \dots \dots (4.2.14)$$

where μ_f = fluid viscosity.

Both the stresses τ and P as nondimensional groups $\tau \rho_s d^2 / \lambda \mu_f^2$ and $G^2 = P \rho_s d^2 / \lambda \mu_f^2$ could be related to a non-dimensional shear rate group $N = \lambda^{1/2} \rho_s d^2 (dV/dy) / \mu_f$ over the entire range of tests. The numerical values of $\tan \phi$ and G^2 for the two limiting conditions are given in SECTION 4.2 .

4.5 COMPARISON OF RESULTS

The values of G^2 and $\tan \phi$ were calculated from EQUATIONS 4.2.2 and 4.3.5 for all test conditions regardless of the type of bed condition. This was done because it was not possible to accurately determine the interface between the fixed bed condition and the suspended region.

The value of λ was calculated from EQUATION 4.4.2 using a value of $C_0 = 0.65$ as determined experimentally by dry compaction of the sand and the average concentration \bar{C}_s obtained by integrating the concentration profiles for values of $C_s > 10\%$. The value of C_0 is reasonably constant for most naturally occurring sands. A friction factor of 0.016 was chosen from FIGURE III-1. The calculated values of G^2 and $\tan \phi$ are listed in TABLE IV-1.

$\tan \phi$ appears to be grouped according to the average solids concentration and flow rate whereas the value of G^2 remains fairly constant for all tests.

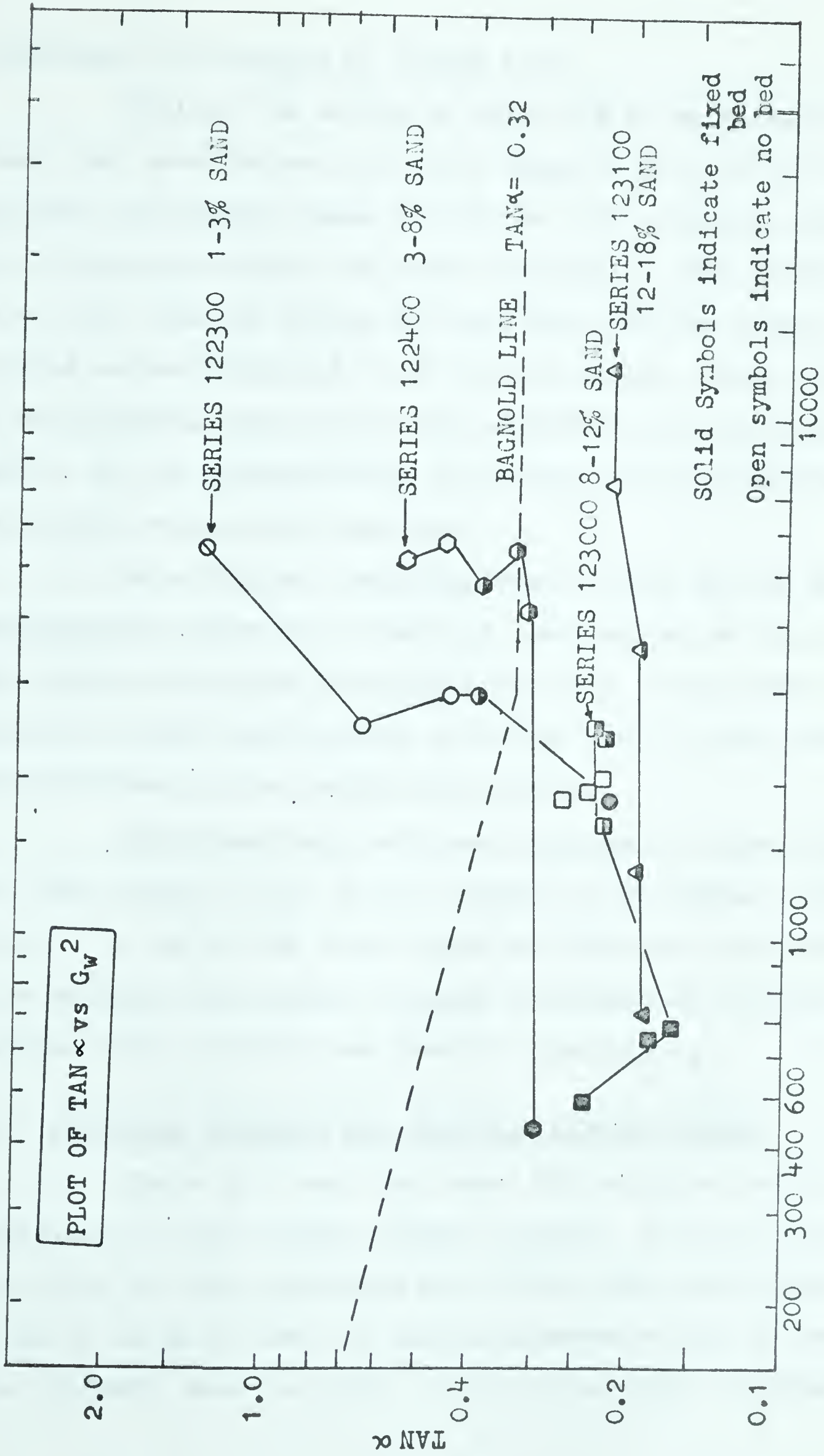
One obvious variable not adequately accounted for in this approach is the pipe wall concentration. It is most logically incorporated by calculating λ from the wall concentration instead of from the average mixture concentration. These values, G_w^2 , are plotted against $\tan \phi$ on

TABLE IV-1

Test No	Interface Inches from Pipe Center	Average Conc \bar{C}_s %	Conc at Floor $C_{s(w)}$ %	Tan α	$G^2 = \frac{\rho_s d^2 p}{\mu_f^2 \lambda}$	$G_w^2 = \frac{\rho_s d^2 p}{\mu_f^2 \lambda_w^*}$	Bed Type
122303	1.4	16.7	35.2	.44	7,300	2,960	N
122304	1.2	14.4	37.1	.40	9,200	2,970	M
122307	1.0	17.7	50.7	.22	12,000	1,890	F
122309	1.4	14.2	35.2	.66	7,200	2,520	N
122310	1.6	11.6	10.8	1.31	5,100	5,470	N
122401	0.8	17.2	37.1	.52	15,000	5,620	N
122402	0.8	17.5	37.1	.46	15,000	5,700	N
122403	0.8	19.6	42.9	.39	15,000	4,650	M
122404	0.8	20.2	44.8	.32	14,900	4,210	M
122405	0.8	18.9	39.0	.34	14,900	5,550	M
122406	0.8	23.8	62.7	.30	14,800	432	F
123001	0.4	23.7	58.7	.21	14,600	1,650	M
123002	0.4	20.4	50.7	.27	18,400	1,850	N
123003	0.4	21.3	50.7	.24	19,200	1,920	N
123004	0.4	22.4	50.7	.23	18,800	2,020	N
123006	0.4	21.8	58.7	.24	19,200	2,540	M
123007	0.4	21.4	54.7	.22	18,900	2,500	M
123008	0.6	25.5	62.7	.25	15,500	500	F
123009	0.4	27.2	66.8**	.18	18,100	640	F
123010	0.4	29.4	79.1**	.17	17,600	680	F
123101	0	25.5	62.7	.19	22,200	710	F
123102	0	22.8	48.7	.21	22,700	5,580	N
123103	0	25.2	54.7	.20	22,000	3,540	M
123104	0	23.1	44.8	.22	22,900	7,370	M
123105	0	22.8	35.2	.21	22,700	12,500	M
123106	0	24.5	60.7	.20	22,300	1,350	F

Note: $\lambda_w = \frac{1}{\left[\frac{0.65}{C_{s(w)}} \right]^{0.33} - 1}$

** Value of 62.7 used in calculating G_w^2



$$G_w^2 = \rho_s d^2 P / \mu_f^2 \lambda_w$$

FIGURE IV - 2

logarithmic coordinates in FIGURE IV-2.

Whereas the values of $\tan \alpha$ are by no means constant they nevertheless fall in a range of 0.17 to 1.3 which includes the Bagnold range of 0.32 to 0.75. The one value of 1.3 falling outside the upper range has a +10% solids zone only 0.36" from the bottom wall and also has the lowest average concentration of 11.6% in this region. This is close to the limiting range below which EQUATION 4.2.1 does not apply. At low concentrations the effect of the intergranular water will become more important.

An additional resisting shear stress due to the intergranular water will result in lower values of $\tan \alpha$ than values calculated from EQUATION 4.3.5. This could explain the trend toward higher values of $\tan \alpha$ at the lower concentrations in the bottom pipe region.

The fixed bed condition in general is identified by lower values of G_w^2 mainly because of the higher values of λ_w . In two of the tests where the fixed bed concentration exceeded the maximum assumed concentration of 65%, a maximum value of 62.7% was used to calculate λ_w .

4.6 EMPIRICAL EQUATION FOR CRITICAL DEPOSIT REGION

There is a very real need for reliable design equations in the critical deposit region. To be of any practical use such equations must follow the traditional trend of being in terms of design parameters such as pressure gradient, mean velocity, solids properties and transport

concentration.

Ansley (1963) found a strong correlation between the nondimensional groups, $(\frac{V_m D}{\nu} \cdot \frac{g D}{V_m^2})$ and $\Phi (= \frac{1 - i_w}{C_{s1w}})$

for his test data with 0.223 mm silica sand in a 2" pipe for the critical deposit region. His equation was:

$$\Phi = 2.45 \times 10^{-21} \left[\frac{V_m D}{\nu} \cdot \frac{g D}{V_m^2} \right]^{4.48} \dots (4.6.1)$$

The group on the right hand side is most conveniently expressed as the ratio of Re/FN^2 and represents the ratio of gravitational to viscous forces for the fluid flowing at velocity V_m in a pipe of diameter D . ν is the kinematic viscosity of the water. The sand properties such as size and density were constant during the tests and therefore do not enter in this equation.

A regression analysis of the present data with 0.355 mm sand in the 4" line yielded the expression;

$$\Phi = 1.44 \times 10^{-21} \left[\frac{DV_m}{\nu} \cdot \frac{g D}{V_m^2} \right]^{4.618} \dots (4.6.2)$$

with a high correlation coefficient of 0.935. The results of these tests are shown in FIGURE IV-3 together with the Ansley data, as a logarithmic plot of Φ vs (Re/FN^2) .

A line fitting both the 2" and 4" test data would have the form;

$$\Phi = K \times 10^{-21} \left[\frac{DV_m}{\nu} \cdot \frac{g D}{V_m^2} \right]^n \dots (4.6.3)$$

with $K = 1.44$ to 2.41

$n = 4.62$ to 4.48

The close agreement between these sets of data indicates that in the critical deposit region, ϕ and therefore the hydraulic gradient, is not critically dependent on particle size in the range 0.223 to 0.335 mm.

4.7 CONCENTRATION GRADIENT

A more general application of EQUATION 4.3.5 will require a prior knowledge of the concentration gradient for particular conditions of flow and transport concentration.

Inspection of the concentration profiles leads to the general observation that the concentration gradient is reasonably independent of flow rate for any given transport concentration in the critical deposit region.

The semi-log plots, FIGURES III-2 to 5, show a fairly well defined straight line relation for the low concentration tests as well as for the upper pipe portions of the high concentration tests. This is in agreement with the findings of other workers (Schmidt, 1925; O'Brien, 1933; Vanoni, 1946; Rouse, 1950) who studied the distribution of fine sediment in turbulent flow. Durand (1952) concluded from his tests that the concentration gradient is independent of mean velocity for sand sizes greater than approximately 2 mm. For smaller sizes the gradient changes with mean velocity.

The upper part of each curve was said to satisfy Rouse's (1950) equation;

$$C_s = K \left[\frac{D}{y'} - 1 \right]^z \quad (4.7.1)$$

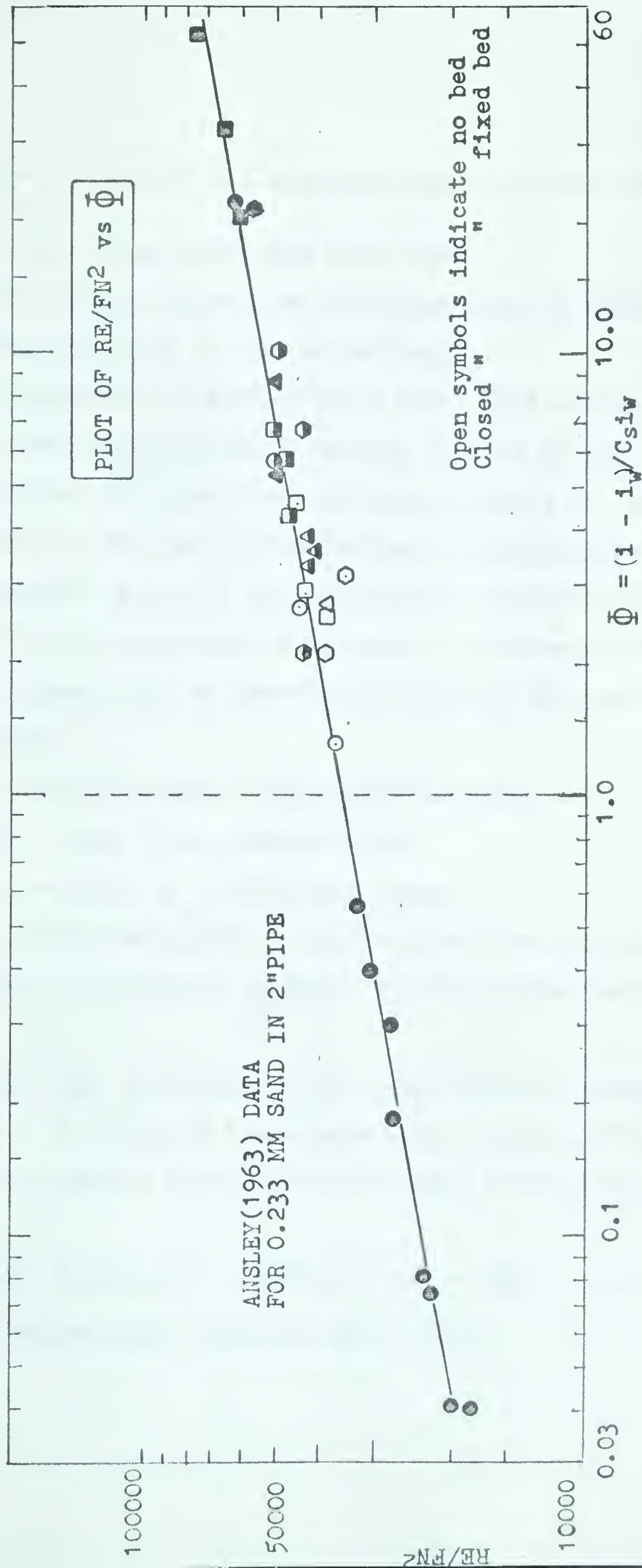


FIGURE IV - 3

where $z = \frac{K'}{V_m}$. K and K' are constants and C_s is the concentration at y' feet above the pipe floor.

No attempt appears to have been made to study the concentration gradient in the bottom region.

Inspection of FIGURE III-6 shows that moving beds have pipe floor concentrations varying from 40 to 60%. The concentration at the pipe floor although subject to the largest error is the only known boundary condition and it appeared logical to use it as a reference concentration. The deviation from the semi-log relationship at higher concentrations also appeared to be associated with the increased depth of this region.

A semi-log plot of $C_s/C_s(w)$ vs y'/y'_B
where, $C_s(w)$ = pipe floor concentration

y'_B = depth of +10% solids region

C_s = concentration y' inches from the interface
showed promise in grouping together all the concentration gradients.

One test from each of the test series is plotted in FIGURE IV-4. In spite of the apparent high degree of scatter, a regression analysis of the 28 data points yielded the equation:

$$\log [C_s/C_s(w)] = 0.74(y'/y'_B) - 0.74 \dots (4.7.2)$$

with a high correlation coefficient of 0.95.

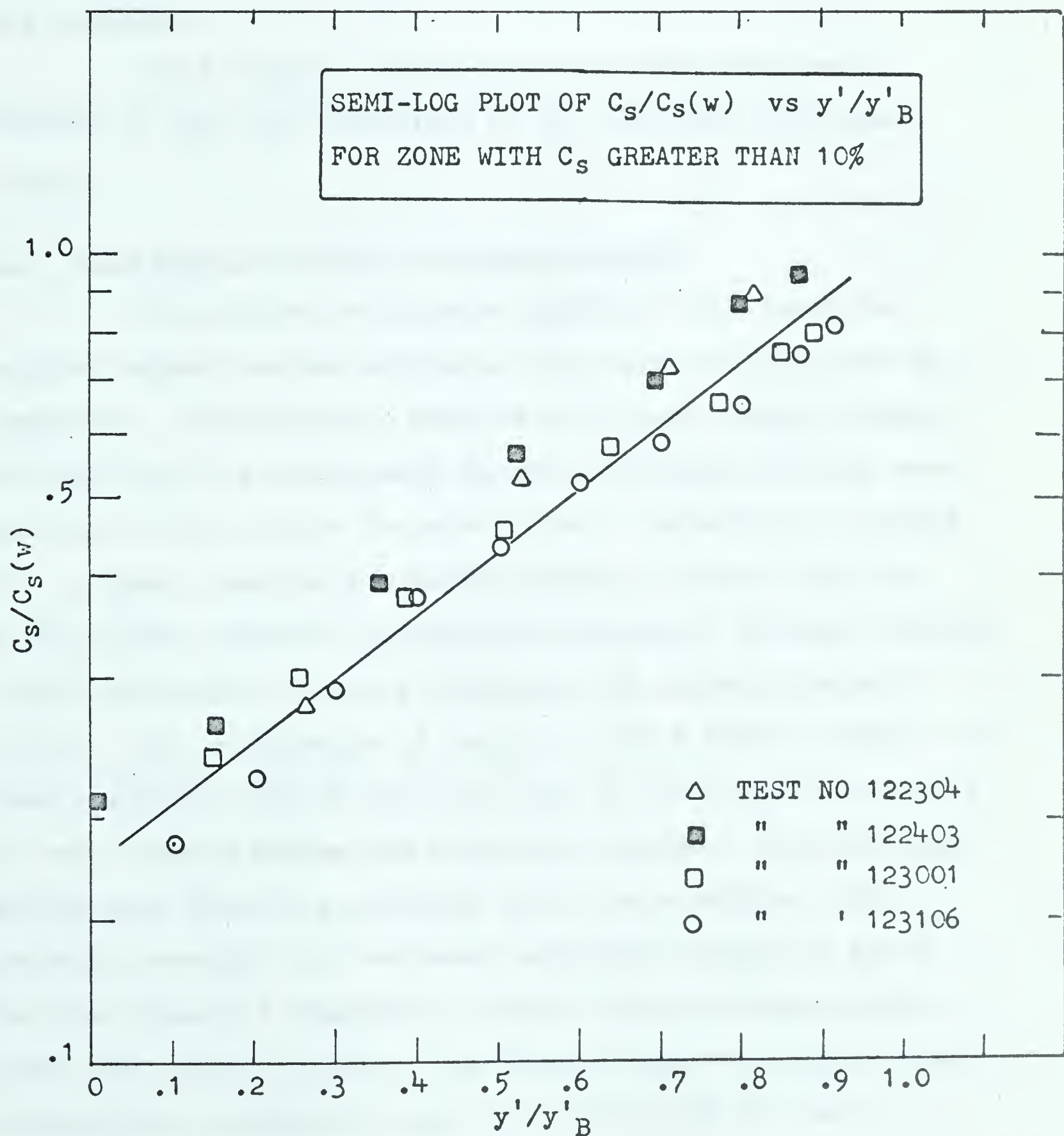


FIGURE IV - 4

CHAPTER V

DISCUSSION OF RESULTS

5.1 GENERAL

This chapter briefly discusses the analyses of CHAPTER IV and the limitations of the equations developed therein.

5.2 FLOW EQUATION BASED ON BAGNOLD CONCEPT

The success with which EQUATION 4.3.5 could be applied depends on how accurately the value of $\tan \alpha$ can be predicted. Unfortunately Bagnold only gives average values of $\tan \alpha$ for his experiments thereby precluding further comparison of the scatter to be expected. Inspection of FIGURE IV - 2 shows remarkably constant values of $\tan \alpha$ (0.17 to 0.27) in the transport condition of practical interest (SERIES 123000 and 123100) where a dense zone of appreciable depth exists. The calculation of $\tan \alpha$ for fixed beds is subject to some inaccuracy due to the fact that no differentiation could be made between moving and stationary solids. The stationary solids were therefore included in the calculation. This probably accounts for the lower calculated values of $\tan \alpha$ for the fixed bed condition. Higher values of $\tan \alpha$ would bring the points closer to the Bagnold line. Excluding these points gives a narrower range of 0.20 to 0.27 for $\tan \alpha$.

Values of G_w^2 are subject to large errors and no reliable classification of the flow regime can be made based on its numerical value. Bagnold's classification would place all the points in the transition region. The fixed beds can be associated with lower values of G_w^2 and therefore can be said to fall closer to the "Viscous" region.

5.3 EMPIRICAL EQUATION FOR CONCENTRATION GRADIENT

EQUATION 4.7.2 shows promise as a practical means of predicting the concentration gradient above the pipe floor and was derived with the data from one fixed and three moving bed conditions. Four values of y'_B (depth of +10% solids region) and $C_s(w)$ were used and the equation therefore adequately reflects the range of conditions tested. y'_B however never extended above the pipe centerline and further testing will be required to establish its validity in this range.

Further tests may show that other variables such as overall solids transport concentration, pipe configuration and possibly flow rate should be accounted for in this equation.

5.4 EMPIRICAL EQUATION BASED ON CONVENTIONAL EXTERNAL PARAMETERS

EQUATION 4.6.2 provides a good means of predicting pressure drops in terms of average transport concentration. It does not, however, include the properties of the solids nor does it present a logical way in which to do so. Its application will therefore always be limited to exactly the range of experimental conditions.

CHAPTER VI

CONCLUSIONS AND RECOMMENDATIONS

6.1 CONCLUSIONS

Development of the Gamma-ray scanner has made possible concentration gradient measurement without disturbing the fluid flow. The test results showed the concentration gradient to be rather insensitive to flow rate in the critical deposit region. In general, moving beds could be identified by pipe floor concentrations of 40 to 60%. Fixed beds generally were associated with pipe floor concentrations exceeding 60%. These pipe floor concentrations are subject to large errors of approximately $\pm 11\%$ solids.

These concentration gradients showed that solids are transported in the lower pipe regions with clear water occupying 25 to 75% of the flow area. On the basis of this observation a simplified model of the flow mechanism could be formulated. The pipe wall shear stress in the top water and low solids concentration region was estimated from a friction factor. The pipe wall shear stress in the bottom region was estimated from the Bagnold "dispersive stress" concept which relates this shear stress to the submerged weight of the solids and a coefficient of friction ($\tan \phi$). The values of $\tan \phi$ from these experiments were found to fall close to the predicted values and were reasonably constant (0.20 to 0.27)

for conditions where the bottom high concentration zone exceeded depths of approximately 1.5".

This approach has considerable potential in that it provides a logical way of being extended to flow systems with different pipe sizes, fluids and particles and is not subject to the extensive experimental verification of the purely empirical approach.

6.2 RECOMMENDATIONS

It is recommended that:

- (a) concentration gradient measurement be carried out with a narrower gamma beam and possibly in larger pipes to increase the accuracy of the floor concentration measurement.
- (b) tests be conducted over a wider range of particle size and density to establish the extent to which $\tan \alpha$ changes.
- (c) active work be carried out to develop a reliable method of determining velocity profiles in solids-fluid mixtures.

LIST OF REFERENCES

LIST OF REFERENCES

1. Ansley, R.W. "Hydraulic Transport of Fluidized Solids in Open-Channel Flow;" - Ph.D. Thesis, University of Alberta, October 1963.

2. Babcock, H.A. "The State of the Art of Transporting Solids in Pipelines;" - paper presented at the American Institute of Chemical Engineers' National Meeting, Denver 1962.

3. Bagnold, R.A. "Experiments on a Gravity-Free Dispersion of Large Solid Spheres in a Newtonian Fluid Under Shear;" Proc. Roy. Soc. A, 225, 49 (1954).

4. Bagnold, R.A. "Flow of Cohesionless Grains in Fluids;" Phil. Trans. A, 249, 235 (1956)

5. Banister J.R. "Particulate Dynamics Research at Sandia Laboratory;" Proc. of the 6th Midwestern Conference of Fluid Mechanics, University of Texas, 1959.

6. Blatch, N.S. "Water Filtration at Washington D.C., Discussion;" - ASCE Trans., Vol. 57, Dec. 1906.

7. Blench, T. "Regime Behaviour of Canals and Rivers;" Butterworth's, 1957.

8. Chamberlain, A.R.;
 Yotsukura, N.;
 Karaki, S.S.;
 Albertson, M.L. "Transport of Material by Fluids in Pipes;" - Paper presented to ASCE Hydraulics Division Conference, Seattle, August 1960.

9. Condolios, E.;
 Chapus, E.E. "Transporting Solid Materials in Pipelines;" - Chemical Engineering, June 1963.

10. Danel, P.F. "Transportation of Sand and Gravel Discussion;" ASCE Trans., Vol. 104, 1939.

11. Daniel, S.M. "Concentration and Velocity Measurement in Horizontal Flow of Solid-Liquid Suspensions;" - M.Sc. Thesis, University of Saskatchewan, April 1963.
12. Daniel, S.M.; Shook, C.A. "Flow of Suspensions in Pipelines;" Paper presented at 14th Canadian Chemical Engineering Conference, October, 1964.
13. Durand, R. "The Hydraulic Transportation of Coal and Solid Material in Pipes;" - Paper presented at The London Colloquium of the National Coal Board, Dec. 1952.
14. Friedlander, S.K. A.I. Ch. E. Journal, 3, 3, P. 381 (1957)
15. Govier, G.W.; Charles, M. "The Hydraulics of the Pipeline Flow of Solid-Liquid Mixtures;" - The Engineering Journal, August 1961.
16. Hazen, A.; Hardy, E.D. "Works for the Purification of the Water Supply of Washington D.C.;" - ASCE Trans., Vol. 57 Dec. 1906.
17. Hinze, J.O. "Momentum and Mechanical-Energy-Balance Equations for a Flowing Homogeneous Suspension With Slip Between the Two Phases;" Appl. Sci. Res. Section A . Vol 11.
18. Howard, C.D.D. "The Effect of Fines on the Pipeline Flow of Sand-Water Mixtures;" - M.Sc. Thesis, University of Alberta, October 1962.
19. Howard, G.W. "Transportation of Sand and Gravel in a Four-Inch Pipe;" - ASCE Trans., Vol. 104, 1939.
20. Hunt, J.N. Proc. Roy. Soc. "A" 224, 1158, (1924).
21. Newitt, D.M.; Richardson, J.F.; Abbott, M.; Turtle, R.B. "Hydraulic Conveying of Solids in Horizontal Pipes;" - Transactions of The Institute of Chemical Engineers, Vol. 33, 1955.

22. O'Brien, M.P.;
Folsom, R.G. "The transportation of Sand in Pipelines;" University of California Publications in Engineering, Nov. 1937.
23. O'Brien, M.P.;
Folsom, R.G. "Transportation of Sand and Gravel Discussion;" - ASCE Trans., Vol. 104, 1939.
24. Schmidt, W. "Der Massenaustausch in Freier Luft und Verwandte Erscheinungen;" Hamburg: H. Grand., 1925.
25. Shook, C.A. Ph.D. Thesis, University of London (1960).
26. Rouse, H. "Engineering Hydraulics;" John Wiley and Sons, 1950.
27. Streeter, V.L. "Handbook of Fluid Dynamics;" McGraw-Hill, 1961.
28. Thomas, D.G. "Transport Characteristics of Suspensions;" American Institute of Chemical Engineering Journal, Vol. 8, No. 3, July 1962.
29. Vanoni, V.A. "Transportation of Suspended Sediment by Water;" ASCE Trans., Vol. 111, 1946.
30. Worster, R.C. "The Hydraulic Transport of Solids;" Proc. Colloq. on Hydraulic Transportation, London, Nov. 1952.
31. "The Transportation of Solids in Steel Pipelines;" Colorado School of Mines, Research Foundation, Inc., Golden, Colo., 1963.
32. "Transport of Materials by Fluids in Pipes;" ASCE Hydraulics Div. Conference, Seattle, Aug. 1960.

PART B

PART BTABLE OF CONTENTS

	<u>PAGE</u>
CHAPTER I	105
CHAPTER II	106
CHAPTER III	112
FIGURE II-1	107a
FIGURE II-2	108
FIGURE III-1	116
FIGURE III-2	117
FIGURE III-3	118
FIGURE III-4	119
FIGURE III-5	120
FIGURE III-6	121
FIGURE III-7	122
PLATE II-1	110a

PART B
CHAPTER I

INTRODUCTION

This investigation has not been brought to any satisfactory conclusion and the purpose of this section is simply to report the investigation and present the test results.

A non-Newtonian clay suspension was used as the carrying fluid in the pipeline and open channel flow experiments conducted by Ansley (1963). It has been claimed that clay-water mixtures up to certain concentrations boost the sand carrying capacity of a given installation. An extensive investigation by Ansley showed that the Bingham Model could be used to describe the rheological behaviour of the slurry. This approach has also been taken by Thomas (1962) in studying the flow of thorium oxide, kaolin and other suspensions in small diameter pipes.

The simplest possible case of single particles settling in a still fluid appeared to be a logical starting point.

PART B
CHAPTER II

EXPERIMENTAL

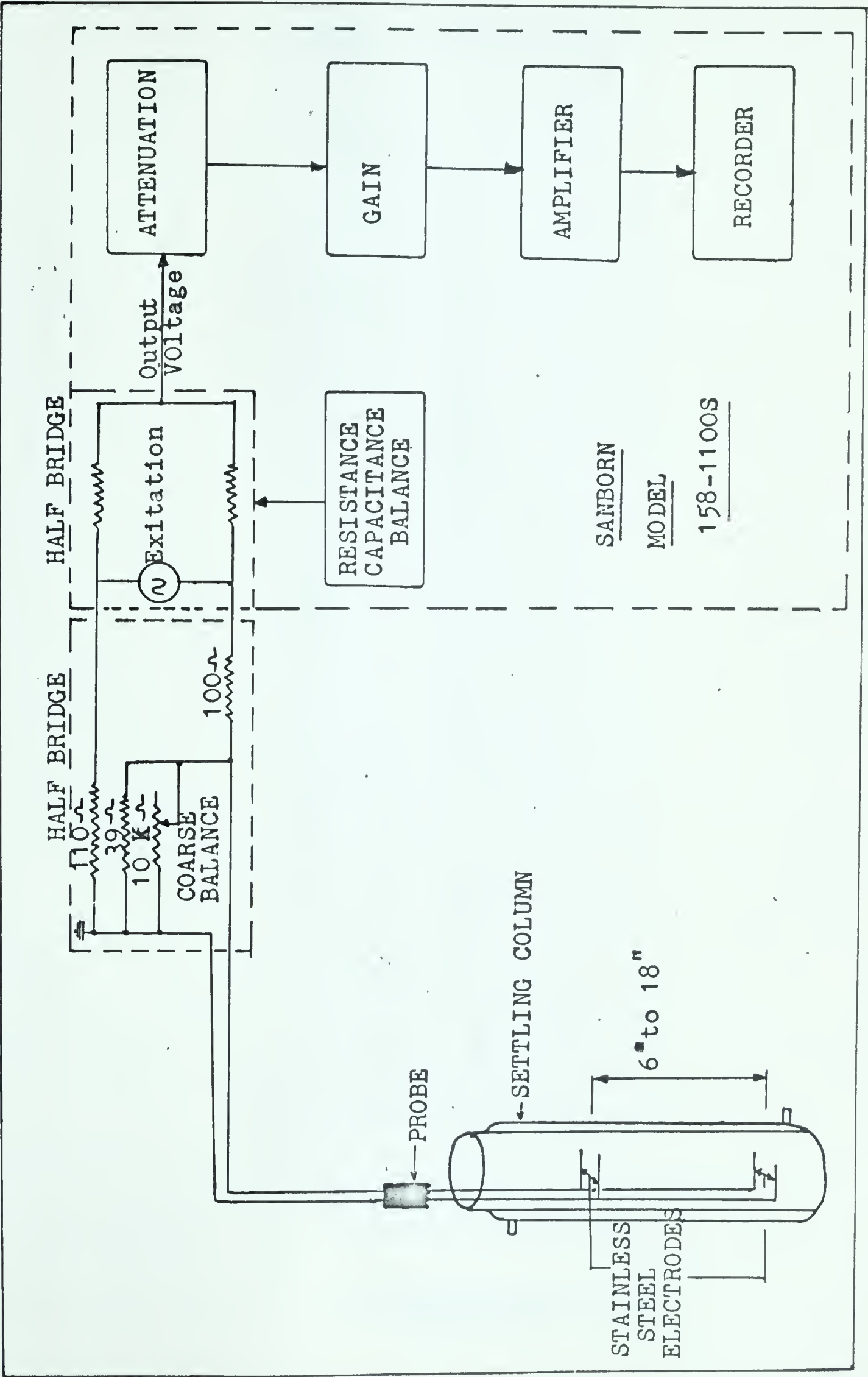
The high turbidity of the clay suspension necessitated development of an electrical technique to replace visual observation of settling particles. The following is a description of the apparatus used.

Tests were conducted in a 2 3/8" diameter by 3' long water jacketed glass column. Settling rates in clear water were obtained by measuring the time taken by single particles to fall between two marks spaced at 2 to 2½ ft. A stop watch measuring to one tenth of a second was used. The first mark was located 9½" below the liquid surface. No significant difference was observed when the marks were located at greater depths, thus indicating that the observed rates could be regarded as the terminal settling velocity of the single particles. A large number of results with the largest particles in water had to be discarded because particles tended to bounce off the walls. For the majority of the particles the column diameter was considered large enough to neglect wall effects. The test temperature was kept constant by circulating water through the column jacket. Settling rates in the clay slurry were obtained by detecting the instantaneous change in conductivity as the particles passed between two sets of electrodes located 6" to 18" apart in the

column. After numerous trials with different types of electrodes, an electrode consisting of two 0.050 inches thick stainless steel wires $1\frac{1}{2}$ " long and spaced at $\frac{3}{8}$ inches in a horizontal plane was found to be satisfactory. The electrical circuit is shown in FIGURE II - 1.

The two sets of electrodes were connected in parallel across one leg of a resistance bridge. The other half of the resistance bridge and the amplification and recording of the AC voltage proportional to the conductivity change between the electrodes was provided by a Sanborn Model 158 - 1100 S amplifier. Resistance and capacitance controls permit balancing of resistance bridge over a wide range of conductivities between the probes. Best results were obtained with minimum amplifier attenuation and occasional adjustment of the resistance and capacitance balance.

A sharp "kick" was recorded whenever a particle passed between either electrode. The exact distance between two adjacent "kicks" together with a fast recorder chart speed gave an accurate and convenient means of calculating particle settling rates. A fair number of "drops", especially with the finer particles sizes, were useless because of the particle missing one or both electrodes. However, a large number of particles could be dropped in a short time so that this was not a serious disadvantage. FIGURE II - 2 shows typical results obtained on the recorder chart. Particle sizes in the range 4 to 16 mesh performed the best with these particular electrodes.



SIMPLIFIED CIRCUIT DIAGRAM

FIGURE II - 1



6 MM BEADS IN 1.242 SG CLAY SLURRY
DISTANCE, 1.5 FT
CHART SPEED, 10 MM PER SEC

TYPICAL RECORDER CHART
FIGURE II -2

Difficulty was experienced in getting readings with single particles smaller than approximately 30 mesh even when smaller electrode spacings were used. Quite a good response was obtained however when a number of particles were dropped at the same time. The maximum weight introduced at one time never exceeded 0.1 gm, thus making it highly unlikely that these readings differed significantly from the terminal settling velocity.

The clay slurry tended to settle in the column and hydrometer readings were taken at frequent intervals at the surface and the slurry was mixed whenever this value dropped below the required value. Hydrometer readings were also taken of samples withdrawn between the electrodes to establish the exact concentration gradient in the column. An average value of the slurry concentration between the electrodes was used in determining the drag coefficient and apparent kinematic viscosity of the fluid. Settling rates were calculated from 10 to 50 readings.

MATERIALS

Two types of silica sand were used.

TYPE 1 SOLIDS - ATHABASCA SAND

This sand has a specific gravity of 2.65 and was obtained from the tailings dump of a tar sand extraction pilot plant at Mildred Lake, Alberta. A large number of pumping tests in a 1" and a 2" pipeline were conducted with this sand at the University of Alberta.

TYPE 2 SOLIDS - OTTAWA SAND

This sand has a 2.64 specific gravity and conformed to ASTM C109 standards. No attempt was made to measure the geometric properties of either of these sands.

Settling tests were done with narrow size fractions obtained by careful sieving between adjacent sizes of screens. All screen fractions were further wet screened by hand to remove under-size material. In the case of the Athabasca sand this procedure was essential since large amounts of fines (-325M) were retained with all the fractions below 100 Mesh.

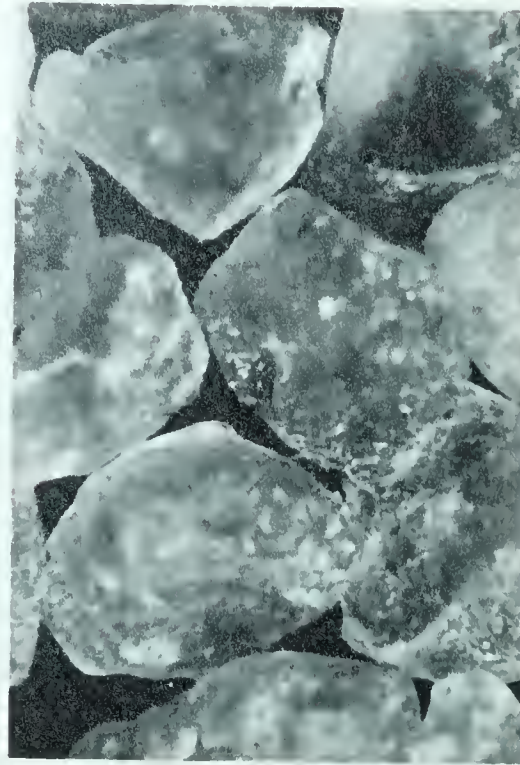
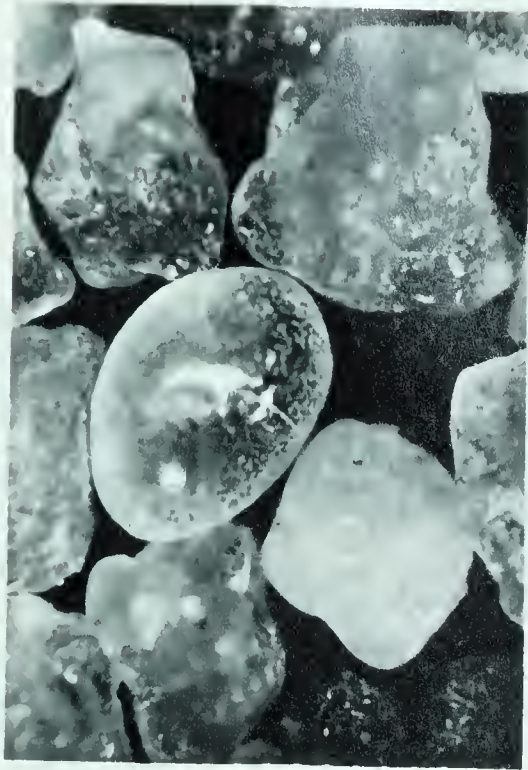
For the Ottawa sand - 18, 20, 25, 30, 35, 40, 45, 50, 60, 70, 80, and 100 Mesh (U. S. Series) fractions were prepared. For the Athabasca sand all fractions down to 200 Mesh were prepared. i.e. 4, 8, 12, 16, 18, 20, 25, 30, 35, 40, 45, 50, 60, 70, 80, 100, 120, 140, 170, 200 Mesh (U. S. Series). PLATE II-1 shows photomicrographs of some of these size fractions.

TYPE 3 SOLIDS - GLASS BEADS

3mm, 4mm, and 6mm diameter, approximately spherical beads with specific gravity of 2.65 manufactured by the Fisher Scientific Company constituted the largest size particles used in the settling tests.

TYPE 4 SOLIDS - GLASS BEADS

Seven sizes - 8-10; 14-16; 16-20; 20-24; 32-35 Taylor Mesh fractions, No. 2 (average diameter, 0.125") and No. 2½ (average diameter 0.098") were used as supplied by



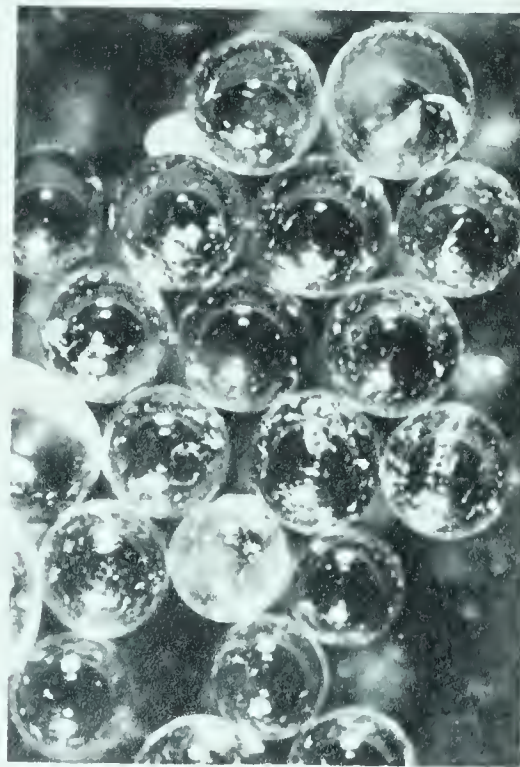
SCALE

0
0.1mm
1.0mm

25 TO 30 MESH

20 TO 25 MESH

TYPE I SOLIDS



SCALE

0
0.1mm
1.0mm

16 TO 20 MESH

30 TO 35 MESH

TYPE 4 SOLIDS

PHOTO-MICROGRAPHS OF SAND [TYPE I] AND BEADS [TYPE 4]
PLATE II - I

the manufacturer at that time, Potters Brothers, Inc., Carlstadt, New Jersey, U.S.A. Density determinations (Davies, M.Sc. Thesis, 1959) give values ranging from 2.47 to 2.555 for various size fractions of these beads. An average value of 2.51 was used for all size fractions rather than using the individual values obtained for each fraction.

The table below lists the density values obtained by Davies.

<u>DENSITIES OF GLASS BEADS - TYPE 4</u>	
<u>SIZE</u>	<u>DENSITY</u> <u>gm/cc</u>
No. 2	2.508
14/16 Mesh	2.520
16/20 Mesh	2.555
20/24 Mesh	2.515
32/35 Mesh	2.470
Average	<u>2.514</u>

CLAY

The clay used in the tests was obtained from a local ceramics company. This material was used as the carrying fluid in a large number of sand pumping tests conducted at the University of Alberta. Rheological investigation showed that water slurries of this material exhibited Bingham Plastic behaviour. The bulk of the clay is less than 200 mesh in size using wet sieving techniques. The specific gravity was reported as 2.65. Preparation of several slurries by mixing an accurately weighed amount of dry clay with a known volume of water indicated this value to be correct. Other properties of this clay are discussed by Ansley (1963).

PART B
CHAPTER III

EXPERIMENTAL RESULTS

Tests were conducted with four fluids. Clear water tests were conducted to enable comparison of the accuracy of the electrode method with visually observed settling rates. Tests at three clay slurry concentrations of 8 volume % solids (1.132 SG), 11.5 volume % (1.189 SG) and 14.5 volume % (1.242 SG) covered the region of interest. Types 1, 2 and 3 solids were used in all the tests. Type 4 solids (2.51 SG glass beads) were used only with the 1.242 SG slurry when it became necessary to gain data over a wider range of Reynolds numbers. All the original experimental readings are listed in APPENDIX D, TABLE D-2 together with the kinematic viscosity and yield stress of each clay slurry.

The following will act as a guide to the test conditions:

Clear Water.....	Tests No. 1.01 to 1.05
1.189 SG clay slurry..	Tests No. 5.01 to 7.03
1.132 SG clay slurry..	Tests No. 8.01 to 9.03
1.242 SG clay slurry..	Tests No. 10.01 to 12.07

All the original test data were punched on IBM cards and a programme was set up to calculate the following:

Average settling rate, W , ft/sec = $\frac{\text{settling distance, ft}}{\text{chart distance, mm} / \text{chart speed, mm/sec}}$

Standard deviation of settling rate, s_w

Drag coefficient, $C_D = \frac{4}{3} \left(\frac{gd}{W^2} \right) \left(\frac{S_s - S_w}{S_w} \right)$

Standard deviation of $C_D = 2s_w C_D / W$

Reynolds Number, $Re = \frac{dW\rho_f}{\mu}$ for water

$$= \frac{dW\rho_f}{\eta} \text{ for clay slurry}$$

Standard deviation of Reynolds Number = $s_W Re/W$

Froude number, $Fr = W/\sqrt{gd}$

Modified Froude number = $W/\sqrt{gd(S_s/S_W-1)}$

Hedstrom number = $\tau_y d^2 \rho_f / \eta^2$

The computer output format (APPENDIX TABLE D-1) lists these quantities together with the test number, average solid sizes and the fluid specific gravity for each test.

CLEAR WATER SETTLING TESTS

Clear water settling tests were conducted by visual observation of particles and by the electrode method. Visual test numbers are 1.01 to 1.15, 3.01 to 4.02. Electrode test numbers are 2.01 to 2.07. Comparison of average settling rates and standard deviations show close correspondence between the two methods. Tests 1.01, 2.05 and 1.06, 2.06 gave average values within 5% of one another. The standard deviations for these fractions were quite high. i.e. 20.8% and 24.5% for the visual method and 27.7% and 15.8% for the electrode method indicating the effect of varying particle sizes and shapes within sieve fractions. The electrode method gives less scatter for the smaller sieve fraction probably because the readings give settling rates for a small cluster of particles rather than individual particles. Comparison of these results with that of other workers is probably most conveniently achieved by the conventional non-dimensional plot of Reynolds

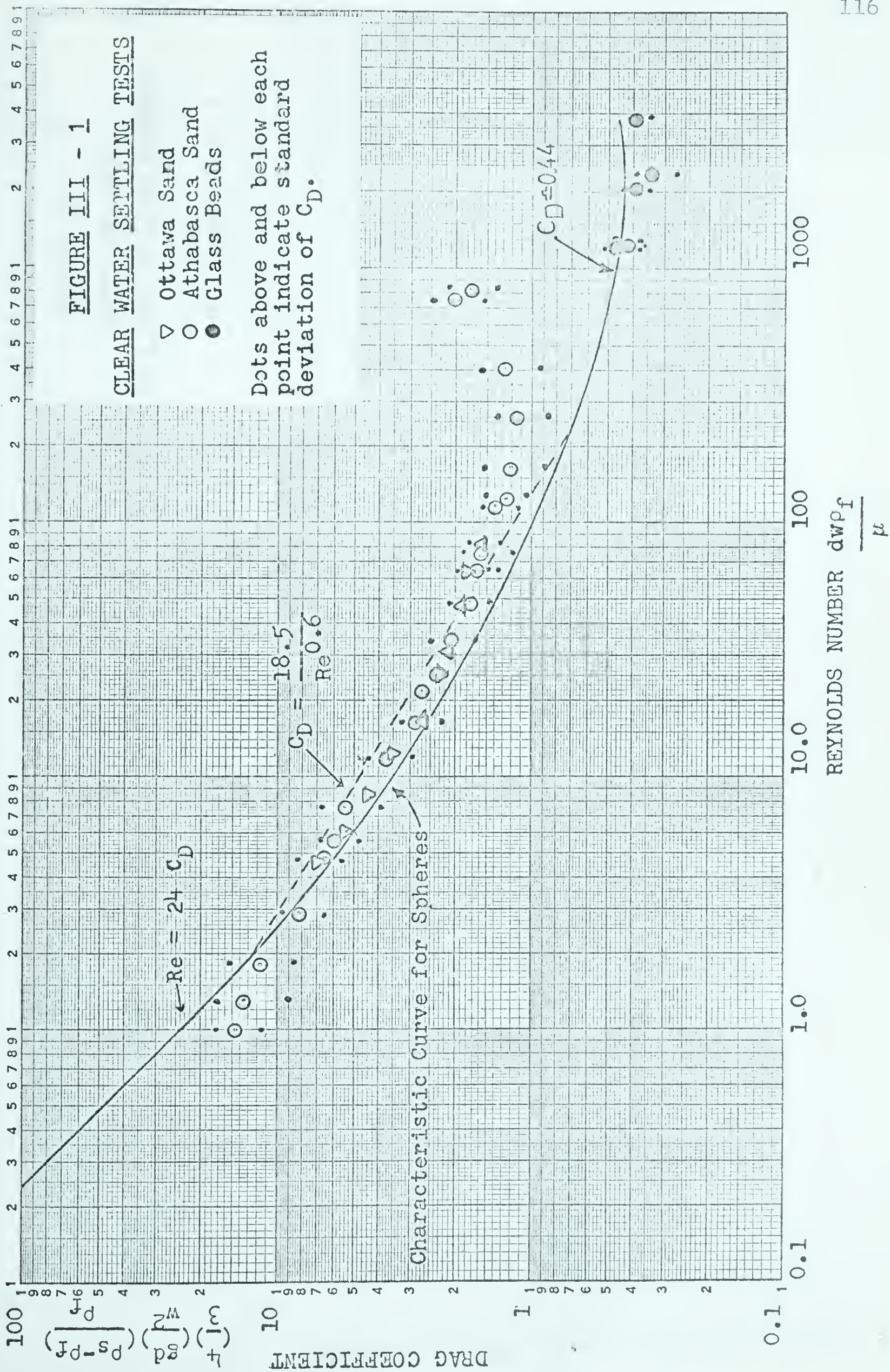
number against the Drag coefficient C_D . These values are plotted in FIGURE III-1. The standard curve for spheres settling in water is also shown on this plot. The test data follow this standard curve fairly well up to Reynolds numbers of 20 to 50 with only minor deviations for the smaller sand sieve fractions. There is also little difference between the Athabasca and Ottawa Sand in this range. The smoothing curve through the points shows a tendency to level off at a drag coefficient of approximately 1.5, which conforms to the observation of other workers.

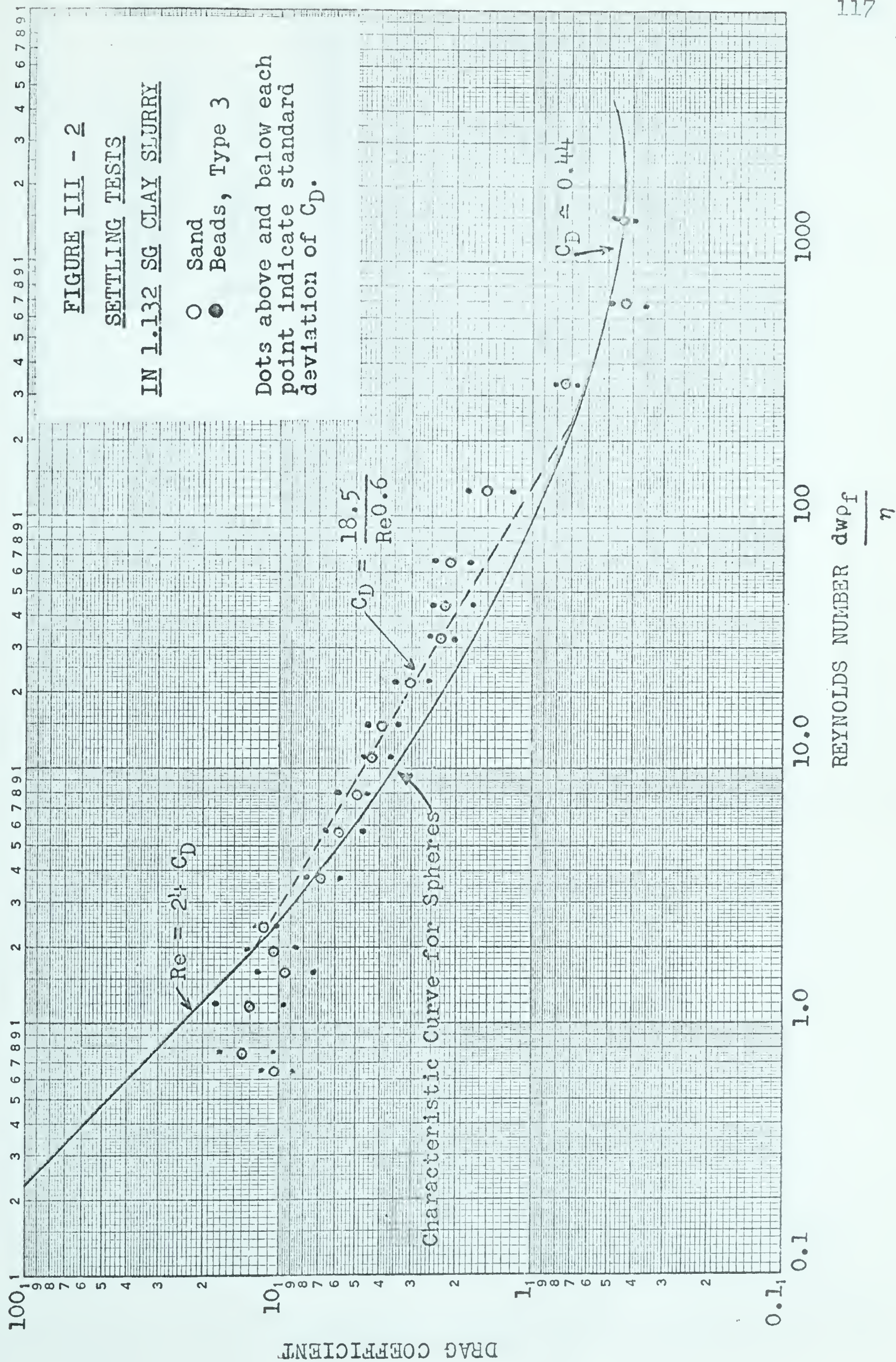
SETTLING TESTS IN CLAY SLURRIES

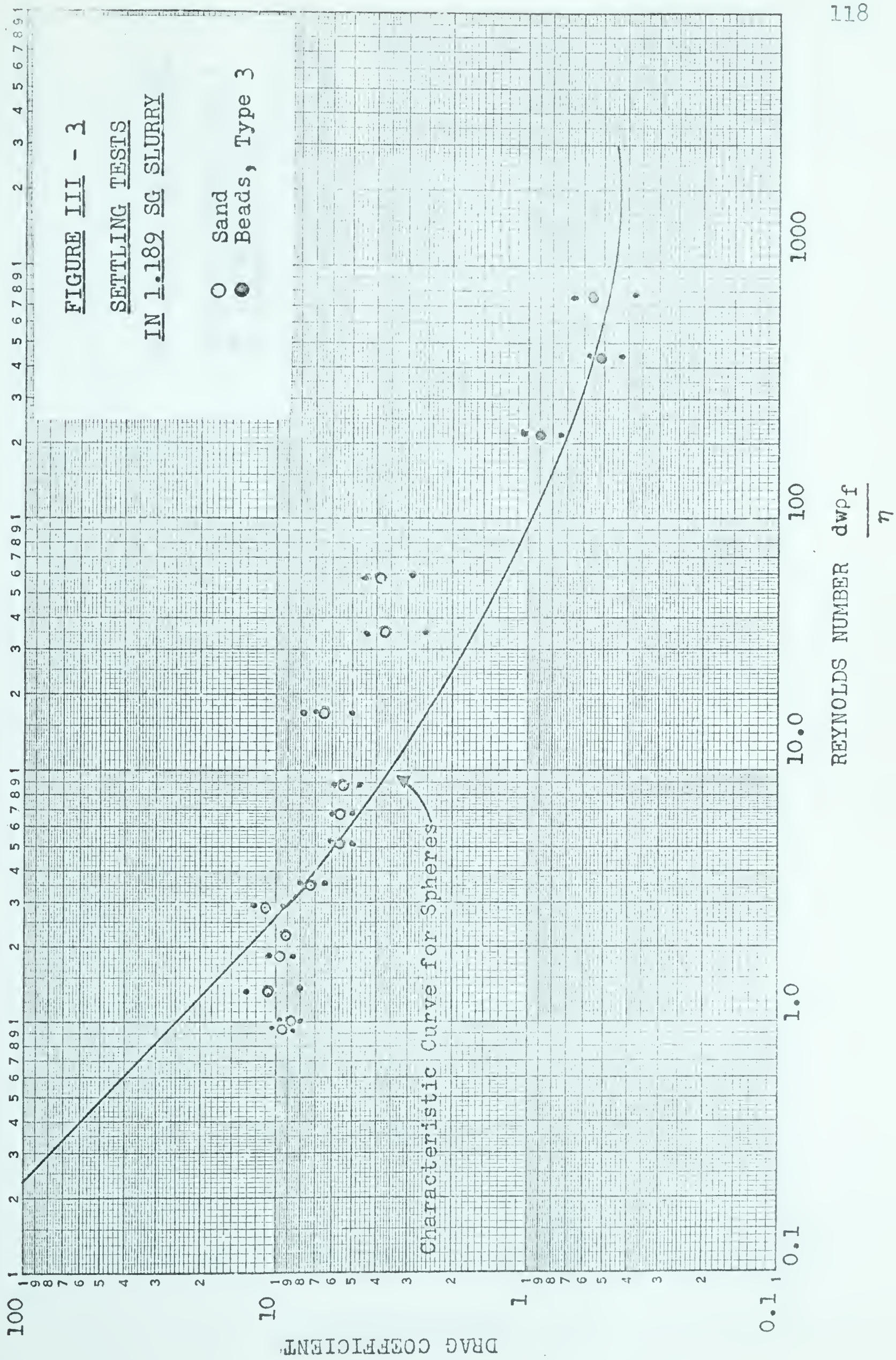
Test results are presented as plots of C_D vs Re in FIGURES III-2 to 5. FIGURE III-2 shows little deviation from the clear water plot for Reynolds numbers greater than 7. FIGURES III-3 and 4 show a marked deviation from the clear water line for Types 1 and 2 solids and for Reynolds numbers greater than 10. An interesting observation is that C_D for the glass spheres (Type 3) always falls on the clear water line. These plots do not give any well defined order to data for the higher clay concentrations. Dimensional analysis shows that

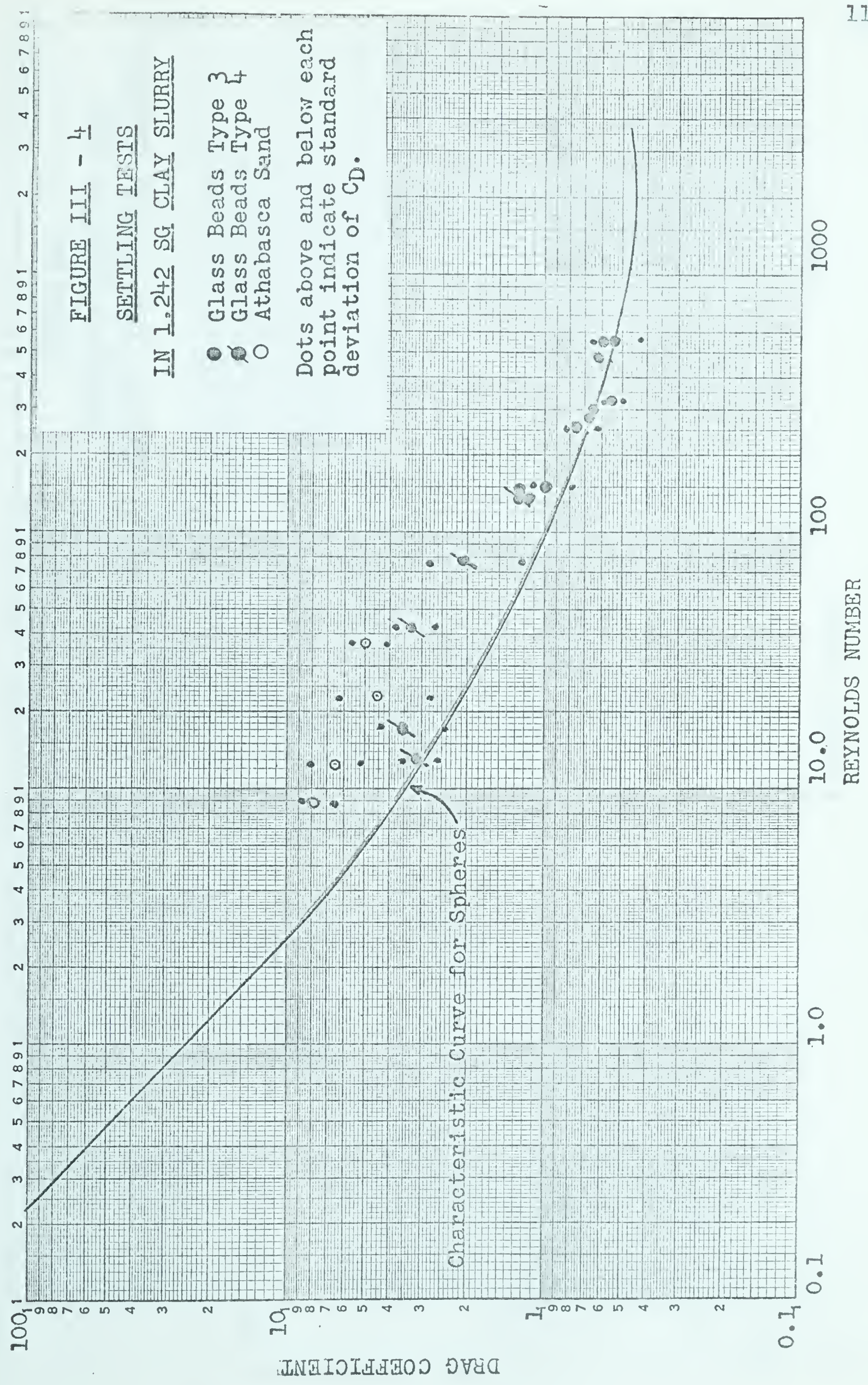
$$C_D = \text{FN}(\text{shape}, Re, He, \frac{\rho_s - \rho_f}{\rho_f})$$

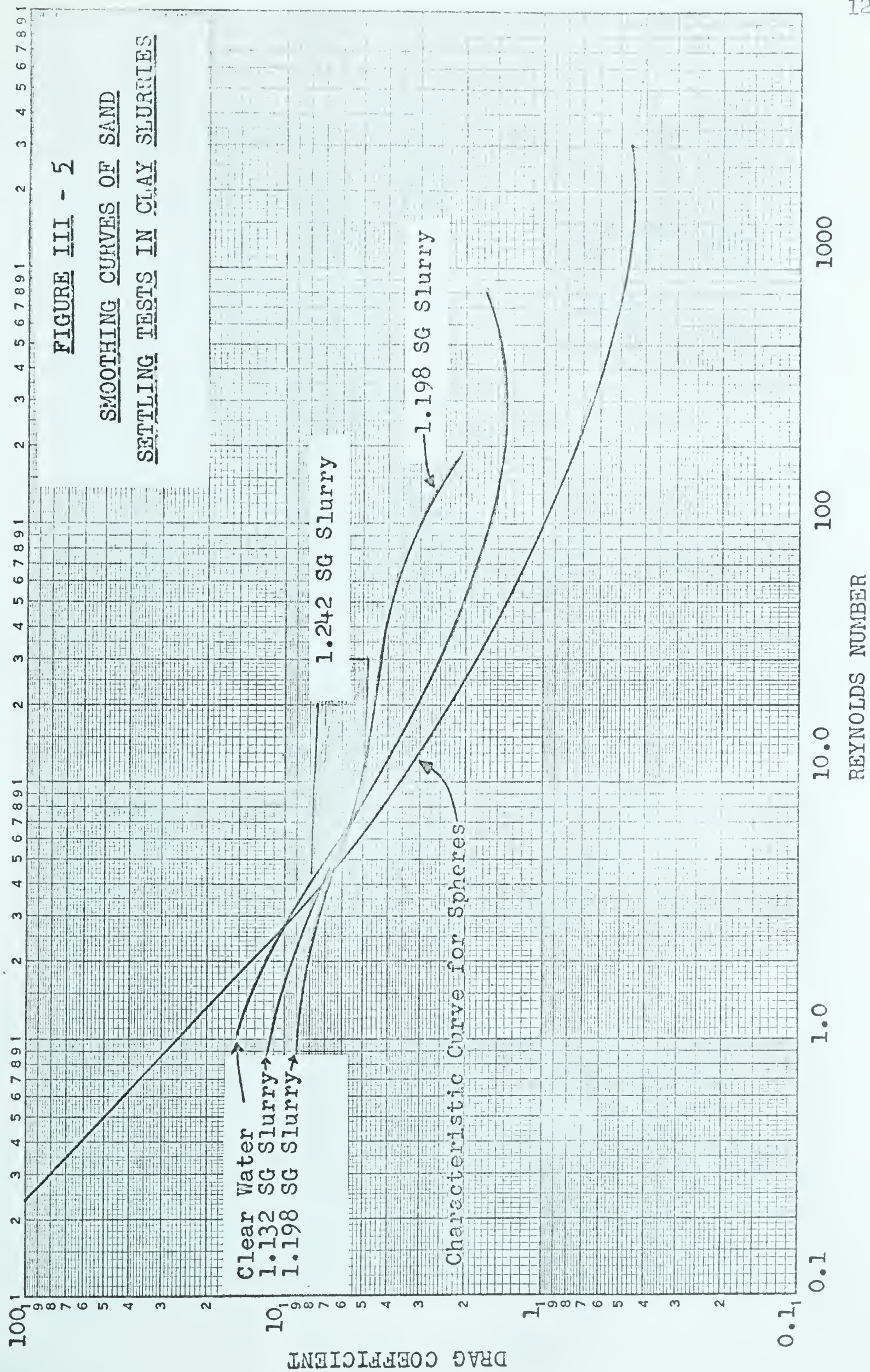
FIGURE III-6 is a logarithmic plot of He vs Re and shows well defined relation for one clay concentration. A fairly orderly grouping results from a logarithmic plot of Re vs He/C_D as shown in FIGURE III-7. The fourth nondimensional group $\frac{\rho_s - \rho_f}{\rho_f}$ appears to separate the test data into a series of parallel lines.

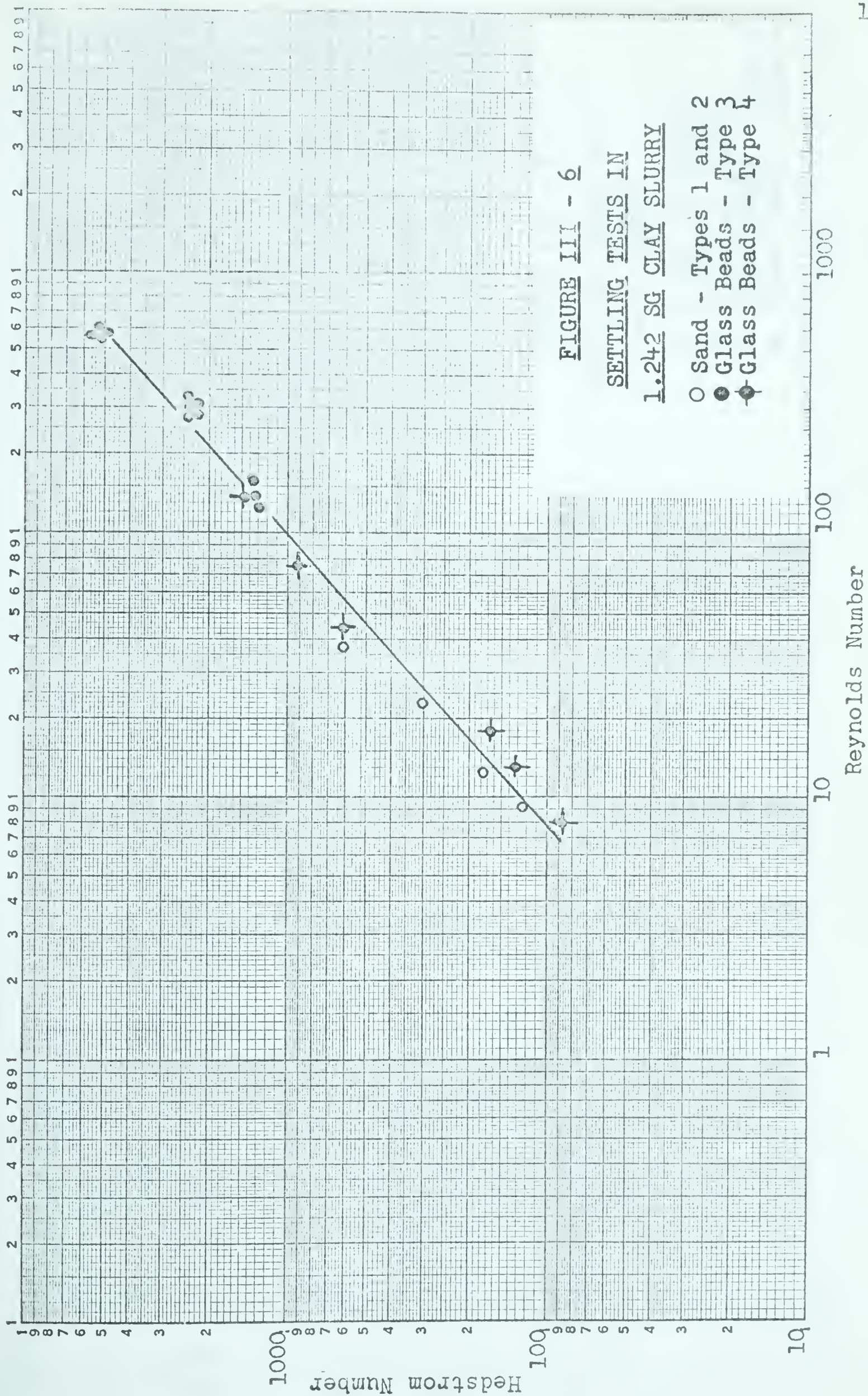


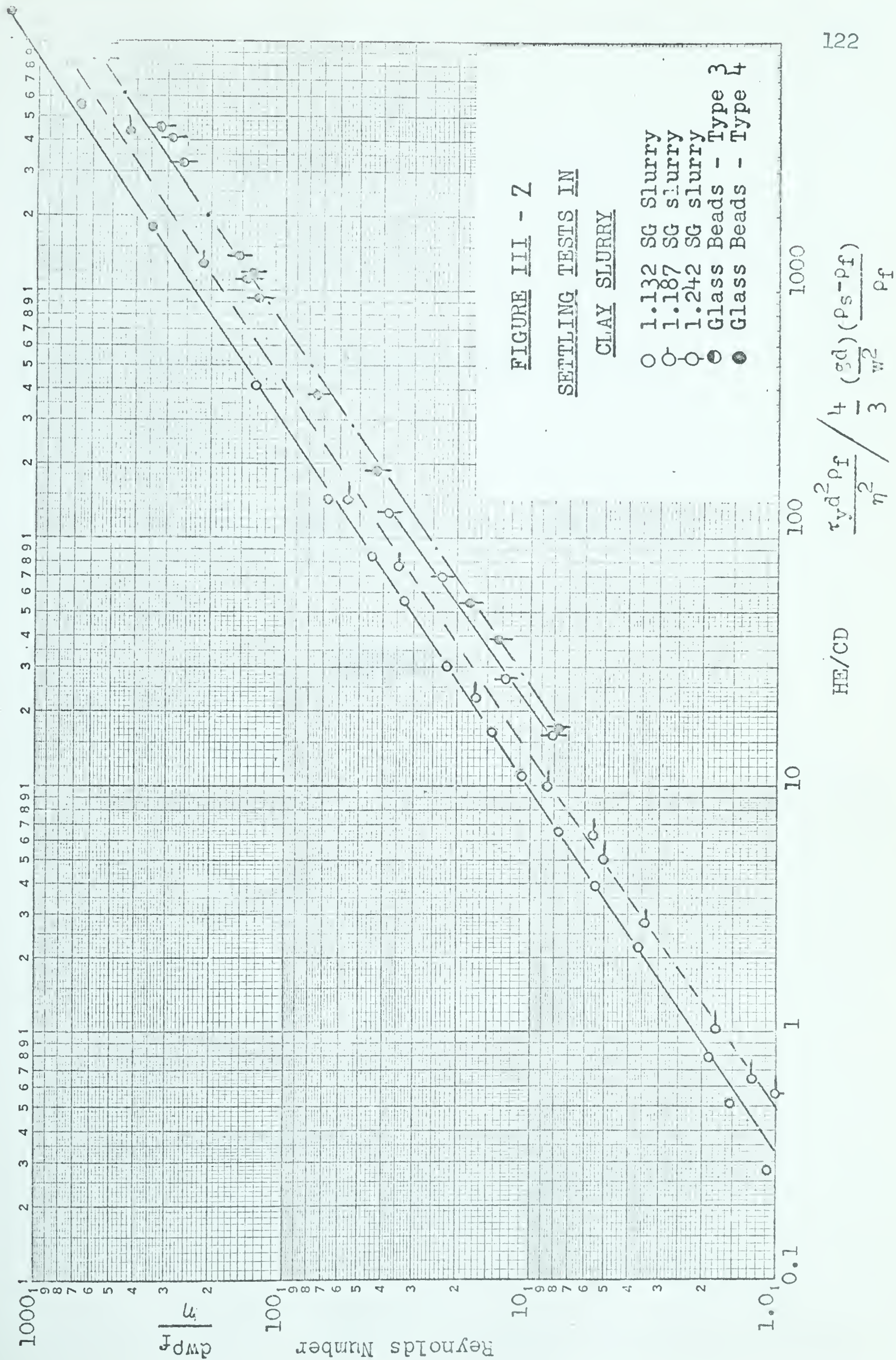












APPENDIX A

APPENDIX AA.1 CALCULATIONS FOR TABLE C-1

$Q' = \text{Reading} \times \text{Factor, USGPM}$

$Q = Q' \times 0.1337/60, \text{ ft}^3/\text{sec}$

$V_m = Q/\pi R^2, \text{ ft/sec}$

$i_w = \frac{\text{Manometer differential (inches)} \times \text{factor}}{600}$

$FN = V_m/\sqrt{gD}$

$Re = VD/\nu$

$\nu = \text{Value taken from FIGURE 1.10, Streeter (1961) at operating temperature}$

$f = \frac{2i_w Dg}{V_m^2}$

A.2 CALCULATIONS FOR TABLE C-2

$\text{Flow, lb/sec} = \frac{\text{weight of slurry in weigh tank, lb}}{\text{time interval, sec}}$

$Q = \text{Flow, lb/sec} / \gamma_m$

Sample at pipe discharge weighed and dried in oven
gives: x weight % solids
 1 - x weight % water

$$C_t = 100 \cdot \frac{x}{2.64} \left/ \left[\frac{x}{2.64} + (1-x) \frac{62.43}{\gamma_w} \right] \right.$$

$$\gamma_m = \frac{C_t}{100} \cdot \gamma_s + \frac{(1-C_t)}{100} \cdot \gamma_w$$

$V_m = Q/\pi R^2 \text{ ft/sec}$

$\gamma_w, \nu = \text{Values from FIGURE 1.10, Streeter (1961) for operating temperature}$

$$V_x = \sqrt{\frac{f}{8}} \cdot V_m \text{ ft/sec}$$

$i, Re, FN \text{ as under A.1}$

A.3 STATISTICAL PARAMETERS

$$\text{Arithmetic Mean} = \bar{x} = \frac{1}{N} \sum_{i=1}^N x_i$$

$$\text{Root Mean Square} = \left[\frac{1}{N} \sum_{i=1}^N x_i^2 \right]^{1/2}$$

$$\text{Standard Deviation} = s = \left[\frac{1}{N} \sum_{i=1}^N (x_i - \bar{x})^2 \right]^{1/2}$$

A.3.1 LINEAR REGRESSION

The best fit straight line of the form $y = ax + b$, assuming that y only is subject to error, gives the following expression for a and b by the method of "least squares".

$$a = \frac{n \sum xy - \sum x \sum y}{n \sum x^2 - (\sum x)^2}$$

$$b = \frac{\sum y - a \sum x}{n}$$

A.3.2 LINEAR REGRESSION OF TRANSFORMED VARIABLE

The best fit equation of the form $Y = CX^a$ is obtained by taking logarithms on both sides, yielding;

$$\log Y = a \log X + \log C$$

$$\text{Let } y = \log Y$$

$$x = \log X$$

$$b = \log C$$

A linear regression on the equation $y = ax + b$ can now be made using the expressions for a and b as under A.3.2.

CORRELATION COEFFICIENT

The correlation coefficient for the y on x linear regression is defined as;

$$r = \frac{n\sum xy - \sum x \sum y}{\sqrt{[n\sum x^2 - (\sum x)^2][n\sum y^2 - (\sum y)^2]}}$$

APPENDIX B

B 1

Flow Meter Reading	Final Weight lb	Initial Weight lb	Differ- ence lb	Time sec	Temp °F	Measured Discharge USGPM	Flow Factor USGPM/ Division
Meter set at 1.823 mv full scale.							
100.0	1600.0	1100.0	500.0	33.60	72	100.10	1.001
71.0	1235.0	879.0	356.0	35.75	72	71.77	1.011
49.5	1457.0	1235.0	222.5	31.90	72	50.27	1.016
Average							1.009
Max. discrepancy = -0.79% or -0.80 GPM							
Meter set at 7.58 mv full scale.							
91.0	1581.5	1117.5	464.0	7.4	78	452.34	4.971
90.0	1556.0	949.0	607.0	9.65	78	453.77	5.042
74.0	1734.5	1426.0	308.5	6.00	78	370.92	5.012
30.0	1583.5	1347.0	236.5	11.20	78	152.33	5.078
20.0	1347.0	1185.5	162.5	11.50	78	101.94	5.097
10.5	1662.5	1583.5	79.0	10.90	78	52.28	4.979
Average							5.030
Max. discrepancy = +1.33% or 6.69 GPM							
Meter set at 3.34 mv full scale.							
10.0	1184.0	874.5	309.5	100.55	82	22.20	2.220
50.0	1494.0	1184.0	310.0	20.45	82	109.41	2.188
100.5	1565.0	1197.5	367.5	11.95	82	221.9	2.208
Average							2.205
Max. discrepancy = +0.68% or 1.50 GPM							

TABLE B-2MAGNETIC FLOW METER CALIBRATION WITH SAND-WATER MIXTURES

Test No	Flow Meter Reading	Weight Flow Rate lb/sec	Temp °F	Vol % Water	Wt. Flow Rate x Vol % Water
063001	23.5	16.18	78	93.5	15.1
063002	14.0	8.08	78	93.5	7.55
06003	21.2	15.25	78	87.5	13.4
06004	16.0	10.70	78	87.5	9.4
06005	19.7	15.20	78	80.8	12.3
07020	21.5	14.6	79	80.8	11.8
07060	29.2	20.2	82	93.5	18.9
07100	22.7	19.52	81	76.1	14.9
07107	58.0	44.44	81	95.5	42.5

APPENDIX B.3GAMMA ATTENUATION TESTS FOR WATER AND SAND.

These tests were carried out by running the scanner carriage to the extremity of its travel distance so that the vertical gamma-beam cleared the pipe. A 3.30 cm diameter by 15 cm long plastic cylinder was clamped over the 1/4" outlet collimating hole so that the gamma-beam passed along the vertical axis of the cylinder. Water was added to the cylinder in 5 cc increments by a precision syringe and through a thin plastic tube. The amplifier signal, E and volume were recorded each time. A factor of 21.7 cc/inch was used to convert the cumulative volumes into path lengths, x_w inches.

Sand attenuation tests were carried out by adding test sand to the cylinder in 5 to 10 gm increments, compacting and levelling the sand with a flat surfaced rubber plunger and then placing the cylinder in the beam path by means of a long handled clamp. The weight of sand divided by the sand SG of 2.64 and conversion factor of 21.7 cc/inch gave the length, x_s , at zero voidage. TABLES B-3.1 and B-3.2 list the test results.

TABLE B-3.1
GAMMA ATTENUATION IN WATER

Temperature 75° F

Water Volume cc	Distance Inches x_w	Chart Reading Volts E	$\ln \left[\frac{E_0}{E} \right]$	$k_w = \ln \left[\frac{E_0}{E} \right] / x_w$
0	0	3.75	0	
15	0.69	3.34	1.150	0.1665
20	0.92	3.18	1.652	0.1800
25	1.15	3.07	1.995	0.1735
30	1.38	2.95	2.395	0.1735
35	1.61	2.85	2.750	0.1709
40	1.84	2.76	3.070	0.1670
45	2.07	2.66	3.430	0.1659
50	2.30	2.56	3.820	0.1600
55	2.53	2.47	4.170	0.1651
60	2.76	2.39	4.510	0.1633
65	2.99	2.31	4.840	0.1616
70	3.22	2.22	5.250	0.1630
75	3.45	2.15	5.550	0.1609
80	3.68	2.07	5.930	0.1611
85	3.91	2.01	6.240	0.1595

Average 0.1661

Std. Dev. 0.0055

TABLE B-3.2
GAMMA ATTENUATION IN SAND

Weight of Sand gm	Volume at Zero Voidage	Distance Inches x_s	Chart Reading Volts E	$\ln \left[\frac{E_0}{E} \right]$	$k_s = \ln \left[\frac{E_0}{E} \right] / x_s$
0		0	3.75		
20	7.58	0.349	3.25	0.1415	0.405
30	11.3	0.521	3.01	0.2190	0.420
35	13.3	0.611	2.85	0.2735	0.447
40	15.1	0.695	2.75	0.3110	0.447
45	17.1	0.786	2.59	0.3715	0.472
55	20.8	0.956	2.44	0.430	0.449
75	28.4	1.308	2.15	0.551	0.421
85	32.2	1.48	2.02	0.619	0.418
90	34.1	1.57	1.91	0.675	0.430
100	37.9	1.74	1.79	0.739	0.424
110	41.7	1.92	1.62	0.839	0.437

Average 0.433

Std. Dev. 0.018

TABLE B-3.3

B 6

STANDARD ABSORPTION CURVES - HORIZONTAL BEAMTop half of Pipe with water, - temp = 79° F, - Flow = 300 USGPM

Inches from Chart Center Line	Location Chart Readings in Volts, E_p and $\ln E_p$						Std Dev $\times 10^{-3}$	% Dev	Average % Dev
	<u>Test No</u>					Average			
	1222s1	1222s2	1223s1	1223s2	1223s3				
0	1.88 .6313	1.89 .6366	1.89 .6366	1.89 .6366	1.88 .6313	1.886 .6345	2.6	0.41	
0.5	1.89 .6366	1.89 .6366	1.89 .6366	1.89 .6366	1.89 .6366	1.890 .6366	0	0	
1.0	1.90 .6419	1.91 .6471	1.91 .6471	1.91 .6471	1.91 .6471	1.908 .64606	2.08	0.322	
1.5	1.93 .6575	1.94 .6627	1.94 .6627	1.94 .6627	1.94 .6627	1.938 .66166	2.08	0.314	
2.0	1.98 .6831	1.99 .6881	1.98 .6831	1.98 .6831	1.99 .6881	1.984 .6851	2.45	0.357	
2.5	2.03 .7080	2.05 .7178	2.05 .7178	2.03 .7080	2.05 .7178	2.042 .7138	4.81	0.675	
3.0	2.13 .7561	2.15 .7655	2.13 .7561	2.13 .7561	2.13 .7561	2.134 .7579	3.76	0.496	
3.5	2.23 .8020	2.27 .8198	2.27 .8198	2.24 .8065	2.25 .8109	2.252 .8118	7.11	0.876	
4.0	2.40 .8755	2.43 .8879	*	2.41 .8796	2.43 .8879	2.417 .8827	5.36	0.608	.450
4.3	2.54 .9322	2.57 .9439	*	2.57 .9439	2.57 .9439	2.562 .94097	5.06	0.538	
4.5	2.65 .9746	2.69 .9895	*	2.68 .9858	2.69 .9895	2.678 .98485	6.11	0.621	
4.7	2.81 1.0332	2.84 1.0438	*	2.81 1.0332	2.82 1.0367	2.820 1.03667	4.34	0.426	.528
4.8	3.00 1.0986	3.00 1.0986	*	3.01 1.1019	2.96 1.0852	2.992 1.09607	6.44	0.587	
E_{Op}	3.70	3.70	3.70	3.70	3.70				

* Air in top of pipe. Values unreliable.

TABLE B-3.4

B 7

STANDARD ABSORPTION CURVES - HORIZONTAL BEAM

Bottom half of pipe with water, - Temp = 79° F, - Flow = 300 USGPM

Location Inches from Chart Center Line	Chart Readings in Volts, E_p and $\ln E$						Std Dev $\times 10^{-3}$	% Dev	Aver- age % Dev
	Test No.								
	1222s1	1222s2	1223s1	1223s2	1223s3	Average			
0.5	1.89 .6366	1.89 .6366	1.90 .6418	1.90 .6418	1.90 .6418	1.896 .6397	2.541	0.381	
1.0	1.91 .6471	1.91 .6471	1.92 .6523	1.91 .6471	1.91 .6471	1.912 .6481	2.08	0.321	
1.5	1.93 .6575	1.93 .6575	1.95 .6678	1.95 .6678	1.94 .6627	1.940 .6626	4.61	0.695	
2.0	1.99 .6881	1.99 .6881	2.00 .6923	1.99 .6881	1.98 .6831	1.990 .6891	3.195	0.464	
2.5	2.04 .7130	2.03 .7080	2.06 .7276	2.06 .7227	2.04 .7130	2.046 .7168	7.18	1.00	
3.0	2.13 .7561	2.11 .7467	2.15 .7655	2.13 .7561	2.13 .7561	2.130 .7561	5.94	0.780	
3.5	2.25 .8109	2.24 .8065	2.28 .8242	2.27 .8198	2.24 .8065	2.256 .8135	7.19	0.884	
4.0	2.41 .8796	2.41 .8796	2.44 .8920	2.43 .8879	2.41 .8796	2.420 .8837	5.23	0.598	.640
4.3	2.55 .9361	2.54 .9322	2.60 .9555	2.55 .9361	2.56 .9400	2.560 .9399	8.15	0.866	
4.5	2.67 .9821	2.66 .9783	2.71 .9970	2.70 .9932	2.67 .9821	2.682 .9865	7.24	0.734	
4.7	2.82 1.0367	2.82 1.0367	2.87 1.0543	2.84 1.0438	2.84 1.0438	2.838 1.0430	6.46	0.618	.739
4.8	2.95 1.0818	3.02 1.1053	3.04 1.1119	3.00 1.0986	3.04 1.1119	3.010 1.1019	11.19	1.015	
E_{op}	3.70	3.70	3.70	3.70	3.70				

TABLE B-3.5

STANDARD ABSORPTION CURVES - VERTICAL BEAMPipe with water, - Temp = 80° F, - Flow = 300 USGPM

Location Inches from Chart Center Line	<u>NORTH HALF</u>			<u>SOUTH HALF</u>		
	Chart Readings E_p and $\ln E_p$			Chart Readings E_p and $\ln E_p$		
	<u>Test No.</u>			<u>Test No.</u>		
	1221s1	1223s3	Average	1221s1	1223s3	Average
0	1.87	1.87	1.87			
0.5	1.87	1.87	1.87	1.87	1.87	1.87
1.0	1.89	1.89	1.89	1.90	1.89	1.895
1.5	1.92	1.91	1.915	1.91	1.92	1.915
2.0	1.96	1.96	1.96	1.96	1.96	1.96
2.5	2.03	2.01	2.02	2.03	2.02	2.025
3.0	2.11	2.10	2.105	2.12	2.11	2.115
3.5	2.22	2.22	2.22	2.25	2.25	2.250
4.0	2.38	2.38	2.38	2.41	2.40	2.405
4.3	2.53	2.53	2.53	2.57	2.56	2.565
4.5	2.65	2.65	2.65	2.65	2.67	2.66
4.7	2.80	2.80	2.80	2.85	2.86	2.855
4.8	3.04	3.04	3.04	3.01	3.01	3.01
E_{op}	3.70	3.70	3.70	3.70	3.70	3.70

TABLE B-3.6

STANDARD PIPE WALL ABSORPTION CURVES AND CALCULATED VALUES OF k_w

HORIZONTAL BEAM - TOP HALF

Location Inches from Chart Center Line	PIPE WALL - TOP HALF				CALCULATION OF		
	Chart Readings			Average $\frac{E_{om}}{E_m}$	$k_w = \ln \left[\frac{E_{op} E_m}{E_{om} E_p} \right] / x$		
	E_m and E_{om} / E_m	Test No.			Path Length Inches x	$\ln^* \left[\frac{E_{op} E_m}{E_{om} E_p} \right]$	k_w
	122001	122002	122003				
0	3.58 1.039	3.50 1.029	3.50 1.034	1.034	3.916	.6413	0.1637
0.5	3.58 1.039	3.50 1.029	3.50 1.034	1.034	3.893	.6382	0.1665
1.0	3.58 1.039	3.48 1.034	3.50 1.034	1.035	3.832	.6281	0.1639
1.5	3.58 1.039	3.48 1.034	3.50 1.034	1.035	3.724	.6125	0.1644
2.0	3.56 1.045	3.48 1.034	3.48 1.040	1.039	3.568	.5850	0.1639
2.5	3.55 1.048	3.48 1.034	3.48 1.040	1.039	3.367	.5562	0.1651
3.0	3.55 1.048	3.45 1.043	3.47 1.043	1.044	3.038	.5074	0.1670
3.5	3.53 1.054	3.43 1.050	3.45 1.049	1.051	2.714	.4466	0.1645
4.0	3.50 1.063	3.38 1.065	3.42 1.058	1.062	2.220	.3660	0.1649
4.3 k_w	3.45 0.1608	3.35 0.1621	3.36 0.1612		1.820		0.1613
4.5 k_w	3.36 0.1502	3.25 0.1498	3.30 0.1561		1.472		0.1521
4.7 k_w	3.27 0.1100	3.10 0.1238	3.16 0.1375		0.9852		0.1237
E_{om}	3.72	3.60	3.62				

* Values of E_{op} and E_p from TABLE B-3.3

TABLE B-3.7

STANDARD PIPE WALL ABSORPTION CURVES AND CALCULATED VALUES OF k_w

HORIZONTAL BEAM - BOTTOM HALF

PIPE WALL - BOTTOM HALF					CALCULATION OF		
Location Inches from Chart Center Line	Chart Readings			Average $\frac{E_{om}}{E_m}$	$k_w = \ln \left[\frac{E_{op} E_m}{E_{om} E_p} \right] / x$		
	E_m and E_{om}/E_m				$\ln^* \left[\frac{E_{op} E_m}{E_{om} E_p} \right]$	Path Length Inches x	k_w
	Test No.						
	122001	122002	122003				
0.5	3.58 1.039	3.50 1.029	3.50 1.034	1.034	0.6355	3.893	0.1631
1.0	3.58 1.039	3.50 1.029	3.50 1.034	1.034	0.6270	3.832	0.1636
1.5	3.58 1.039	3.50 1.029	3.50 1.034	1.034	0.6119	3.724	0.1643
2.0	3.57 1.042	3.49 1.031	3.48 1.040	1.037	0.5839	3.568	0.1636
2.5	3.56 1.045	3.47 1.037	3.46 1.046	1.042	0.5516	3.367	0.1638
3.0	3.53 1.054	3.46 1.040	3.45 1.049	1.047	0.5062	2.038	0.1666
3.5	3.53 1.054	3.45 1.043	3.45 1.049	1.048	0.4485	2.714	0.1652
4.0	3.48 1.069	3.42 1.052	3.41 1.062	1.061	0.3653	2.220	0.1645
4.3 k_w	3.44 0.1594	3.36 0.1648	3.36 0.1615			1.820	0.1619
4.5 k_w	3.35 0.1478	3.30 0.1595	3.27 0.1492			1.4724	0.1521
4.7 k_w	3.16 0.1030	3.12 0.1240	3.10 0.1112			0.9852	0.1127
E_{om}	3.72	3.60	3.62				

* Values of E_{op} and E_p from TABLE B-3.4

TABLE B-3.8

STANDARD PIPE WALL ABSORPTION CURVES AND CALCULATED VALUES OF k_w

VERTICAL BEAM - NORTH HALF

Location Inches from Chart Center Line	Chart Readings E_m Test No.		Average E_m	CALCULATION OF $k_w = \ln \left[\frac{E_{op} E_m}{E_{om} E_p} \right] / x$		
	122001	122002		$\ln^* \left[\frac{E_{op} E_m}{E_{om} E_p} \right]$	Path Length Inches x	k_w
0	3.58	3.60	3.59	0.6382	3.916	0.1629
0.5	3.60	3.60	3.60	0.6413	3.8932	0.1646
1.0	3.60	3.60	3.60	0.6308	3.8320	0.1646
1.5	3.60	3.60	3.60	0.6136	3.724	0.1645
2.0	3.60	3.60	3.60	0.5939	3.568	0.1664
2.5	3.58	3.58	3.58	0.5585	3.367	0.1659
3.0	3.57	3.57	3.57	0.5122	3.038	0.1686
3.5	3.54	3.55	3.54	0.4549	2.714	0.1676
4.0	3.50	3.51	3.50	0.3736	2.220	0.1683
4.3 k_w	3.43 0.1608	3.45 0.1629			1.820	0.1619
4.5 k_w	3.30 0.1400	3.38 0.1559			1.472	0.1480
4.7 k_w	3.25 0.1380	3.27 0.1435			0.9852	0.1408
E_o	3.75	3.75	3.75			

* Values of E_{op} and E_p from TABLE B-3.5

TABLE - B-3.9

STANDARD PIPE WALL ABSORPTION CURVES AND CALCULATED VALUES OF k_w

VERTICAL BEAM - SOUTH HALF

Location Inches from Chart Center Line	Chart Readings E_m		Average E_m	CALCULATION OF $k_w = \ln \frac{E_{op} E_m}{E_{om} E_p} / x$		
	Test No 122001	No 122002		$\ln^* \frac{E_{op} E_m}{E_{om} E_p}$	Path Length Inches x	k_w
0.5	3.60	3.60	3.60	0.6413	3.8932	0.1646
1.0	3.60	3.60	3.60	0.6233	3.8320	0.1626
1.5	3.60	3.60	3.60	0.6157	3.724	0.1653
2.0	3.60	3.58	3.59	0.5914	3.5684	0.1657
2.5	3.60	3.58	3.59	0.5579	3.3670	0.1656
3.0	3.59	3.57	3.58	0.5110	3.038	0.1682
3.5	3.56	3.55	3.56	0.4440	2.714	0.1635
4.0	3.50	3.48	3.49	0.3591	2.220	0.1618
4.3 k_w	3.48 0.1601	3.43 0.1521			1.820	0.1561
4.5	**	3.30	3.30	0.202	1.4724	0.1372
4.7	**	3.28	3.28	0.1255	0.9852	0.1275
E_{om}^{***}	3.75	3.75				

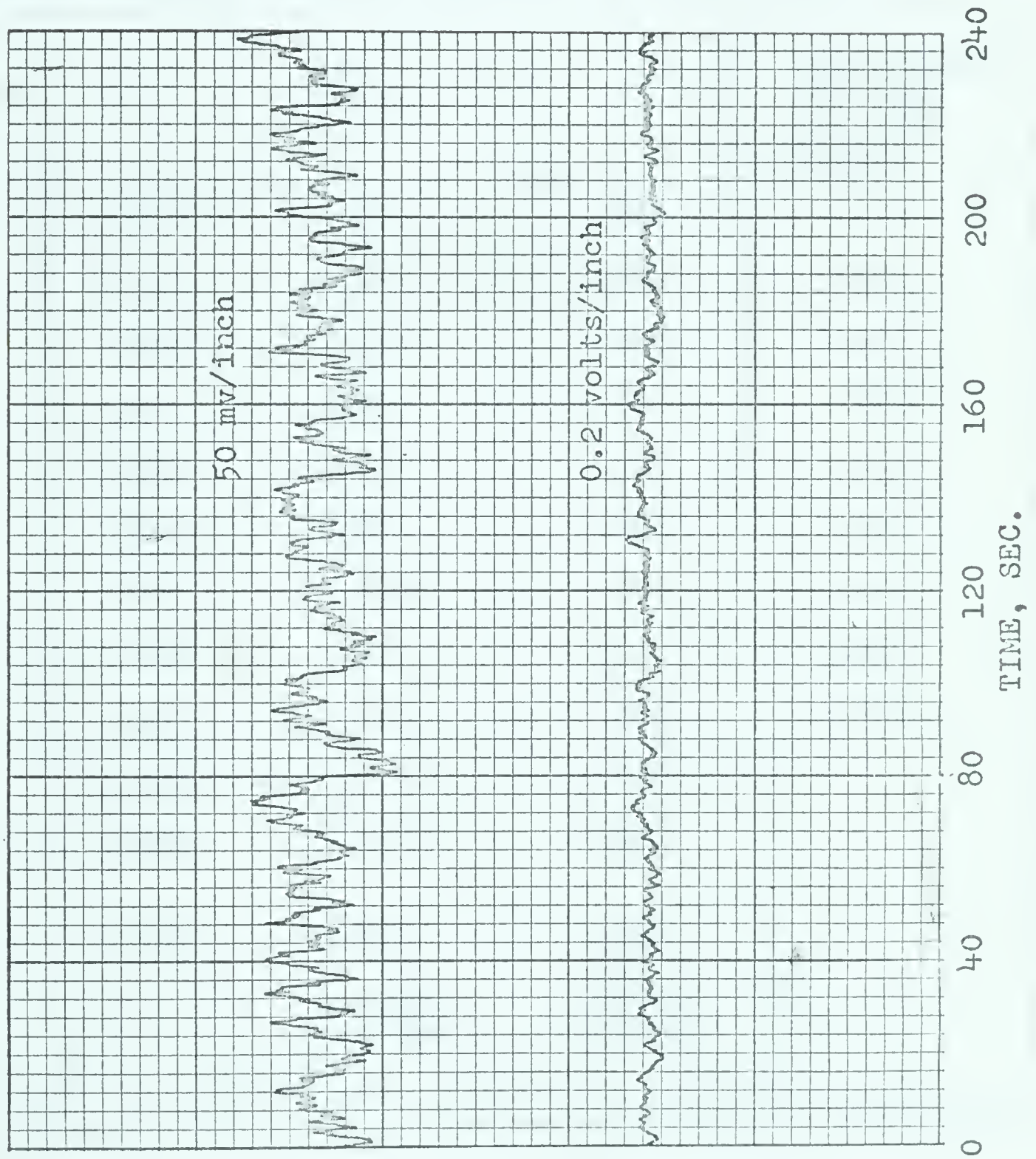
* Values of E_{op} and E_p from TABLE B-3.5

** Values unreliable

*** Average value

Time Record of output signal with reference plate in position

[illegible]



RANDOM VARIATION OF GAMMA OUTPUT SIGNAL

FIGURE B-4

TABLE B-5

PIPE INSIDE DIAMETER AND WALL MEASUREMENTS

Inside diameter readings taken at 5° intervals.

WALL THICKNESS INCHES	ID Inches			MEASUREMENT AT ONE LOCATION INCHES
.049	3.922	3.929	3.889	3.922
.049	3.920	3.931	3.888	3.921
.048	3.906	3.933	3.889	3.921
.049	3.906	3.933	3.887	3.923
.049	3.906	3.935	3.908	3.923
.049	3.885	3.934	3.920	3.923
.048	3.890	3.930	3.927	3.921
.048	3.894	3.930	3.936	3.921
.049	3.900	3.929	3.928	3.923
.048	3.904	3.928	3.925	
Average .049	3.919	3.919	3.927	
	3.921	3.912	3.921	
		Average -	3.9156	
		Std Dev -	0.0154	

TABLE B-6

CHART DISTANCES IN INCHES BETWEEN LIMIT SWITCHES AND BETWEEN
LIMIT SWITCH AND CHART CENTERLINE

TEST NO	LIMIT TO CENTER	LIMIT TO LIMIT	LIMIT TO CENTER	LIMIT TO LIMIT	MEASURED CARRIAGE DISPLACEMENT INCHES
122406	2.075	4.420	2.225	4.420	
123001	2.075	4.400	2.235	4.420	
123002	2.080	4.440	2.230	4.425	
123003	2.080	4.430	2.235	4.420	
123004	2.070	4.420	2.230	4.420	
123005	2.080	4.430	2.235	4.420	
123006	2.080	4.430	2.230	4.430	
123007	2.080	4.430	2.225	4.415	
123008	2.085	4.435	2.225	4.410	4.485
123009	2.075	4.435	2.230	4.430	4.480
123010	2.070	4.425	2.225	4.420	4.480
123101	2.085	4.450	2.230	4.445	4.482
123102	2.080	4.460	2.235	4.445	4.477
123103	2.075	4.445	2.230	4.450	4.483
123104	2.075	4.450	2.235	4.440	4.482
123105	2.065	4.450	2.230	4.435	4.484
123106	2.080	4.450	2.230	4.445	4.477
123107	2.080	4.440	2.230	4.430	4.483
AVERAGE	2.077	4.440	2.230	4.435	4.481
STD DEV x 10 ⁻³	5.06	9.7	3.525	12.05	2.62
	<u>VERTICAL SCAN</u>		<u>HORIZONTAL SCAN</u>		

$$\text{Conversion Factor } F = \frac{L}{L_c} = \frac{4.481}{4.435} = 1.008$$

$$\text{Standard Error of } F \quad \frac{\partial F}{\partial L} = \frac{1}{L_c} \quad \frac{\partial F}{\partial L_c} = -\frac{L}{L_c^2}$$

$$s_f^2 \approx \left(\frac{1}{L_c}\right)^2 s_L^2 + \left(\frac{L}{L_c^2}\right)^2 s^2 L_c = \left(\frac{1}{L_c}\right)^2 \left[s_L^2 + \left(\frac{L}{L_c}\right)^2 s^2 L_c \right]$$

$$s_f = \frac{1}{L_c} \left[6.81 \cdot 10^{-6} + (1.008)^2 \cdot 145.0 \cdot 10^{-6} \right]^{1/2}$$

$$= \frac{1}{L_c} \left[6.8 + 147 \right]^{1/2} \cdot 10^{-3} = \frac{12.4}{4.435} = 2.8 \cdot 10^{-3} = 0.0028$$

TABLE B-7PIPE CENTER LOCATED BY MEASUREMENT

<u>MEASUREMENT</u>	<u>INCHES</u>
Shaft to Pipe Wall	0.103
Pipe Wall	0.049
Pipe Radius	1.958
Shaft Radius	0.125
Total	<u>2.235</u>
Equivalent chart distance;	
2.230 X 1.008	<u>2.248</u>
Difference	- .013 or -0.58%

This is considered reasonable agreement and within the limits of accuracy of the measurements.

TABLE B-8.1

SAMPLING ACCURACY

Flow meter reading 21.5, - Temperature 79° F, - Flow 15 lb/sec.

TOTAL WEIGHT gm	DRY WEIGHT gm	TARE WEIGHT	WATER WEIGHT	SAMPLE WEIGHT	WT% WATER
709.45	444.32	266.14	265.13	443.31	59.81
653.72	435.35	295.58	218.37	358.12	60.98
634.36	415.78	267.89	218.58	366.47	59.64
573.90	369.28	254.26	204.62	319.64	64.02
561.48	356.44	236.81	205.04	334.67	61.27
601.27	381.95	252.56	219.32	348.71	62.89
582.57	429.80	333.73	152.77	248.84	61.39
634.30	422.47	289.66	211.83	344.64	61.47
652.41	408.79	268.02	243.62	384.39	63.33
561.37	370.90	253.69	190.47	307.68	61.90
612.03	412.78	298.03	199.25	324.00	61.50
594.47	415.08	298.50	178.39	295.97	60.27
766.24	514.93	408.26	251.31	408.26	61.55
742.92	503.35	359.17	239.57	383.75	62.43
726.97	502.40	359.01	224.57	367.96	61.03
605.90	386.62	248.95	219.28	356.95	61.44
694.16	493.35	358.19	200.81	335.97	59.78
Average -					61.45
Standard Deviation -					±1.19

TABLE B-8.2
SAMPLING ACCURACY

Flow meter reading 29.2, - Temperature 82° F, - Flow 20 lb/sec.

TOTAL WEIGHT gm	DRY WEIGHT gm	TARE WEIGHT	WATER WEIGHT	SAMPLE WEIGHT	WT% WATER
562.11	312.11	266.00	250.00	296.11	84.43
605.25	342.46	295.43	262.79	309.82	84.82
583.01	317.74	267.74	265.27	315.27	84.14
500.28	289.80	254.12	210.48	246.16	85.51
517.61	280.04	236.68	237.57	280.93	84.59
561.62	301.28	252.40	260.34	309.22	84.20
783.57	473.60	420.15	309.97	363.42	85.24
547.53	327.37	289.50	220.16	258.03	85.32
566.39	313.93	267.89	252.46	298.50	84.58
483.65	289.60	253.55	194.05	230.10	84.33
551.25	338.47	299.88	212.78	251.37	84.65
538.09	332.96	297.37	205.13	240.72	85.21
635.25	398.94	357.82	236.31	277.43	85.17
589.63	394.33	358.02	195.30	231.61	84.32
722.40	415.32	358.90	307.08	363.50	84.48
527.69	289.70	248.80	237.99	278.89	85.31
673.68	405.89	358.02	267.79	315.66	84.83
853.21	489.94	425.07	363.27	428.14	84.83
721.04	473.38	423.41	247.66	297.63	83.21
807.22	480.01	426.93	327.21	380.29	86.02
733.80	411.70	353.93	322.10	379.87	84.79
598.45	342.36	300.91	256.09	297.54	86.07
639.52	341.82	290.48	297.70	349.04	85.29
840.00	482.10	420.90	357.90	419.10	85.40
838.24	484.72	424.02	353.52	414.22	85.35
832.72	485.77	427.03	346.95	405.69	85.52
725.56	467.22	420.77	258.34	304.79	84.75
915.30	503.34	430.00	411.96	485.30	84.89
858.03	491.36	429.93	366.67	428.10	85.65
Average -					84.92
Std Dev -					±1.98

TABLE B - 9
SAND GRAIN SIZE DISTRIBUTION

U.S. SIEVE NO	% RETAINED ON	% FINER THAN	$\ln(d)$	d, mm	$\frac{d}{0.355}$
30	.8	99.9	.526	.59	1.66
35	16.7	99.1	.694	.50	1.41
40	34.8	82.4	.866	.42	1.18
45	17.2	47.6	1.050	.35	.985
50	12.6	17.8	1.214	.297	.836
60	8.2	9.6	1.387	.250	.704
70	5.1	4.5	1.561	.210	.591
80	2.1	2.4	1.731	.177	.498
100	1.7	0.7	1.904	.149	.420
120	0.3	0.4	2.079	.125	.352
140	0.2	0.2	2.254	.105	.296
Pan	0.2				
$d = \text{Sieve opening in mm}$					

APPENDIX C

TABLE C-1
CLEAR WATER PUMPS IN 4 INCH LINE

FLOW		DIFFERENTIAL		TEMP. OF	KIN. VISC. X 10 ⁶	FLOW USGPM	MEAN VEL. FPS	FROUDE NUMBER FN	REYNOLDS NUMBER Re	FRICT. FACTOR f
READ. %	FACT.	PRESSURE- INCH	FACT.							
50.0	5.050	47.00	0.598	74.0	10.07	297.95	7.94	2.438	257748.3	0.016
55.0	5.040	41.00	0.598	74.0	10.07	277.20	7.38	2.269	239798.1	0.016
44.0	5.450	30.00	0.598	75.1	9.94	239.80	6.39	1.962	210157.4	0.015
40.0	5.040	24.00	0.598	75.0	9.94	201.60	5.37	1.650	176679.5	0.017
35.0	5.046	19.75	0.598	75.0	9.94	176.61	4.70	1.445	154778.6	0.019
30.0	5.340	14.00	0.598	75.0	9.94	160.20	4.27	1.311	140397.1	0.016
24.5	5.040	10.63	0.598	76.0	9.82	123.48	3.29	1.011	109538.6	0.021
20.0	5.040	6.63	0.598	76.0	9.82	100.80	2.69	0.825	89419.2	0.019
17.5	4.970	5.31	0.598	76.0	9.82	86.98	2.32	0.712	77155.1	0.021
15.0	4.970	4.06	0.598	77.0	9.69	74.55	1.99	0.610	67020.2	0.022
14.0	4.970	3.45	0.598	77.0	9.69	69.58	1.85	0.569	62552.2	0.021
13.0	4.970	3.00	0.598	77.0	9.69	64.61	1.72	0.529	58084.2	0.021
11.5	4.970	2.75	0.598	77.0	9.69	57.16	1.52	0.468	51382.2	0.025
10.5	4.970	2.19	0.598	77.0	9.69	52.18	1.39	0.427	46914.2	0.024
9.5	4.970	1.88	0.598	78.0	9.56	47.22	1.26	0.386	43023.3	0.025
48.0	4.970	10.00	1.972	86.0	8.68	238.56	6.36	1.952	239419.7	0.016
9.0	4.970	1.30	0.598	86.0	8.68	44.73	1.10	0.366	44891.2	0.019
14.5	4.970	3.70	0.598	86.0	8.68	72.06	1.92	0.590	72324.7	0.021
20.0	4.970	7.20	0.598	86.0	8.68	99.40	2.65	0.813	99758.2	0.022
25.0	4.970	3.30	1.972	86.0	8.68	124.25	3.31	1.017	124697.8	0.020
30.0	5.100	4.40	1.972	86.0	8.68	153.00	4.08	1.252	153551.4	0.017
35.0	5.050	6.10	1.972	86.0	8.68	176.75	4.71	1.446	177386.9	0.018
40.0	5.050	7.40	1.972	86.0	8.68	202.00	5.38	1.653	202727.9	0.017
45.0	5.050	34.70	0.598	84.0	8.87	227.25	6.05	1.860	223183.6	0.020
50.0	5.050	10.60	1.972	82.0	9.10	252.50	6.73	2.066	241714.1	0.015
60.0	5.050	15.60	1.972	82.0	9.10	303.00	8.07	2.480	290056.9	0.016
65.0	5.050	19.00	1.972	82.0	9.10	328.25	8.74	2.686	314228.3	0.016
70.0	5.050	20.90	1.972	82.0	9.10	353.50	9.42	2.893	338399.7	0.015
75.0	5.050	23.20	1.972	82.0	9.10	378.75	10.09	3.100	362571.1	0.015
80.0	5.320	27.20	1.972	82.0	9.10	426.40	11.36	3.490	408185.7	0.014
60.0	5.050	15.10	1.972	82.0	9.10	303.00	8.07	2.480	290056.9	0.015
28.0	0.148	0.02	0.598	78.0	9.56	4.14	0.11	0.034	3776.1	0.034
28.5	0.148	0.02	0.598	78.0	9.56	4.22	0.11	0.035	3843.5	0.033
40.0	0.148	0.05	0.598	78.0	9.56	5.92	0.16	0.048	5394.4	0.042
45.0	0.148	0.09	0.598	78.0	9.56	7.25	0.19	0.059	6608.2	0.051
50.0	0.148	0.10	0.598	80.0	9.56	8.73	0.22	0.071	7956.8	0.039
70.0	0.148	0.12	0.598	80.0	9.30	10.36	0.28	0.085	9704.2	0.033
78.0	0.148	0.15	0.598	80.0	9.30	11.54	0.31	0.094	10813.2	0.033
90.0	0.148	0.17	0.598	80.0	9.30	13.32	0.35	0.109	12476.8	0.028
100.0	0.148	0.22	0.598	78.0	9.56	14.80	0.39	0.121	13486.1	0.030
30.0	0.148	0.21	0.120	80.0	9.30	4.44	0.12	0.036	4158.9	0.063
40.0	0.148	0.30	0.120	80.0	9.30	5.92	0.16	0.048	5545.2	0.051
75.0	0.148	0.60	0.120	80.0	9.30	11.10	0.30	0.091	10397.3	0.029
50.5	0.218	0.15	0.598	80.0	9.30	11.01	0.29	0.090	10312.1	0.037
58.5	0.218	0.20	0.598	80.0	9.30	12.75	0.34	0.104	11945.7	0.036
70.0	0.218	0.25	0.598	80.0	9.30	15.26	0.41	0.125	14294.0	0.032
80.0	0.218	0.28	0.598	80.0	9.30	17.44	0.46	0.143	16336.0	0.027
90.5	0.218	0.35	0.598	80.0	9.30	19.73	0.53	0.161	18480.1	0.027

TABLE C-1 - continued
CLEAR WATER RUNS IN 4 INCH LINE

FLOW READ. %	FLOW FACT.	DIFFERENTIAL PRESSURE		TEMP. OF	KIN. VISC. X 10 ⁶	FLOW USGPM	MEAN VEL. FPS	FOUDES NUMBER FN	REYNOLDS NUMBER Re	FRICT. FACTOR f
		INCH	FACT.							
100.5	0.218	0.42	0.598	80.0	0.20	21.91	0.58	0.179	20522.1	0.026
10.0	2.126	0.48	0.598	81.0	0.20	21.26	0.57	0.174	20130.6	0.031
20.0	2.126	1.50	0.598	81.0	0.20	42.52	1.13	0.348	40261.3	0.025
29.8	2.126	3.20	0.598	81.0	0.20	63.35	1.69	0.518	59989.3	0.024
40.0	2.126	5.55	0.598	81.0	0.20	85.04	2.27	0.696	80522.5	0.023
50.0	2.126	8.05	0.598	81.0	0.20	106.30	2.83	0.870	100653.2	0.021
60.2	2.126	11.15	0.598	81.0	0.20	127.99	3.41	1.047	121186.4	0.020
70.0	2.126	14.75	0.598	81.0	0.20	148.82	3.96	1.218	140914.4	0.020
80.0	2.126	19.80	0.598	81.0	0.20	170.08	4.52	1.392	161045.0	0.019
89.5	2.126	23.20	0.598	81.0	0.20	190.28	5.07	1.557	180169.1	0.019
100.5	2.126	27.55	0.598	81.0	0.20	213.66	5.69	1.749	202312.8	0.018
80.0	2.126	6.13	1.872	81.0	0.20	170.08	4.52	1.392	161045.0	0.020
60.0	2.126	3.50	1.872	81.0	0.20	127.56	3.40	1.044	120783.8	0.020
50.0	2.126	2.50	1.872	81.0	0.20	106.30	2.83	0.870	100653.2	0.020
40.0	2.126	1.63	1.872	81.0	0.20	85.04	2.27	0.696	80522.5	0.021
30.0	2.197	0.88	1.872	81.0	0.20	65.91	1.76	0.539	62408.7	0.019
20.0	2.197	0.50	1.872	81.0	0.20	43.94	1.17	0.360	41605.8	0.024
22.5	4.962	2.50	1.872	82.0	0.10	111.64	2.97	0.914	106875.9	0.019
30.0	4.962	4.50	1.872	82.0	0.10	148.86	3.97	1.218	142501.2	0.019
40.0	4.962	7.75	1.872	82.0	0.10	198.48	5.29	1.624	190001.6	0.018
49.5	4.962	10.88	1.872	82.0	0.10	245.62	6.54	2.010	235127.0	0.017
60.0	4.962	15.38	1.872	82.0	0.10	297.72	7.92	2.426	285002.4	0.016
70.0	4.962	20.56	1.872	82.0	0.10	347.34	9.25	2.843	332502.9	0.016
81.0	4.962	27.81	1.872	82.0	0.10	401.92	10.71	3.289	384753.3	0.016
91.5	4.962	35.06	1.872	82.0	0.10	454.02	12.10	3.716	434628.7	0.016
95.0	4.962	37.50	1.872	82.0	0.10	471.39	12.56	3.858	451253.9	0.016

TABLE C-2
SAND - WATER RUNS

Test No	Flow lb/sec	Q ft ³ /sec	V _m ft/sec	Ct %	Temp OF	ν ft ² /sec x10 ⁶	SG Mix-ture	FN	i	f	Re	V _x ft/sec
122303.	43.59	0.6783	8.11	2.00	79.00	9.4	1.03	2.5042	0.0527	0.0168	280745.1	0.372
122302.	43.59	0.6799	8.13	1.85	79.00	9.4	1.03	2.5100	0.0527	0.0167	281404.4	0.372
122303.	43.59	0.6767	8.09	2.15	79.00	9.4	1.03	2.4983	0.0527	0.0169	280088.9	0.372
122304.	38.35	0.5921	7.08	2.50	79.00	9.4	1.04	2.1859	0.0449	0.0168	245060.9	0.343
122304.	38.35	0.5903	7.06	2.69	79.00	9.4	1.04	2.1792	0.0449	0.0189	244316.6	0.343
122304.	38.35	0.5939	7.10	2.30	79.00	9.4	1.03	2.1925	0.0449	0.0187	245809.8	0.343
122307.	30.31	0.4740	5.67	1.68	78.00	9.6	1.02	1.7500	0.0334	0.0218	193532.6	0.296
122307.	30.31	0.4756	5.69	1.48	78.00	9.6	1.02	1.7557	0.0334	0.0217	194161.3	0.296
122307.	30.31	0.4725	5.65	1.88	78.00	9.6	1.03	1.7444	0.0334	0.0220	192907.9	0.296
122309.	52.00	0.7995	9.56	2.76	79.00	9.6	1.04	2.9518	0.0718	0.0165	326433.5	0.434
122309.	52.00	0.7997	9.57	2.74	79.00	9.6	1.04	2.9524	0.0718	0.0165	326501.3	0.434
122309.	52.00	0.7994	9.56	2.77	79.00	9.6	1.04	2.9512	0.0718	0.0165	326365.7	0.434
122310.	62.49	0.9662	11.56	2.41	79.00	9.6	1.04	3.5669	0.0998	0.0157	394458.4	0.512
122310.	62.49	0.9671	11.57	2.35	79.00	9.6	1.04	3.5703	0.0998	0.0157	394826.7	0.512
122310.	62.49	0.9653	11.55	2.46	79.00	9.6	1.04	3.5636	0.0998	0.0157	394090.8	0.512

Note: First row of each test is calculated from average value of Ct.

TABLE C-2 - continued

SAND - WATER RUNS

Test No	Flow lb/sec	Q ft ³ /sec	V _m ft/sec	C _t %	Temp OF	ν ft ² /sec x10 ⁶	SG Mix-ture	FN	i	f	Re	V _x ft/sec
122401.	61.56	0.8896	10.64	6.82	80.00	9.3	1.11	3.2842	0.1042	0.0193	373341.2	0.523
122401.	61.56	0.8961	10.72	6.33	80.00	9.3	1.10	3.3085	0.1042	0.0191	376101.5	0.523
122401.	61.56	0.8831	10.56	7.32	80.00	9.3	1.12	3.2603	0.1042	0.0196	370621.1	0.523
122402.	54.36	0.7871	9.41	6.69	80.00	9.3	1.11	2.9058	0.0883	0.0209	330327.5	0.482
122402.	54.36	0.7816	9.35	7.16	80.00	9.3	1.11	2.8857	0.0883	0.0212	328045.1	0.482
122402.	54.36	0.7926	9.48	6.23	80.00	9.3	1.10	2.9262	0.0883	0.0206	332641.8	0.482
122403.	48.44	0.7112	8.51	5.77	81.00	9.2	1.09	2.6258	0.0755	0.0219	301743.2	0.445
122403.	48.44	0.7135	8.54	5.55	81.00	9.2	1.09	2.6343	0.0755	0.0218	302715.2	0.445
122403.	48.44	0.7090	8.48	5.98	81.00	9.2	1.09	2.6174	0.0755	0.0221	300777.4	0.445
122404.	46.50	0.6891	8.24	5.13	79.00	9.4	1.08	2.5440	0.0686	0.0212	285209.1	0.425
122404.	46.50	0.6877	8.23	5.26	79.00	9.4	1.08	2.5389	0.0686	0.0213	284638.6	0.425
122404.	46.50	0.6905	8.26	5.00	79.00	9.4	1.08	2.5491	0.0686	0.0211	285782.0	0.425
122405.	41.20	0.6098	7.29	5.22	79.00	9.4	1.08	2.2511	0.0615	0.0243	252378.3	0.402
122405.	41.20	0.6048	7.23	5.76	79.00	9.4	1.09	2.2327	0.0615	0.0247	250308.2	0.402
122405.	41.20	0.6148	7.35	4.67	79.00	9.4	1.07	2.2699	0.0615	0.0239	254482.9	0.402

TABLE C-2 - continued

SAND - WATER RUNS

Test No	Flow lb/sec	Q ft ³ /sec	V_m ft/sec	Ct %	Temp OF	ν ft ² /sec x10 ⁶	SG Mix-ture	FW	i	f	Re	V_x ft/sec
122406.	34.98	0.5221	6.24	4.66	78.00	9.6	1.07	1.9274	0.0593	0.0319	213142.3	0.395
122406.	34.98	0.5319	6.36	3.45	78.00	9.6	1.05	1.9637	0.0593	0.0308	217159.1	0.395
122406.	34.98	0.5126	6.13	5.87	78.00	9.6	1.09	1.8924	0.0593	0.0331	209271.3	0.395
123001.	46.70	0.6365	7.61	10.90	82.00	9.1	1.18	2.3499	0.0714	0.0259	273004.0	0.433
123001.	46.70	0.6443	7.71	10.03	82.00	9.1	1.16	2.3787	0.0714	0.0253	276352.5	0.433
123001.	46.70	0.6289	7.52	11.77	82.00	9.1	1.19	2.3218	0.0714	0.0265	269735.7	0.433
123002.	59.95	0.8111	9.70	11.44	82.00	9.1	1.18	2.9944	0.0911	0.0203	347876.5	0.489
123002.	59.95	0.8162	9.76	10.98	82.00	9.1	1.18	3.0134	0.0911	0.0201	350091.2	0.489
123002.	59.95	0.8060	9.64	11.89	82.00	9.1	1.19	2.9755	0.0911	0.0206	345689.7	0.489
123003.	56.40	0.7610	9.10	11.64	83.00	9.0	1.19	2.8094	0.0821	0.0208	330745.4	0.464
123003.	56.40	0.7604	9.10	11.69	83.00	9.0	1.19	2.8073	0.0821	0.0208	330507.6	0.464
123003.	56.40	0.7615	9.11	11.59	83.00	9.0	1.19	2.8114	0.0821	0.0208	330983.6	0.464
123004.	50.74	0.7055	8.44	9.50	83.00	9.0	1.15	2.6047	0.0774	0.0228	306646.0	0.451
123004.	50.74	0.6872	8.22	11.37	83.00	9.0	1.18	2.5369	0.0774	0.0241	298672.3	0.451
123004.	50.74	0.7249	8.67	7.63	83.00	9.0	1.12	2.6761	0.0774	0.0216	315057.2	0.451

TABLE C-2 - continued

SAND - WATER RUNS

Test No	Flow lb/sec	Q ft ³ /sec	V _m ft/sec	Ct %	Temp OF	\sqrt{v} ft ² /sec x10 ⁶	SG Mix-ture	FN	i	f	Re	V _x ft/sec
123005.	44.85	0.6189	7.40	10.03	83.00	9.0	1.16	2.2850	0.0652	0.0250	269008.2	0.414
123005.	44.85	0.6305	7.54	8.73	83.00	9.0	1.14	2.3277	0.0652	0.0241	274038.2	0.414
123005.	44.85	0.6078	7.27	11.32	83.00	9.0	1.18	2.2438	0.0652	0.0259	264159.6	0.414
123006.	49.92	0.6752	8.08	11.45	82.00	9.1	1.18	2.4927	0.0752	0.0242	289599.3	0.444
123006.	49.92	0.6729	8.05	11.70	82.00	9.1	1.19	2.4842	0.0752	0.0244	288612.2	0.444
123006.	49.92	0.6775	8.10	11.20	82.00	9.1	1.18	2.5013	0.0752	0.0240	290593.3	0.444
123007.	44.30	0.6160	7.37	9.49	81.00	9.2	1.15	2.2741	0.0674	0.0261	261322.9	0.421
123007.	44.30	0.6199	7.42	9.04	81.00	9.2	1.14	2.2887	0.0674	0.0257	263010.0	0.421
123007.	44.30	0.6120	7.32	9.94	81.00	9.2	1.16	2.2596	0.0674	0.0264	259657.2	0.421
123008.	34.75	0.5077	6.07	6.07	79.00	9.4	1.10	1.8745	0.0628	0.0357	210153.4	0.406
123008.	34.75	0.5087	6.08	5.94	79.00	9.4	1.09	1.8779	0.0628	0.0356	210539.3	0.406
123008.	34.75	0.5068	6.06	6.19	79.00	9.4	1.10	1.8711	0.0628	0.0359	209768.9	0.406
123009.	30.82	0.4587	5.49	4.83	78.00	9.6	1.08	1.6935	0.0577	0.0403	187283.1	0.389
123009.	30.82	0.4588	5.49	4.82	78.00	9.6	1.08	1.6938	0.0577	0.0403	187315.4	0.389
123009.	30.82	0.4586	5.49	4.84	78.00	9.6	1.08	1.6932	0.0577	0.0403	187250.8	0.389

TABLE C-2 - continued

SAND - WATER RUNS

Test No	Flow lb/sec	Q ft ³ /sec	V_m ft/sec	Ct %	Temp OF	\sqrt{V} ft ² /sec x 10 ⁶	SG Mixture	FW	i	f	Re	V_x ft/sec
123101.	25.64	0.3892	4.66	3.57	78.00	9.6	1.06	1.4369	0.0465	0.0451	158901.5	0.349
123101.	25.64	0.3882	4.64	3.73	78.00	9.6	1.06	1.4333	0.0465	0.0453	158506.9	0.349
123101.	25.64	0.3902	4.67	3.41	78.00	9.6	1.05	1.4405	0.0465	0.0448	159298.1	0.349
123101.	45.64	0.6158	7.37	11.61	80.00	9.3	1.19	2.2733	0.0817	0.0317	258427.2	0.463
123101.	45.64	0.6269	7.50	10.32	80.00	9.3	1.17	2.3146	0.0817	0.0305	263122.7	0.463
123101.	45.64	0.6050	7.24	12.90	80.00	9.3	1.21	2.2335	0.0817	0.0328	253896.2	0.463
123102.	62.69	0.8128	9.72	14.56	81.00	9.2	1.24	3.0007	0.0989	0.0220	344818.6	0.510
123102.	62.69	0.7982	9.55	15.93	81.00	9.2	1.26	2.9470	0.0989	0.0228	338652.1	0.510
123102.	62.69	0.8278	9.90	13.19	81.00	9.2	1.21	3.0563	0.0989	0.0212	351213.8	0.510
123103.	58.78	0.7522	9.00	15.55	82.00	9.1	1.25	2.7772	0.0955	0.0248	322648.3	0.501
123103.	58.78	0.7495	8.96	15.83	82.00	9.1	1.26	2.7670	0.0955	0.0250	321456.6	0.501
123103.	58.78	0.7550	9.03	15.27	82.00	9.1	1.25	2.7875	0.0955	0.0246	323848.9	0.501
123104.	58.17	0.7407	8.86	15.95	83.00	9.0	1.26	2.7346	0.0945	0.0253	321947.7	0.498
123104.	58.17	0.7342	8.78	16.62	83.00	9.0	1.27	2.7107	0.0945	0.0257	319134.2	0.498
123104.	58.17	0.7473	8.94	15.27	83.00	9.0	1.25	2.7590	0.0945	0.0249	324811.3	0.498

TABLE C-2 - continued

SAND - WATER RUNS

Test No	Flow lb/sec	Q ft ³ /sec	V _m ft/sec	Ct %	Temp OF	γ ft ² /sec x10 ⁶	SG Mixture	FN	1	f	Re	V _x ft/sec
123105.	56.84	0.7216	8.63	16.16	83.00	9.0	1.26	2.6641	0.0899	0.0253	313641.9	0.486
123105.	56.84	0.7144	8.55	16.94	83.00	9.0	1.27	2.6375	0.0899	0.0258	310512.3	0.486
123105.	56.84	0.7290	8.72	15.39	83.00	9.0	1.25	2.6912	0.0899	0.0248	316835.3	0.486
123106.	50.70	0.6320	7.56	17.59	83.00	9.0	1.29	2.3332	0.0836	0.0307	274692.5	0.469
123106.	50.70	0.6270	7.50	18.21	83.00	9.0	1.30	2.3148	0.0836	0.0312	272519.9	0.469
123106.	50.70	0.6371	7.62	16.97	83.00	9.0	1.27	2.3520	0.0836	0.0302	276900.0	0.469

TABLE C-3

GAMMA-RAY POINT CONCENTRATIONS, Cs

Test No	± Inches from Centerline												
	0	.2	.4	.6	.8	1.0	1.2	1.4	1.6	1.73	1.80	1.88	
122303	0.51	0.51 1.02	0.51 1.55	1.04 1.57	1.06 2.67	0. 2.77	0. 4.66	0.61 8.86	2.80 16.15	1.67 24.67	5.27 31.11	3.61 35.15	Top Horiz. Bottom Horiz.
122303	3.65	3.14 3.14	3.69 3.15	3.19 2.67	2.71 2.71	2.23 1.67	1.75 1.16	1.88 3.10	2.14 1.41	3.39 3.35	3.21 1.06	14.71 7.17	Top Vert. Bottom Vert.
122304	0.	0. 0.	0. 0.	0. 0.52	0. 1.06	0. 2.21	0. 4.06	0. 10.18	1.39 20.04	0. 27.49	2.10 33.46	1.80 37.07	
122304	4.18	3.67 3.67	3.69 3.69	3.19 2.67	3.26 2.71	2.23 2.23	1.16 1.74	0.62 1.85	0. 0.70	0.84 2.51	0. 1.06	1.82 8.98	
122307	0.	0. 8.46	0. 4.72	0.52 4.78	1.06 4.86	0. 3.90	0. 4.06	0.61 3.73	1.39 0.70	1.67 0.	5.27 4.24	9.08 7.20	
122307	6.89	6.38	5.31	4.28	1.62	2.80	2.34	1.25	0.	1.69	1.07	0.	
122309	0.	0. 0.	0. 0.	0. 0.	0. 0.53	1.11 0.	9.59 0.	19.74 0.	27.41 1.39	38.17 0.83	42.22 5.27	52.49 5.43	
122309	3.12	2.61 2.61	3.15 2.62	2.65 1.59	2.16 1.62	1.11 1.11	1.16 1.74	1.25 3.10	0.71 0.70	0.84 2.51	1.07 1.06	3.64 7.17	
122310	0.	0.51 1.02	0.51 1.03	0.52 2.10	0.53 2.67	0. 2.77	0. 5.25	0.61 6.92	2.10 9.35	2.51 15.53	7.40 15.12	9.08 10.84	
122310	2.59	2.61 2.08	3.15 2.62	2.65 1.59	2.16 1.62	1.67 1.11	1.16 1.16	1.88 2.47	2.14 0.70	3.39 2.51	4.29 0.	9.15 3.57	
122401	1.54	1.54 3.61	1.03 4.72	0.52 5.87	0.53 8.80	0. 10.91	0. 15.19	0.61 19.74	2.10 27.29	1.67 32.28	4.21 32.28	7.25 37.07	
122401	7.44	6.93 6.93	6.41 6.41	6.49 5.96	6.06 6.06	5.66 5.66	4.72 5.30	5.06 6.92	5.04 5.72	5.11 6.76	6.46 6.43	7.30 8.98	
122402	1.54	1.02 3.09	0.51 4.18	0. 5.87	0.53 8.23	0. 10.91	0. 15.83	0. 21.17	0.70 27.29	1.67 33.25	5.27 32.28	5.43 37.07	
122402	7.44	7.48 7.48	7.52 7.52	7.05 6.53	6.63 6.06	6.25 5.66	5.93 4.70	5.71 6.27	5.04 3.55	6.84 4.20	8.64 2.13	14.71 10.80	
122403	1.54	1.02 2.56	1.03 3.65	1.04 5.32	1.06 8.80	0.55 11.51	0.58 17.14	1.23 24.79	1.39 30.61	2.51 37.18	4.21 40.66	3.61 42.87	C
122403	8.00	7.48 6.93	7.52 7.52	7.05 6.53	6.63 6.63	6.25 6.25	5.33 5.91	4.42 6.27	4.31 4.99	5.11 5.91	4.29 3.20	3.64 12.62	9

TABLE C-3 - continued

GAMMA-RAY POINT CONCENTRATIONS, C_s

Test No	0	± Inches from Centerline								1.6	1.73	1.80	1.88
		.2	.4	.6	.8	1.0	1.2	1.4					
122404	1.54	1.02	1.03	0.52	0.53	0.55	0.	0.	2.10	1.67	5.27	5.43	
122404	7.44	2.56	3.12	5.32	8.23	12.12	17.80	24.79	32.30	38.17	43.10	44.82	
		8.04	8.08	7.05	7.20	6.25	5.93	5.06	3.58	5.11	4.29	0.	
122405	1.54	8.04	7.52	7.09	7.20	6.83	5.91	7.56	4.99	6.76	6.43	16.29	
122405	7.44	1.02	1.03	1.04	1.59	1.10	0.	1.23	2.10	2.51	3.15	7.25	
		2.56	3.12	4.78	7.66	10.91	17.14	24.06	28.94	37.18	40.66	38.99	
122406	1.02	6.93	6.96	6.49	5.50	5.66	4.72	3.78	1.42	2.54	2.14	0.	
		6.93	6.96	6.53	6.06	6.25	4.70	4.99	3.55	4.20	3.20	10.80	
122406	6.89	1.02	0.51	0.	1.06	0.	0.	0.	0.	0.	0.	0.	
123001	3.63	2.05	3.12	3.70	7.09	12.12	17.80	27.75	42.79	56.88	60.80	62.70	
		7.48	7.52	7.61	7.20	5.66	3.53	4.42	2.14	2.54	2.14	0.	
123001	12.55	6.38	8.08	7.65	7.20	7.42	5.91	5.63	4.99	6.76	6.43	14.45	
123002	5.23	2.58	1.55	1.04	1.06	0.	0.	0.61	0.70	0.83	3.15	1.80	
		6.81	9.67	13.87	17.77	22.33	28.14	33.89	38.34	43.21	48.05	58.67	
123002	10.82	12.62	12.68	12.24	11.89	11.63	10.27	10.99	9.47	9.47	7.55	5.47	
		12.62	12.10	11.71	11.30	11.02	12.11	12.84	10.89	12.86	11.90	19.98	
123002	5.23	3.63	2.59	2.63	1.59	0.55	0.	1.85	2.10	0.83	6.33	7.25	
123002	10.82	7.91	9.67	12.10	15.92	19.04	23.21	27.75	32.30	39.17	40.66	50.71	
		10.88	10.93	9.90	10.11	10.41	9.64	10.32	7.98	8.59	10.84	5.47	
123003	4.69	10.88	10.93	9.95	10.11	10.41	10.22	11.50	10.89	13.75	11.90	23.70	
123003	11.39	3.10	2.59	2.10	1.59	0.55	0.	0.61	1.39	2.51	5.27	7.25	
		7.36	9.11	12.10	15.92	19.69	25.30	30.79	34.86	39.17	43.10	50.71	
123003	11.39	10.88	10.93	10.48	10.11	9.21	8.39	8.33	7.24	6.84	7.55	0.	
123004	4.16	11.45	10.93	9.95	10.11	10.41	10.22	11.50	10.14	11.98	11.90	21.83	
123004	11.97	2.58	2.07	1.57	1.06	0.55	0.58	0.61	2.10	1.67	5.27	5.43	
		7.36	9.11	12.10	16.53	21.00	27.43	33.11	36.59	42.19	44.33	50.71	
123004	11.97	11.45	12.10	11.06	11.30	10.41	10.27	10.32	7.24	9.47	9.74	9.15	
123004	11.97	5.83	5.31	4.85	4.93	10.41	10.22	10.84	9.39	8.49	9.70	18.13	

TABLE C-3 - continued
GAMMA-RAY POINT CONCENTRATIONS, C_s

Test No	0	± Inches from Centerline								1.73	1.80	1.88
		.2	.4	.6	.8	1.0	1.2	1.4	1.6			
123005	3.10	3.10 5.73	2.59 6.89	2.10 10.36	1.59 15.30	0.55 19.04	0.58 26.00	1.85 31.56	3.51 37.46	2.51 44.23	5.27 49.30	5.43 58.67
123005	12.55	11.45 12.03	11.51 11.51	11.65 11.12	11.30 11.30	10.41 10.41	9.64 10.85	10.32 11.50	7.98 10.14	8.59 10.23	8.64 10.80	5.47 19.98
123006	3.10	2.58 5.73	1.55 8.55	1.04 12.10	0.53 15.92	0. 19.69	0. 26.00	0. 31.56	0.70 35.72	0.83 42.19	5.27 46.80	3.61 54.67
123006	12.55	11.45 12.03	11.51 11.51	11.65 11.12	10.70 11.30	9.81 10.41	9.64 10.85	10.32 12.17	7.98 10.89	7.72 11.10	8.64 11.90	5.47 19.98
123007	3.10	1.54 5.20	0.51 7.44	1.04 10.94	1.06 15.30	0. 19.69	0. 26.71	0. 31.56	1.39 34.86	0. 43.21	4.21 48.05	1.80 54.67
123007	11.39	10.88 10.88	10.36 11.51	10.48 9.95	10.11 10.70	9.21 9.81	15.42 9.59	8.99 10.13	7.98 8.65	8.59 11.10	7.55 8.61	3.64 14.45
123008	2.06	1.02 3.09	0.51 7.44	0. 7.53	0. 15.30	0. 19.04	0. 23.21	0. 35.46	0. 47.36	0. 54.72	0. 56.92	0. 62.70
123008	8.55	10.88 9.16	8.65 10.36	11.65 8.80	9.52 11.89	9.21 9.21	9.01 9.59	5.71 10.13	6.50 6.45	5.98 9.35	5.37 9.70	1.82 14.45
123009	2.06	1.54 4.67	0.51 7.44	0. 12.10	0.53 17.77	0. 24.35	0. 31.80	1.23 43.63	1.39 52.06	0.83 57.97	4.21 60.80	3.61 66.76
123009	13.73	13.80 13.80	13.87 13.87	14.63 12.90	13.71 14.32	12.86 12.86	11.53 12.11	9.65 12.17	7.98 9.39	7.72 10.23	6.46 8.61	5.47 16.29
123010	1.54	0.51 3.61	0.51 6.89	0. 11.52	0.53 20.30	0. 27.10	0. 39.45	0. 49.65	0.70 52.06	0. 59.07	2.10 68.75	0. 79.14
123010	14.91	14.99 14.39	15.07 14.46	14.03 13.50	14.32 13.71	14.11 14.11	12.17 13.39	10.32 12.84	5.77 9.39	5.11 10.23	5.37 8.61	0. 18.13

TABLE C-3 - continued
GAMMA-RAY POINT CONCENTRATIONS, C_s

Test No	0	+ Inches from Centerline								1.73	1.80	1.88
		.2	.4	.6	.8	1.0	1.2	1.4	1.6			
123101	8.51	5.77 12.41	3.65 15.49	2.63 20.01	1.59 24.21	0.55 27.10	0. 31.80	0. 36.26	0.70 39.22	0.83 45.25	3.15 49.30	0. 62.70
123101	15.51	14.99 14.99	15.67 15.07	15.24 14.11	14.54 14.32	13.49 14.11	14.11 14.69	14.40 14.88	13.26 16.22	13.92 17.33	14.18 17.49	9.15 25.57
123102	9.06	6.85 11.83	5.26 14.90	4.23 17.51	2.67 20.54	1.10 23.67	0.58 28.14	1.23 32.33	2.10 34.86	1.67 40.17	3.15 41.88	3.61 48.74
123102	13.73	13.21 13.21	12.68 12.68	12.83 12.90	13.10 12.50	12.86 12.86	12.17 12.75	12.34 14.88	10.98 13.91	12.13 16.43	10.84 17.49	0. 27.44
123103	9.63	7.95 12.98	5.80 16.09	4.23 18.13	3.21 22.89	2.21 25.72	2.32 29.59	3.73 35.46	4.22 38.34	2.51 43.21	5.27 46.80	7.25 54.67
123103	13.73	13.80 13.80	13.87 13.87	12.83 12.90	13.71 12.50	12.86 12.86	12.81 12.75	13.03 14.20	11.74 13.91	13.02 16.43	11.95 15.24	3.64 25.57
123104	7.95	6.85 11.83	4.18 13.71	3.16 17.51	3.21 21.59	2.21 25.03	1.15 28.87	1.85 33.11	3.51 35.72	3.35 42.19	6.33 44.33	10.92 44.82
123104	14.91	14.39 14.39	14.46 14.46	14.63 14.11	13.71 13.71	12.86 13.49	13.46 14.69	13.03 15.56	11.74 14.68	12.13 18.23	11.95 17.49	0. 31.22
123105	7.40	5.77 10.69	3.65 14.90	2.63 16.89	1.66 21.59	0.55 25.03	0. 29.59	1.23 33.11	2.10 36.59	1.67 40.17	6.33 41.88	9.08 35.15
123105	14.91	14.39 14.39	14.46 15.07	13.43 14.11	13.71 13.71	13.49 13.49	13.46 14.04	13.71 14.88	11.74 13.91	13.02 15.53	11.95 16.36	5.47 23.70
123106	7.95	5.23 11.26	4.72 13.71	2.63 17.51	1.59 22.89	0.55 26.41	0. 31.80	0. 36.26	1.39 39.22	1.67 45.25	3.15 49.30	5.43 60.68
123106	16.12	15.60 14.99	15.67 15.67	15.85 14.71	14.32 14.94	14.11 14.11	14.11 14.04	14.40 16.94	13.26 15.44	13.92 17.33	16.42 15.24	14.71 25.57

TABLE C - 4

C 13

FLOW ACCURACYFlow meter reading 21.5 - Temperature 79° F

FINAL WEIGHT lb	INITIAL WEIGHT lb	DIFF. lb	TIME sec	FLOW lb/sec
1046.0	868.0	178.0	12.20	14.59
1045.0	866.0	179.0	12.25	14.61
1046.0	866.0	180.0	12.25	14.69
1045.0	866.0	181.5	12.40	14.63
1050.5	867.0	183.5	12.40	14.79
1047.5	868.0	179.5	12.10	14.83
1044.0	868.0	176.0	11.85	14.80
1046.0	868.5	177.5	11.95	14.85
1042.0	869.0	173.0	11.80	14.66
1044.0	869.0	175.0	11.80	14.83
1046.0	869.5	176.5	11.87	14.86
1047.0	870.0	177.0	12.0	14.75
1049.0	871.0	178.0	12.0	14.83
1048.0	872.0	176.0	11.8	14.91
1050.0	872.0	178.0	11.9	14.95
1047.5	872.5	175.0	11.67	14.99
1050.0	872.5	177.5	11.85	14.98
Average, Calculated				14.79
Actual				14.80
Std Dev, Calculated				±0.13
Actual				±0.15
				or ±1%

Flow meter reading 29.2 - Temperature 82° F

FINAL WEIGHT lb	INITIAL WEIGHT lb	DIFF. lb	TIME sec	FLOW lb/sec
981.0	836.5	144.5	6.95	20.79
975.5	837.0	138.5	6.70	20.67
972.0	837.5	134.5	6.60	20.38
981.0	838.0	143.0	7.05	20.28
979.0	839.0	140.0	6.90	20.29
Average				20.5
Std Dev, Calculated				±0.2
Actual				±0.5
				or ±2.5%

CHECK ON REPRODUCIBILITYFlow meter reading 60.0 - Temperature 79° F
Transport Concentration - 2.1 Volume %

TEST NO.	INITIAL WEIGHT lb	FINAL WEIGHT lb	DIFFERENCE lb	TIME seconds	FLOW lb/ sec	DIFFERENCE lb
122303	1106.00	1598.90	492.90	11.15	43.59	
122308	1059.00	1521.50	462.50	10.60	43.63	0.04

C.5 ACCURACY OF CONCENTRATION MEASUREMENT BY GAMMA-RAY INSTRUMENT, C_s

The standard errors of the measured quantities of EQUATIONS 2.12 and 2.16 are summarized in this section. The standard error of C_s is calculated at four points in the pipe and for values of C_s close to actual test conditions. These points and concentrations are:

Distance from pipe center, inches . . .	0	0.6	1.2	1.8
Concentration, %	5	10	30	50

C.5.1 STANDARD ERROR OF PATH LENGTH, x

$$x = 2[R^2 + (y \cdot F)^2]^{1/2} \quad (2.10.1)$$

$$\text{Standard error, } s_x = \left[\left(\frac{\partial x}{\partial R} \cdot s_R \right)^2 + \left(\frac{\partial x}{\partial F} \cdot s_F \right)^2 \right]^{1/2}$$

$$= \frac{4}{x} \left[(R^2 \cdot s_R)^2 + (y^2 \cdot F \cdot s_F)^2 \right]^{1/2} \quad . (C-5.1)$$

All measured and calculated values are listed below.

$$R = 3.916" \quad s_R = 0.0077" \quad (\text{TABLE B-5})$$

$$F = 1.008 \quad s_F = 0.0028 \quad (\text{TABLE B-6})$$

y , inches	0	0.6	1.2	1.8
x , inches	3.916	3.724	3.079	1.472
s_x , inches	0.015	0.016	0.020	0.048

C.5.2 STANDARD ERROR OF $k = k_s - k_w$

$$k_s = 0.443/\text{inch} \quad s_{k_s} = 0.018/\text{inch} \quad (\text{TABLE B-3.1})$$

$$k_w = 0.166/\text{inch} \quad s_{k_w} = 0.0055/\text{inch} \quad (\text{TABLE B-3.2})$$

$$\text{Standard error, } s_k = \left[(s_{k_s})^2 + (s_{k_w})^2 \right]^{1/2} \quad (C-5.2)$$

TABLE C-5

ACCURACY OF TRANSPORT CONCENTRATION DURING TEST RUNS

Test No	<u>VOLUME % SAND</u>			Root Mean Square of Deviations
	Sample 1	Sample 2	Deviation from Average	
122303	1.85	2.15	0.15	± 0.44
122304	2.69	2.30	0.18	
122307	1.48	1.88	0.22	
122309	2.74	2.77	0.02	
122310	2.35	2.46	0.56	
122401	6.33	7.32	0.50	
122402	7.16	6.23	0.46	
122403	5.98	5.55	0.26	
122404	5.26	5.00	0.13	
122405	5.76	4.67	0.54	
122406	3.45	5.87	1.21	
123007	9.04	9.94	0.45	
123008	5.94	6.19	0.12	
123009	4.84	4.82	0.01	
123010	3.73	3.41	0.16	
123001	10.03	11.77	0.87	± 0.80
123002	10.98	11.87	0.44	
123003	11.69	11.59	0.50	
123006	11.70	11.20	0.25	
123101	10.31	12.90	1.29	
123102	15.93	13.19	1.37	
123103	15.83	15.27	0.28	
123104	16.62	15.27	0.68	
123105	16.94	15.39	0.78	
123106	18.21	16.97	0.62	
			Overall	± 0.61

$$= \pm 0.0188$$

$$= \pm 0.019/\text{inch}$$

$$k = 0.267 \pm 0.019/\text{inch}$$

This value of k is used for the 17 points $\pm 1.6''$ from the pipe center.

C.5.3 STANDARD ERROR OF $k = 1.61 k_w$

The values of k_w in the end regions where $y > \pm 1.6''$ were obtained from the pipe scanning tests (TABLES B-3.6, 3.7, 3.8 and 3.9) and are summarized below.

TABLE C-5.2

y, inches x, inches	1.72 1.82	1.8 1.472	1.88 0.985
k_w	.1608 .1621 .1612 .1594 .1648 .1615 .1608 .1629 .1601 .1521	.1502 .1498 .1561 .1478 .1598 .1492 .1400 .1559 .1372	.1100 .1238 .1375 .1030 .1240 .1112 .1380 .1435 .1275
Average	<u>.1606</u>	<u>.1495</u>	<u>.1242</u>
s_{k_w}	.0044	.0070	.0159
s_k		.0200	

STANDARD ERROR OF FACTOR, $1.61 = \left(\frac{k_s}{k_w} - 1 \right)$

Standard error, $s_{1.61} = \frac{1}{k_w} \left[(s_{k_s})^2 + (k_s \cdot s_{k_w})^{1/2} \right] \quad (C-5.3.1)$
 $= \pm 0.110$, where values of k_s , k_w , s_{k_s} ,
and s_{k_w} are those listed under C-5.2.

Standard error of 1.61 k_w :

$$s_k = \left[(1.61 s_{k_w})^2 + (k_w \cdot s_{1.61})^2 \right]^{1/2} \dots (C-5.3.2)$$

= ± 0.020 for values of k_w and s_{k_w} at $y = 1.8''$

from TABLE C-5.2 .

i.e. $k = 1.61 k_w \pm 0.020$ at $y = 1.8''$.

C.5.4 STANDARD ERROR OF $\ln E = \ln(E) - \ln(E_p)$

The standard deviations of the readings at the 23 points listed in TABLES B-3.3 and 3.4 expressed as a percentage of the value at each point appear to be fairly random but show somewhat poorer accuracy in the end regions as would be expected. These values are listed in TABLE C-5.4 and are averaged separately for the center, end and overall pipe areas.

From this table, standard errors are found to be:

$$\begin{aligned} s_{\ln E} = s_{\ln E_p} &= 0.0052 \ln(E) \text{ for } y \leq \pm 1.6'' \\ &= 0.0063 \ln(E) \text{ for } y > \pm 1.6'' \end{aligned}$$

TABLE C-5.4

STANDARD DEVIATIONS OF $\ln(E_p)$ FROM HORIZONTAL BEAM

SCANNING TESTS

VALUES FROM TABLES B-3.3 and B-3.4

Location \pm Inches from Pipe Center	Top % Dev	Bottom % Dev	Overall Averages % Dev
0	0.41		
0.2	0	0.381	
0.4	0.322	0.321	
0.6	0.314	0.695	
0.8	0.357	0.464	
1.0	0.675	1.000	
1.2	0.496	0.780	
1.4	0.876	0.884	
1.6	0.608	0.598	
Average	0.45	0.64	0.52
1.72	0.538	0.866	
1.80	0.621	0.734	
1.88	0.426	0.618	
Average	0.53	0.74	0.63
Overall			0.56

Standard error of $\ln e = \ln(E_p/E)$,

$$\begin{aligned}
 s_{\ln e} &= \left[(s_{\ln E})^2 + (s_{\ln E_p})^2 \right]^{1/2} \\
 &= 0.0052 \left[(\ln E)^2 + (\ln E_p)^2 \right]^{1/2} \\
 &\quad \text{for } y \leq \pm 1.8'' \\
 &= 0.0063 \left[(\ln E)^2 + (\ln E_p)^2 \right]^{1/2} \\
 &\quad \text{for } y > \pm 1.8''
 \end{aligned}$$

Values of $s_{\ln e}$ are calculated for concentrations of 5, 10, 30, and 50% at distances 0, 0.6, 1.2, 1.8 inches from the pipe center as shown in TABLE C-5.5 .

TABLE C-5.5

y, inches	0	0.6	1.2	1.8
C_s , %	5	10	30	50
$\ln(E_p)$	0.6345	0.6626	0.7561	1.0430
$\ln(E)$	0.5822	0.5632	0.5095	0.8658
v	0.0523	0.0994	0.2466	0.1772
$s_{\ln e}$	0.0045	0.0045	0.0048	0.0085

C.5.5 STANDARD ERROR OF C_s

The standard error of C_s is calculated from;

$$s_{C_s}^2 = \left(\frac{\partial C_s}{\partial \ln e} \cdot s_e \right)^2 + \left(\frac{\partial C_s}{\partial k} \cdot s_k \right)^2 + \left(\frac{\partial C_s}{\partial x} \cdot s_x \right)^2 \dots (C-5.1)$$

where s_e , s_k , s_x are the standard errors of quantities

$\ln(E_p/E)$, $k = 0.267/\text{inch}$, path length x are given under the preceding sections.

$\frac{\partial C_s}{\partial \ln e}$, $\frac{\partial C_s}{\partial k}$, $\frac{\partial C_s}{\partial x}$ are partial derivatives of the equation,

$$C_s = \frac{100 \ln e}{kx}$$

and their values substituted in EQUATION C-5.1 simplify to;

$$s_{C_s} = \frac{100}{kx} \left[s_{\ln e}^2 + \left(\frac{\ln E s_k}{k} \right)^2 + \left(\frac{\ln E s_x}{x} \right)^2 \right]^{1/2} \dots (C-5.2)$$

The values of each term and computation of s_{C_s} at the 4 points and for the 4 concentrations are given in TABLE C-5.6 .

TABLE C-5.6
SAMPLE CALCULATION FOR ACCURACY OF CONCENTRATION
BY GAMMA-RAY INSTRUMENT

Location, y Inches below Pipe center	0	0.6	1.2	1.8
Concentration, C_s	5	10	30	50
x, Inches	3.916	2.724	3.079	1.472
s_x	0.015	0.016	0.020	0.048
lne	0.0523	0.0994	0.2466	0.1772
s_{lne}	0.0045	0.0045	0.0048	0.0085
k	0.267	0.267	0.267	0.241
s_k	0.019	0.019	0.019	0.020
1 $(s_{lne})^2 \cdot 10^6 *$	19.98	20.43	23.04	72.25
2 $(\frac{lne s_k}{k})^2 \cdot 10^6 *$	13.84	50.27	308.01	217.04
3 $(\frac{lne s_x}{k})^2 \cdot 10^6 *$	8.59	35.74	341.14	1245.41
$\Sigma 1,2,3 \cdot 10^6 *$	40.96	106.44	672.19	1534.70
$100(\Sigma 1,2,3)^{1/2} *$.64	1.0317	2.51	3.91
$\frac{100}{kx} [\Sigma 1,2,3]^{1/2} *$	1.0456	.9943	.8221	.3548
s_{C_s}	.61	1.04	3.05	11.0

* Based on data before rounding off to
3 significant figures.

TABLE C-6

COMPARISON OF SAND CONCENTRATION FROM INTEGRATED
GAMMA-RAY CONCENTRATION PROFILES (\bar{C}_s)
WITH TRANSPORT CONCENTRATION (C_t)
OBTAINED BY SAMPLING AT PIPE DISCHARGE

Test No	Horizontal Beam	Vertical Beam	Average	Sample Average C_t	Deviation From Average	Root Mean Square Deviation
122303	3.12	2.72	2.92	2.00	0.46	± 1.09
122304	2.64	2.78	2.71	2.50	0.21	
122309	2.31	2.02	2.16	2.76	0.60	
122310	2.31	2.09	2.20	2.41	0.21	
122401	5.31	6.20	5.75	6.82	1.07	
122402	6.06	6.50	6.28	6.69	0.41	
122403	6.80	6.45	6.63	5.77	0.86	
122404	8.58	7.35	7.96	5.13	2.83	
122405	6.59	5.73	6.16	5.22	0.94	
123007	9.52	10.45	9.99	9.49	0.50	
123001	10.72	11.81	11.26	10.90	0.36	± 1.95
123002	10.04	10.48	10.26	11.44	1.18	
123003	10.22	10.23	10.23	11.64	1.41	
123004	11.56	9.37	10.46	9.50	0.96	
123006	9.83	11.06	10.45	11.45	1.00	
123101	13.67	14.82	14.24	11.61	2.63	
123102	12.89	13.03	12.96	14.56	1.60	
123103	14.62	13.40	14.01	15.55	1.54	
123104	13.14	14.21	13.68	15.95	2.27	
123105	12.52	14.09	13.30	16.16	2.86	
123106	13.27	15.22	14.25	17.59	3.34	

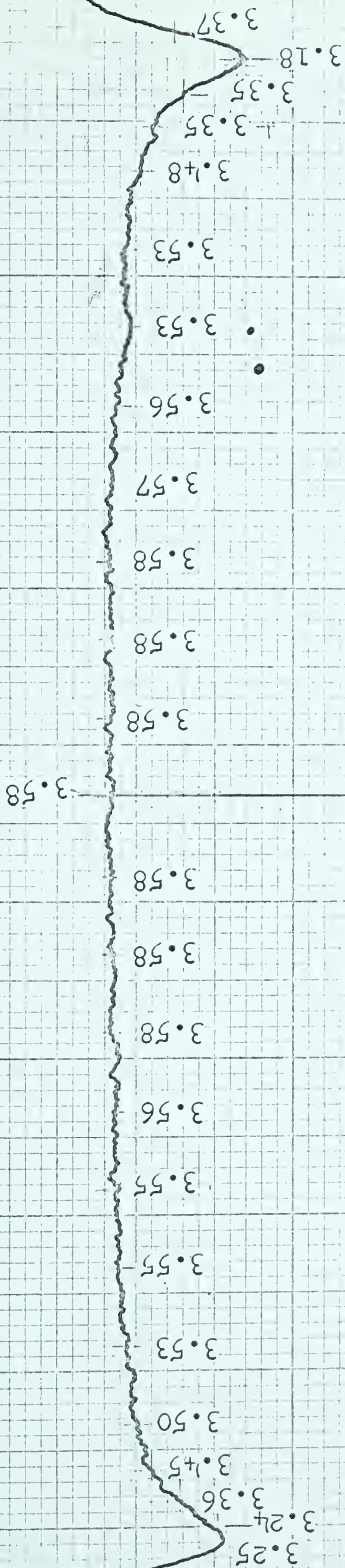
Note: Tests with fixed beds have been omitted.

APPENDIX C

STANDARD PIPE WALL ABSORPTION CURVES

TESTS # 122001 to 122003

TEST NO. I22001
HORIZONTAL BEAM



START

VALUES UNRELIABLE

TEST NO. 122001
VERTICAL BEAM

3.48
3.43
3.38

3.50

3.56

3.59

3.60

3.60

3.60

3.60

3.60

3.58

3.60

3.60

3.60

3.60

3.58

3.57

3.54

3.50

3.43

3.30

3.22

3.25

START

3.62

3.10
3.12

3.30

3.36

3.42

3.45

3.46

3.47

3.49

3.50

3.50

3.50

3.50

3.50

3.48

3.48

3.48

3.48

3.45

3.43

3.38

3.35

3.25

3.10
3.13

TEST NO. I22002
HORIZONTAL BEAM

[illegible]

3.30

3.43

3.48

3.55

3.57

3.58

3.58

3.60

3.60

3.60

3.60

3.60

3.60

3.60

3.60

3.58

3.57

3.55

3.51

 3.45

3.28

• 26

3.28

3.50

$$3.36$$

3.16
3.25
3.30

 3.145 3.17

87.8

3.148

3.50

3.50

3.50

1

3.50

- 050 -

50.

841.9

9+1.

 $\xi + 1$

5+1.

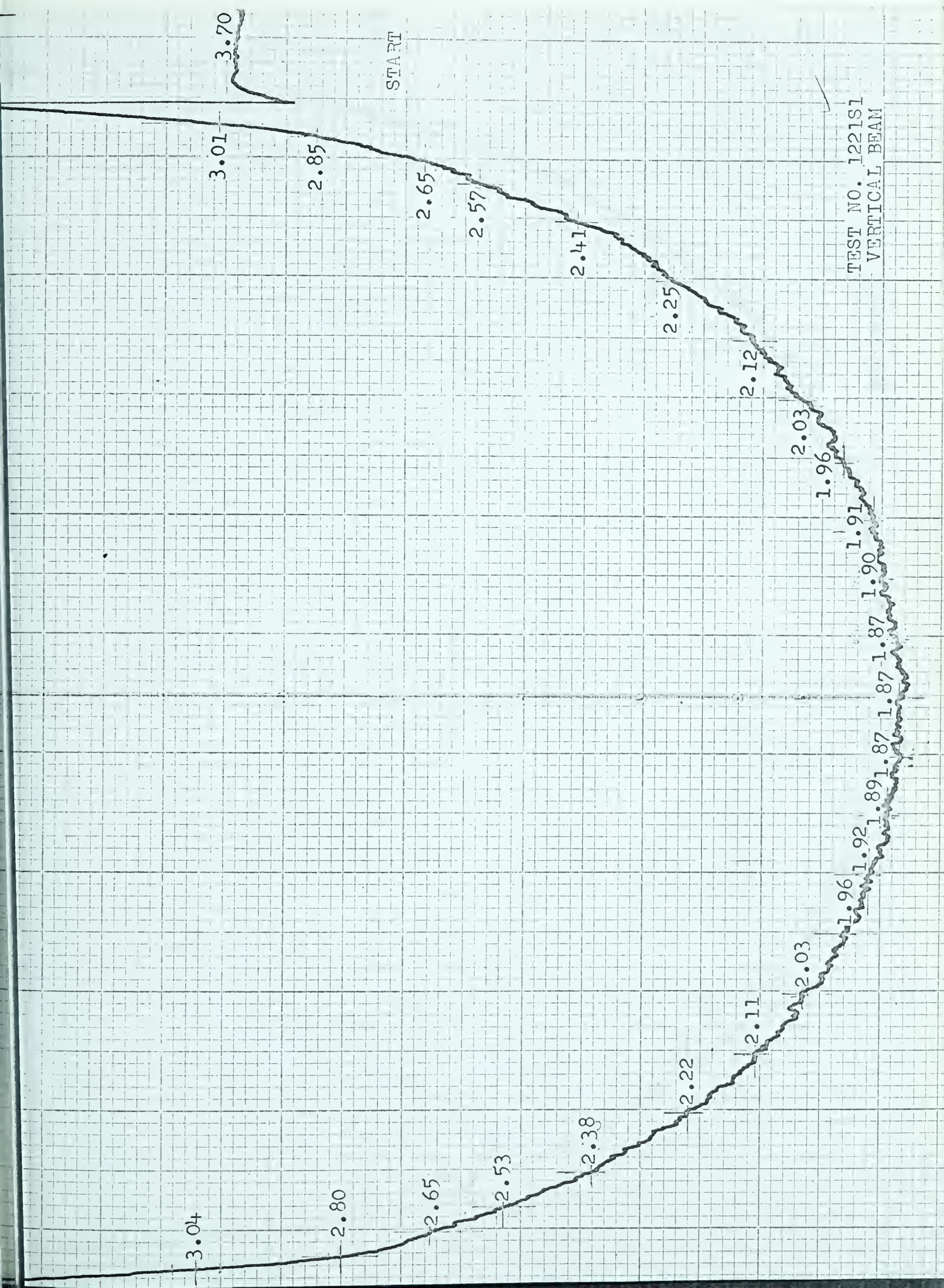
I + 1

3.

APPENDIX C

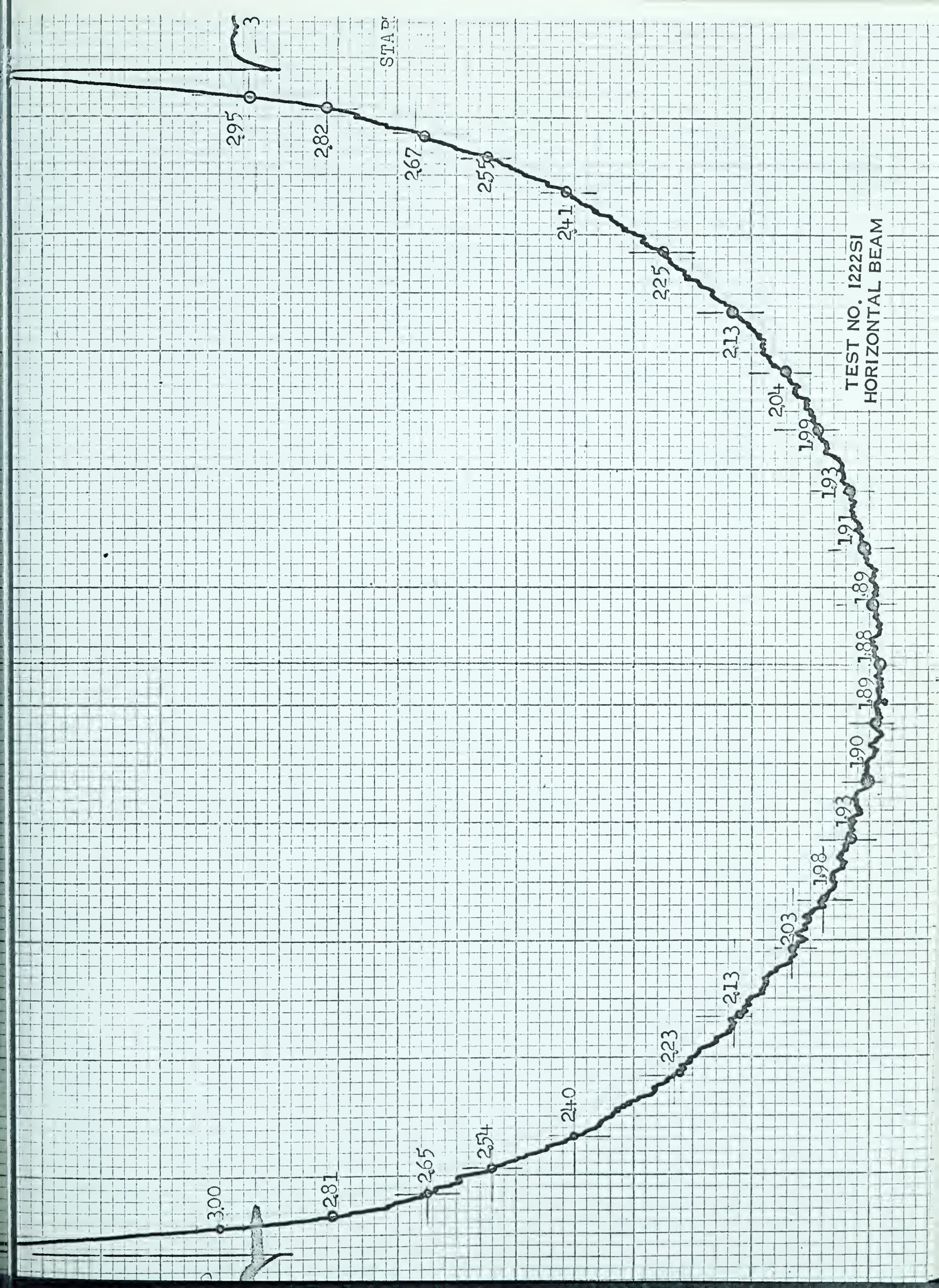
STANDARD ABSORPTION CURVES OF PIPE WITH WATER

TESTS # 1221S1 to 1223S3



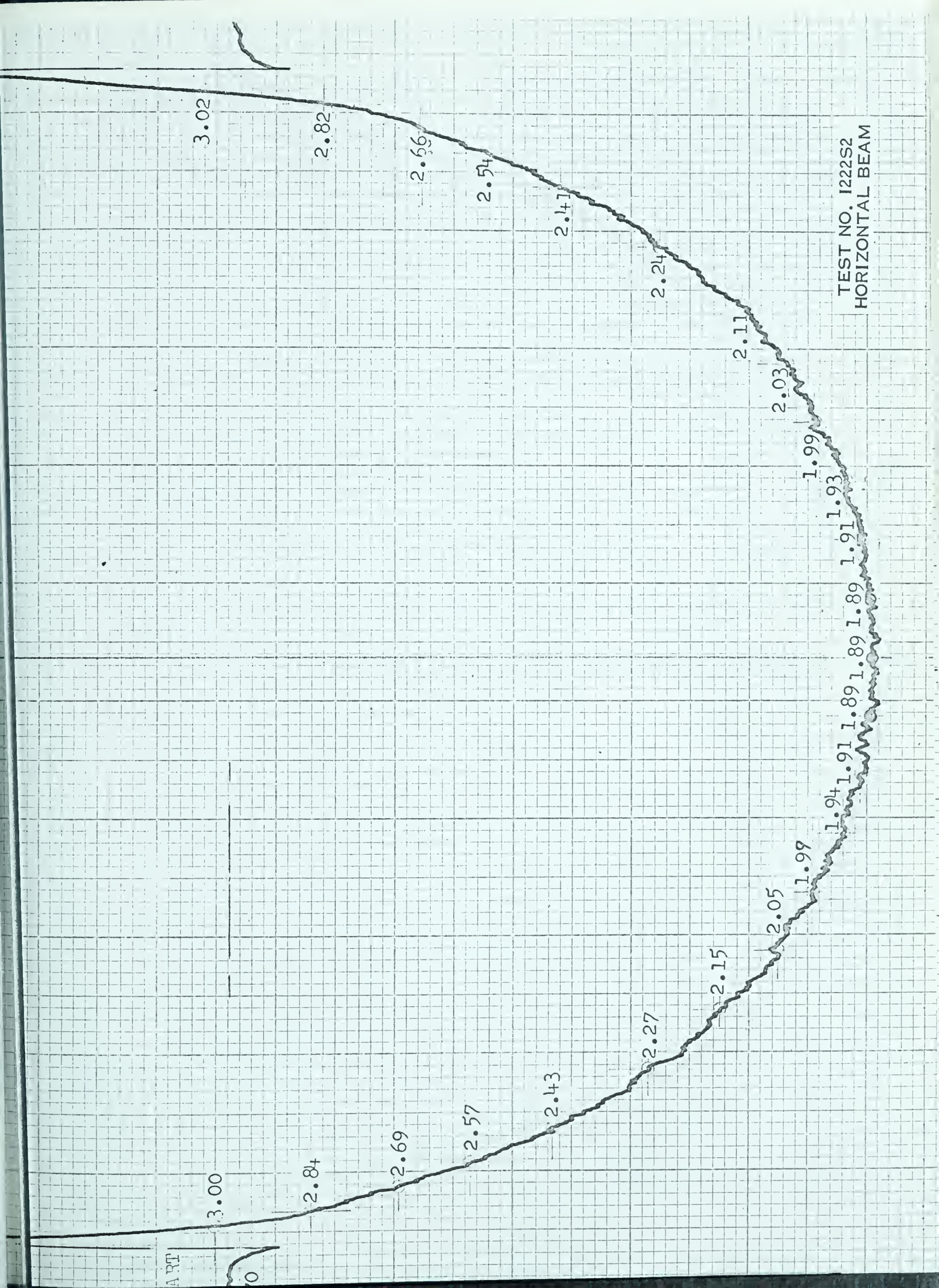
START

TEST NO. 1221S1
VERTICAL BEAM



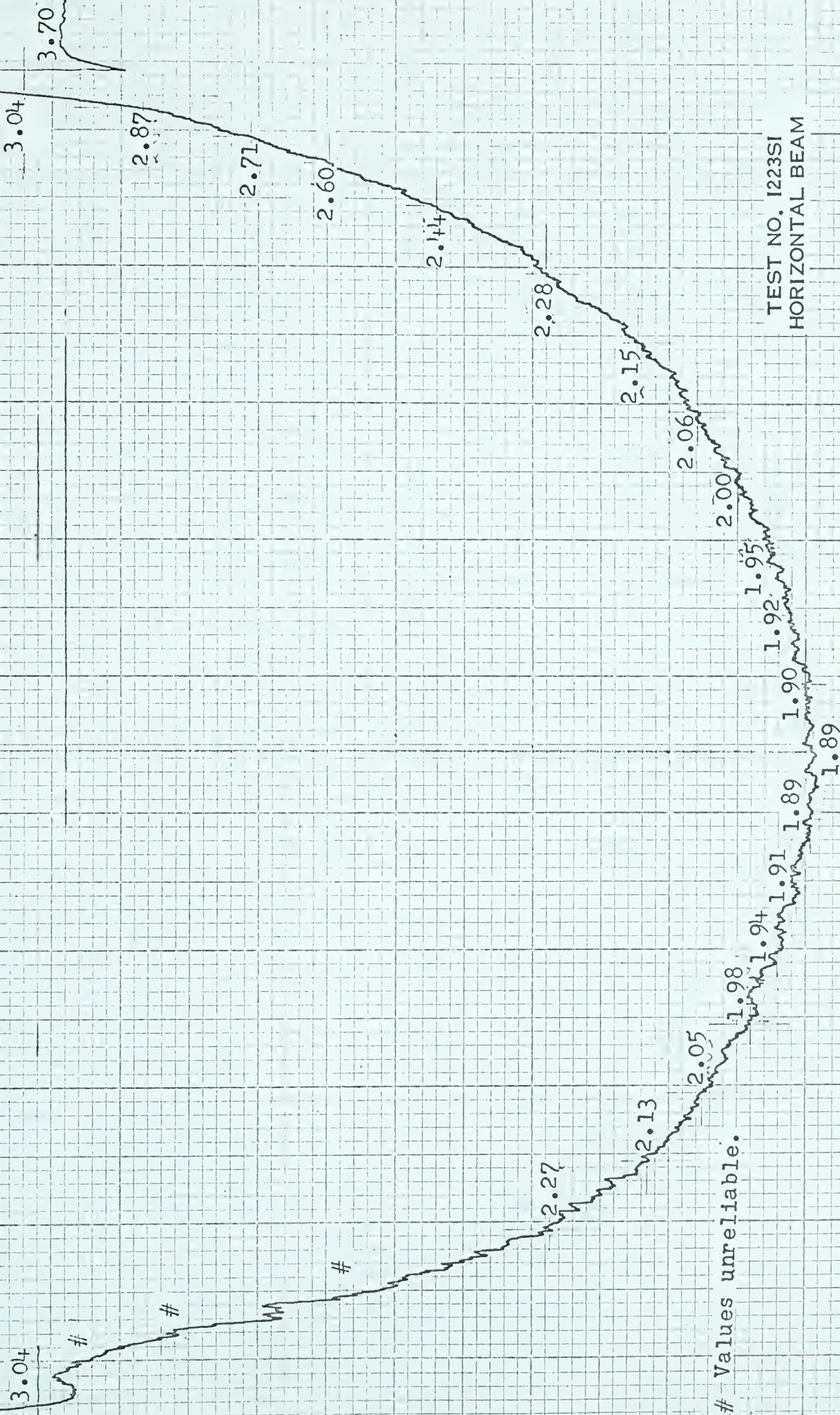
TEST NO. 1222SI
HORIZONTAL BEAM

STAP



TEST NO. I222S2
HORIZONTAL BEAM

START



Values unreliable.

TEST NO. 1223SI
HORIZONTAL BEAM

START

TEST NO. I223S2
HORIZONTAL BEAM

3.01

2.81

2.68

2.57

2.41

2.24

2.13

2.03

1.98

1.94

1.91

1.90

1.89

1.89

2.06

2.13

2.27

2.43

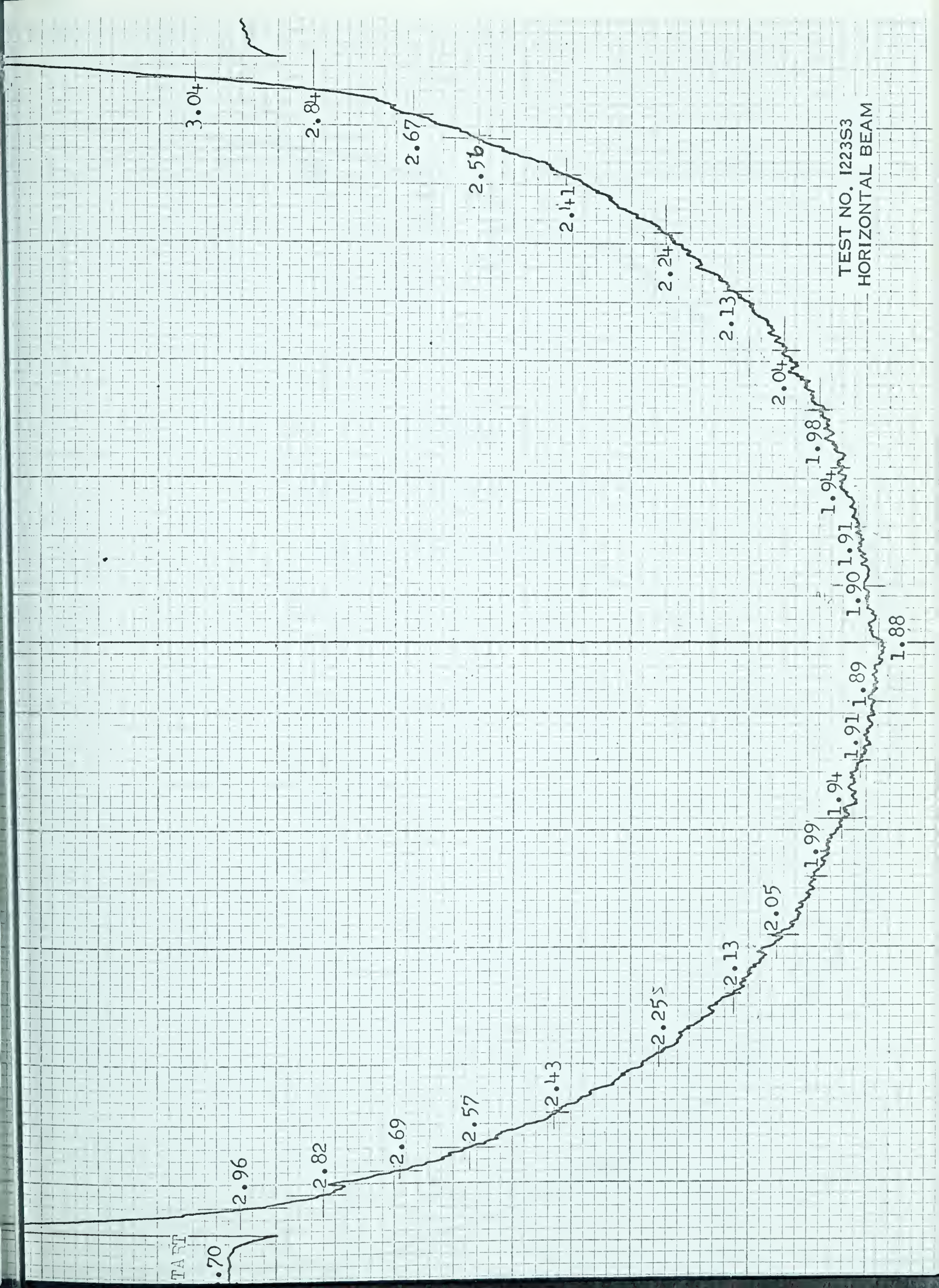
2.55

2.70

2.84

3.00

3.70



START

3.01

3.70

2.86

2.67

2.56

2.40

2.25

2.11

2.02

1.96

1.92

1.89

1.87

1.89

1.87

1.87

1.89

1.91

2.01

1.96

2.10

2.22

2.38

2.53

2.65

2.80

3.04

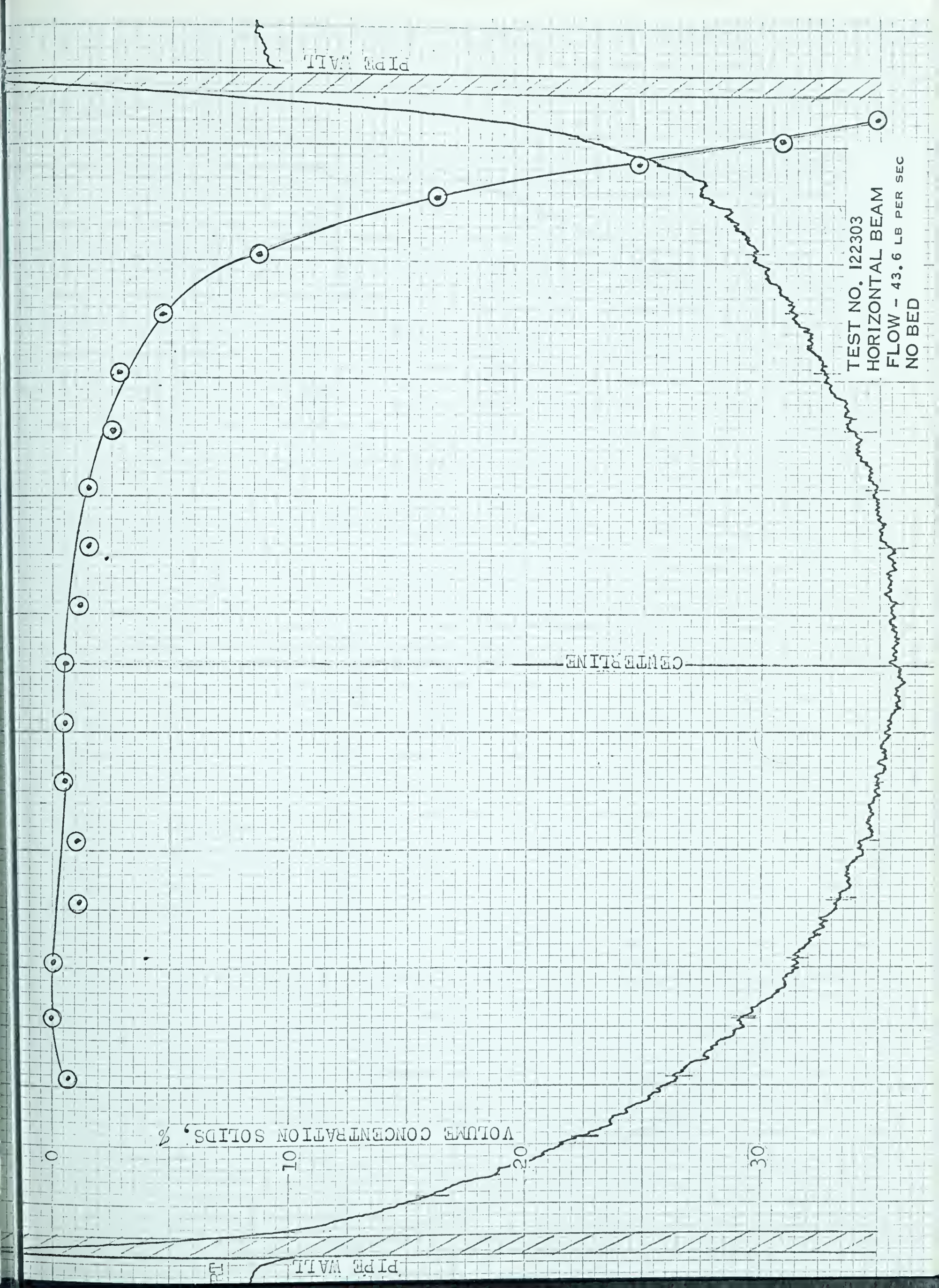
TEST NO. 1223S3

VERTICAL BEAM

APPENDIX C

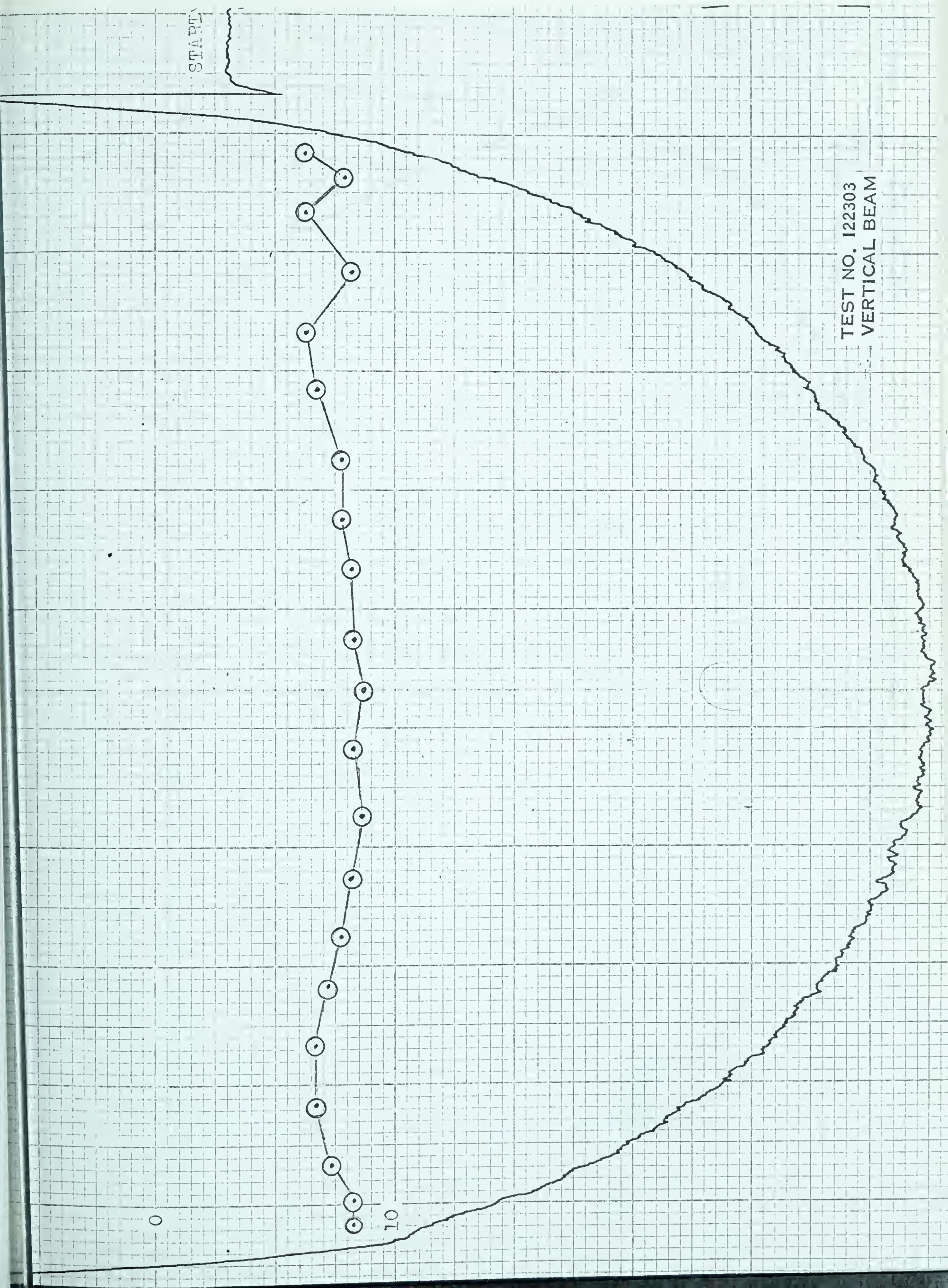
TEST RUN ABSORPTION CURVES

TESTS # 122303 to 123106

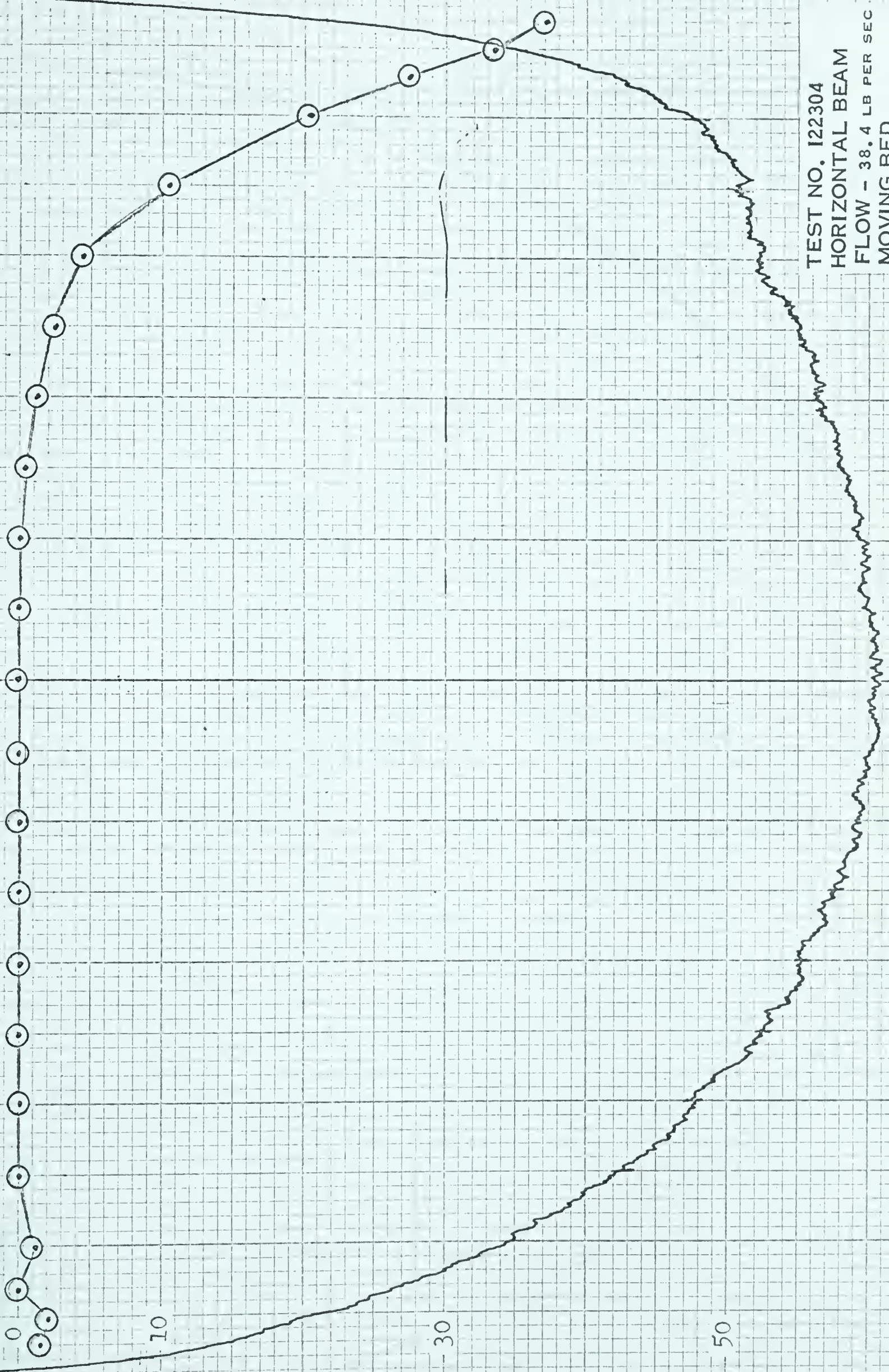


START

TEST NO. 122303
VERTICAL BEAM



TEST NO. 122304
HORIZONTAL BEAM
FLOW - 38.4 LB PER SEC.
MOVING BED



TEST NO. 122304
VERTICAL BEAM

START

TEST NO. 122304
VERTICAL BEAM

VOLUME CONCENTRATION SOLIDS, %

0

10

20

30

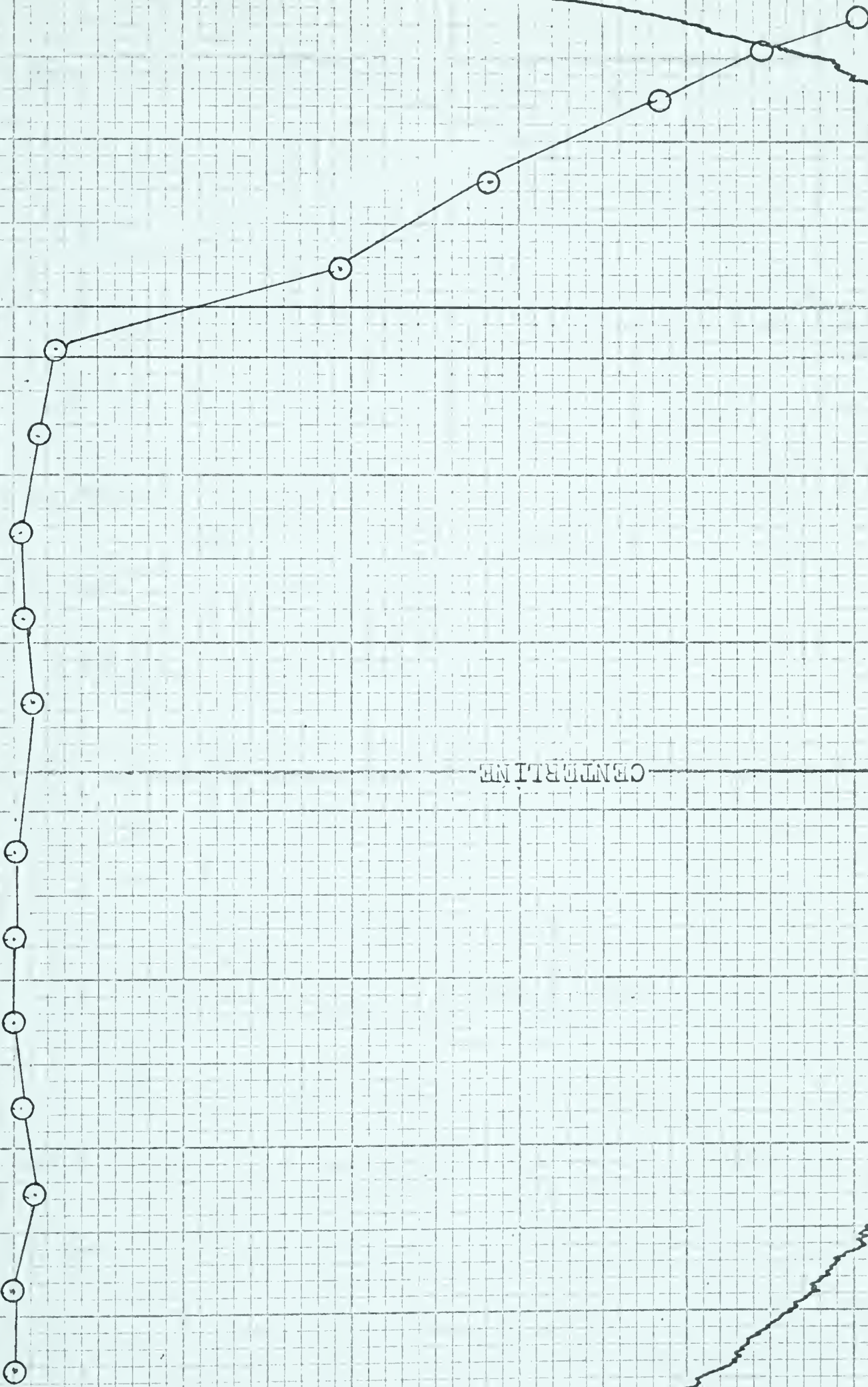
40

PIPE WALL

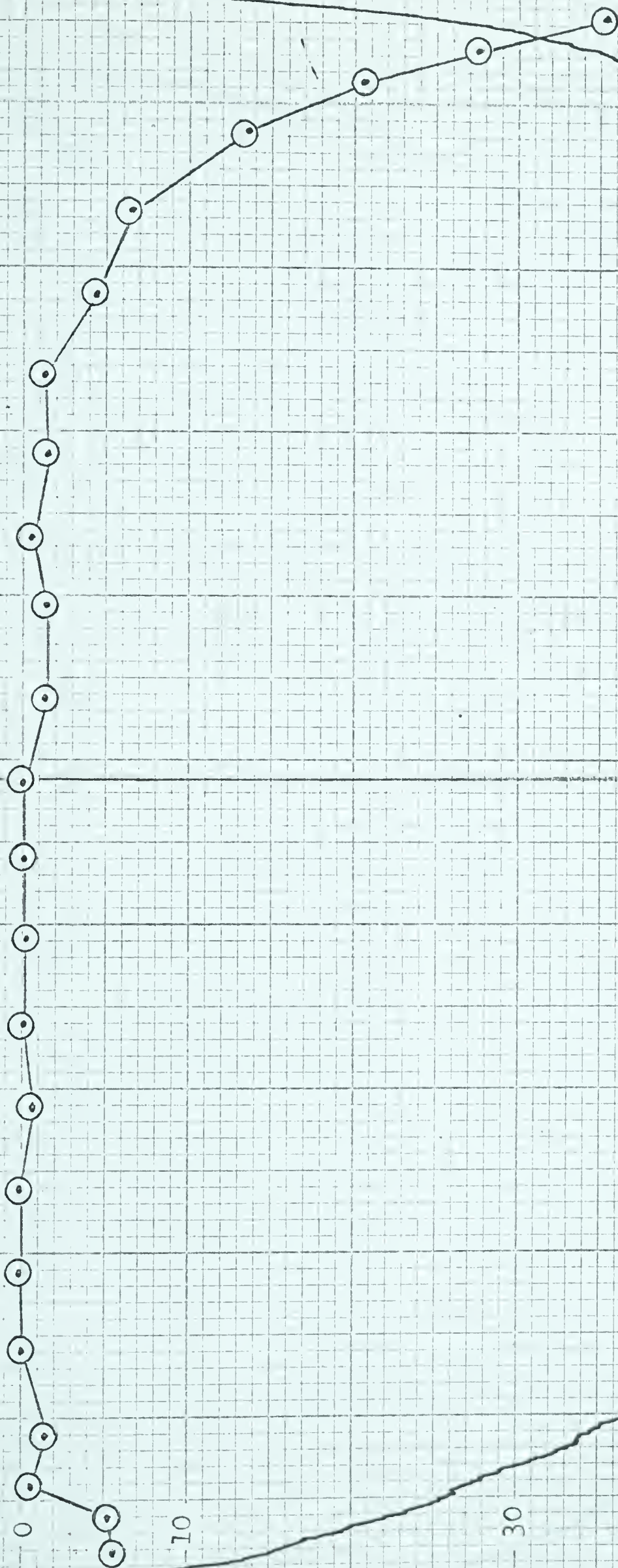
CENTRELINE

PIPE WALL

TEST NO. 122307
HORIZONTAL BEAM
FLOW - 30.3 LB PER SEC
FIXED BED



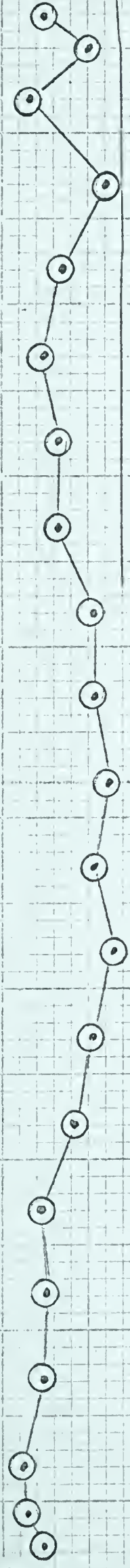
TEST NO. 122309
HORIZONTAL BEAM



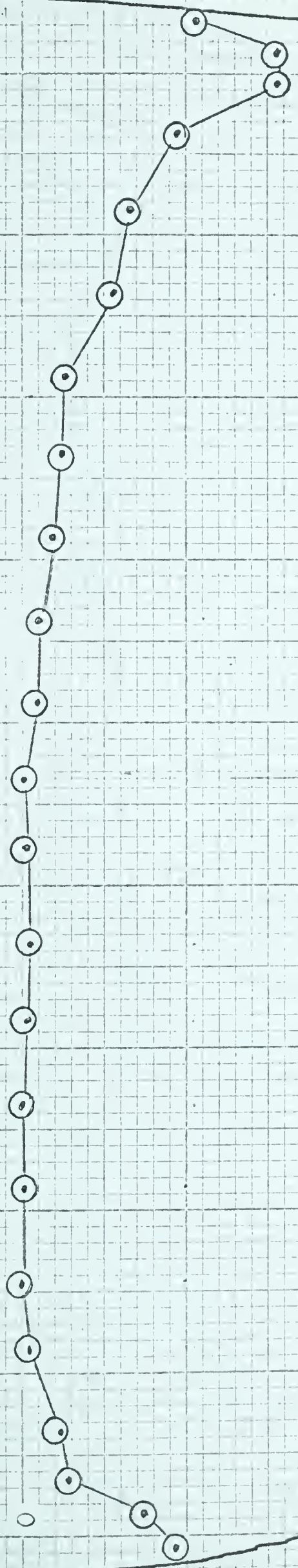
START

TEST NO. 122309
VERTICAL BEAM
FLOW - 52.0 LB PER SEC
NO BED

10

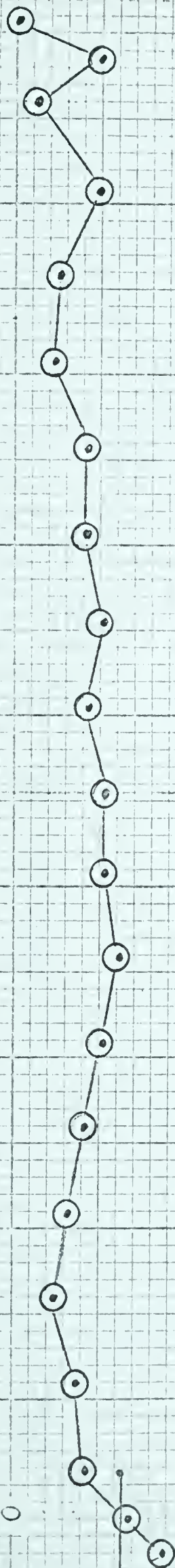


TEST NO. 122310
HORIZONTAL BEAM
FLOW - 62.5 LB PER SEC
NO BED



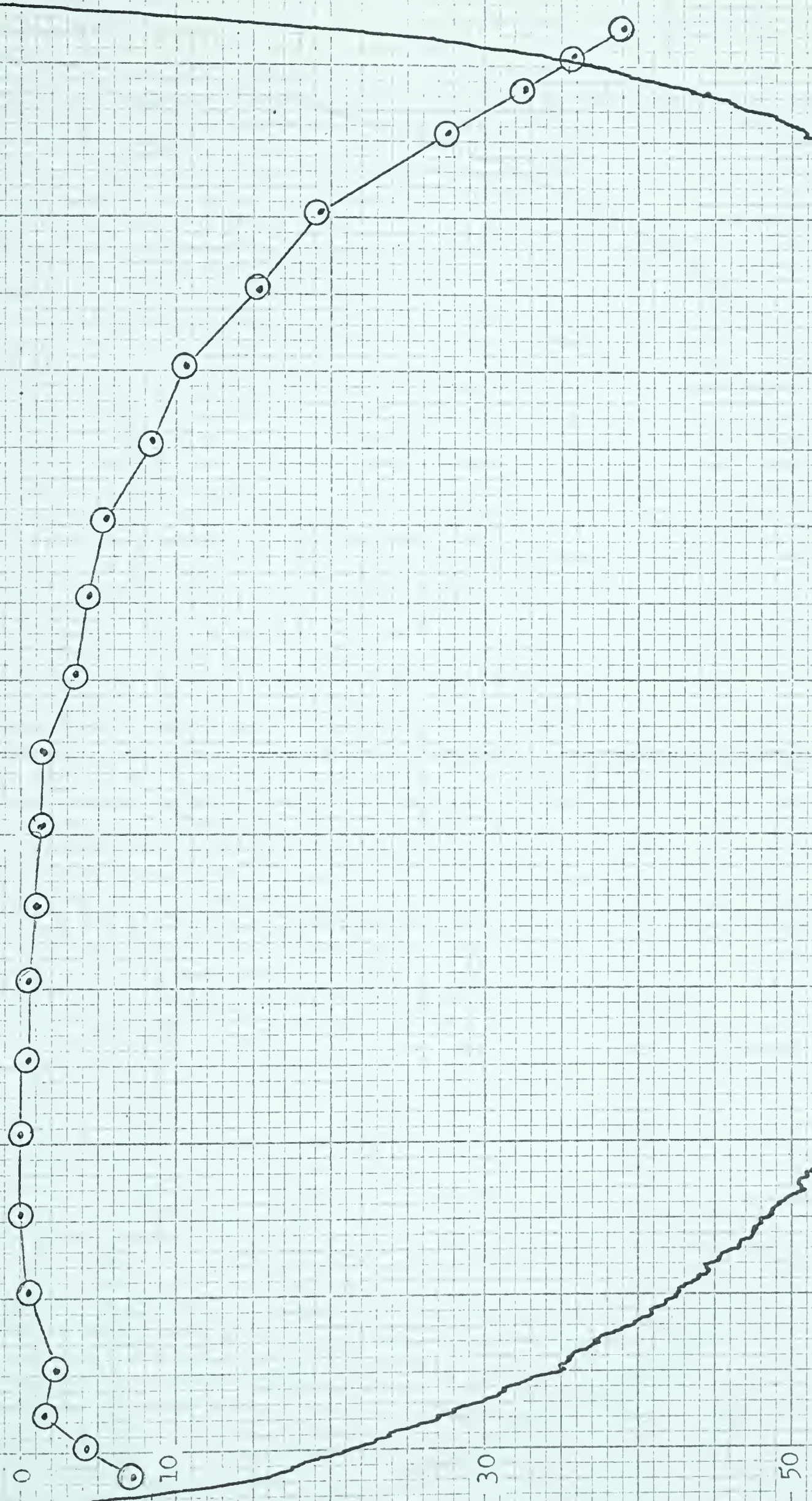
10

TEST NO. 122310
VERTICAL BEAM

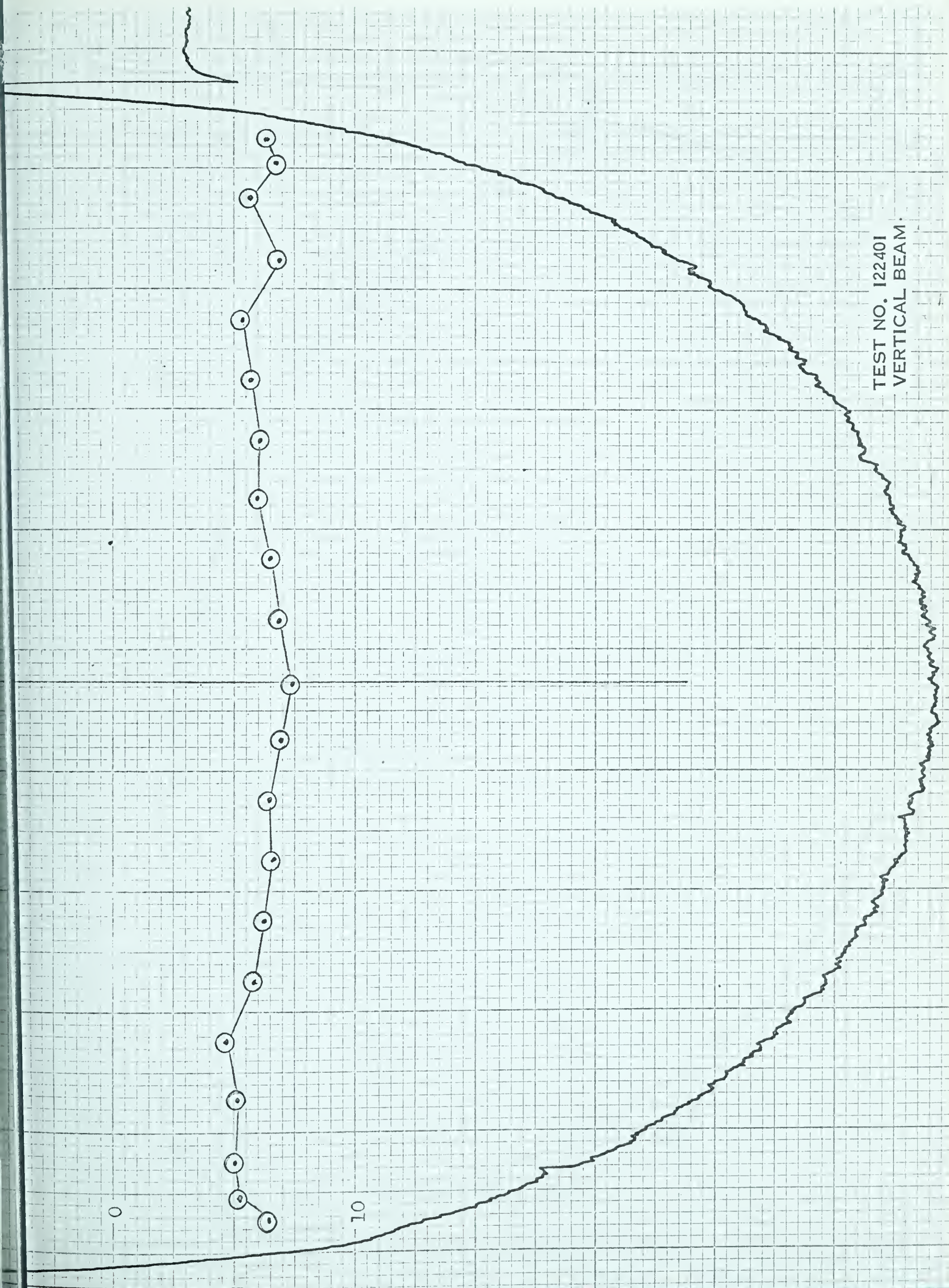


10

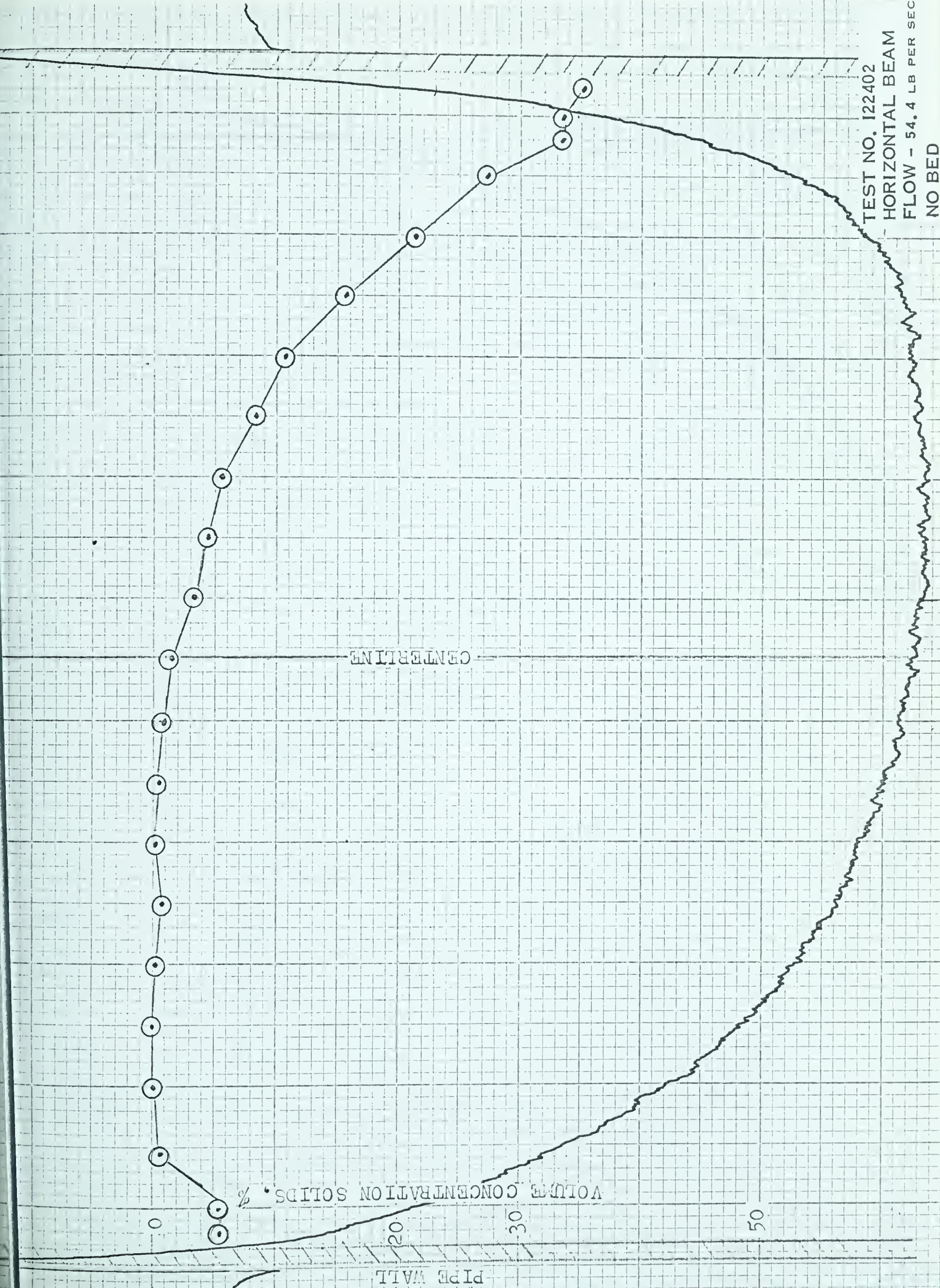
TEST NO. 122401
HORIZONTAL BEAM
FLOW - 61.6 LB PER SE
NO BED



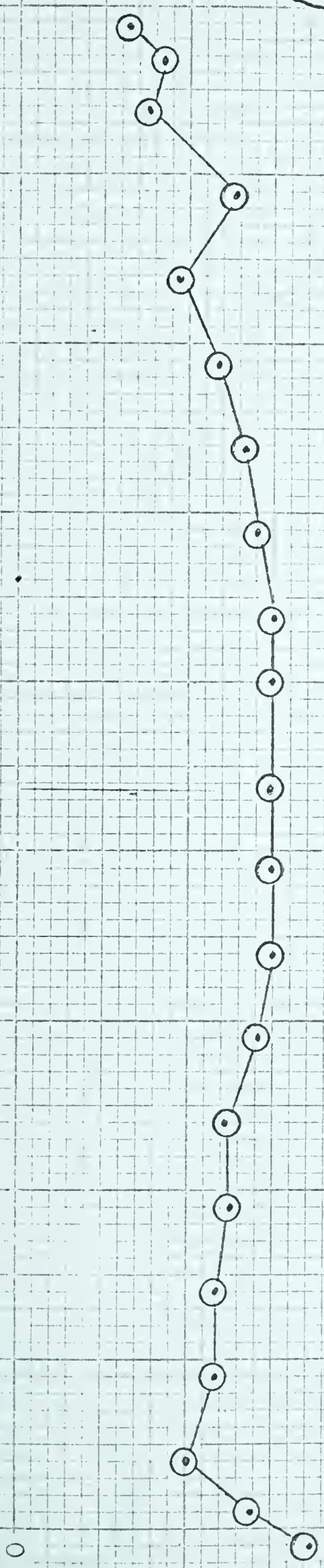
TEST NO. 122401
VERTICAL BEAM.



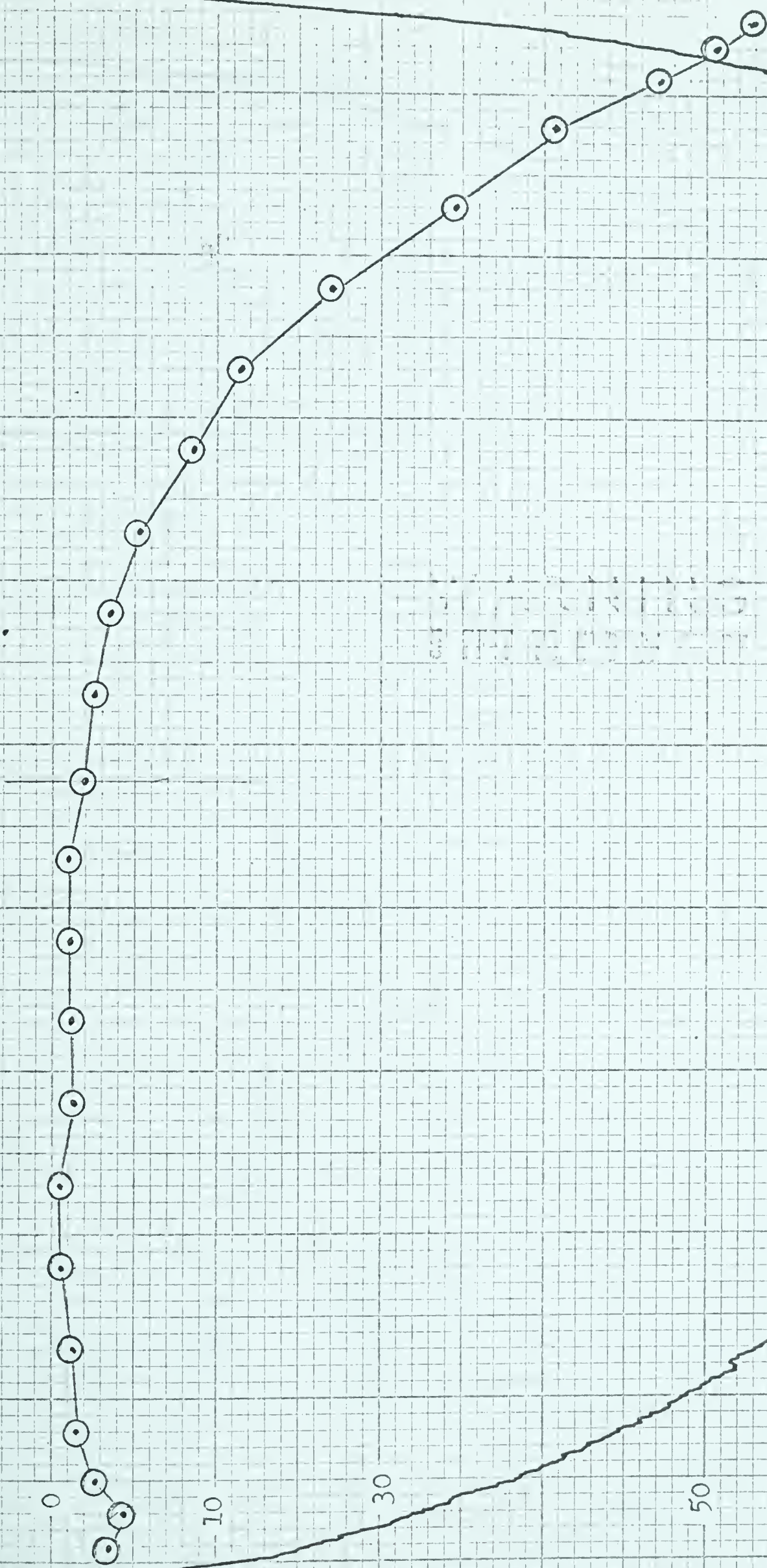
TEST NO. 122402
HORIZONTAL BEAM
FLOW - 54.4 LB PER SEC
NO BED



TEST NO. 122402
VERTICAL BEAM



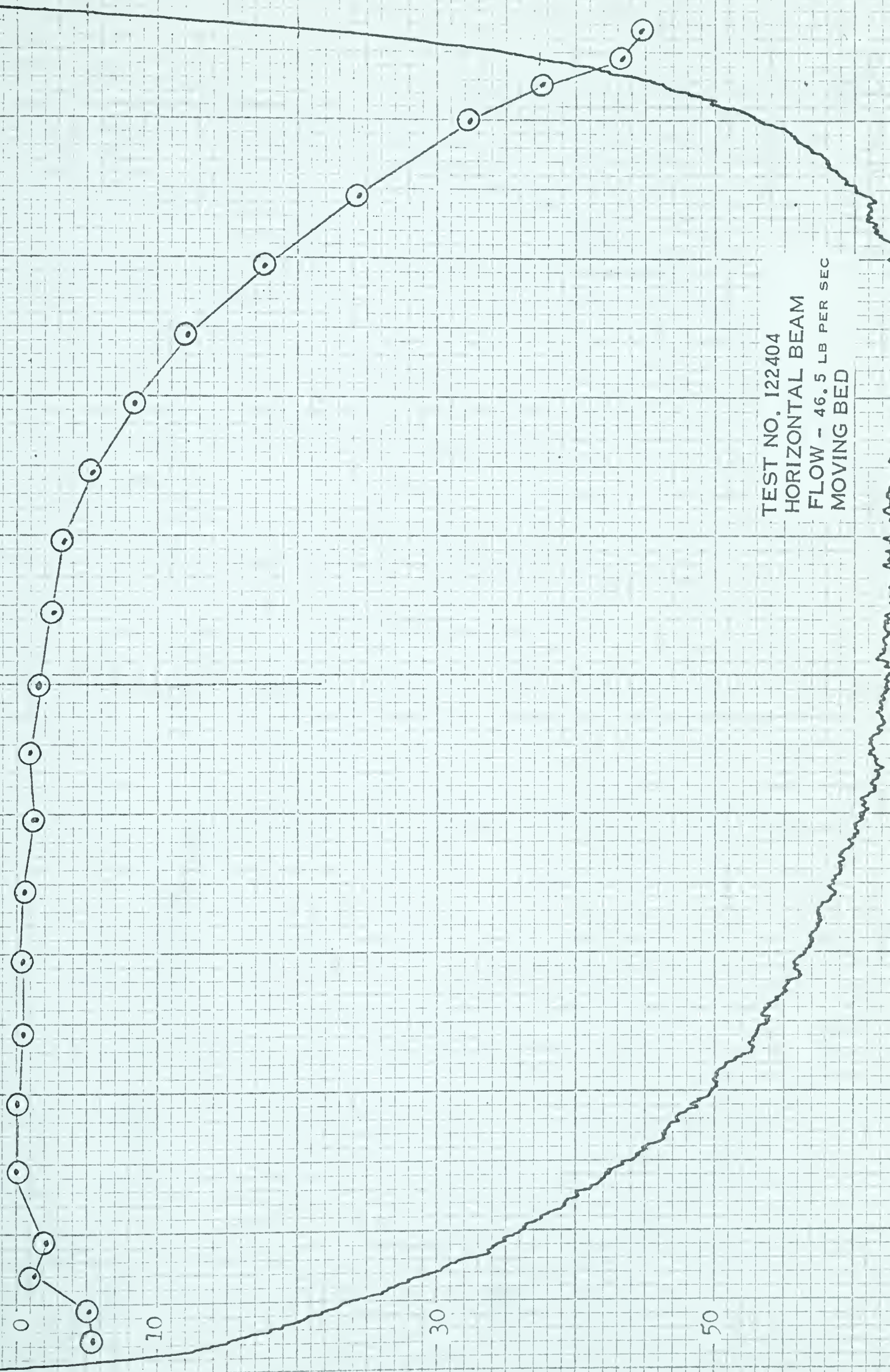
TEST NO. 122403
HORIZONTAL BEAM
FLOW - 48.4 LB PER SEC
MOVING BED



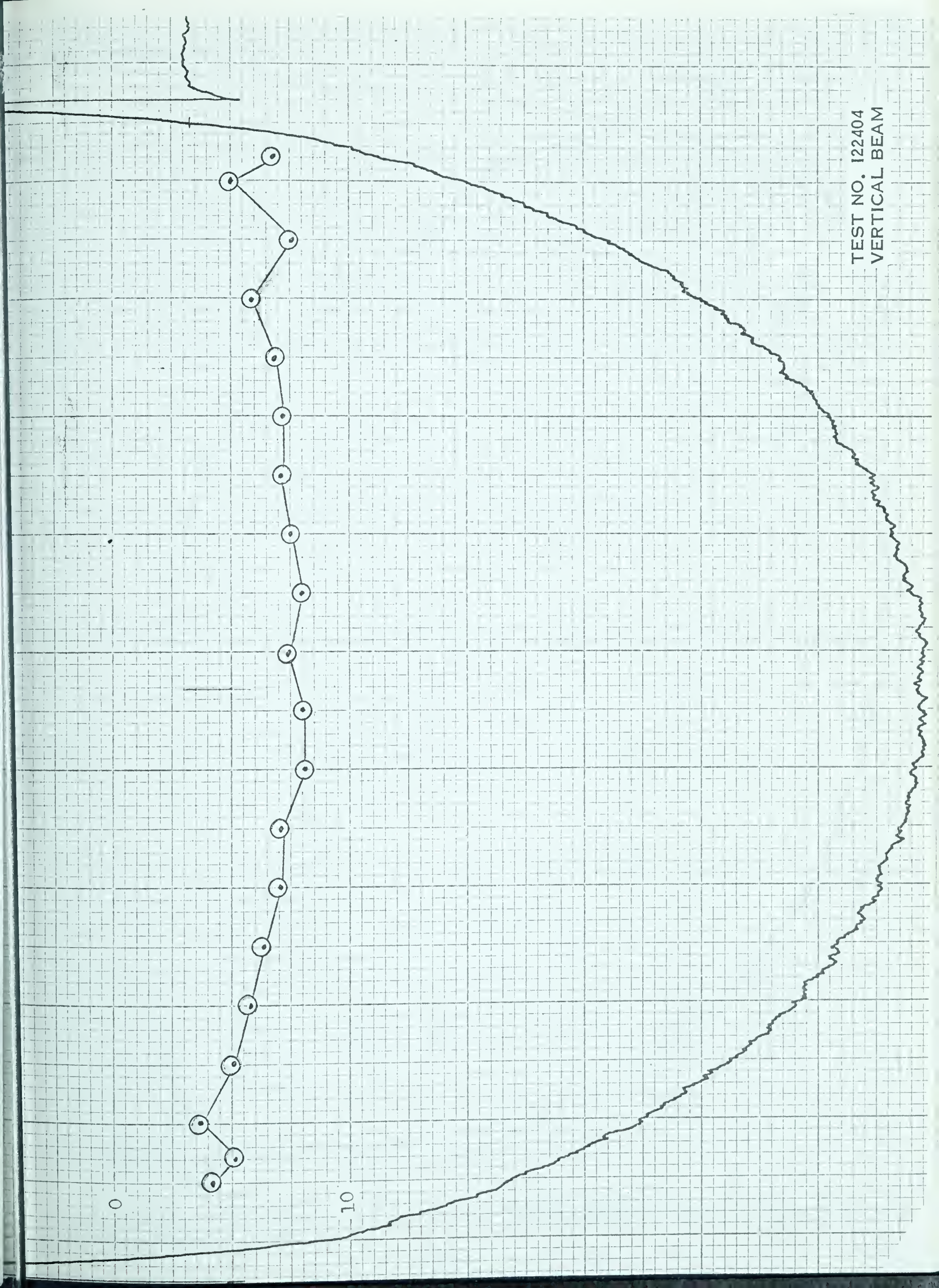
TEST NO. 122403
VERTICAL BEAM



TEST NO. 122404
HORIZONTAL BEAM
FLOW - 46.5 LB PER SEC
MOVING BED



TEST NO. 122404
VERTICAL BEAM

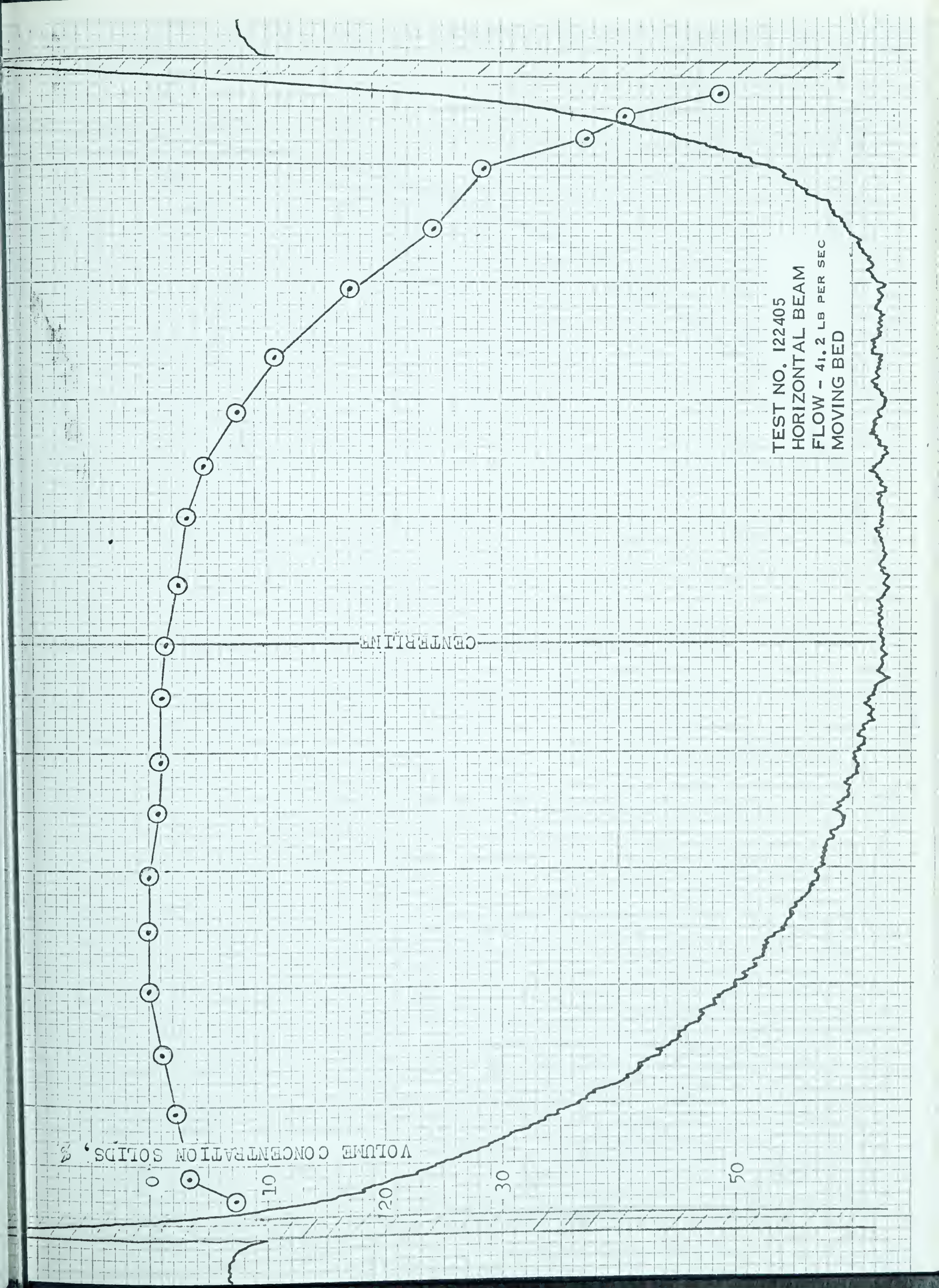


TEST NO. 122405
HORIZONTAL BEAM
FLOW - 41.2 LB PER SEC
MOVING BED

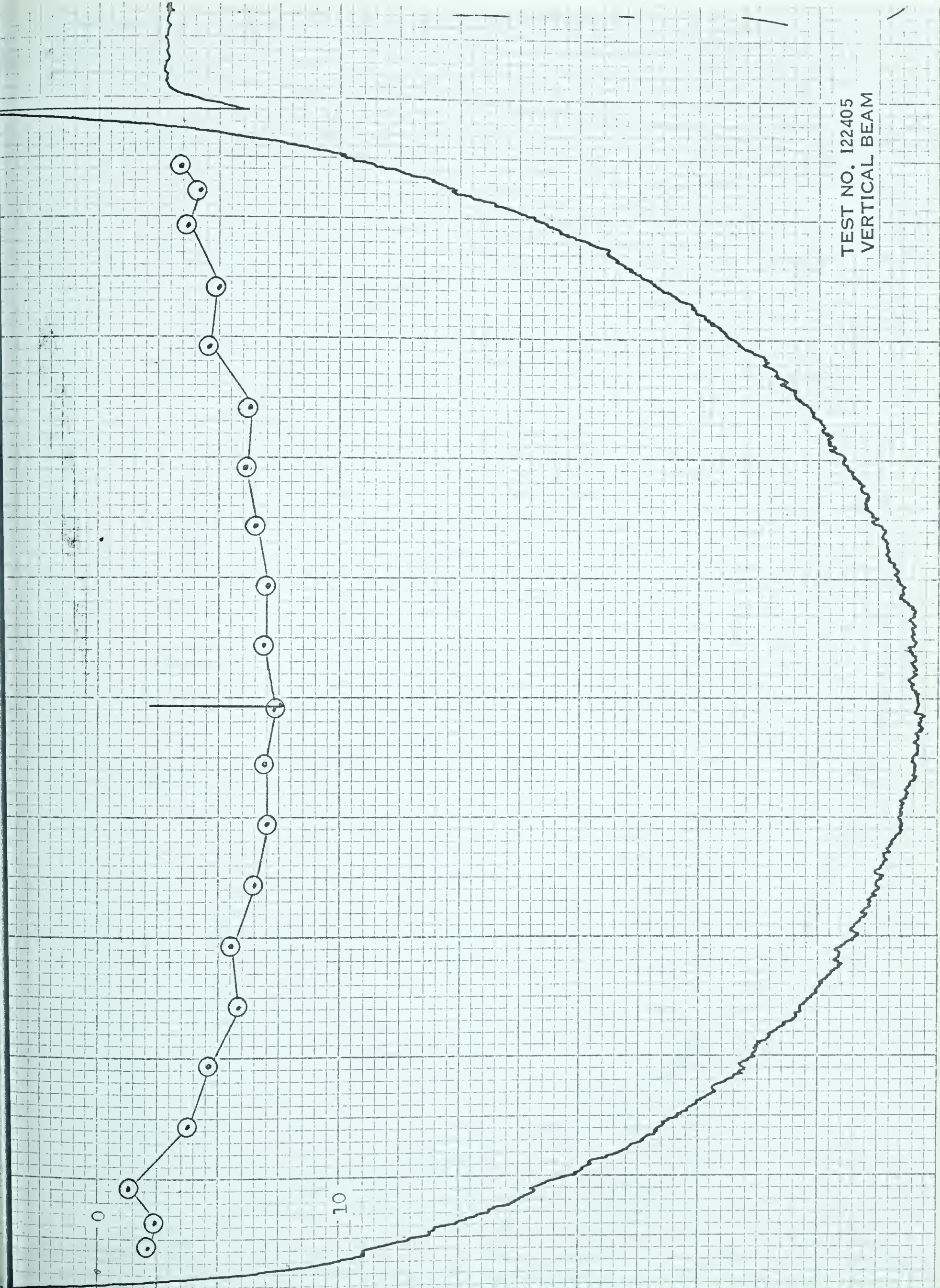
CENTRIFUGAL

VOLUME CONCENTRATION SOLIDS, %

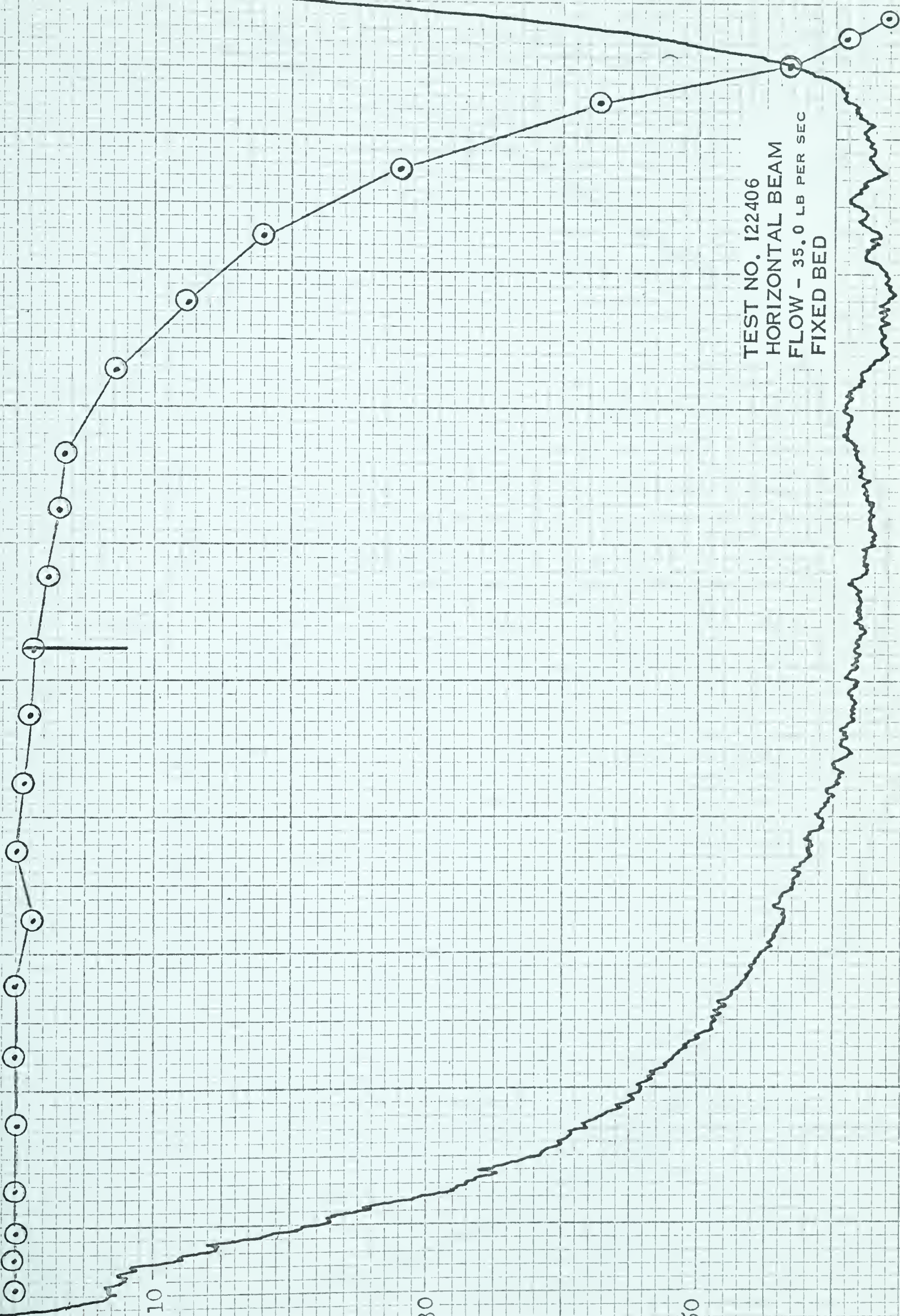
0 10 20 30 50



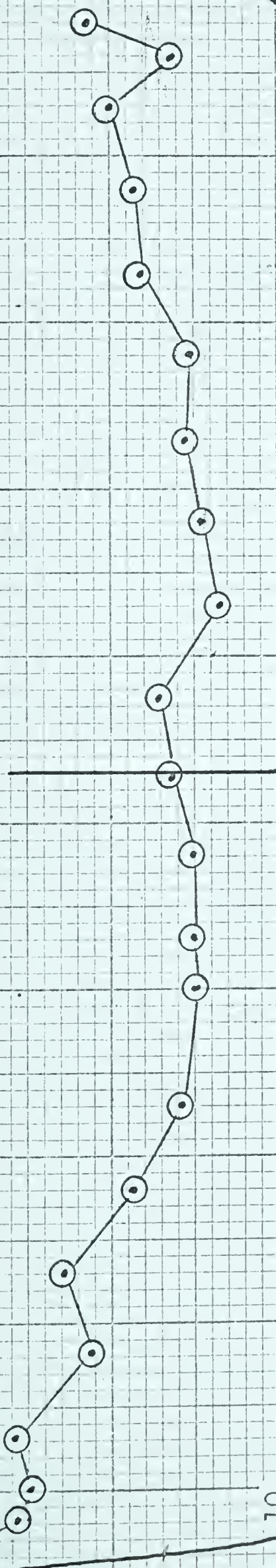
TEST NO. 122405
VERTICAL BEAM



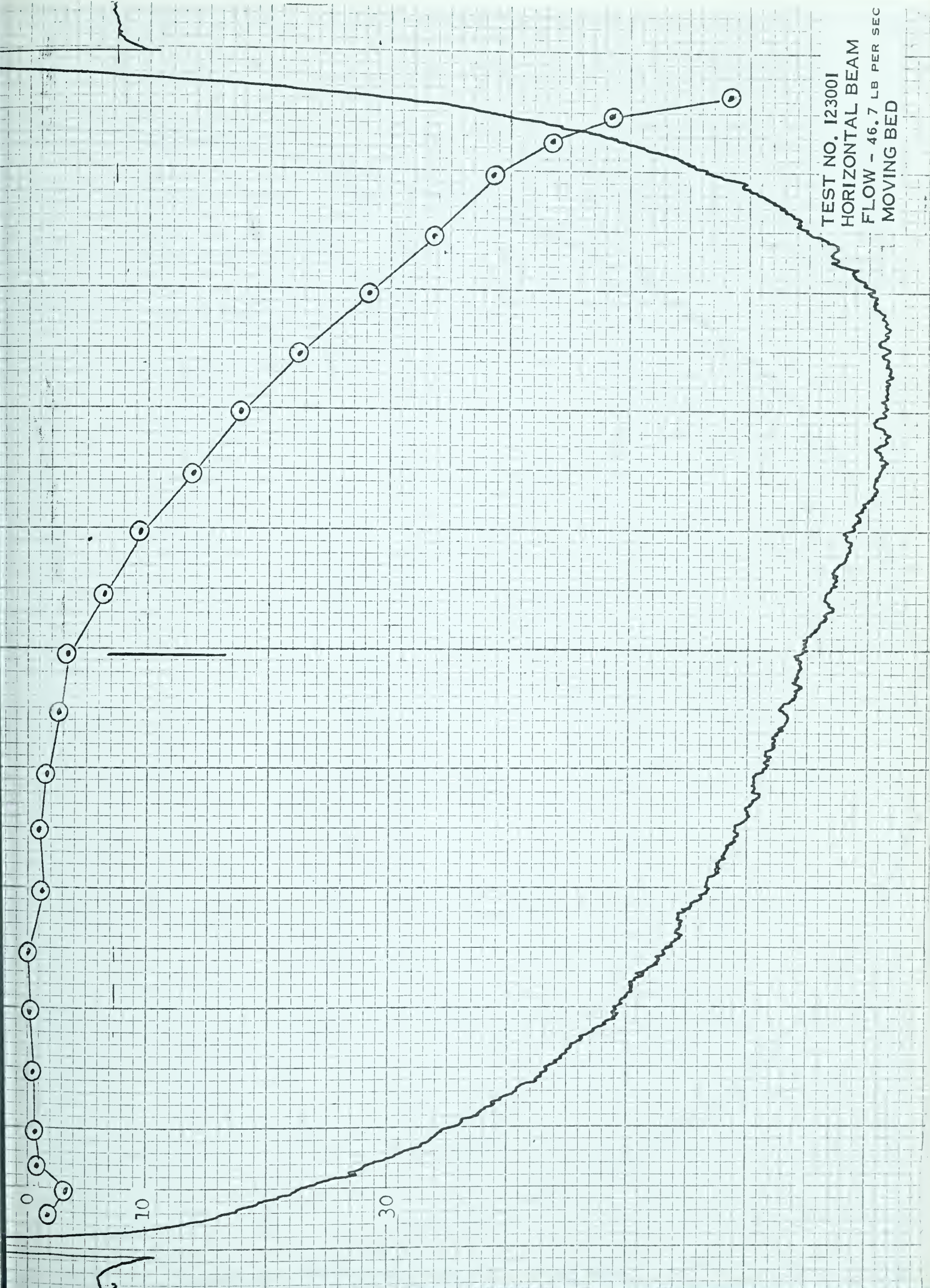
TEST NO. I22406
HORIZONTAL BEAM
FLOW - 35.0 LB PER SEC
FIXED BED



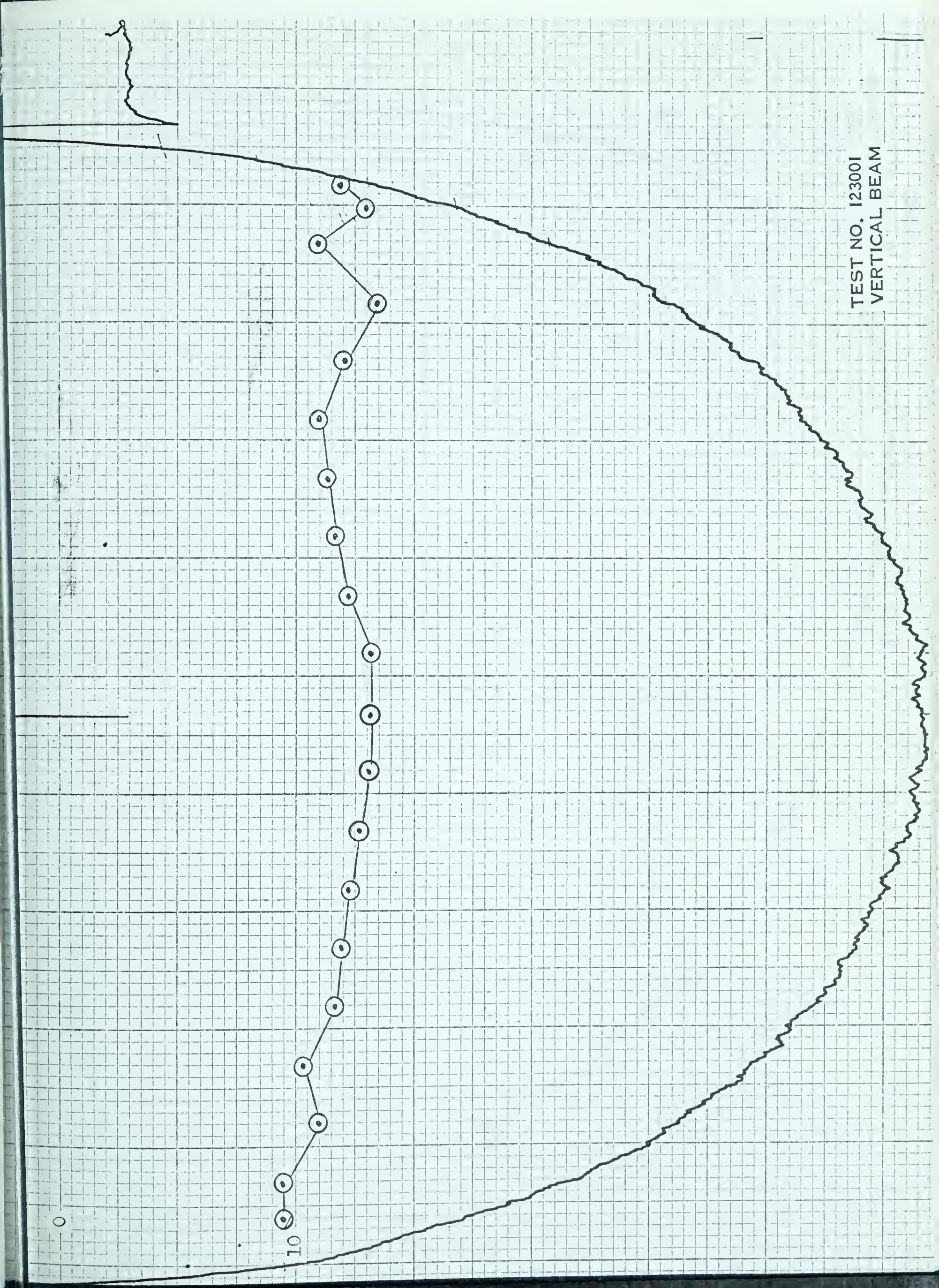
TEST NO. 122406
VERTICAL BEAM



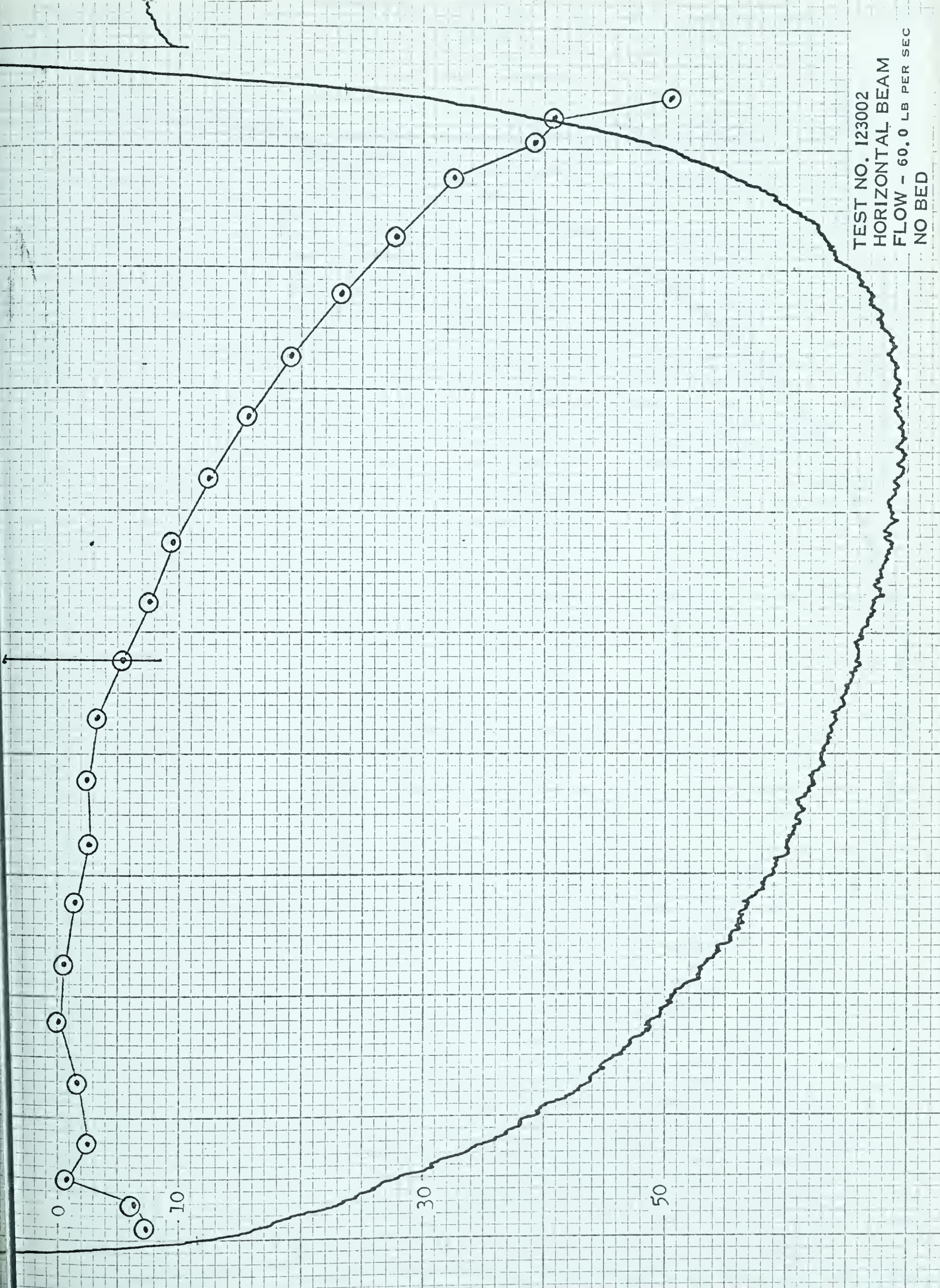
TEST NO. 123001
HORIZONTAL BEAM
FLOW - 46.7 LB PER SEC
MOVING BED



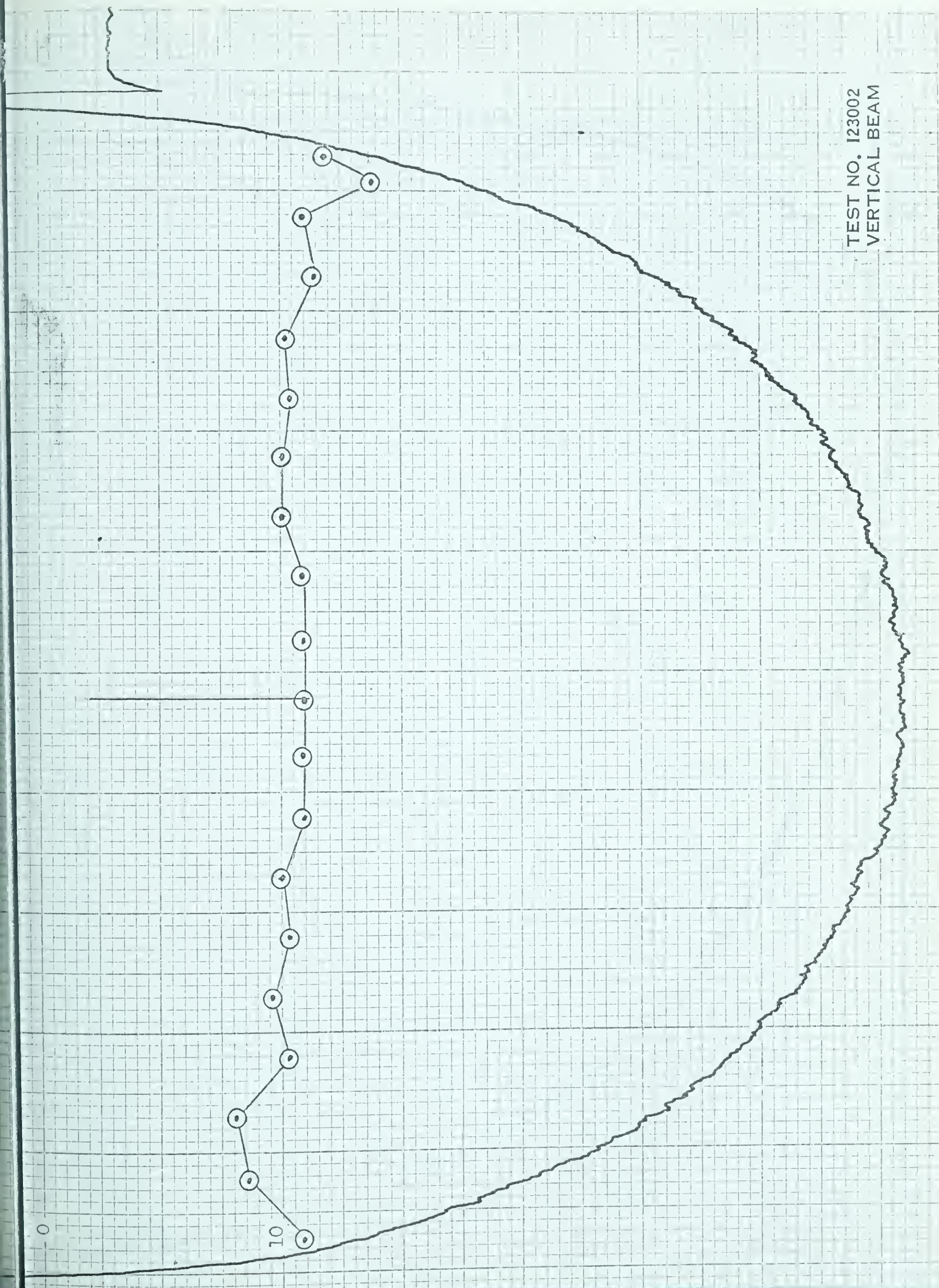
TEST NO. 123001
VERTICAL BEAM



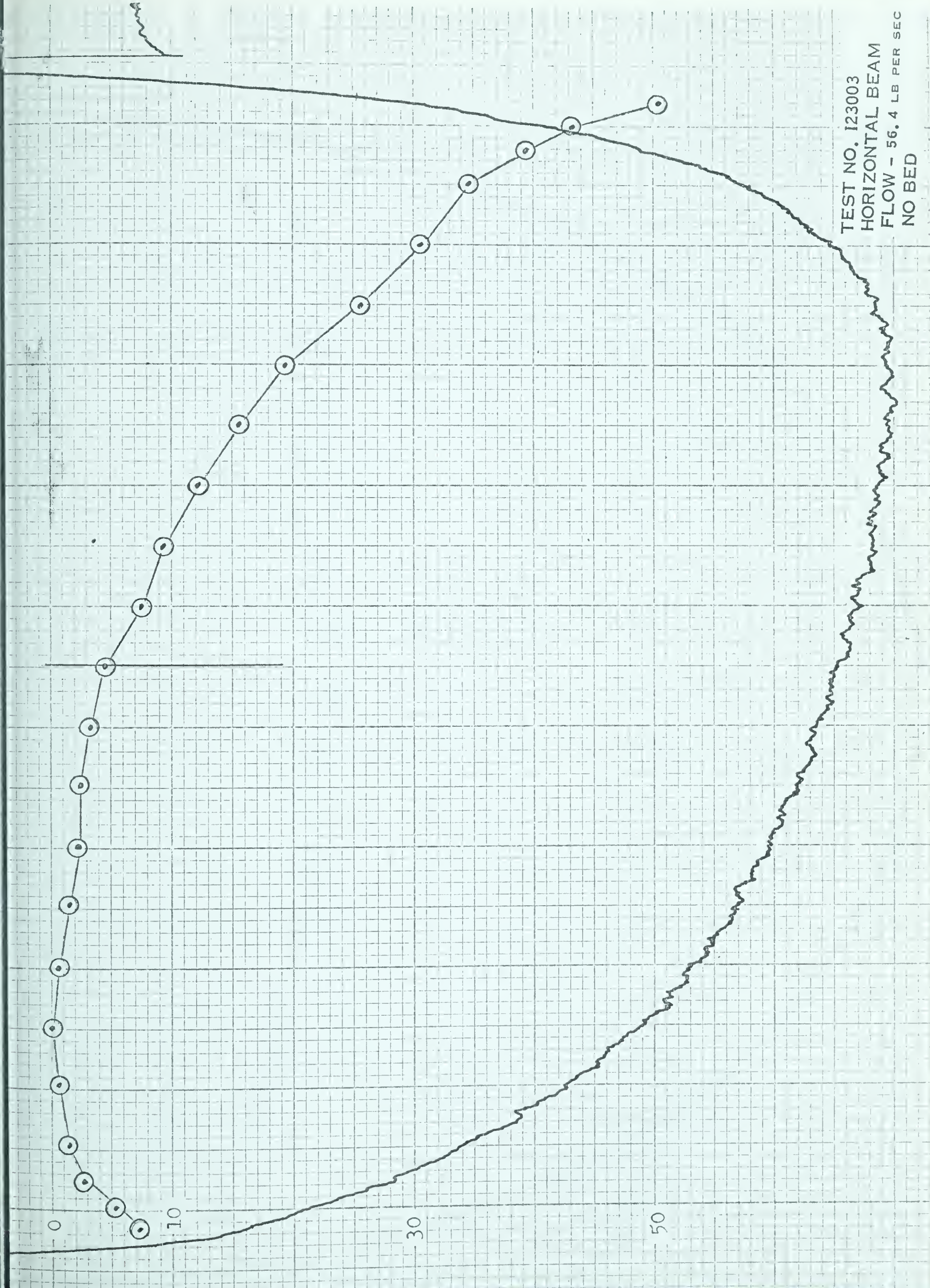
TEST NO. 123002
HORIZONTAL BEAM
FLOW - 60.0 LB PER SEC
NO BED



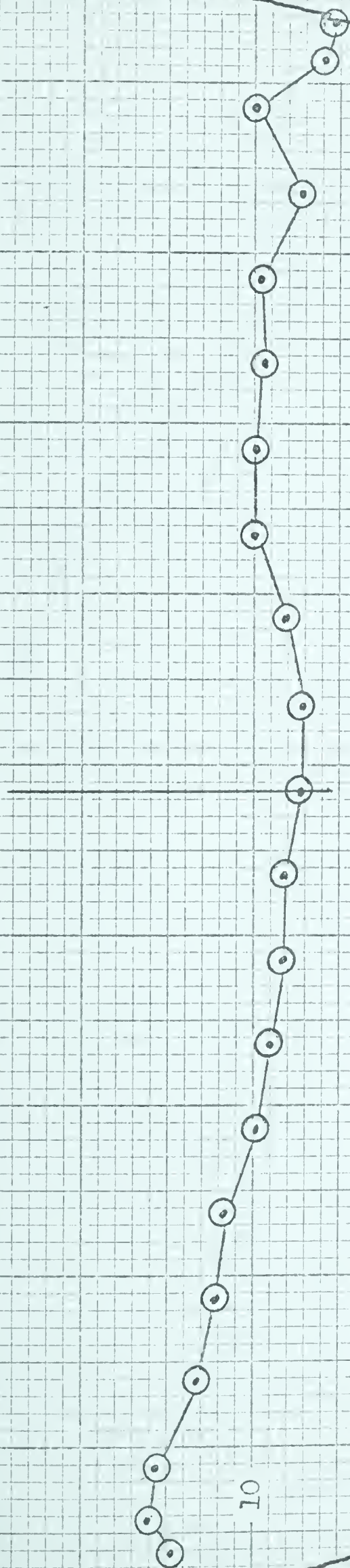
TEST NO. 123002
VERTICAL BEAM



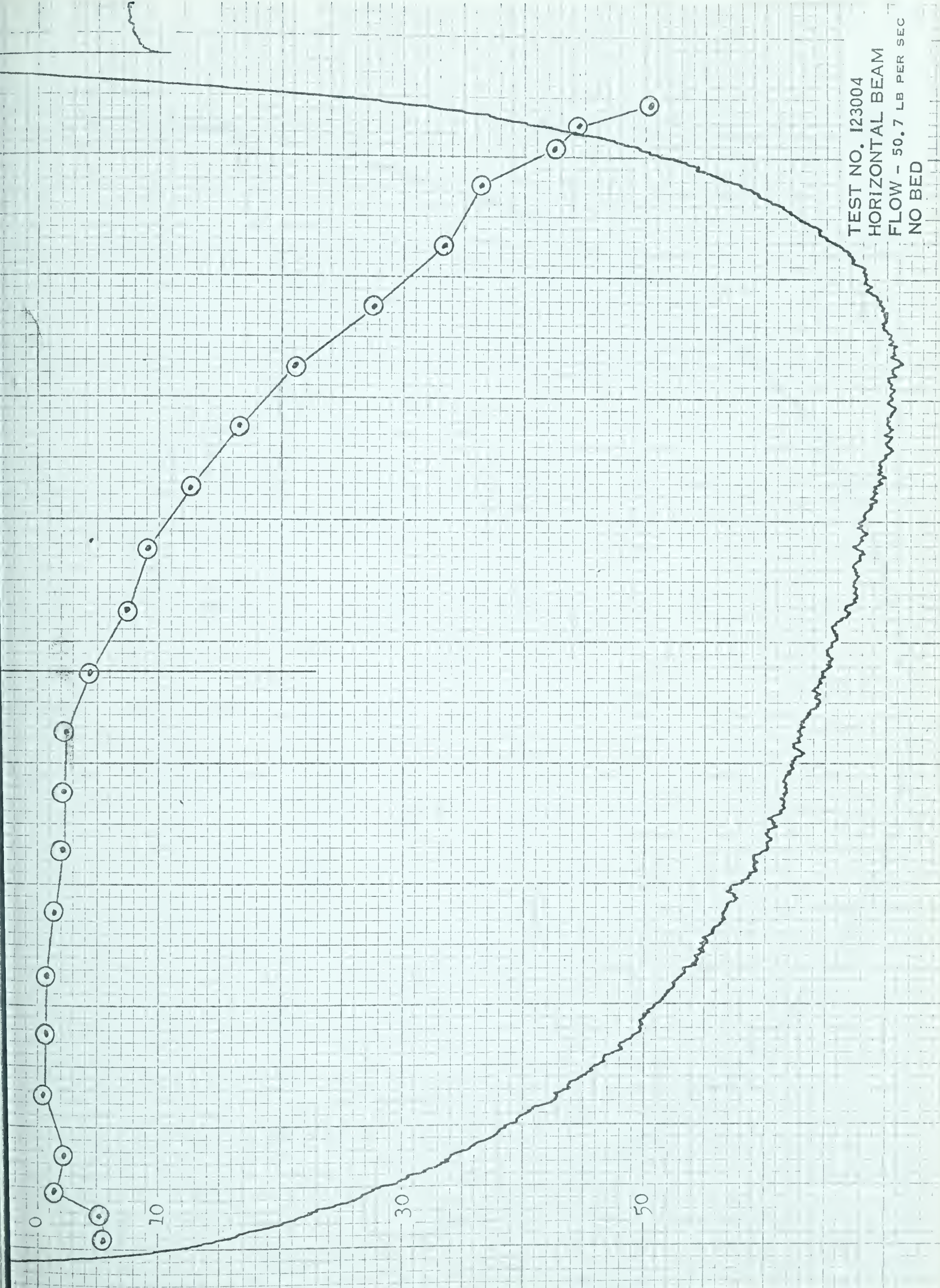
TEST NO. 123003
HORIZONTAL BEAM
FLOW - 56.4 LB PER SEC
NO BED



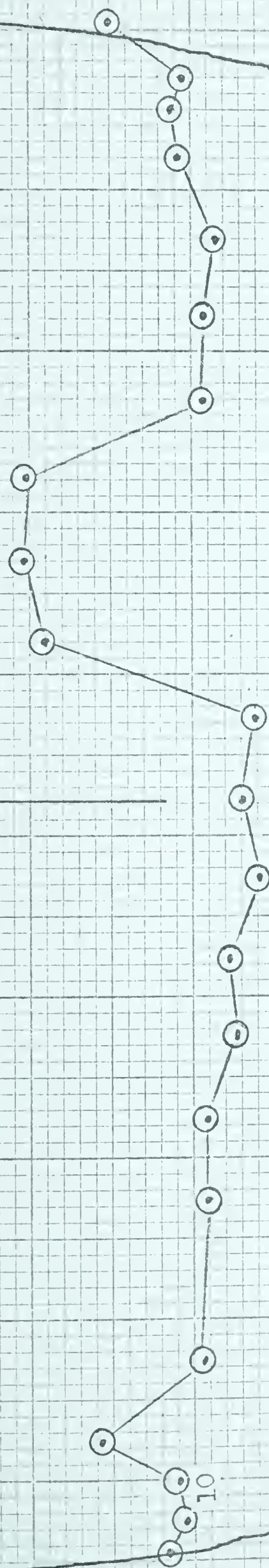
TEST NO. 123003
VERTICAL BEAM



TEST NO. 123004
HORIZONTAL BEAM
FLOW - 50.7 LB PER SEC
NO BED



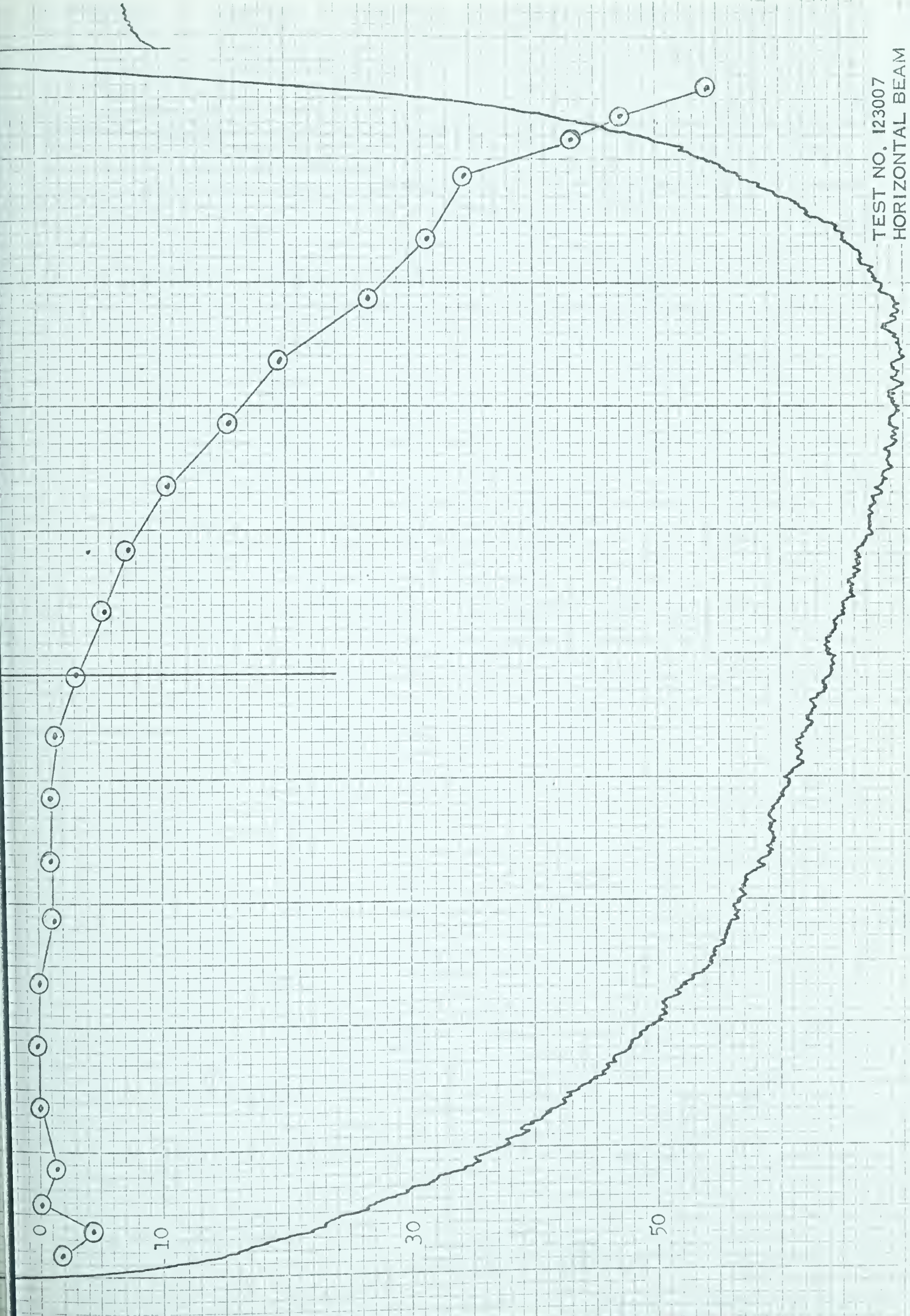
TEST NO. 123004
VERTICAL BEAM



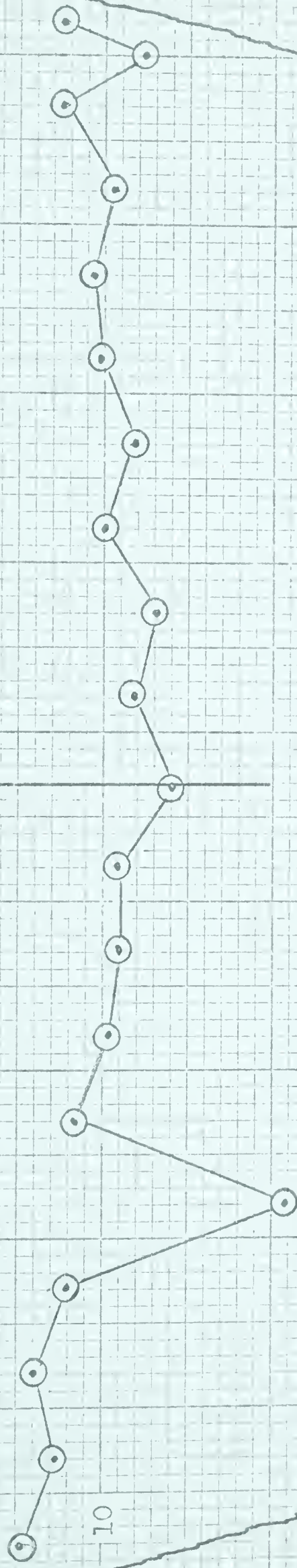
TEST NO. 123006
VERTICAL BEAM



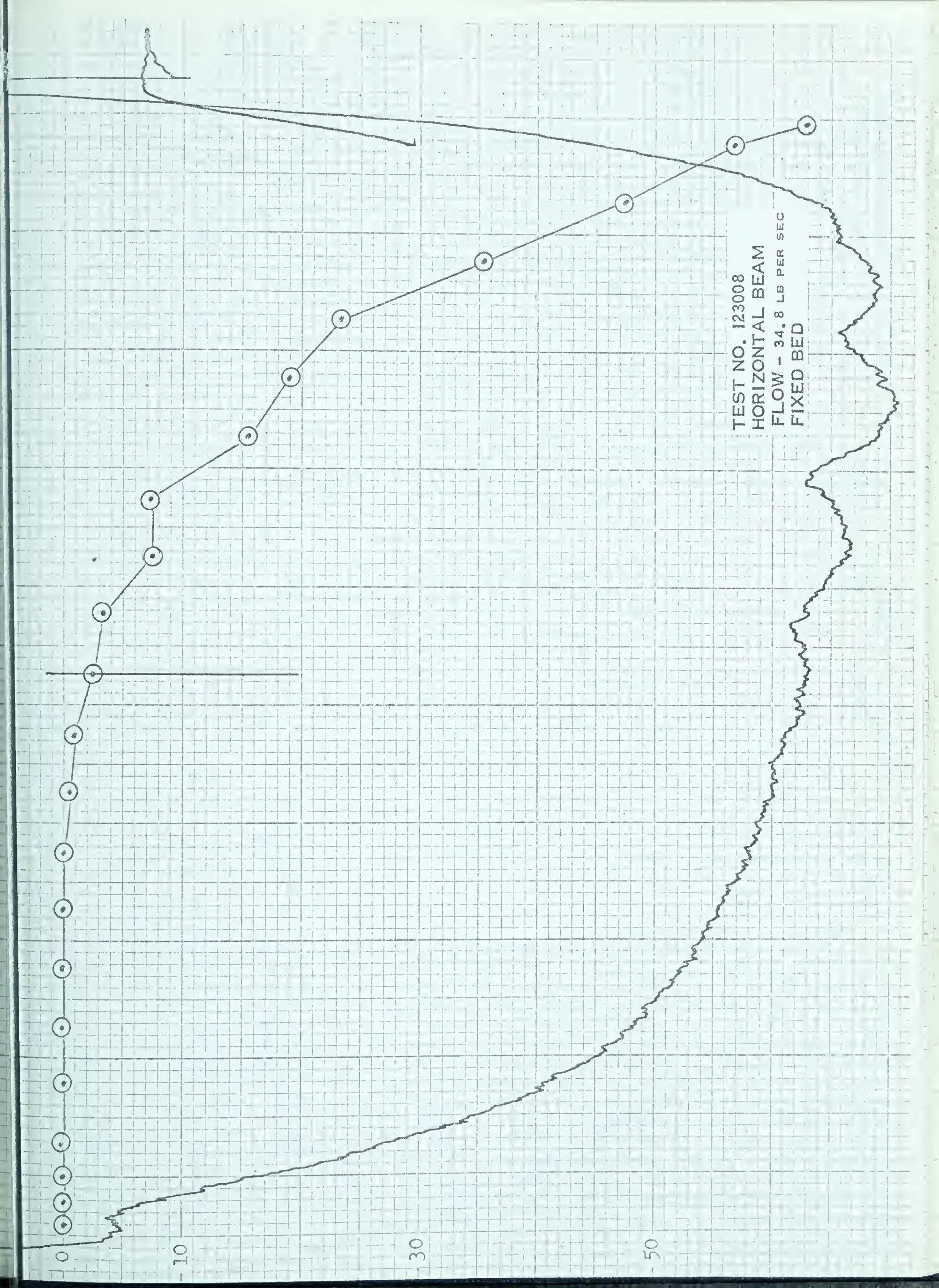
TEST NO. 123007
HORIZONTAL BEAM
FLOW - 44.3 LB PER SEC
MOVING BED



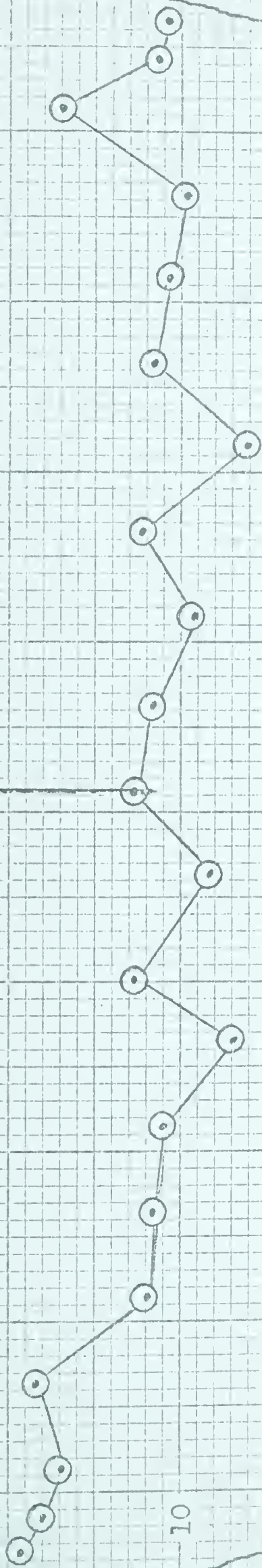
TEST NO. 123007
VERTICAL BEAM



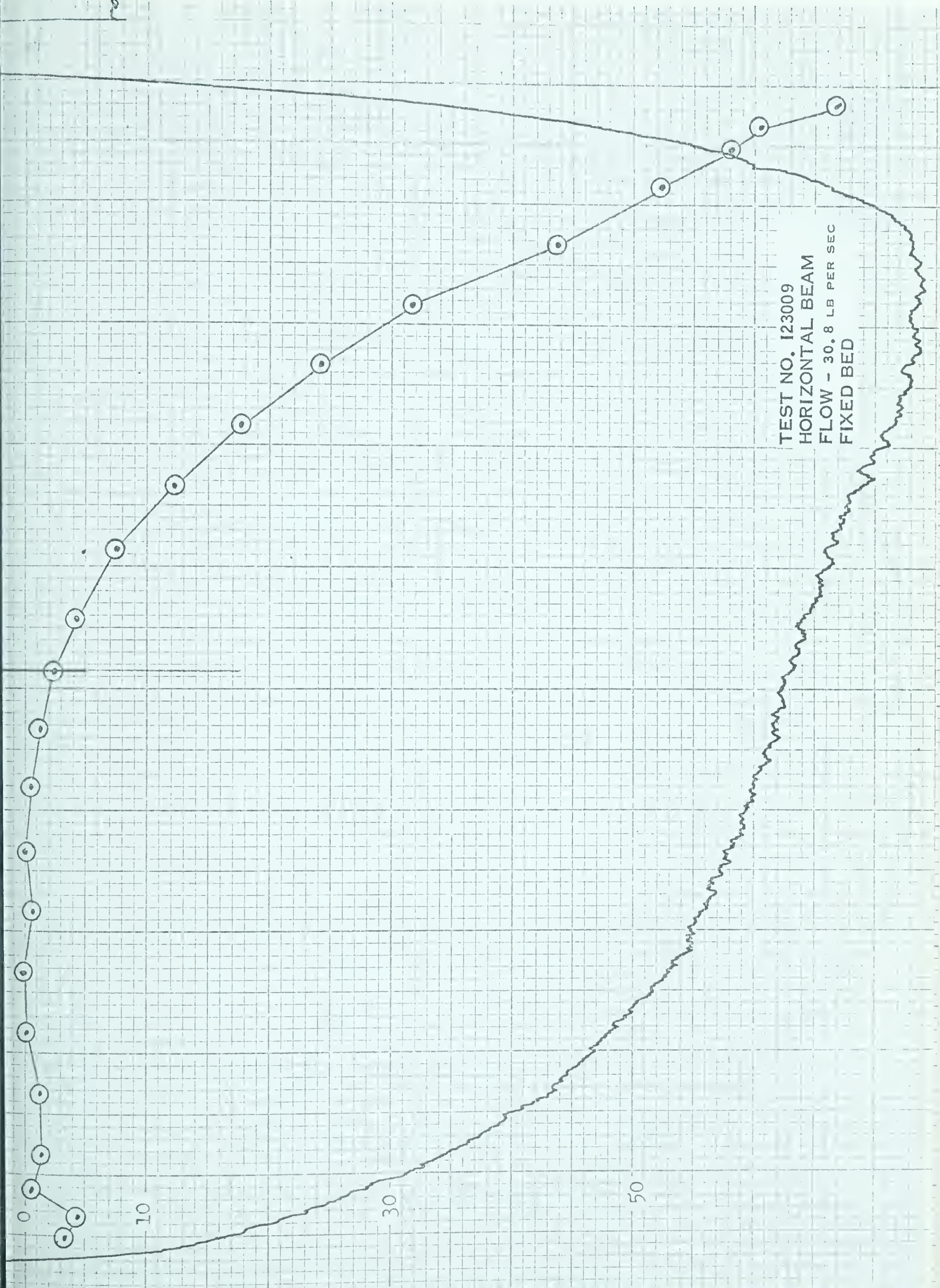
TEST NO. 123008
HORIZONTAL BEAM
FLOW - 34.8 LB PER SEC
FIXED BED



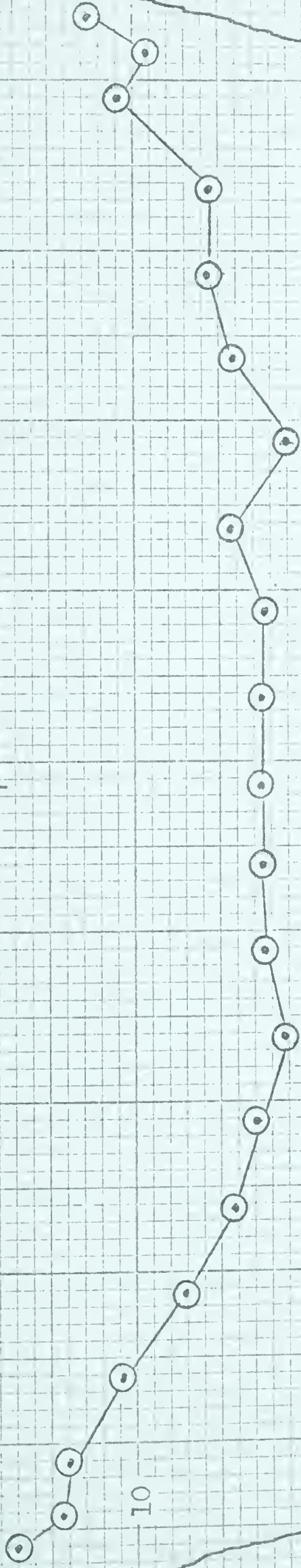
TEST NO. 123008
VERTICAL BEAM



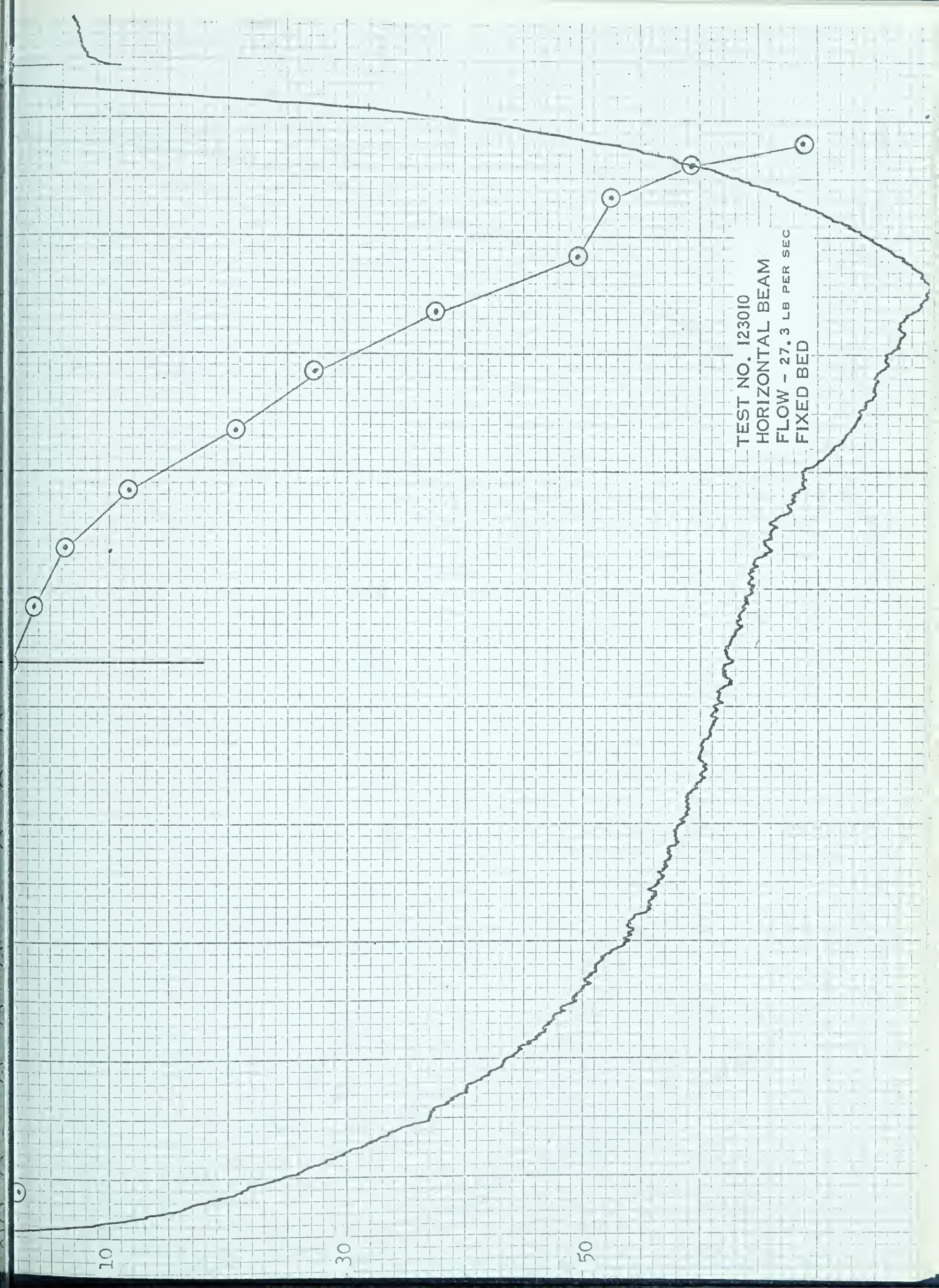
TEST NO. 123009
HORIZONTAL BEAM
FLOW - 30.8 LB PER SEC
FIXED BED



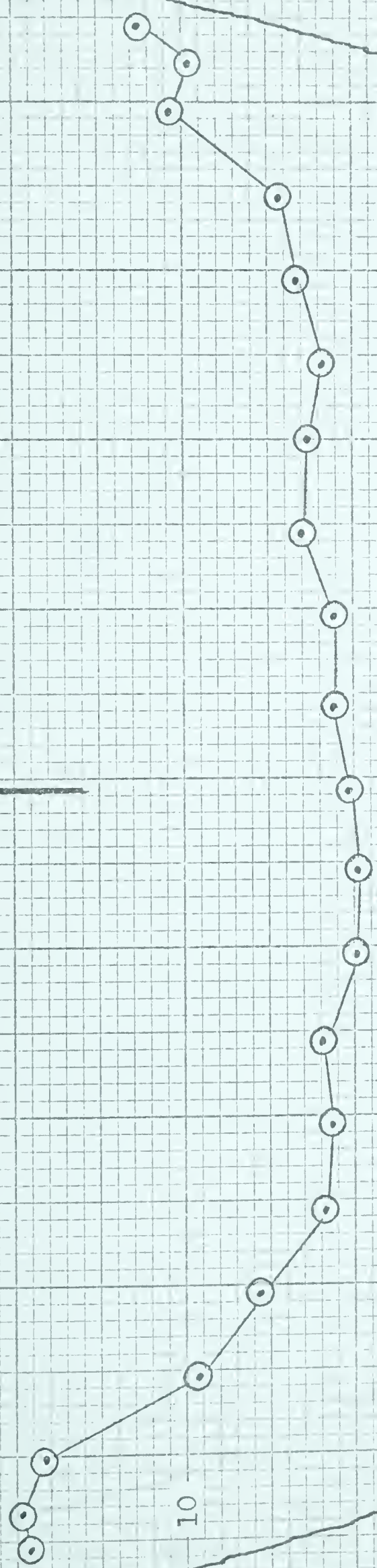
TEST NO. 123009
VERTICAL BEAM



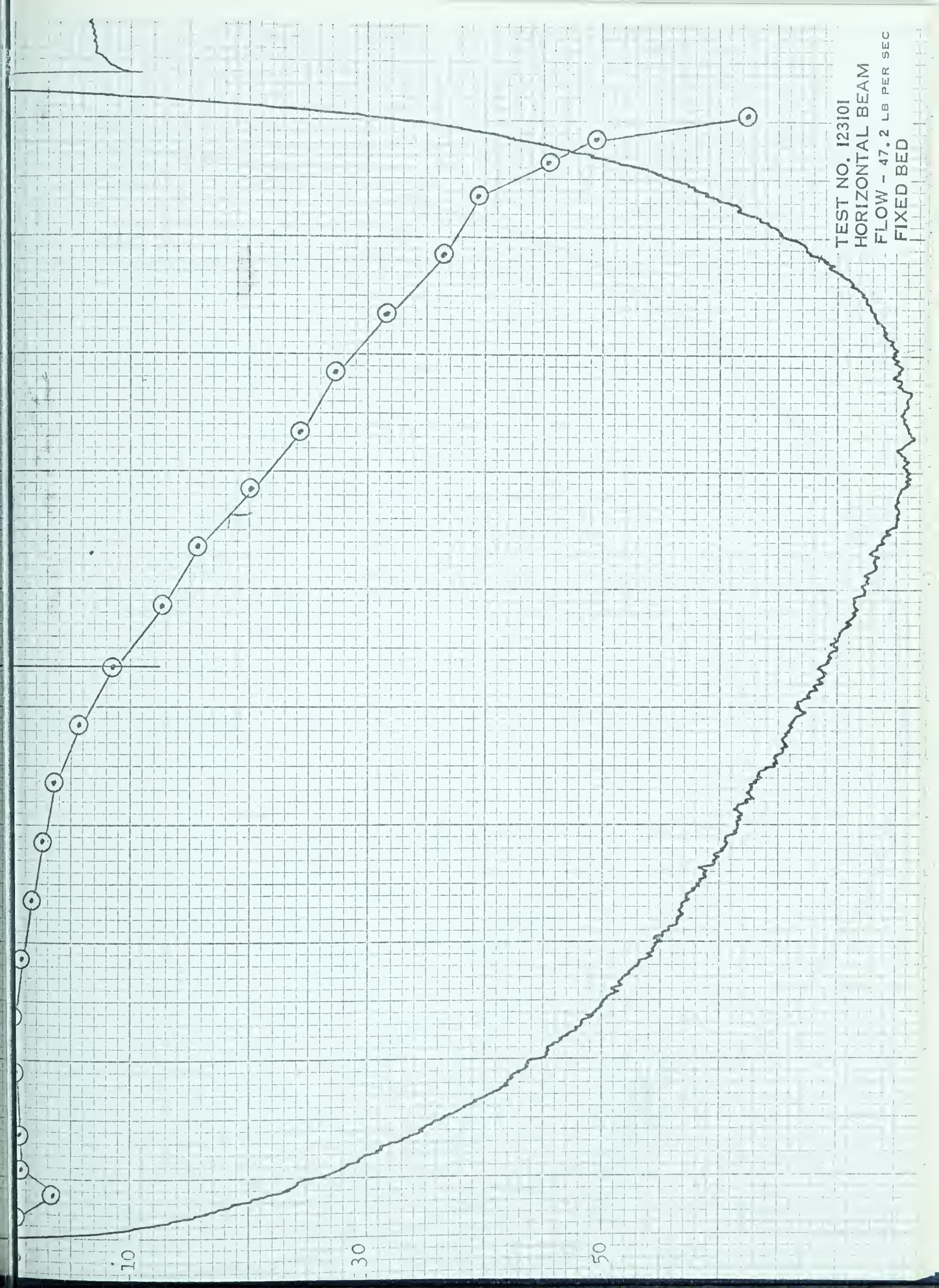
TEST NO. 123010
HORIZONTAL BEAM
FLOW - 27.3 LB PER SEC
FIXED BED



TEST NO. 123010
VERTICAL BEAM

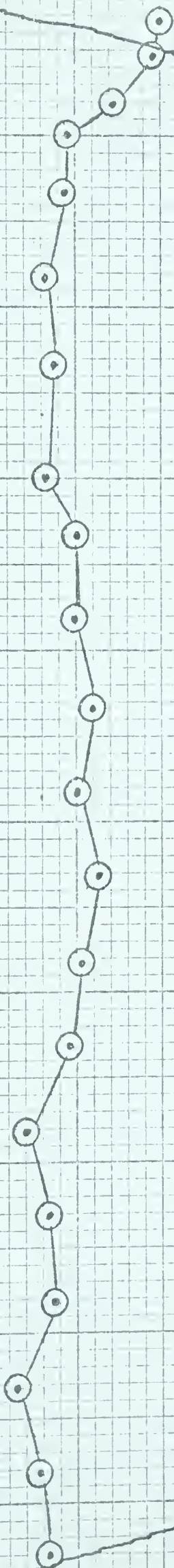


TEST NO. 123101
HORIZONTAL BEAM
FLOW - 47.2 LB PER SEC
FIXED BED

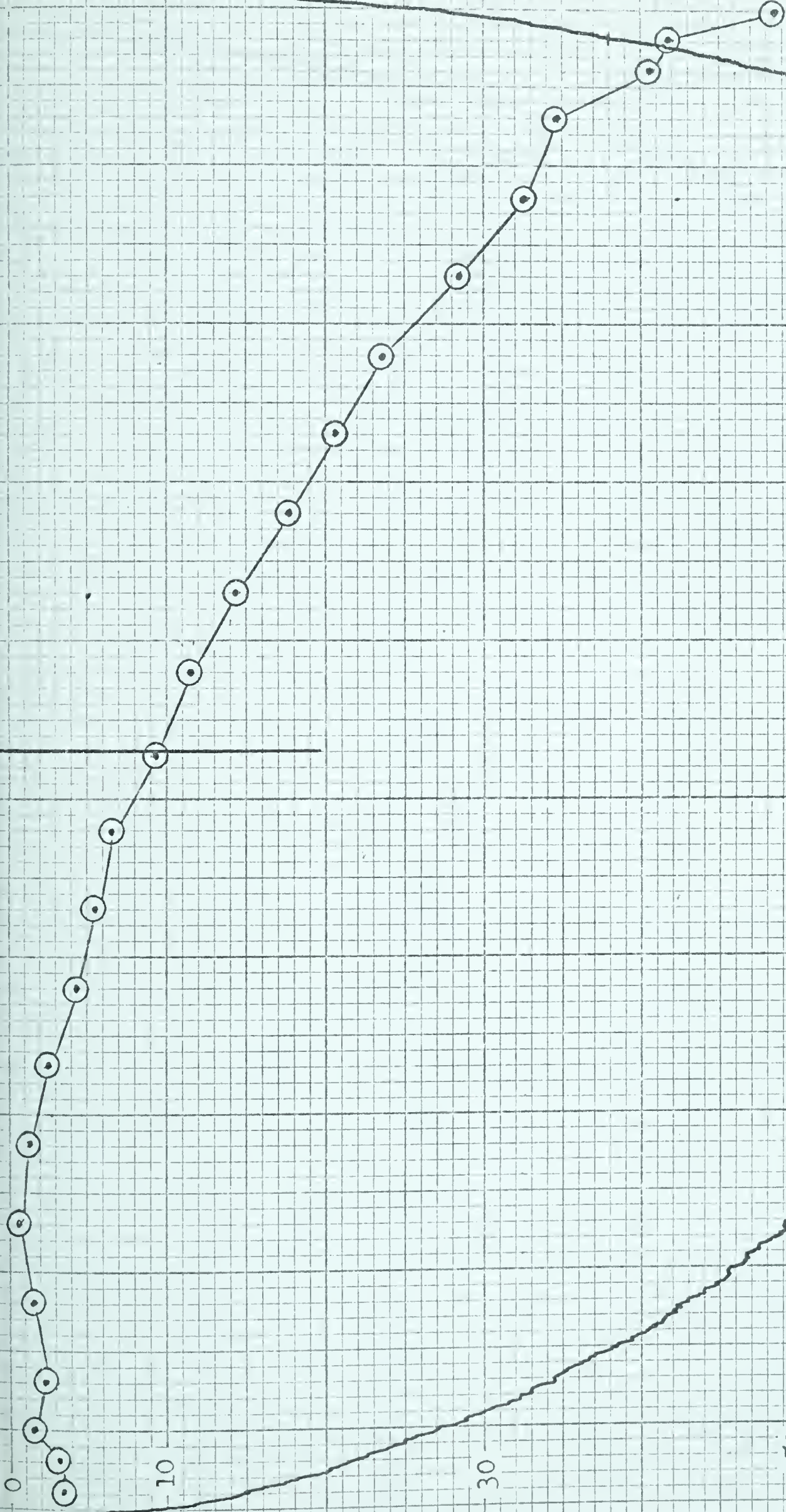


TEST NO. 123101
VERTICAL BEAM

10

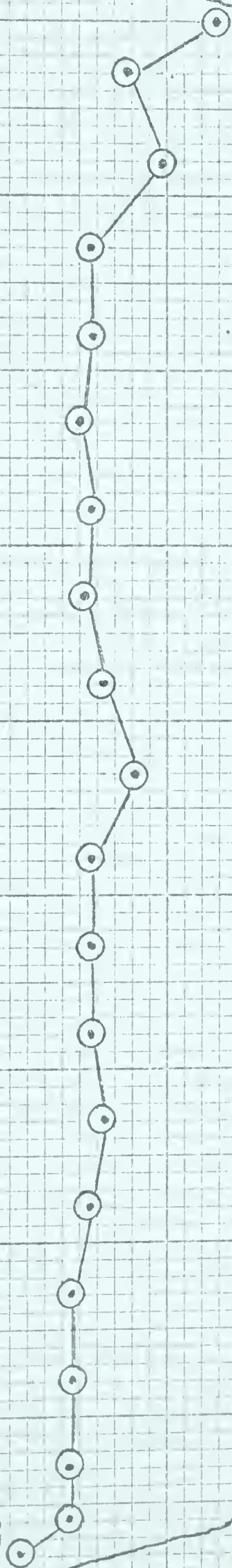


TEST NO. 123102
HORIZONTAL BEAM
FLOW - 62.7 LB PER SEC
NO BED

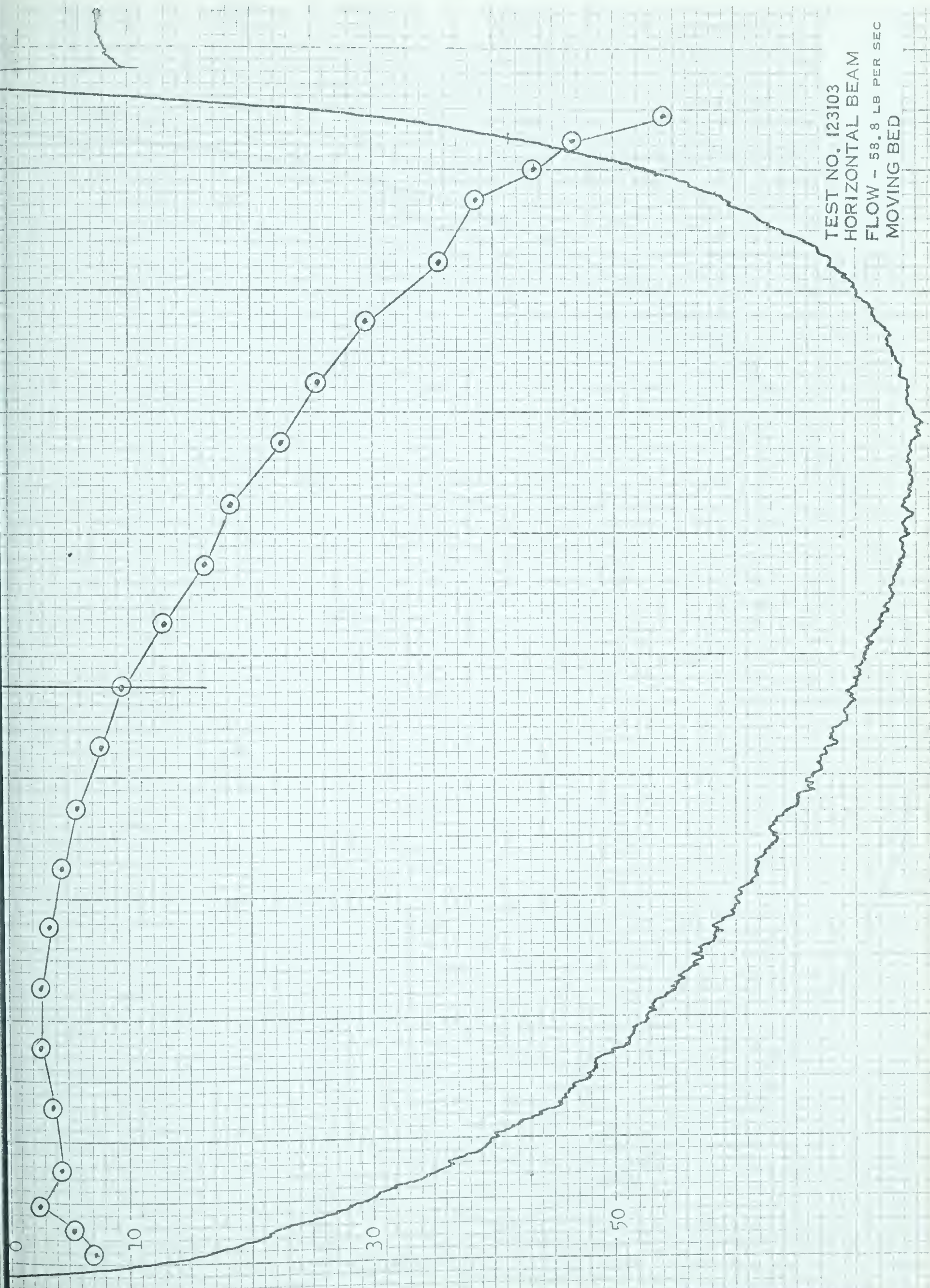


TEST NO. 123102
VERTICAL BEAM

10

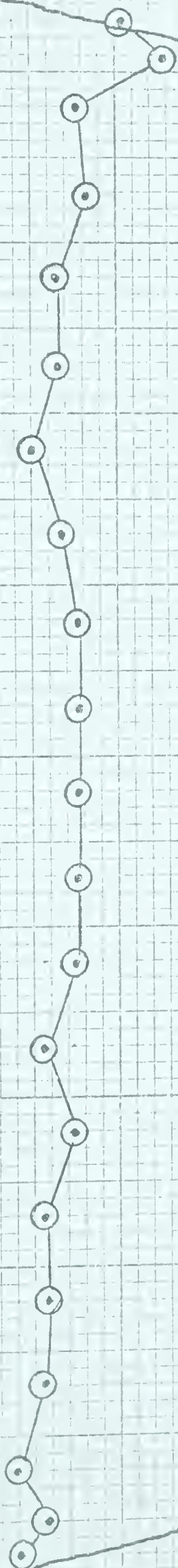


TEST NO. 123103
HORIZONTAL BEAM
FLOW - 58.8 LB PER SEC
MOVING BED

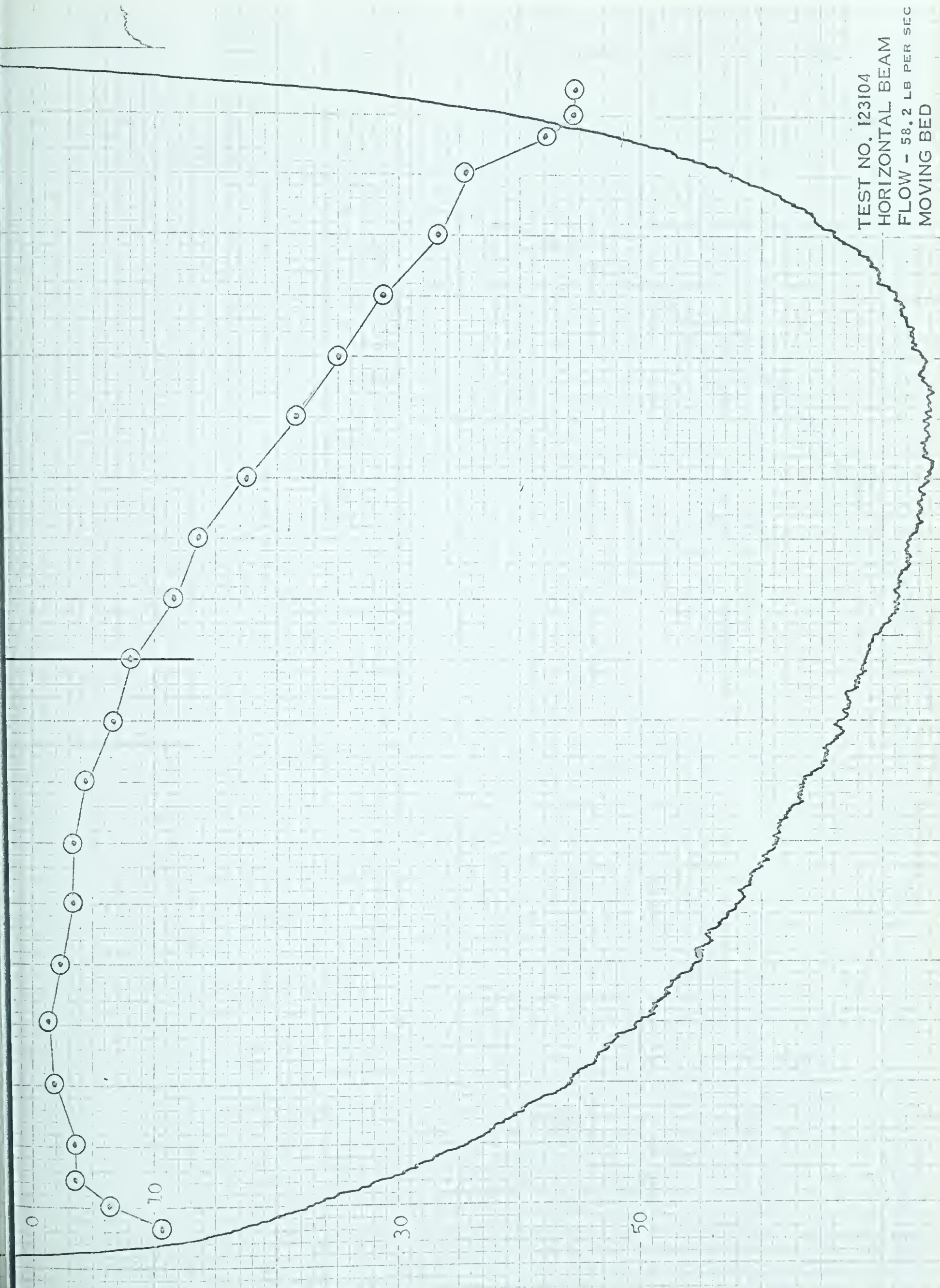


TEST NO. 123103
VERTICAL BEAM

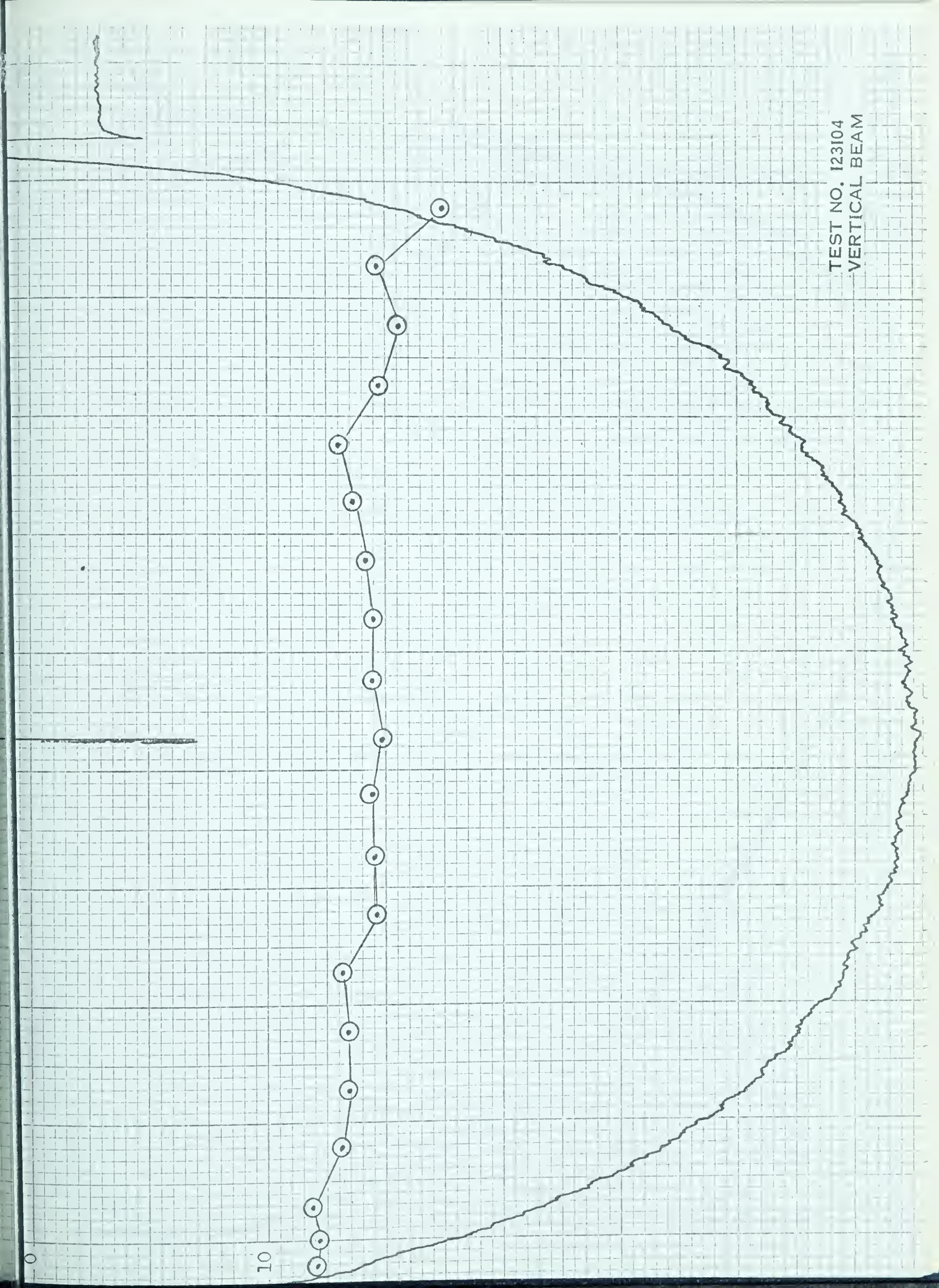
10



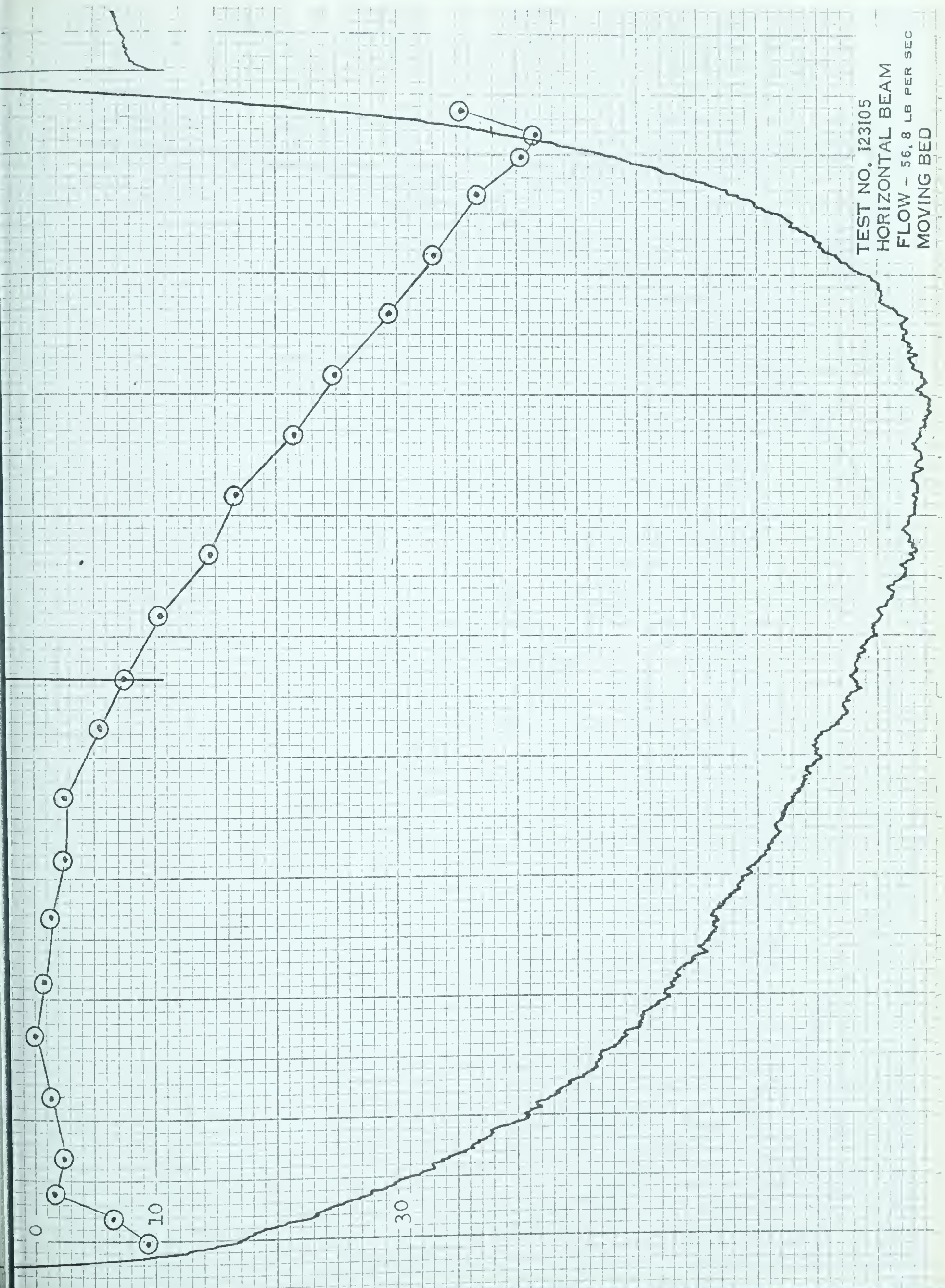
TEST NO. 123104
HORIZONTAL BEAM
FLOW - 58.2 LB PER SEC
MOVING BED



TEST NO. 123104
VERTICAL BEAM



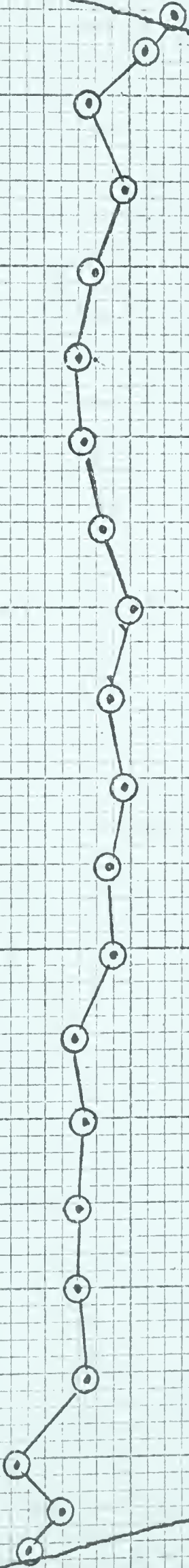
TEST NO. 123105
HORIZONTAL BEAM
FLOW - 56.8 LB PER SEC
MOVING BED



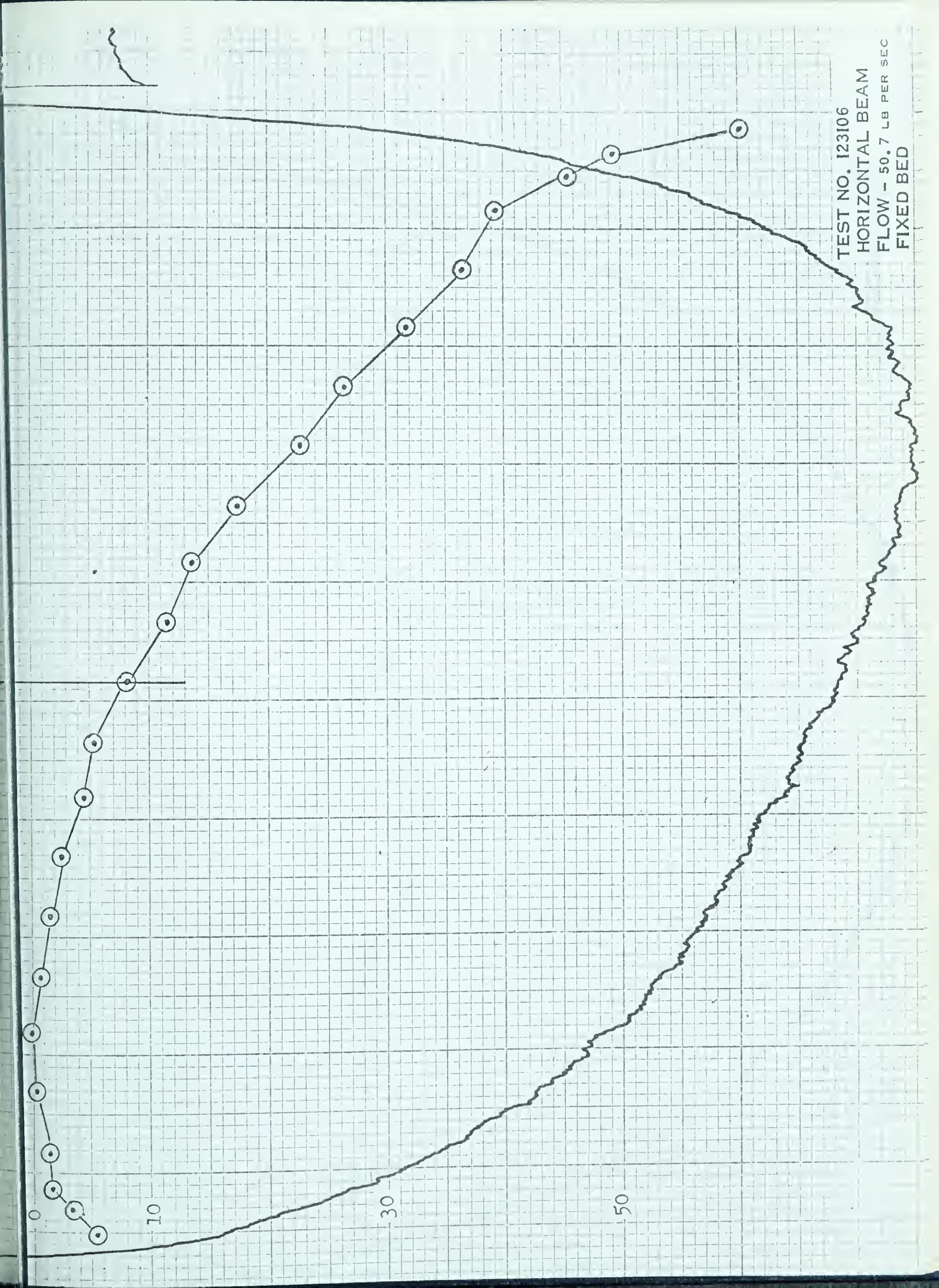
TEST NO. 123105
VERTICAL BEAM

0

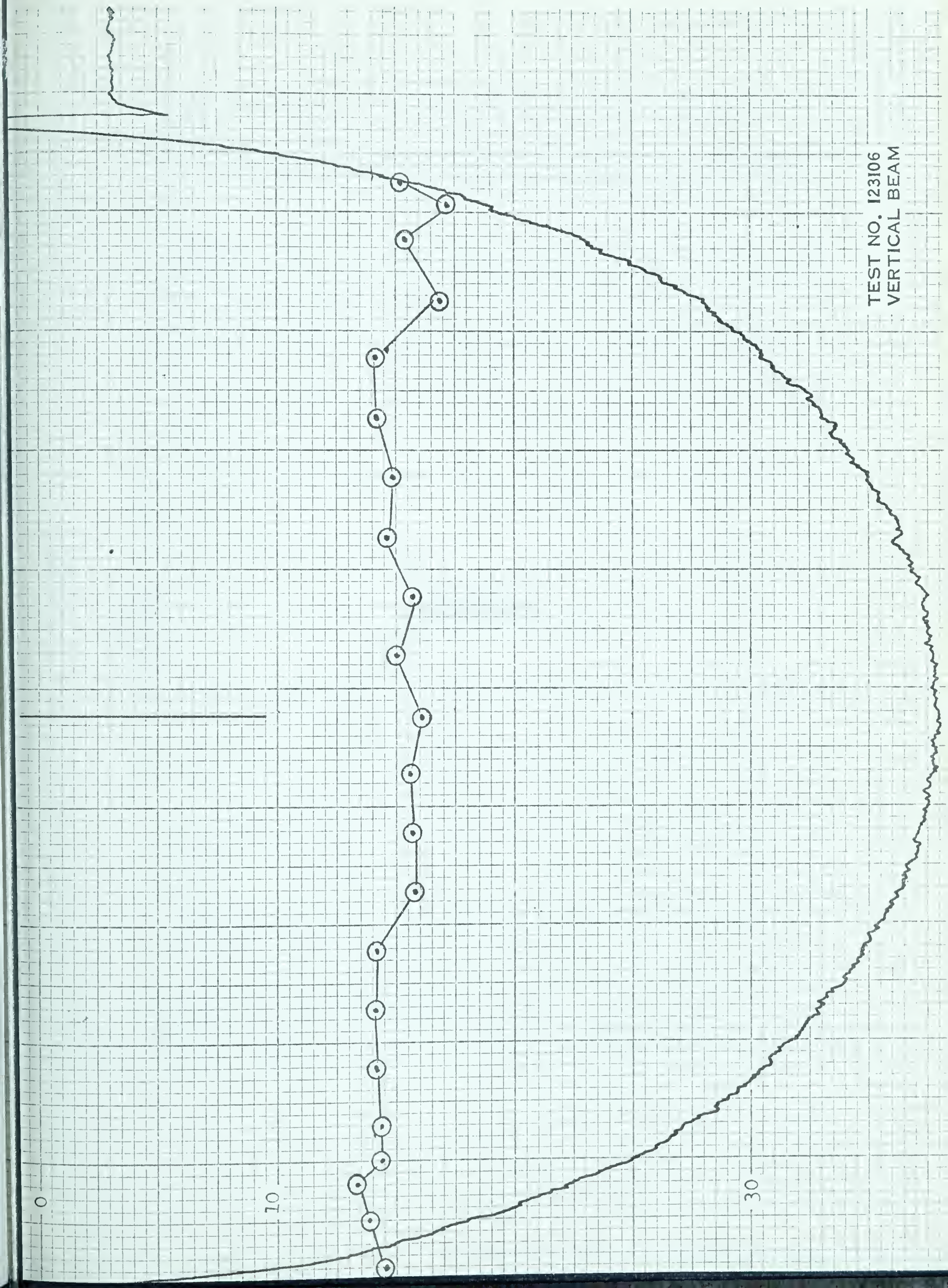
10



TEST NO. 123106
HORIZONTAL BEAM
FLOW - 50.7 LB PER SEC
FIXED BED



TEST NO. 123106
VERTICAL BEAM



APPENDIX D

TABLE D-1
SETTLING TEST RESULTS

TEST NO	DIA INCHES	FLUID S.G.	VEL FPS	STD DEV	DRA G COEF	STD DEV	REYNOLD NO	STD DEV	FR NO	MOD FR NO	HF NO	SOLID TYPE
1.01	0.03625	1.000	0.407	0.045	1.29	0.28	124.2	13.6	1.305	1.016	0.	1
1.02	0.03055	1.000	0.345	0.040	1.52	0.35	88.6	10.3	1.204	0.937	0.	1
1.03	0.02560	1.000	0.305	0.029	1.62	0.31	65.8	6.3	1.165	0.907	0.	1
1.04	0.02150	1.000	0.272	0.024	1.72	0.30	49.2	4.4	1.132	0.882	0.	1
1.05	0.01810	1.000	0.230	0.022	2.02	0.39	35.0	3.4	1.043	0.812	0.	1
1.06	0.01520	1.000	0.201	0.092	2.22	2.04	25.7	11.8	0.996	0.775	0.	1
1.07	0.01230	1.000	0.162	0.016	2.76	0.53	16.8	1.6	0.892	0.695	0.	1
1.08	0.01080	1.000	0.132	0.012	3.68	0.70	12.0	1.1	0.773	0.601	0.	1
1.09	0.00910	1.000	0.100	0.014	5.37	1.50	7.7	1.1	0.640	0.498	0.	1
1.10	0.00770	1.000	0.088	0.007	5.89	0.94	5.7	0.5	0.611	0.476	0.	1
1.11	0.00710	1.000	0.078	0.007	6.84	1.29	4.7	0.4	0.567	0.442	0.	1
1.12	0.00540	1.000	0.063	0.006	7.95	1.52	2.9	0.3	0.526	0.409	0.	1
1.13	0.00450	1.000	0.047	0.008	11.81	3.74	1.8	0.3	0.431	0.336	0.	1
1.14	0.00380	1.000	0.041	0.007	13.59	4.72	1.3	0.2	0.402	0.313	0.	1
1.15	0.00320	1.000	0.037	0.004	14.04	3.36	1.0	0.1	0.396	0.308	0.	1
2.01	0.14030	1.000	0.639	0.074	2.03	0.47	755.0	87.9	1.042	0.811	0.	1
2.02	0.07990	1.000	0.606	0.075	1.28	0.32	407.8	50.2	1.310	1.020	0.	1
2.03	0.05650	1.000	0.544	0.065	1.13	0.27	258.7	30.8	1.397	1.088	0.	1
2.04	0.04315	1.000	0.460	0.067	1.20	0.35	167.2	24.2	1.353	1.053	0.	1
2.05	0.03625	1.000	0.387	0.040	1.43	0.29	117.9	12.1	1.239	0.965	0.	1
2.06	0.01230	1.000	0.164	0.012	2.70	0.38	17.0	1.2	0.902	0.702	0.	1
2.07	0.14030	1.000	0.686	0.087	1.76	0.45	810.6	102.7	1.119	0.871	0.	1
3.01	0.03055	1.000	0.341	0.024	1.55	0.22	87.7	6.2	1.191	0.927	0.	2
3.02	0.02560	1.000	0.295	0.019	1.74	0.22	63.5	4.1	1.125	0.876	0.	2
3.03	0.02150	1.000	0.258	0.018	1.91	0.26	46.7	3.2	1.073	0.836	0.	2
3.04	0.01810	1.000	0.227	0.018	2.08	0.33	34.5	2.7	1.028	0.800	0.	2
3.05	0.01520	1.000	0.199	0.017	2.26	0.39	25.5	2.2	0.986	0.767	0.	2
3.06	0.01230	1.000	0.163	0.016	2.73	0.54	16.9	1.7	0.897	0.699	0.	2
3.07	0.01080	1.000	0.136	0.014	3.43	0.71	12.4	1.3	0.801	0.624	0.	2
3.08	0.00910	1.000	0.114	0.013	4.17	0.97	8.7	1.0	0.727	0.566	0.	2
3.09	0.00770	1.000	0.095	0.009	5.08	0.92	6.1	0.6	0.658	0.512	0.	2
3.10	0.00710	1.000	0.079	0.013	6.65	2.16	4.7	0.8	0.575	0.448	0.	2

TABLE D-1 - continued

TEST NO	DIA INCHES	FLUID S.G.	SETTLING TEST RESULTS					FR NO	MOD FR NO	HE NO	SOLID TYPE
			VEL FPS	STD DEV	DRA COEF	STD DEV	REYNOLD NO				
4.01	0.23600	1.000	1.934	0.086	0.37	0.03	3841.4	2.430	1.892	0.	3
4.02	0.15750	1.000	1.717	0.152	0.32	0.06	2276.0	2.641	2.056	0.	3
4.03	0.15750	1.000	1.543	0.061	0.29	0.03	2046.3	2.374	1.848	-0.	3
4.04	0.11800	1.000	1.319	0.068	0.40	0.04	1310.5	2.245	1.825	-0.	3
4.05	0.11800	1.000	1.233	0.121	0.46	0.09	1224.7	2.191	1.706	0.	3
5.01	0.02560	1.189	0.145	0.008	5.38	0.61	8.7	0.552	0.408	54.51	2
5.02	0.02150	1.189	0.131	0.006	5.50	0.46	6.6	0.546	0.493	38.45	2
5.03	0.01810	1.189	0.121	0.005	5.46	0.43	5.1	0.548	0.494	27.25	2
5.04	0.01520	1.189	0.098	0.005	7.00	0.76	3.5	0.484	0.436	19.22	2
5.05	0.01080	1.189	0.070	0.003	9.66	0.82	1.8	0.412	0.371	9.70	2
5.06	0.00910	1.189	0.061	0.007	10.79	2.65	1.3	0.390	0.351	6.89	2
5.07	0.01520	1.189	0.078	0.006	10.95	1.62	2.8	0.387	0.349	19.22	2
5.08	0.00710	1.189	0.058	0.003	9.13	0.80	1.0	0.424	0.382	4.19	2
5.09	0.00710	1.189	0.061	0.008	8.51	2.32	1.0	0.439	0.396	4.19	2
6.01	0.14030	1.189	0.372	0.032	4.47	0.78	122.0	0.606	0.546	1637.33	1
6.02	0.07990	1.189	0.305	0.035	3.78	0.87	57.0	0.658	0.594	531.02	1
6.03	0.05650	1.189	0.267	0.035	3.50	0.92	35.2	0.684	0.617	265.53	1
6.04	0.04315	1.189	0.170	0.019	6.53	1.45	17.2	0.501	0.452	154.88	1
6.05	0.00710	1.189	0.060	0.005	8.63	1.30	1.0	0.436	0.393	4.19	1
7.01	0.11800	1.189	0.764	0.065	0.89	0.15	211.1	1.358	1.225	1158.20	3
7.02	0.15750	1.189	1.174	0.094	0.50	0.08	440.1	1.805	1.628	2134.74	3
7.03	0.23600	1.189	1.374	0.223	0.55	0.18	759.0	1.727	1.558	4632.81	3
8.01	0.07990	1.132	0.509	0.063	1.48	0.36	132.4	1.100	0.950	616.36	1
8.02	0.05650	1.132	0.360	0.033	2.10	0.39	66.1	0.924	0.797	308.20	1
8.03	0.04315	1.132	0.311	0.026	2.15	0.36	43.6	0.912	0.788	179.76	1
8.04	0.03625	1.132	0.277	0.017	2.27	0.28	32.6	0.887	0.766	126.87	1
8.05	0.03055	1.132	0.220	0.019	3.03	0.53	21.9	0.769	0.664	90.11	1
8.06	0.02560	1.132	0.177	0.015	3.90	0.67	14.8	0.677	0.584	63.27	1
8.07	0.02150	1.132	0.157	0.010	4.16	0.52	11.0	0.656	0.566	44.63	1
8.08	0.01810	1.132	0.133	0.016	4.88	1.16	7.9	0.605	0.523	31.63	1
8.09	0.01520	1.132	0.113	0.010	5.68	1.03	5.6	0.561	0.484	22.31	1
10	0.01230	1.132	0.094	0.008	6.72	1.18	3.8	0.516	0.445	14.61	1

TABLE D-1 - continued

SETTLING TEST RESULTS

TEST NO	DIA INCHES	FLUID S.G.	VEL FPS	STD DEV	DRAO COEF	STD DEV	REYNOLD NO	STD DEV	FR NO	MOD FR NO	HE NO	SOLID TYPE
8.11	0.01080	1.132	0.067	0.004	11.37	1.28	2.4	0.1	0.297	0.342	11.26	1
8.12	0.00910	1.132	0.065	0.010	10.20	3.16	1.9	0.3	0.419	0.362	8.00	1
8.13	0.00770	1.132	0.062	0.009	9.50	2.66	1.6	0.2	0.434	0.375	5.72	1
8.14	0.00710	1.132	0.050	0.008	13.87	4.28	1.1	0.2	0.359	0.310	4.87	1
8.15	0.00540	1.132	0.044	0.006	13.65	3.50	0.8	0.1	0.362	0.313	2.82	1
8.16	0.00450	1.132	0.046	0.004	10.00	1.62	0.7	0.1	0.423	0.365	1.96	1
9.01	0.11800	1.132	0.874	0.039	0.74	0.07	335.6	14.9	1.553	1.341	1344.32	3
9.02	0.15750	1.132	1.343	0.111	0.42	0.07	688.4	56.8	2.065	1.783	2394.97	3
9.03	0.23600	1.132	1.623	0.044	0.43	0.02	1246.7	33.7	2.039	1.761	5377.28	3
10.01	0.07990	1.242	0.256	0.021	4.96	0.82	37.0	3.1	0.552	0.519	608.96	1
10.02	0.05650	1.242	0.225	0.044	4.53	1.70	23.0	4.5	0.577	0.542	304.50	1
10.03	0.04315	1.242	0.162	0.018	6.64	1.45	12.7	1.4	0.477	0.448	177.61	1
10.04	0.03625	1.242	0.137	0.011	7.83	1.20	9.0	0.7	0.439	0.413	125.35	1
11.01	0.23600	1.242	1.345	0.166	0.53	0.13	575.1	70.9	1.690	1.588	5312.75	3
11.02	0.23600	1.242	1.296	0.113	0.57	0.10	554.0	48.2	1.628	1.529	5312.75	3
11.03	0.15750	1.242	1.104	0.040	0.52	0.04	315.1	11.5	1.699	1.596	2366.23	3
11.04	0.15750	1.242	1.132	0.069	0.50	0.06	323.0	19.7	1.741	1.635	2366.23	3
11.05	0.11800	1.242	0.652	0.059	1.12	0.20	139.4	12.7	1.159	1.089	1328.19	3
11.06	0.11800	1.242	0.709	0.074	0.95	0.20	151.5	15.7	1.259	1.183	1328.19	3
11.07	0.11800	1.242	0.589	0.084	1.38	0.39	125.9	18.0	1.046	0.983	1328.19	3
11.08	0.15750	1.242	0.932	0.059	0.73	0.09	266.0	16.8	1.434	1.347	2366.23	3
11.09	0.15750	1.242	1.037	0.057	0.59	0.07	295.8	16.3	1.595	1.498	2366.23	3
11.10	0.23600	1.242	1.252	0.115	0.61	0.11	535.5	49.0	1.574	1.478	5312.75	3
11.11	0.23600	1.242	1.249	0.093	0.61	0.09	534.1	39.7	1.570	1.474	5312.75	3
12.01	0.07990	1.242	0.299	0.031	3.25	0.67	43.3	4.5	0.647	0.640	608.05	4
12.02	0.04350	1.242	0.217	0.034	3.37	1.05	17.1	2.7	0.636	0.629	180.50	4
12.03	0.03590	1.242	0.205	0.015	3.13	0.46	13.3	1.0	0.660	0.653	122.94	4
12.04	0.03020	1.242	0.146	0.018	5.19	1.27	8.0	1.0	0.512	0.507	87.00	4
12.05	0.02150	1.242	0.170	0.025	2.72	0.80	6.6	1.0	0.708	0.701	44.09	4
12.06	0.12500	1.242	0.602	0.024	1.26	0.10	136.3	5.4	1.039	1.028	1490.44	4
12.07	0.09900	1.242	0.415	0.086	2.08	0.86	73.7	15.3	0.809	0.801	916.11	4

NOTE

TYPE 1 SOLIDS - ATHABASCA SAND

TYPE 2 SOLIDS - OTTAWA SAND

TYPE 3 SOLIDS - 3MM, 4MM, 6MM GLASS BEADS

TYPE 4 SOLIDS - 2.5 SG GLASS BEADS

TABLE D-2
SETTLING TEST DATA

TEST NO	MESH	TEMP	DIST FT	FLUID S.G.	NO OF TESTS	CHART SPEED	KIN VISC	YIELD STRESS	READINGS
1.01	18.20	75.0	2.0	1.000	33	0.	0.99	0.	
5.20	4.60	5.50		4.90	4.60	5.50	5.60	4.60	4.90 5.10
4.50	4.20	4.10		5.70	5.40	4.90	5.50	5.40	5.80 5.00
5.40	4.90	5.30		4.60	4.00	6.00	4.20	4.40	5.00 4.60
5.60	4.20	4.00							
1.02	20.25	75.0	2.0	1.000	33	0.	0.99	0.	
4.70	4.60	6.70		7.10	4.70	5.30	5.90	6.80	6.30 6.60
5.40	5.20	6.20		6.30	6.00	6.00	5.70	5.80	5.60 6.10
5.40	5.70	7.00		5.80	5.50	6.90	5.70	5.30	6.10 5.70
5.00	6.80	6.10							
1.03	25.30	75.0	2.0	1.000	33	0.	0.99	0.	
6.90	7.20	5.90		5.90	6.90	7.00	5.90	6.20	7.90 7.10
6.90	6.90	6.70		7.20	6.20	6.60	6.90	5.90	7.50 7.10
8.60	6.00	6.20		7.00	6.20	7.50	6.00	6.00	6.30 5.90
5.90	5.90	5.90							
1.04	30.35	75.0	2.0	1.000	33	0.	0.99	0.	
7.60	6.70	6.50		6.90	7.60	7.60	7.10	7.20	8.10 6.00
7.10	7.20	7.40		8.50	9.00	7.50	6.70	6.50	8.30 7.00
8.00	6.90	7.40		7.20	7.70	7.60	8.70	7.40	7.20 6.70
6.80	8.20	7.40							
1.05	35.40	75.0	2.0	1.000	33	0.	0.99	0.	
8.30	9.40	9.20		8.50	8.70	7.90	8.20	10.00	7.00 8.50
9.70	8.30	9.90		8.60	10.00	7.90	9.20	8.70	9.40 9.70
10.40	7.70	10.70		9.20	7.70	8.10	8.30	8.80	8.90 8.20
8.60	7.70	8.50							
1.06	40.45	75.0	2.0	1.000	33	0.	0.99	0.	
9.40	11.30	9.40		9.80	9.90	10.00	11.10	11.10	12.20 10.00
11.30	10.40	12.20		10.60	10.00	11.70	2.80	11.70	11.10 12.80
10.90	11.40	12.70		10.10	9.90	10.70	9.80	10.40	9.60 11.00
11.10	13.40	11.90							
1.07	45.50	75.0	2.0	1.000	33	0.	0.99	0.	
12.70	14.60	11.70		12.60	12.30	12.30	10.50	11.80	10.80 14.40
10.10	14.80	11.30		12.40	13.60	12.00	14.00	12.00	12.10 10.60
13.90	13.50	13.50		11.30	14.00	13.00	11.60	12.20	12.50 11.60
12.60	11.70	12.80							

TABLE D-2 - continued

SETTLING TEST DATA										READINGS	
TEST NO	MESH	TEMP	DIST FT	FLUID S.G.	NO OF TESTS	CHART SPEED	KIN VISC	YIELD STRESS			
1.08	50.60	75.0	2.0	1.000	33	0.	0.99	0.	14.60	13.70	
15.20	14.80	16.60	14.60	18.10	18.10	18.90	17.10	16.10	14.20	12.20	
14.40	15.30	13.90	12.50	15.00	15.00	14.70	17.30	13.30	15.20	16.10	
15.80	14.70	16.30	15.50	16.50	16.50	16.60	15.30	16.10			
15.80	14.40	15.40									
1.09	60.70	75.0	2.0	1.000	33	0.	0.99	0.	22.50	20.90	
15.90	18.00	19.30	17.10	18.80	18.80	19.70	17.50	24.40	20.90	23.90	
15.30	18.00	19.70	20.70	17.10	17.10	21.40	17.90	26.50	19.20	22.20	
24.30	19.00	19.10	20.60	21.90	21.90	19.40	20.20	17.10			
22.80	23.30	28.00									
1.10	70.80	75.0	2.0	1.000	33	0.	0.99	0.	23.10	23.90	
25.90	22.10	22.30	25.50	22.60	22.60	23.50	21.90	21.90	22.20	22.20	
23.30	22.10	23.80	18.60	20.50	20.50	21.30	23.20	21.40			
22.20	23.30	22.30	22.20	22.60	22.60	27.50	23.10	22.10			
30.30	23.80	22.40									
1.11	80.10	76.0	2.0	1.000	33	0.	0.99	0.	25.10	25.90	
30.20	24.00	23.70	27.00	24.60	24.60	28.00	25.90	27.80	29.10	27.50	
26.40	24.70	23.90	23.20	27.20	27.20	29.50	23.00	27.50	24.00	28.10	
20.10	22.20	24.70	28.30	28.00	28.00	26.20	24.70	28.50			
25.10	22.60	23.60									
1.12	10.12	76.0	2.0	1.000	33	0.	0.99	0.	29.20	37.40	
28.60	29.60	27.60	29.80	28.00	28.00	29.70	34.90	27.50	31.60	28.40	
37.70	43.70	29.20	31.30	34.30	34.30	34.00	35.50	30.60	31.50	35.30	
32.40	32.30	29.30	31.40	33.50	33.50	32.40	31.90	31.40			
33.20	29.20	30.50									
1.13	12.14	76.0	1.0	1.000	33	0.	0.99	0.	22.00	22.20	
18.40	24.40	18.50	25.80	31.80	31.80	18.60	19.50	20.80	19.00	20.30	
21.60	22.10	20.50	23.30	16.60	16.60	17.10	19.30	23.50	23.40	18.30	
15.60	19.40	24.30	25.90	32.00	32.00	23.20	20.00	26.20			
18.50	23.50	19.50									
1.14	14.17	76.0	0.5	1.000	33	0.	0.99	0.	13.70	15.20	
10.40	13.60	11.20	13.30	11.00	11.00	10.00	12.20	10.90	17.70	10.70	
9.40	9.70	16.60	11.70	11.40	11.40	12.40	11.60	17.40	9.80	15.50	
13.90	10.10	16.40	16.40	10.30	10.30	12.70	13.50	11.60			
12.70	12.50	13.90									

TABLE D-2 - continued

SETTLING TEST DATA										READINGS	
TEST NO	MESH	TEMP	DIST FT	FLUID S.G.	NO OF TESTS	CHART SPEED	KIN VISC	YIELD STRESS			
1.15	17.20	76.0	0.5	1.000	33	0.	0.99	0.			
13.20	11.60	12.20	13.30	11.90	11.90	10.80	11.50	13.40		12.90	13.80
14.40	14.40	14.80	14.70	14.00	14.00	17.10	12.10	14.10		12.80	16.80
13.60	14.70	13.20	15.60	14.60	14.60	19.60	13.40	14.80		14.20	14.40
13.60	14.00	11.10									
2.01	4.80	77.0	1.5	1.000	5	5.0	0.99	0.			
10.00	14.50	11.50	11.50	12.00	12.00						
2.02	8.12	79.0	1.5	1.000	29	5.0	0.99	0.			
10.50	11.50	12.50	13.00	15.00	15.00	12.00	10.00	14.00		10.00	14.00
12.00	15.00	13.00	14.00	13.50	13.50	12.50	14.50	11.00		11.00	13.00
10.50	13.00	13.00	14.50	12.00	12.00	12.50	11.50	10.50		14.50	
2.03	12.16	79.0	1.5	1.000	20	5.0	0.99	0.			
13.50	12.00	14.50	12.00	17.00	17.00	13.00	13.50	13.00		17.00	14.00
13.00	16.50	13.50	18.00	12.00	12.00	15.00	15.00	12.50		12.00	13.00
2.04	16.18	79.0	1.0	1.000	37	5.0	0.99	0.			
13.50	18.50	16.00	11.00	10.00	10.00	12.00	10.50	11.00		10.00	11.50
13.50	13.00	11.00	10.00	9.00	9.00	11.50	12.00	11.00		10.00	12.00
13.00	11.00	12.00	10.00	9.50	9.50	9.00	11.00	9.00		11.00	9.00
11.50	10.50	9.50	10.50	10.00	10.00	9.00	9.50				
2.05	18.20	75.0	1.0	1.000	57	5.0	0.99	0.			
17.00	13.00	14.50	14.00	13.00	13.00	13.00	13.00	11.50		12.00	15.00
14.50	13.50	12.00	12.00	12.00	12.00	12.00	13.50	12.50		14.00	13.00
13.00	14.00	12.00	12.50	14.50	14.50	13.00	14.50	13.00		12.00	11.50
12.00	15.00	12.50	11.50	12.00	12.00	11.50	13.00	11.50		11.50	14.00
13.00	16.00	11.00	12.50	12.50	12.50	16.00	10.50	12.00		14.00	15.00
13.00	16.00	15.00	11.50	13.00	13.00	12.00	12.00				
2.06	45.50	74.0	1.5	1.000	36	2.5	0.99	0.			
23.00	25.00	26.00	24.00	27.00	27.00	23.00	20.00	23.00		24.00	24.00
25.00	24.00	24.00	21.00	24.00	24.00	24.00	23.00	23.00		22.00	23.00
23.00	22.00	23.00	22.00	22.00	22.00	19.00	23.00	22.00		21.00	21.00
23.00	24.00	22.00	23.00	25.00	25.00	21.00					
2.07	4.80	75.0	1.0	1.000	16	5.0	0.99	0.			
9.50	8.50	6.50	7.00	6.00	6.00	8.00	7.50	7.50		7.00	7.50
8.00	9.00	7.00	7.00	6.00	6.00	6.50					

TABLE D-2 - continued

SETTLING TEST DATA										READINGS	
TEST NO	MESH	TEMP	DIST FT	FLUID S.G.	NO OF TESTS	CHART SPEED	KIN VISC	YIELD STRESS			
3.01	20.25	75.0	2.0	1.000	32	0.	0.99	0.			
6.00	7.20	6.50		4.90	5.60	5.50	6.20	5.40	5.60	5.80	
5.50	5.70	5.20		5.60	5.90	6.20	6.10	5.80	6.00	5.80	
5.90	6.20	6.50		5.80	5.80	6.10	6.30	5.70	5.80	6.00	
6.30	5.70										
3.02	25.30	75.0	2.0	1.000	32	0.	0.99	0.			
7.20	6.60	7.20		6.90	7.00	6.50	7.00	6.10	6.20	7.00	
6.30	7.20	7.20		7.20	7.40	7.50	7.00	6.50	6.30	6.90	
6.00	6.20	6.80		6.60	7.20	6.70	7.50	6.90	6.80	6.10	
7.30	6.70										
3.03	30.35	75.0	2.0	1.000	32	0.	0.99	0.			
7.70	8.00	7.60		7.60	8.70	8.10	7.70	7.20	8.20	8.80	
7.90	8.10	8.50		6.80	7.60	6.70	7.20	8.20	7.60	7.30	
7.80	7.90	7.50		7.00	7.90	7.30	8.10	7.80	8.70	7.80	
7.40	8.70										
3.04	35.40	75.0	2.0	1.000	32	0.	0.99	0.			
8.00	8.70	9.00		9.00	8.60	8.60	8.40	9.80	9.60	9.10	
9.60	9.00	10.20		10.80	9.70	8.90	7.90	8.20	7.90	8.40	
8.60	9.30	8.20		8.60	8.50	7.60	8.30	9.00	8.80	9.50	
10.20	8.40										
3.05	40.45	7.5	2.0	1.000	32	0.	0.99	0.			
9.50	10.20	11.00		9.70	8.60	10.90	10.40	10.90	9.10	8.40	
10.60	10.60	10.30		12.50	10.40	10.40	9.70	9.70	9.40	9.30	
10.00	10.80	8.50		10.10	10.30	11.70	9.50	10.20	10.30	9.50	
11.00	10.40										
3.06	45.50	7.5	2.0	1.000	32	0.	0.99	0.			
12.30	14.30	11.40		11.10	11.90	10.90	13.30	11.00	11.40	12.40	
13.80	11.70	15.90		12.40	12.40	13.00	12.80	11.90	12.00	10.70	
14.30	12.40	12.30		12.20	14.90	12.00	13.20	12.20	10.90	10.80	
14.20	10.60										
3.07	50.60	75.0	2.0	1.000	32	0.	0.99	0.			
10.60	12.10	13.40		15.20	13.00	16.00	14.70	14.00	13.80	15.30	
15.30	19.30	14.70		15.90	13.80	15.00	14.70	15.60	15.70	14.60	
14.70	15.00	15.70		14.90	14.40	14.90	15.40	16.40	15.30	14.90	
13.60	16.10										

TABLE D-2 - continued

SETTLING TEST DATA										
TEST NO	MESH	TEMP	DIST FT	FLUID S.G.	NO OF TESTS	CHART SPEED	KIN VISC	YIELD STRESS	READINGS	
3.08	60.70	75.0	2.0	1.000	32	0.	0.99	0.	15.60	17.20
15.40	17.30	15.00	20.80	14.20	19.20	19.20	15.20	21.90	16.40	20.30
16.30	22.70	17.90	16.90	17.30	17.10	17.10	18.90	19.60	16.70	15.70
16.50	20.60	15.40	19.60	17.40	19.90	19.90	17.20	17.50		
19.00	20.90									
3.09	70.80	75.0	2.0	1.000	32	0.	0.99	0.	21.80	19.50
20.00	21.20	19.40	19.50	19.50	20.30	20.30	22.90	20.10	21.60	22.20
25.30	22.80	21.00	21.00	22.70	22.20	22.20	21.50	20.70	21.90	23.50
22.90	21.00	21.90	21.60	19.10	20.40	20.40	15.90	26.00		
20.50	21.80									
3.10	80.10	75.0	2.0	1.000	32	0.	0.99	0.	32.00	32.00
24.20	21.10	26.80	33.80	33.20	28.60	28.60	22.90	21.10	20.80	26.30
27.90	22.80	20.90	21.40	23.00	23.10	23.10	25.20	18.20	26.30	27.40
24.90	23.00	29.60	23.60	31.30	28.20	28.20	28.30	22.00		
22.90	35.00									
4.01	6.00	77.0	2.5	1.000	11	0.	0.99	0.	1.35	1.20
1.40	1.25	1.30	1.35	1.35	1.30	1.30	1.25	1.25		
1.25										
4.02	4.00	77.0	2.5	1.000	12	0.	0.99	0.	1.45	2.00
1.40	1.40	1.40	1.35	1.55	1.40	1.40	1.45	1.45		
1.40	1.40									
4.03	4.00	77.0	1.5	1.000	3	2.5	0.99	-0.		
2.50	2.50	2.30								
4.04	3.00	77.0	2.5	1.000	10	1.0	0.99	-0.	1.80	2.00
1.80	1.90	1.90	2.10	2.00	1.90	1.90	1.80	1.80	5.50	6.50
4.05	3.00	77.0	1.5	1.000	14	5.0	0.99	0.		
5.50	6.00	7.00	5.50	6.50	5.50	5.50	5.50	5.50		
7.00	7.00	6.50	6.50							
5.01	25.30	76.0	1.0	1.189	17	2.5	3.56	0.035	17.00	18.00
17.00	17.00	17.00	19.00	17.00	16.00	16.00	17.00	20.00		
16.00	17.00	17.00	16.00	18.00	18.00	18.00	18.00			
5.02	30.35	76.0	1.0	1.189	10	2.5	3.56	0.035	19.00	19.00
21.00	18.00	19.00	19.00	19.00	20.00	20.00	18.00	19.00		

TABLE D-2 - continued

SETTLING TEST DATA										READINGS	
TEST NO	MESH	TEMP	DIST FT	FLUID S.G.	NO OF TESTS	CHART SPEED	KIN VISC	YIELD STRESS			
5.03	35.40	76.0	1.0	1.189	4	2.5	3.56	0.035			
22.00	21.00	20.00	20.00								
5.04	40.45	76.0	1.0	1.189	9	2.5	3.56	0.035			
26.00	27.00	24.00	26.00	27.00	25.00	25.00	23.00	26.00	27.00		
5.05	50.60	76.0	1.0	1.189	15	2.5	3.56	0.035			
36.00	39.00	37.00	33.00	37.00	36.00	36.00	36.00	35.00	34.00	34.00	
35.00	36.00	34.00	37.00	37.00							
5.06	60.70	76.0	1.0	1.189	9	2.5	3.56	0.035			
45.00	35.00	45.00	45.00	35.00	47.00	47.00	40.00	36.00	47.00		
5.07	45.50	76.0	1.0	1.189	35	2.5	3.56	0.035			
29.00	30.00	31.00	26.00	31.00	35.00	35.00	30.00	35.00	37.00	32.00	
32.00	35.00	31.00	37.00	31.00	35.00	35.00	32.00	32.00	34.00	32.00	
32.00	33.00	34.00	31.00	33.00	33.00	31.00	28.00	32.00	34.00	30.00	
33.00	30.00	32.00	32.00	34.00							
5.08	80.10	74.0	1.0	1.189	18	2.5	3.56	0.035			
42.00	43.00	47.00	41.00	41.00	45.00	45.00	42.00	40.00	42.00	43.00	
43.00	43.00	45.00	40.00	45.00	41.00	41.00	43.00	45.00			
5.09	80.10	76.0	1.0	1.189	23	2.5	3.56	0.035			
35.00	33.00	35.00	55.00	48.00	45.00	45.00	50.00	44.00	41.00	42.00	
35.00	41.00	40.00	38.00	49.00	53.00	53.00	41.00	44.00	40.00	35.00	
38.00	39.00	47.00									
6.01	4.80	76.0	1.0	1.189	8	5.0	3.56	0.035			
14.50	13.00	12.00	16.00	14.00	12.50	12.50	12.50	14.00			
6.02	8.12	76.0	1.5	1.189	54	5.0	3.56	0.035			
28.50	28.50	23.50	26.50	23.00	23.00	23.00	25.50	23.00	27.00	24.00	
25.50	21.00	22.00	29.00	30.00	32.00	32.00	25.00	25.00	24.00	26.50	
26.50	32.00	26.50	24.00	21.00	21.00	21.00	25.00	25.00	25.00	26.00	
25.50	20.00	23.50	25.00	22.00	22.00	27.00	22.00	24.00	26.00	22.00	
23.00	30.00	25.00	23.00	30.00	25.00	25.00	20.00	21.50	21.50	22.50	
26.00	23.50	23.00	32.00								
6.03	12.16	76.0	1.5	1.189	19	2.5	3.56	0.035			
14.00	18.00	15.00	16.00	11.00	13.00	13.00	15.00	14.00	18.00	13.00	
12.00	15.00	15.00	11.00	14.00	14.00	14.00	16.00	14.00	14.00		

TABLE D-2 - continued

SETTLING TEST DATA

TEST NO	MESH	TEMP	DIST FT	FLUID S.G.	NO OF TESTS	CHART SPEED	KIN VISC	YIELD STRESS	READINGS
6.04	16.18	76.0	1.5	1.189	51	2.3	3.56	0.035	
19.00	20.00	24.00	19.00	18.00	18.00	17.00	19.00	20.00	17.00 19.00
18.00	23.00	19.00	23.00	20.00	20.00	19.00	22.00	19.00	19.00 19.00
18.00	22.20	21.00	23.00	17.00	17.00	18.00	19.00	20.00	18.00 21.00
19.00	18.00	20.00	22.00	20.00	20.00	18.00	21.00	18.00	25.00 24.00
27.00	25.00	24.00	23.00	22.00	22.00	22.00	20.00	21.00	21.00 21.00
25.00									
6.05	80.10	70.6	1.0	1.189	31	2.5	3.56	0.035	
40.00	36.00	40.00	41.00	40.00	40.00	40.00	35.00	37.00	45.00 48.00
40.00	42.00	41.00	42.00	40.00	40.00	39.00	45.00	44.00	41.00 45.00
46.00	45.00	45.00	48.00	42.00	42.00	42.00	43.00	40.00	40.00 44.00
40.00									
7.01	3.00	75.0	1.5	1.189	33	5.0	3.56	0.035	
9.00	9.50	10.50	10.00	8.00	8.00	10.50	10.00	10.50	9.00 10.00
10.00	10.00	8.50	10.50	9.50	9.50	10.50	10.50	10.50	10.50 10.50
9.50	10.50	9.00	10.00	8.50	8.50	10.50	11.00	9.50	10.50 10.50
8.50	11.00	9.00							
7.02	4.00	75.0	1.5	1.189	30	5.0	3.56	0.035	
6.00	6.00	7.00	6.50	6.00	6.00	6.00	7.00	6.50	5.50 6.50
6.00	5.50	6.50	6.00	6.50	6.50	7.00	6.00	7.00	6.50 6.00
6.50	7.50	6.50	6.50	7.50	7.50	6.50	6.00	6.00	7.50 6.50
7.03	6.00	75.0	1.5	1.189	21	5.0	3.56	0.035	
5.00	5.50	4.00	5.00	5.00	5.00	4.50	7.00	6.00	6.50 6.50
5.00	5.00	6.00	6.50	5.50	5.50	4.50	5.60	4.50	6.50 6.50
7.00									
8.01	8.12	79.0	1.5	1.132	9	2.5	2.56	0.020	
10.00	6.50	7.00	7.00	9.00	9.00	7.00	7.00	7.00	7.00
8.02	12.16	79.0	1.5	1.132	17	2.5	2.56	0.020	
10.00	10.00	10.00	12.00	10.00	10.00	10.00	10.00	10.00	10.00 13.00
11.00	10.00	13.00	10.00	9.00	9.00	10.00	11.00		
8.03	16.18	76.0	1.5	1.132	12	2.5	2.56	0.020	
12.00	11.00	13.00	12.00	13.00	13.00	14.00	11.00	11.00	12.00 14.00
12.00	11.00								

TABLE D-2 - continued

SETTLING TEST DATA

TEST NO	MESH	TEMP	DIST FT	FLUID S.G.	NO OF TESTS	CHART SPEED	KIN VISC	YIELD STRESS	READINGS
8.04	18.20	76.0	1.5	1.132	18	2.5	2.56	0.020	
13.00	13.00	12.00	14.00	13.00	14.00	14.00	14.00	15.00	14.00 14.00
14.00	14.00	14.00	12.00	14.00	14.00	15.00	13.00	13.00	
8.05	20.25	76.0	1.5	1.132	12	2.5	2.56	0.020	
15.00	17.00	17.00	15.00	18.00	15.00	18.00	18.00	18.00	20.00 17.00
18.00	18.00								
8.06	25.30	76.0	1.5	1.132	20	2.5	2.56	0.020	
19.00	22.00	20.00	20.00	21.00	22.00	22.00	22.00	23.00	23.00 25.00
25.00	23.00	21.00	20.00	19.00	20.00	20.00	19.00	23.00	20.00 19.00
8.07	30.35	76.0	1.5	1.132	20	2.5	2.56	0.020	
26.00	25.00	24.00	25.00	24.00	24.00	24.00	25.00	23.00	21.00 25.00
21.00	21.00	24.00	24.00	24.00	24.00	24.00	24.00	24.00	24.00 26.00
8.08	35.40	76.0	1.0	1.132	28	2.5	2.56	0.020	
16.00	15.00	16.00	16.00	18.00	16.00	16.00	22.00	19.00	20.00 18.00
16.00	22.00	21.00	21.00	20.00	23.00	23.00	23.00	21.00	20.00 21.00
18.00	18.00	18.00	18.00	18.00	19.00	19.00	19.00	20.00	
8.09	40.45	76.0	1.0	1.132	24	2.5	2.56	0.020	
19.00	20.00	21.00	22.00	21.00	24.00	24.00	21.00	23.00	23.00 24.00
23.00	19.00	19.00	19.00	22.00	24.00	24.00	26.00	24.00	23.00 23.00
23.00	25.00	23.00	23.00						
8.10	45.50	76.0	1.0	1.132	12	2.5	2.56	0.020	
35.00	26.00	28.00	25.00	25.00	29.00	29.00	26.00	25.00	25.00 28.00
26.00	25.00								
8.11	50.60	76.0	1.0	1.132	20	2.5	2.56	0.020	
36.00	38.00	36.00	36.00	38.00	37.00	37.00	38.00	39.00	37.00 35.00
38.00	32.00	34.00	41.00	36.00	37.00	37.00	40.00	39.00	38.00 38.00
8.12	60.70	76.0	1.0	1.132	26	2.5	2.56	0.020	
38.00	38.00	40.00	39.00	42.00	38.00	38.00	54.00	52.00	39.00 46.00
52.00	36.00	34.00	36.00	28.00	34.00	34.00	44.00	36.00	40.00 42.00
34.00	38.00	38.00	36.00	28.00	36.00	36.00			

TABLE D-2 - continued

SETTLING TEST DATA

TEST NO	MESH	TEMP	DIST FT	FLUID S.G.	NO OF TESTS	CHART SPEED	KIN VISC	YIELD STRESS	READINGS
8.13	70.80	76.0	1.0	1.132	50	2.5	2.56	0.020	
48.00	45.00	49.00	36.00	38.00	40.00	42.00	44.00	30.00	38.00
32.00	42.00	40.00	58.00	52.00	40.00	48.00	36.00	52.00	45.00
43.00	34.00	40.00	37.00	45.00	31.00	52.00	45.00	43.00	34.00
40.00	37.00	45.00	31.00	34.00	38.00	45.00	38.00	40.00	38.00
45.00	39.00	40.00	39.00	35.00	42.00	39.00	39.00	42.00	38.00
8.14	80.10	76.0	0.5	1.132	20	2.5	2.56	0.020	
23.00	22.00	29.00	23.00	22.00	21.00	30.00	32.00	27.00	29.00
24.00	33.00	28.00	23.00	28.00	33.00	23.00	24.00	24.00	19.00
8.15	10.12	76.0	0.5	1.132	21	2.5	2.56	0.020	
35.00	30.00	31.00	25.00	30.00	31.00	25.00	23.00	40.00	25.00
30.00	31.00	32.00	33.00	27.00	27.00	28.00	25.00	25.00	30.00
30.00									
8.16	12.14	76.0	0.5	1.132	12	2.5	2.56	0.020	
25.00	28.00	25.00	30.00	27.00	25.00	25.00	25.00	25.00	30.00
30.00	30.00								
9.01	3.00	79.0	1.5	1.132	10	5.0	2.56	0.020	
8.50	8.00	8.50	8.50	8.50	8.00	9.00	9.00	9.00	9.00
9.02	4.00	79.0	1.5	1.132	6	10.0	2.56	0.020	
12.50	10.50	11.00	11.00	12.50	10.00				
9.03	6.00	79.0	1.5	1.132	2	10.0	2.56	0.020	
9.00	9.50								
10.01	8.12	79.0	1.5	1.242	23	2.5	4.60	0.070	
15.00	15.00	16.00	14.50	14.60	14.50	15.50	12.50	16.00	14.50
16.50	14.00	16.50	15.00	14.00	15.00	17.00	14.00	14.00	15.50
14.00	12.00	14.00							
10.02	12.16	79.0	1.5	1.242	10	2.5	4.60	0.070	
11.00	17.00	20.00	15.00	19.00	20.00	15.00	18.00	18.00	19.00
10.03	16.18	79.0	1.5	1.242	10	2.5	4.60	0.070	
24.00	29.00	23.00	25.00	21.00	20.00	21.00	22.00	22.00	27.00
10.04	18.20	79.0	1.5	1.242	17	2.5	4.60	0.070	
29.00	30.00	26.00	23.00	27.00	30.00	28.00	27.00	29.00	27.00
30.00	27.00	28.00	26.00	30.00	24.00	27.00			

TABLE D-2 - continued

SETTLING TEST DATA

TEST NO	MESH	TEMP	DIST FT	FLUID S.G.	NO OF TESTS	CHART SPEED	KIN VISC	YIELD STRESS	READINGS
12.02	14.16	7.3	1.5	1.242	11	2.5	4.60	0.070	
15.50	14.50	17.00	15.00	14.50	16.00	16.00	19.00	21.00	17.50 21.00
24.00									
12.03	16.20	73.0	1.5	1.242	12	2.5	4.60	0.070	
18.50	16.50	20.00	19.00	16.50	21.00	21.00	19.00	20.00	17.00 18.00
18.00	17.50								
12.04	20.24	73.0	1.5	1.242	11	2.5	4.60	0.070	
29.00	28.00	28.00	27.00	33.00	22.00	22.00	23.50	23.50	23.00 28.00
22.50									
12.05	32.35	73.0	1.5	1.242	10	2.5	4.60	0.070	
24.00	18.00	24.00	22.50	26.50	23.00	23.00	18.00	18.50	24.50 26.00
12.06	3.20	8.0	1.0	1.242	52	10.0	4.60	0.070	
17.00	17.00	17.50	15.50	16.00	16.50	16.50	16.50	16.00	16.50 15.50
17.00	16.50	17.50	16.50	16.50	16.00	16.00	17.50	17.50	16.00 16.00
16.50	17.00	17.00	17.50	17.50	17.00	17.00	17.00	17.00	16.50 16.50
16.50	16.00	17.50	16.50	17.50	17.50	17.50	17.50	17.50	16.00 16.50
16.50	17.00	17.00	16.00	18.00	16.00	16.00	15.50	17.00	16.00 15.50
15.50	16.00								
12.07	2.50	80.0	1.0	1.242	52	5.0	4.60	0.070	
12.00	12.00	11.00	11.00	10.00	11.00	11.00	10.50	11.00	11.00 10.50
12.00	11.50	11.00	11.50	11.50	11.50	11.50	11.00	11.50	11.50 12.00
12.00	11.00	11.50	11.00	11.00	11.00	11.00	11.50	12.00	11.50 11.50
13.00	13.00	12.00	12.00	11.50	12.00	12.00	12.00	12.50	12.00 12.00
11.50	11.50	11.50	12.00	12.00	12.00	12.00	12.00	12.50	12.00 13.00
12.0	12.0								

NOTE

20.25 IN MESH COLUMN REFERS TO 20-25 SIEVE FRACTION
 80.10 REFERS TO 80-100 SIEVE FRACTION
 10.12 REFERS TO 100-120
 12.14 REFERS TO 120-140
 14.17 REFERS TO 140-170
 17.20 REFERS TO 140-170 SIEVE FRACTION
 MESH COLUMN FOR TYPE 3 SOLIDS REFERS TO PARTICLE SIZE IN MM
 TEMP IN DEG F
 CHART SPEED IN MM/SEC
 KINEMATIC VISCOSITY IN SQ FT/SEC
 YIELD STRESS IN LB/ SQ FT
 READINGS IN SEC IF CHART SPEED IS ZERO
 READINGS IN MM IF CHART SPEED NOT ZERO

B29832